NBSIR 80-2188

# Joint US-USSR Seminar on Mathematical Methods for Estimating the Fire Endurance of Structural Assemblies

R. S. Levine, Editor

Center for Fire Research
National Engineering Laboratory
U.S. Department of Commerce
National Bureau of Standards
Washington, DC 20234

December 1980

Final Report

U.S. DEPARTMENT OF COMMERCE

NATIONAL BUREAU OF STANDARDS

NBSIR 80-2188

# JOINT US-USSR SEMINAR ON MATHEMATICAL METHODS FOR ESTIMATING THE FIRE ENDURANCE OF STRUCTURAL ASSEMBLIES

R. S. Levine, Editor

Center for Fire Research
National Engineering Laboratory
U.S. Department of Commerce
National Bureau of Standards
Washington, DC 20234

December 1980

Final Report

Joint US-USSR Seminar on Mathematical Methods for
Estimating the Fire Endurance of Structural Assemblies


R. S. Levine, Editor


FOREWORD


    This publication is a compilation of papers presented May 14, 1980,
at a Joint US-USSR Seminar on "Mathematical Methods for Estimating the
Fire Resistance of Structural Assemblies".  The seminar was arranged by
the US-USSR Panel on Fire Resistance of Buildings and Structures as a
part of their continuing protocol (agreement) to cooperate in this
field.  This panel is organized within the framework of the US-USSR
agreement on cooperation in the field of housing and other construction,
for which the Department of Housing and Urban Development serves as the
U.S. Executive Agency.  Dr. Robert S. Levine of the National Bureau of
Standards, Center for Fire Research and Dr. Igor G. Romanenkov, Laboratory
Chief, Central Research Institute of Building Construction, GOSSTROY,
are the Co-Chairmen of the Fire Panel.

    This is the first of a series of planned yearly joint seminars on
specific applied fire safety research topics.  The Soviet papers were
translated into English by the Soviets, but editorial changes have been
made by U.S. personnel who are expert in the particular subject.  It is
intended that the original authors' meanings have not been changed.  In
some cases, the U.S. presentations are not yet available as published
papers, or were summaries of work that has already been published else-
where.  Hence, one of the U.S. presentations is in the form of slides
and commentary.  These presentations, in the form given, are intended to
represent up-to-date U.S. technology.

    The agenda of the Joint Seminar is presented on pages v and vi.
The papers are published here in the order they appear in the agenda.
The positions and affiliations of the Soviet speakers are given on page
vii.

## TABLE OF CONTENTS

AGENDA

U.S.-U.S.S.R. PANEL ON FIRE RESISTANCE OF BUILDINGS AND STRUCTURES

Joint Seminar

May 14, 1980                    9:00 a.m.              B119 Polymers (Bldg. 224)


"MATHEMATICAL METHODS FOR ESTIMATING
THE FIRE RESISTANCE OF STRUCTURAL ASSEMBLIES"


9:00 a.m.       Announcements and Plans
                    Dr. Robert S. Levine, Center for Fire Research,
                    National Bureau of Standards

9:10            Welcome
                    Ms. Nina Shafran, Office of International Affairs,
                    Department of Housing and Urban Development

9:15-9:45       Basic Principles of Calculation of Building Structures'
                Fire Resistance Limits, A. I. Yakovlev

9:45-10:15      Behavior of Inorganic Materials in Fire, M. S. Abrams,
                Portland Cement Association

10:15-10:45     Calculation of the Fire Resistance for Flexural Reinforced
                Concrete Structures, V. V. Zhukov and V. N. Samoylenko

10:45-11:00     Coffee Break

11:00-11:30     A Mathematical Model of Heat Flow in Concrete Beams Based
                on the Results of Thirty-two Full Scale Fire Tests, T. D.
                Lin and M. S. Abrams, Portland Cement Association

11:30-12:00     Calculation Method for Determining the Possibility of
                Concrete Spalling Due to Fires, V. V. Zhukov

12:00-1:00      Lunch

| | |
|---|---|
| 1:00-1:30 | Calculating Fire Endurance for Steel Structural Members Located on the Outer Walls of Buildings, R. G. Gewain, American Iron and Steel Institute |
| 1:30-2:00 | Fire Resistance Calculation Methods for Steel Structures A. I. Yakovlev |
| 2:00-2:30 | Reliability Analysis of Fire-Exposed Light-Frame Wood Floor Assemblies, E. Schaffer, Forest Products Laboratory. Presented by F. Woeste, Virginia Institute of Technology. |
| 2:30-3:00 | Basic Principles of Calculating the Fire Resistance of Timber Structures, G. M. Kirpichenkov and I. G. Romanenkov |
| 3:00-3:15 | Coffee Break |
| 3:15-3:45 | Approach to the Fire Resistance Design for Light Wall Panels Using Effective Materials, V. N. Zigern-Korn and I. G. Romanenkov |
| 3:45-4:15 | Sprinkler Systems: An Approach to Active Fire Resistance, J. Hankins, Factory Mutual Research Corporation |
| | Adjourn |

POSITIONS AND AFFILIATIONS OF THE SOVIET SPEAKERS

I. G. Romanenkov

    Laboratory Chief at Central Research Institute of Building
Constructions, USSR State Construction Committee


A. I. Yakovlev

    Department Chief at All-Union Research Institute of Antifire
Defense Institute, USSR Ministry of Internal Affairs


V. V. Zhukov

    Laboratory Chief of Research Institute of Concrete and
Ferro-Concrete, USSR Construction Committee

# BASIC PRINCIPLES OF CALCULATION OF BUILDING STRUCTURES' FIRE RESISTANCE LIMITS

Dr. A. I. Yakovlev
VNIIPO, Ministry of Interior of the USSR

Fire resistance limits of building structures are calculated according to two indexes: (a) load bearing capacity failure due to strength reduction, temperature creep development, thermal expansion and pyrolysis of structural materials in the process of heating; (b) heating of the unexposed surface to 140°C due to heat transfer process.

Generally, the calculation process consists of two parts: heat transfer analysis and stress analysis.

The heat transfer calculations aim at temperature field determining the different sections of the structure and is performed by solving the problem as a case of unsteady state conductive heat transfer. It goes without saying that the heating index of the fire resistance limit of structures is determined solely by the heat transfer calculation.

The stress analysis determines the load bearing capacity of a structure under heating on the basis of ultimate equilibrium equations and deformations considering the variation of physical-mechanical properties with temperature and the pyrolysis rate of building materials under high temperatures.

In general outline, the concept of calculating the fire resistance limit with regard to load bearing capacity failure is shown in figure 1. In figure 1 the abscissa indicates heating time, t. The ordinate indicates the durability of the heated structure (for bending elements, $M_{p,t}$, bending moment; or for compression and tension numbers, $N_{p,t}$, longitudinal force). On the right vertical axis is shown the nominal load value ($M_H$ and $N_H$, respectively) required for the structure.

The temperatures in the sections of the structure are determined for certain periods by heat transfer calculations. Then the stress analysis calculation is made, the results of which form the load bearing capacity reduction curve of the structure exposed to heating. The calculated time during which the load bearing capacity of structure is reduced to the working load value is the calculated fire resistance of the structure.

This is the general principle of fire resistance calculation with regard to load bearing capacity failure. It is applicable to every structure. However, there are particular cases when there is no necessity of determining the load bearing capacity reduction curve, but it is possible to determine the fire endurance by merely calculating a section temperature. The temperature so determined is termed "critical" and it causes the load bearing capacity failure, i.e. fire resistance limit. Then the time necessary for heating the structure to this critical temperature is

1

calculated by solving the inverse heat transfer problem. The time
mentioned is considered to be the fire resistance limit. This is the
way to calculate the bending capacity of reinforced concrete elements
and of steel structures. Their failure takes place due to heating of
the reinforcement and flange to the critical temperature that is regarded
as uniformly distributed over the sections of these elements due to high
heat conductivity of metal. As the fire resistance estimation generally
starts with a heat transfer calculation, we shall first examine the
calculation methods.

I. Heat Transfer Calculation

The initial and boundary conditions of the calculation are as follows:

Initial conditions:

the temperature over the structure's section is uniform and
identical with ambient temperature – $t_H = 20°C$.

Boundary conditions:

a) compartment fire temperature – $t_B$ varies according to the
"standard curve":

$$t_B = 345 \log (8 \tau + 1), °C,$$

where $\tau$ – in min.;

b) the coefficient of heat transfer from the fire to the exposed
surface of the structure – $\alpha$ – is estimated according to the
formula:

$$\alpha = 25 + 4.96 \, S_{np} \frac{\left(\dfrac{t_B + 273}{100}\right)^4 - \left(\dfrac{t_o + 273}{100}\right)^4}{t_B - t_o} ,$$

$$kcal, \, m^{-2}, \, t^{-1}, \, °C^{-1}$$

where $S_{np} = \dfrac{1}{\dfrac{1}{S_B} + \dfrac{1}{S_o} - 1}$ – the given emissivity of the system

between the furnace and the surface of the structure;
$S_B = 0.85$ – the emissivity of the furnace fire box ambient;
$S_o$ – the emissivity of the structure's exposed surface;
$t_o$ – the temperature of the structure's exposed surface;

c) the coefficient of heat transfer from the unexposed surface of
the structure to the ambient – $\alpha'$ – with $t_H = 20°C$ is estimated
according to the formula:

2

$$\alpha' = 1.3^3\sqrt{t'_o - t_H} + 4.96\ S'_o\ \frac{\left(\dfrac{t'_o + 273}{100}\right)^4 - \left(\dfrac{t_H + 273}{100}\right)^4}{t'_o - t_H}\ ,$$

$$\text{kcal, } m^{-2},\ t^{-1},\ {}^{\circ}C^{-1}$$

where $t'_o$ – the exposed surface temperature;

$S'_o$ – the emissivity of the unexposed surface.

The heat transfer calculation also takes into account the nonlinearity of the internal heat transmission and heat absorption for evaporation of free water in the pores of material (negative heat source).

The nonlinear heat transmission is taken into account by the straight line dependence of the thermal conductivity – $\lambda_t$ and heat capacity – $C_t$ – on temperature – t

$$\lambda_t = A \pm B.t,\ C_t = C + D.t$$

where A and C are the initial values of thermal conductivity and heat capacity;

B and D are the coefficients of thermal conductivity and heat capacity change with regard to temperature.

The influence of material moisture content on the change of the temperature field in the exposed structure section takes place due to moisture trans-mission and water evaporation in the pores of the material.

As it is necessary to provide the coincidence of experimental and calculated curves of structure's heating at critical temperatures 100°C and higher, to simplify the process, the calculation is made without taking moisture transmission into consideration. It is assumed that the initial moisture content of the layers does not change and water evaporation takes place in one layer after another. The evaporation starts at 100°C and requires 539 kcal/kg. As a result, the process of heating the structure is retarded. The phenomenon mentioned above is taken into account in the heat transfer equations used in the calculation.

The majority of building structures have one dimension that is significantly more or less than the other two. If the dimension in question is less than two others, for example, the width of flat enclosing structures, the temperature variations are considered to occur solely in the direction of the dimension in question, i.e. a one-dimension analysis is solved. In case one dimension is more than two others, for example, the length of beams, columns and cross-bars, the temperature calculation is made in the cross-section in the other two directions, i.e. a two-dimensional analysis is solved.

The above mentioned heat transfer evaluation conditions indicate the necessity of taking into account the internal and external nonlinearity plus the internal (negative) heat sources. Therefore, it is practically

3

impossible to obtain analytical solutions of the equations even for a single-dimension heat flow. The similar solutions available for engineering design are likely to be obtained only with certain simplifying assumptions, for example, introduction of constant (taken at some average temperature) heat transfer coefficients and application of first order boundary condition. With these assumptions the analytical solution for heating time – $\tau$ – of the exposed surface is possible for one-dimensional heat flow. To calculate the heating time – $\tau$ – of the reinforcement of concrete solid slabs to a critical temperature for one-dimensional heat flow the following analytical solution is used:

$$\tau = \left( \frac{k + \dfrac{y + k_1\, d}{\sqrt{A_{np}}}}{2\chi} \right)^2 \quad \text{hrs.}$$

where k is a temperature variation coefficient of the exposed surface dependent on the density – $\gamma_c$ – of dry concrete (table 1).

Table 1

| $\gamma_{c_1}$ kg·m$^{-3}$ | 100 and less | 1000 | 1500 | 2000 | 2300 | 2450 |
|---|---|---|---|---|---|---|
| k, hr$^{1/2}$ | 0.46 | 0.55 | 0.58 | 0.60 | 0.62 | 0.65 |

y – is the thickness of the concrete cover
d – is the reinforcement bar's diameter
$k_1$ – is a coefficient of the rod's metal mass influence on its heating, depending on the dry concrete density – $\gamma_c$ (table 2)

Table 2

| $\gamma_{c_1}$ kg·m$^{-3}$ | 500 and less | 800 | 1100 | 1400 | 1700 | 2000 and more |
|---|---|---|---|---|---|---|
| $k_1$ | 1.0 | 0.9 | 0.8 | 0.7 | 0.6 | 0.5 |

$A_{np}$ – is the given thermal diffusivity coefficient of concrete, m$^2$ · hr$^{-1}$.

$$A_{np} = \frac{\gamma_{t,cp}}{(C_{t,cp} + 0.012\, p)\, \gamma_c}$$

$\gamma_{t,cp}$ and $C_{t,cp}$ are the average values of concrete thermal conductivity and heat capacity, evaluated at 450°C;

p – concrete moisture content, weight %;

χ – Gauss' error function evaluated according to the formula:

$$\text{erp}\chi = \frac{1250 - T_{A,kp}}{1250 - t_H}$$

$T_{A,kp}$ – is the reinforcement critical temperature, °C.

The analytical time determination – $\tau$ – for the unexposed surface of the structure to reach 140°C (fire resistance limit on the basis of heating), applying the same simplification, may be introduced as:

$$\tau = 2.3 \frac{(\delta + K\sqrt{A'_{np}})^2}{A_{np} \cdot \mu_1^2} \; \log \left( \frac{A_1}{\dfrac{1}{1 + B_i} - \dfrac{140}{1250 - t_H}} \right) \text{ hrs.}$$

where $\delta$ is the structure depth, m;

$B_i$ – Biot number

$$B_i = \frac{\alpha'_{cp}}{\lambda'_{t,cp}} (\delta + k \sqrt{A'_{np}})$$

$\alpha'_{cp} = 4 + 7.4\ S'$ is the average heat transfer coefficient of the unexposed surface, to the ambient air $t_H = 20°C$; including radiation

$\lambda'_{t,cp}$ is the average heat thermal conductivity, evaluated at $t = 250°C$

$A'_{np}$ is the given thermal diffusivity coefficient at $t = 250°C$

$\mu_1$ and $A_1$ are the first characteristic equations' roots (table 3).

Table 3

| $B_i$ | $\mu_i$ | $A_i$ |
|---|---|---|
| 0 | 1.5708 | 1.2735 |
| 0.1 | 1.632 | 1.1865 |
| 0.2 | 1.6887 | 1.1037 |
| 0.3 | 1.7414 | 1.0329 |
| 0.4 | 1.7906 | 0.9758 |
| 0.5 | 1.8366 | 0.9246 |
| 0.6 | 1.8798 | 0.8812 |
| 0.7 | 1.9203 | 0.8406 |
| 0.8 | 1.9586 | 0.8038 |
| 0.9 | 1.9947 | 0.7710 |
| 1.0 | 2.0288 | 0.7415 |
| 1.5 | 2.1746 | 0.6253 |
| 2.0 | 2.2889 | 0.5435 |
| 2.5 | 2.3723 | 0.4889 |
| 3.0 | 1.4557 | 0.4342 |
| 4.0 | 2.5704 | 0.3587 |
| 5.0 | 2.6537 | 0.3065 |
| 6.0 | 2.7165 | 0.2692 |
| 7.0 | 2.6558 | 0.238 |
| 8.0 | 2.8044 | 0.2133 |
| 9.0 | 2.8363 | 0.1934 |
| 10.0 | 2.8628 | 0.1763 |

The differential numerical methods utilized by means of a computer are the universal ones for solving the unsteady state heat transfer tasks without simplifying preconditions, and are applicable for practically any structure. The method of elementary heat balance is one of them.

According to this method, the heat balance equations are derived for a series of ultimate elements that are chosen arbitrarily in the structure by means of a grid attached to its section. Square-, rectangular- or triangular-celled grids are used subject to the section configuration.

The heat balance equation of the ultimate element 1 m long and $\Delta X . \Delta Y$ square with a node XY (fig. 2) for the rectangular grid is given below:

$$\left( A + B \frac{t_{x-1,y} + t_{x,y}}{2} \right) \frac{\left( t_{x-1,y} - t_{x,y} \right) \Delta y \cdot \Delta \tau \cdot 1}{\Delta \chi} +$$

$$\left( A + B \frac{t_{x+1,y} + t_{x,y}}{2} \right) \frac{\left( t_{x+1,y} - t_{x,y} \right) \Delta y \cdot \Delta \tau \cdot 1}{\Delta \chi} + \left( A + B \frac{t_{x,y-1} + t_{x,y}}{2} \right)$$

$$\frac{\left( t_{x,y-1} - t_{x,y} \right) \Delta \chi \cdot \Delta \tau \cdot 1}{\Delta y} + \left( A + B \frac{t_{x,y+1} + t_{x,y}}{2} \right) \left( \frac{\left( t_{x,y} - t_{x,y+1} \right) \Delta \chi \cdot \Delta \tau \cdot 1}{\Delta y} \right) =$$

$$\gamma_c \, \Delta \chi \cdot \Delta y \cdot 1 (C + D \cdot t_{x,y}) (t_{x,y,\Delta \tau} - t_{x,y}) +$$

$$\frac{\gamma_c \cdot \Delta \chi \cdot \Delta y \cdot p \cdot r \cdot 1}{100}$$

where r is the latent heat, $kcal/kg^{-1}$.

The temperature – $t_{x,y}$, $\Delta \tau$ – evaluation formula at the node point in a certain time interval, $\Delta \tau$, is derived by the present equation.

The formulas for all the nodes as well as edge conditions are the computer algorithms for structural fire resistance evaluation on the basis of the heat transfer analysis. In case of a one-dimensional heat flow, e.g. along the y-axis, the nodal temperatures along the x-axis become equal to each other

$$(t_{x,y} = t_{x-1,y} = t_{x+1,y}),$$

and the evaluation algorithm is simplified.

Of concern is that the nodal locations are properly specified and the heat balance equations properly derived for reinforced concrete and protected steel structures with distinctly variable material heat transfer analysis characteristics. The section temperature of bent reinforcement bars and of straight reinforcement profiles walls thickness is considered constant in reinforced concrete structures. Therefore, the bent reinforcement bars' nodes are located in their section's center.

The nodes of the straight reinforcement profiles are located along the length of the walls and flanges in their thickness center. The application of the grid to coated steel structure profiles is carried out analogously. The methods of locating grid nodes in reinforced concrete, steel and laminar nonbearing structure sections as well as heat balance equation types for the nodes are more precisely described in the reports in this seminar dedicated to the fire resistance calculation of the structures mentioned above.

## II. Static Stress Analysis Calculation

As has been already mentioned, this type of calculation is carried out in case the fire resistance of the structure is determined by bearing capacity loss (collapse).

As follows from the basic equilibrium equations, the load-bearing capacity (durability) is affected by the fire destruction according to loss of strength of the structural materials under high temperature conditions. The section diminution due to pyrolysis is taken into consideration in structures made of combustible materials.

### a) Reinforced Concrete Structures

The heating of statically determinate building structures at the bottom results in their failure; as a rule the failure takes place at the cross-section of the maximum bending moment. Sheer failure by diagonal tension is a rare phenomenon and can be prevented by stirrup reinforcement near the bearing points.

The destruction in the cross-section of almost all the slabs and beams takes place due to the tensile reinforcement's heating to its critical temperature. At this temperature a rapid increase in creep occurs due to the working stresses. Thus the reinforcement capacity at the critical temperature is reduced to the value of the working stresses. Therefore, the critical temperature – $T_{a,kp}$ – for the fire endurance estimate of a standard bending structure according to the heat transfer calculation is derived from the strength vs. temperature diagram of the reinforcement steel. The working stress values are calculated from the equilibrium of the cross-section.

In the case of concrete flexural members, such as beams, where the tension reinforcement is by means of bars manufactured from various classes of steel, and the concrete in the compression zone may be heated to high temperatures, the fire endurance time is estimated according to figure 1 for both the tension and compression zones. For all these cases the load bearing capacity of the structure is estimated for definite time periods by substituting the concrete strength values in the ultimate equilibrium equations.

Statically indeterminate flexural structures are subjected to stress redistribution under heating. In this regard the beam members with support restraint undergo a reduction of the bending moments at mid-span and an increase of bending moments at the supports. In the ultimate equilibrium conditions the bearing capacity is based on the residual strength of the supporting and mid-span sections.

When slabs supported along four sides with approximately equal sides sag significantly, their compressed area moves to the sides and the compressive area becomes extended over the width of the slab. Owing to considerable stress reduction the tensile reinforcement's critical temperature is assumed to be 800°C. If the ratio of the sides increases, the reinforcement critical temperature falls to the value noted for simple beam members.

The brittle failure of columns with axial compression is accompanied by concrete crushing over the whole of the cross-section and also by bulging of the longitudinal reinforcement.

The columns load bearing capacity in the ultimate equilibrium conditions is found by summing up the load bearing capacity of the concrete section and of the reinforcement at high temperatures.

Due to considerable temperature variation through the solid column cross-section (more than 200 x 200 mm) the deformation of the central slightly heated layers is significantly less than the intensely heated periphery layers. Therefore, the columns maximum deformation in the ultimate equilibrium condition takes place solely in the cooler concrete at the center of the section. Because of this load transfer, the strength of the outer concrete layers is only partially available.

In this connection the concrete section bearing capacity of solid columns should be estimated considering the temperature creep deformations of loaded concrete. The data may be obtained by testing concrete samples in an apparatus capable of imposing constant load while a specimen is heated according to the concrete heating curve for the fire resistance test on structures.

The temperature variations through thin-walled columns sections having dimensions 200 x 200 mm or less are insignificant. The concrete deformation of the section of the thin-walled columns at ultimate loading may be considered to be the same, and concrete ultimate strength for all the layers is reached. That results in nearly equal fire endurance limits (approximately 1 hr.) for columns with section dimensions 200 x 200 mm and, for example, double-T columns with walls thickness of 60 mm. Columns with section dimensions 300 x 300 mm and double-T columns with walls thickness of 120 mm have an endurance of approximately 2 hrs.

b) Steel Structures

To calculate the fire resistance limit of steel structures it is necessary to determine their heating time to critical temperature. The temperature value is evaluated according to point of plasticity or to the elastic modulus curve of steel structures when heated depending on their mode of failure. Bearing capacity loss of compressed elements may take place due to loss of strength and also loss of integrity. The failure mode depends on the type of structure, steel characteristics, element elasticity, type of support and working load value. Accordingly, the plastic limit and the modulus of elasticity of the steel are used in the ultimate equilibrium equations. The critical temperatures are determined according to the curves with regard to these characteristics.

9

c) <u>Timber Structures</u>

Timber structure failure at fire exposure takes place due to functional section reduction resulting from timber charring and also due to reduction of mechanical properties of the heated timber cross-section.

The time of complete failure is determined according to general case scheme (figure 1). Of concern is that in the calculated heating time periods the structure's bearing capacity depends on the cross-section's size and its durability under heated condition. The reduction in the modulus of elasticity of the timber in the compression zone of the heated cross-section is also taken into consideration with the view of determining the critical force affecting the structure's stability and failure.
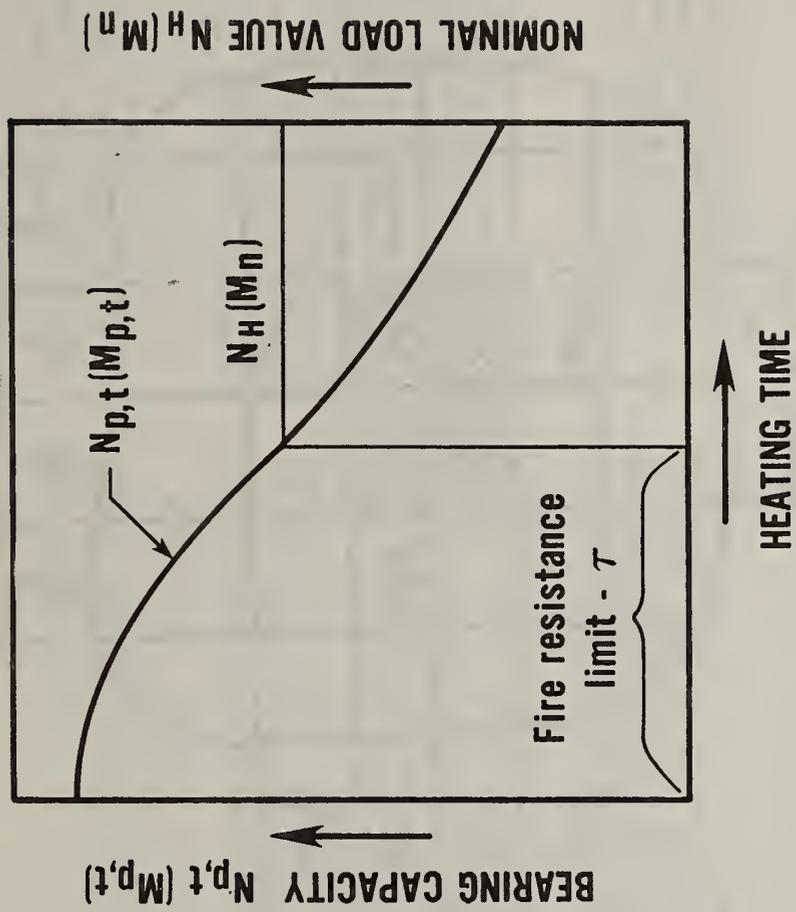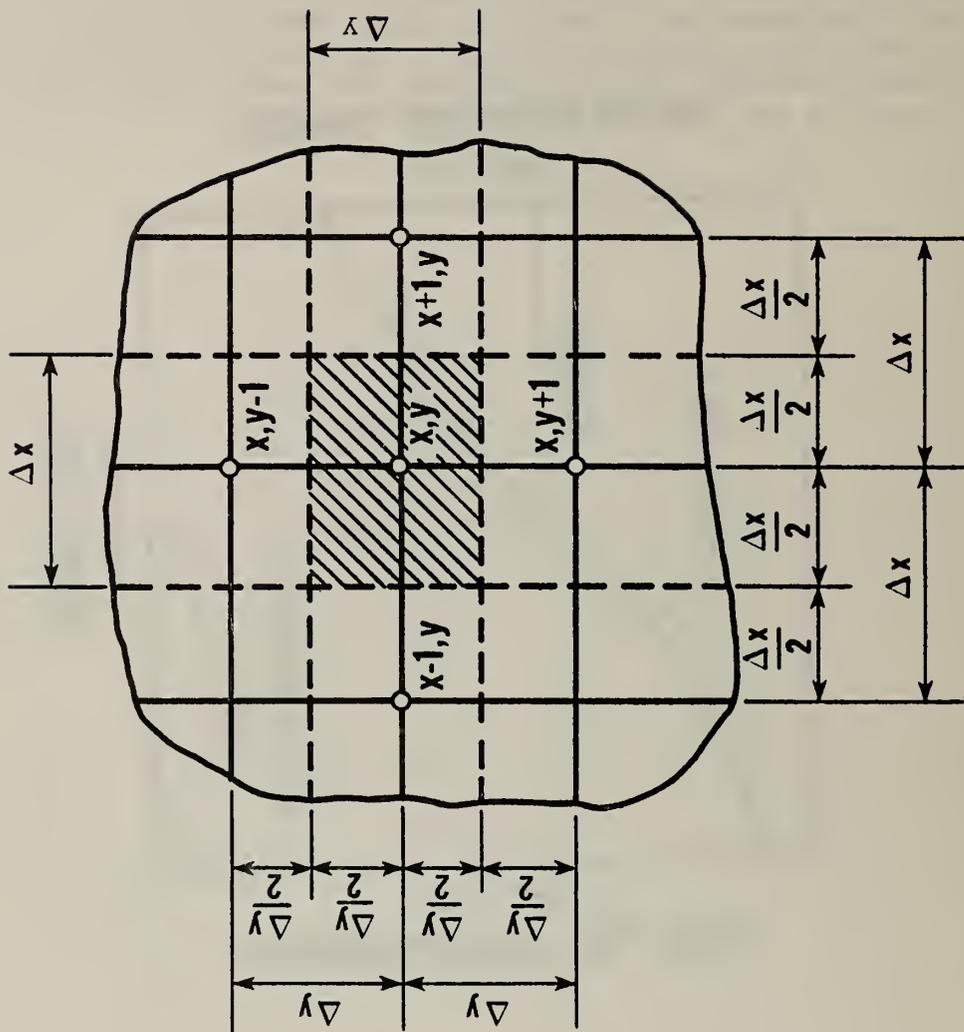
NOMINAL LOAD VALUE $N_H$ ($M_n$)

$N_{p,t}$ ($M_{p,t}$)

$N_H$ ($Mn$)

Fire resistance limit - $\tau$

HEATING TIME

BEARING CAPACITY $N_{p,t}$ ($M_{p,t}$)

Figure 1

11

Figure 2

12

*M. S. Abrams*[1]

# Behavior of Inorganic Materials in Fire *

**ABSTRACT:** Behavior of inorganic materials exposed to fire depends upon the time-temperature relationship during exposure. Exposing these materials to heat generally causes significant changes in strength, elastic, and thermal properties. Temperature-distribution information developed during exposure and changes in properties occurring over the exposure temperature range are essential for evaluating the behavior of a structure where these materials are used.

This report provides information on changes in strength, elastic, and thermal properties due to increasing temperatures for various concretes, steels, and concrete masonry. Also, some thermal-property information is given for common brick, gypsum, ceiling tile, plasterboard, and asbestos-board. Use of temperature distribution and property information in predicting the performance of fire-exposed structures is described.

Finally, information on some actual fires in structures is presented to demonstrate how a knowledge of the behavior of inorganic materials exposed to fire can be used to predict the performance of structures.

**KEY WORDS:** inorganic materials, concrete, steel, concrete masonry, brick, gypsum wallboard, asbestos board, ceiling tile, thermal expansion, modulus of elasticity, stress-strain, creep strain, compressive strength, Poisson's ratio, split cylinder tensile strength, elevated temperature, thermal conductivity, thermal diffusivity, specific heat, temperature distributions, rational design, simple support, continuity, axial restraint, heat transmission criteria, structural integrity, equivalent thickness, design aids, system analysis, actual fires

during or after a fire, are very rare. Where parts of a building have failed structurally, damage usually occurred after a much longer period of fire exposure than that for which the member was designed.

Well-designed fire-resistive steel structures have generally performed well during fires. Collapse of steel structures or parts of the structure during fire exposure has not been frequent. Where such failures have occurred, they were associated with a reduction of the strength and elastic properties of the materials during the fire or inadequate design for the intended occupancy.

Reasons are complex for the excellent performance record during fire of structures utilizing fire-resistive inorganic materials. Consequently, design of such structures for fire has been based on observed field performance and on results of standard fire tests of individual members of the structure [1].[2] Both these methods have shortcomings. Field performance depends upon interpretation of behavior by the observer and designer. Furthermore, actual behavior of structural members in a building generally cannot be simulated in a standard fire test. These shortcomings have resulted in conservative design with many redundant safety factors.

In the past 20 years, information has become available on high temperature properties of inorganic materials. Also, temperature distributions in structural members are available from tests or can be generated from analytical models. More information is available for concrete and steel than for other inorganic materials. This paper presents information on the effect that elevated temperatures have on important properties of some inorganic materials, and typical temperature distributions are given. This information is applied in predicting behavior of structures exposed to fire.

## Material Properties

Knowledge of changes in properties of materials over a wide temperature range is required to predict performance of structures exposed to fire. Most of this information for materials has become available during the past two decades. Effects of temperature on selected material properties are described below.

### Thermal Expansion

In structures where expansion of heated materials is resisted by surrounding elements, thermal expansion information is indispensible in designing for fire. Information for some inorganic materials has been reported in the literature.

Many fires have occurred in different types of fire-resistive structures during the past 50 years. In general, these buildings have performed well structurally, even during severe fire exposure. Spread of fire, both within the building and to adjacent structures, has often been prevented by the fire-resistive nature of the inorganic materials used in the structures. Reports of collapse of a concrete structure or members of that structure,

[1]Manager, Fire Research Section, Portland Cement Association, Skokie, Ill. 60077.

[2]The italic numbers in brackets refer to the list of references appended to this paper.

13

*Concrete*—Expansion data for concrete made with different aggregates are shown in Fig. 1 [2]. Thermal expansion is not a linear function of temperature but increases with increasing temperature. Sanded expanded-shale concrete has the most nearly linear and lowest expansion-versus-temperature relationship over the temperature range of 20 to 875°C (68 to 1607°F). These data were obtained by Cruz using a dilatometric method but results have not yet been published. Philleo [3] performed tests on a carbonate-aggregate concrete using a different technique. He obtained somewhat higher values at temperatures above 375°C (707°F) than those obtained by Cruz.

Dettling [4] pointed up that thermal expansion of concrete is influenced by cement, water content, aggregate type, and age. Anderberg and Thelandersson [5] investigated the effect of different load levels on thermal expansion of a siliceous-aggregate concrete heated at a rate of 5°C (9°F)/min. Thermal expansion was strongly reduced as the stress level increased (as shown in Fig. 2). They also presented data on the influence of rate of heating and moisture conditioning pretreatment on the deformation of concrete under sustained load.

*Concrete Masonry*—Thermal expansion of 16 different concretes used in masonry units was reported by Harmathy and Allen [6]. Siliceous and carbonate aggregate concretes exhibited the largest length change, reaching values of about 1.2 to 1.4 percent at 875°C (1607°F). Most sanded and unsanded expanded slag, expanded-shale, and expanded-clay concretes had a maximum length change between 0.1 and 0.5 percent at 760°C (1400°F). Pumice concretes exhibited considerable shrinkage at temperatures above 315°C (600°F).

*Steel*—Figure 3 [7] shows the average thermal expansion for ferrite steels over a temperature range of 90 to 650°C (194 to 1202°F). The coefficient of expansion for steel does not vary linearly but increases as temperature increases. Expressed in mm/mm/°C (in./in./°F), the coefficient of expansion $\alpha$ is $11 + 0.0036\theta$ millionths ($6.1 + 0.0020\theta$ millionths), where $\theta$ is the temperature. The perlite-austenite transformation of steel, which occurs at about 700 to 850°C (1292 to 1562°F), is accompanied by contraction.

Anderberg et al [8] presented information on the thermal expansion for three German reinforcing steels [9] which showed that expansion is nearly linear to a temperature of 675°C (1247°F) for these steels. Between 300 and 675°C (572 and 1247°F), lower expansion values were obtained for prestressing steel than for hot-rolled or cold-twisted reinforcing steels.

## Modulus of Elasticity

In designing fire-resistive structures, it is important to consider the effects of elevated temperatures on the modulus of elasticity of materials. Such information is available for several types of concretes and steels.

*Concrete*—Values for modulus of elasticity of concrete made with three types of aggregates are shown in Fig. 4 [10]. All three concretes experienced a rapid loss in elastic modulus as temperature increased. At 200°C (392°F),



FIG. 2—*Effect of load levels on concrete deformation* [5].



FIG. 1—*Thermal expansion of concrete* [2].

14

the modulus is from 70 to 80 percent of the room temperature value. At 400°C (752°F), the modulus is from 40 to 50 percent of the original value. Data were obtained by Cruz [10] by an optical method. From these data, it appears that aggregate type and concrete strength do not significantly affect moduli at high temperatures.

Anderberg and Thelandersson [5] obtained information on the modulus of elasticity for a concrete having similar properties as the siliceous-aggregate concrete used by Cruz. Their results agree well with these shown in Fig. 4 for the siliceous aggregate concrete.

Philleo [3] obtained values for modulus of elasticity of a carbonate-aggregate concrete using a dynamic method. His results agree closely with those obtained by Cruz [10] up to about 375°C (707°F). From 375 to 650°C (707 to 1202°F), Philleo obtained higher values. Harmathy [11] and Saeman and Washa [12] determined modulus of elasticity in compression and found little change up to about 200°C (392°F).

Steel—Modulus of elasticity of steel decreases with increasing temperature [7,13] (shown in Fig. 5). The modulus for ferrite steels decreases linearly with temperature to about 500°C (932°F). Above this temperature, the modulus decreases more rapidly. This relationship is also representative of hot-rolled alloyed bars used in prestressed concrete.

Anderberg [8,14] reported modulus of elasticity data for cold-drawn steel. From the data, it appears that the modulus of cold-drawn steel is lower by as much as 20 percent than that of hot-rolled steel over a temperature range of 20 to 700°C (68 to 1292°F).

Pettersson et al [15] gives the modulus of elasticity (secant modulus) as a function of steel temperature for different values of the ratio of steel stress to yield stress at room temperature. His curves show that the modulus of elasticity generally decreases as the ratio of stress to yield stress at room



FIG. 5—Modulus of elasticity of steel [7].
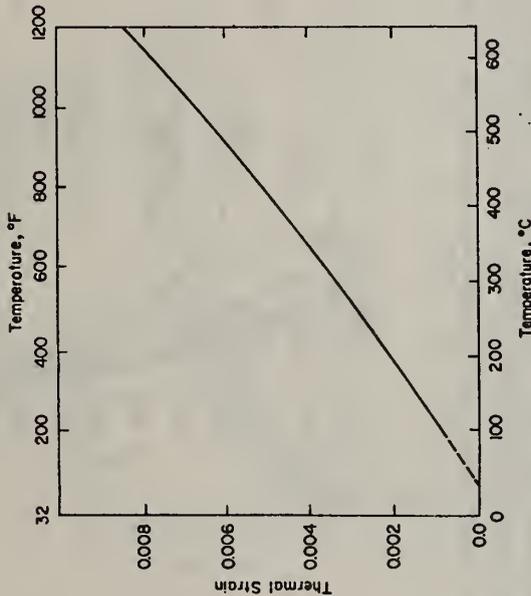


FIG. 3—Thermal expansion of ferrite steels [7].
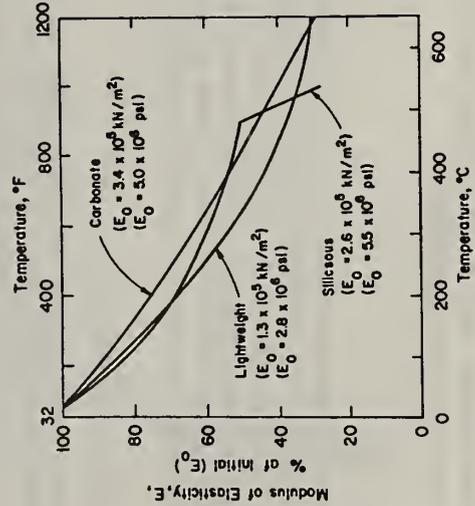


FIG. 4—Modulus of elasticity of concrete [10].

15
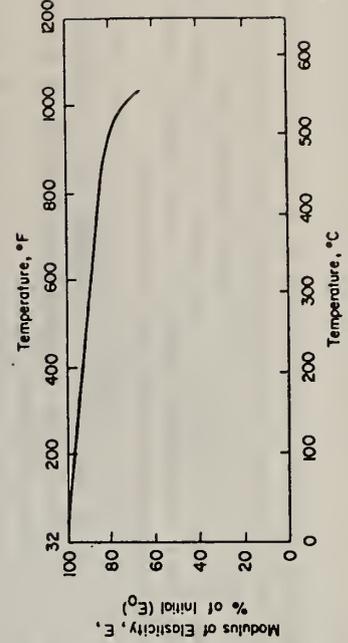
temperature increases. Also, as this ratio increases, the elastic modulus begins to decrease at lower temperatures.

### Poisson's Ratio

Information is given on the effect of elevated temperature on Poisson's ratio only for concrete. Philleo [3] and Cruz [10] reported results on Poisson's ratio for various concretes at elevated temperatures. Although Philleo indicated a decrease in Poisson's ratio with increasing temperature, both he and Cruz pointed out that results were erratic and no general trend of temperature effects on Poisson's ratio clearly was evident.

### Stress-Strain Relationships

Stress-strain information for inorganic materials has become more important in prediction of behavior of structures both during and after fires. Information is presented for concrete, steel, and concrete masonry materials.

*Concrete*—Kordina and Schneider [16] studied the stress-strain response of normal-weight concretes at variable temperatures under a number of loading conditions. More recently, Anderberg and Thelandersson [5] presented additional information on stress-strain relations of concrete at different temperatures. This information is shown in Fig. 6. Tests were con-
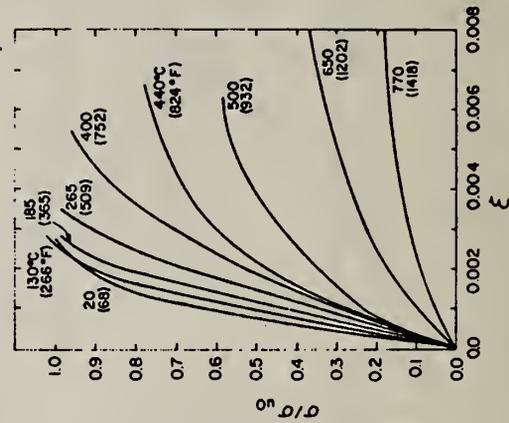
FIG. 6—*Stress-strain relations for different temperatures* [5].

---

ducted on specimens conditioned at 65 percent relative humidity and 20°C (68°F) that were heated without any load. A short-duration loading was used. Curves in Fig. 6 show that with increasing temperature ultimate stress decreases and ultimate strain increases. From each stress-strain curve, three characteristic parameters can be defined: elastic modulus, ultimate compressive strength, and ultimate strain.

*Concrete Masonry*—Complete data between 25 and 760°C (77 and 1400°F) on stress-strain relationships in compression of a lightweight masonry concrete (expanded shale aggregate) were reported by Harmathy [11]. Some of the data are shown in Fig. 7.

*Steel*—Stress-strain relationships for several types of steel have been reported by Harmathy and Stanzak [17]. Curves for ASTM A36 steel are shown in Fig. 8. Figure 9 shows a family of stress-strain curves for ASTM A421 prestressing steel. Curves were obtained utilizing a normal strain rate during test. Stress-strain curves for these steels were also obtained in tests using slow and fast strain rates.

### Creep

To describe the high temperature behavior of reinforced concrete, steel, and other inorganic materials, short-term creep characteristics of these materials must be known. Creep information for steel has been available
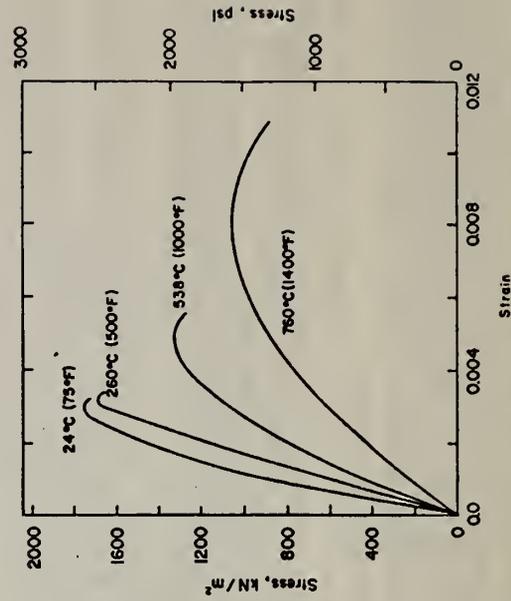
FIG. 7—*Stress-strain curves for lightweight masonry concrete at various high temperatures* [11].

for some time. Only recently has this type of strain information become available for concrete. Little information is available for other inorganic materials used in buildings.

*Concrete*—Some data on creep at high temperatures of a carbonate aggregate concrete were reported by Cruz [18]. Figure 10 shows data graphically for a 5-h test period. After heating to test temperature, a load equal to 45 percent of room-temperature strength of the concrete was maintained during the test period. For this concrete, creep increased with temperature only moderately to 320°C (608°F). Above this point, the increase in creep was much greater. Mukaddam and Bresler [19] and Mukaddam [20] also conducted experimental and theoretical studies on creep of concrete at variable temperatures. Nasser and Neville [21] reported that age, moisture conditioning, type and strength of concrete, and stress-strain ratio affect creep of concrete at high temperatures.

More recently, Anderberg and Thelandersson [5] conducted creep measurements on concrete under sustained load at constant temperature. In these tests, the unloaded specimen was heated to about 400°C (752°F) while the thermal expansion developed. The load was applied after the temperature reached equilibrium, sustained during 3 h, and then removed. The test was terminated by cooling the specimen which gave rise to a decrease in strain. The time-dependent creep strain under the sustained load and temperature was small compared to the thermal expansion.



FIG. 10—*Creep of a carbonate aggregate concrete at various temperatures* [18] (*applied stress = 12.42 MN/m² (1800 psi), $f_c'$ = 27.6 MN/m² (4000 psi).*
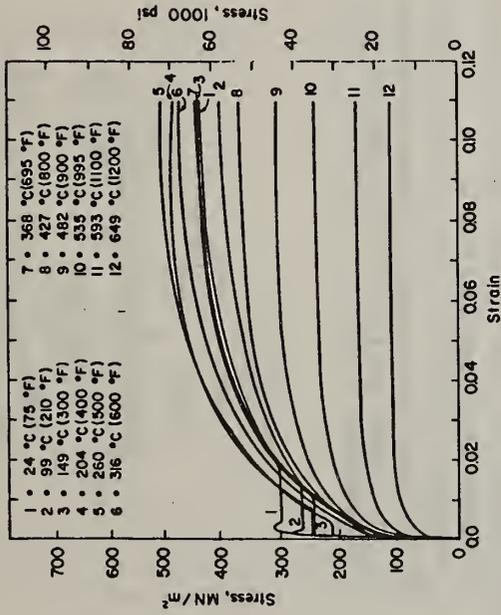


FIG. 8—*Stress-strain curves for an ASTM A36 steel* [17].
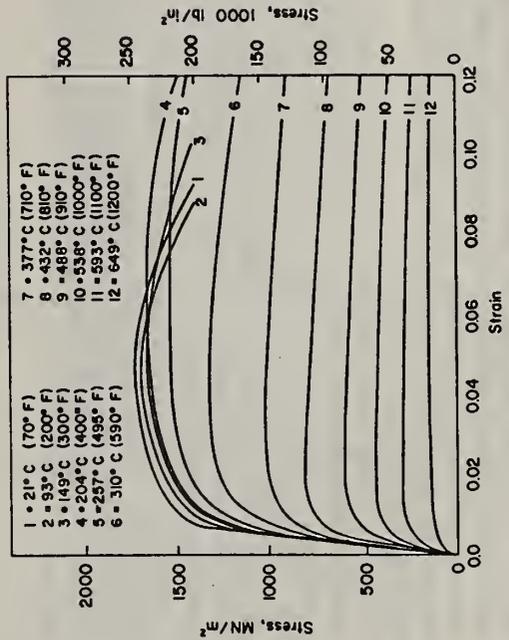


FIG. 9—*Stress-strain curves for an ASTM A421 steel* [17].

FIG. 12—*Effect of temperature and stress level on creep* [5].

Harmathy showed [23,24] that the creep strain can be satisfactorily described by the following equation

$$\epsilon_t = \frac{\epsilon_{to}}{\ln 2} \cosh^{-1}(2^{Z\theta/\epsilon_{to}}) \qquad (2)$$

where

$\epsilon_t$ = creep strain, mm/mm (in./in.),
$Z$ = Zener-Hollomon parameter, h$^{-1}$, and
$\epsilon_{to}$ = (unnamed) creep parameter, mm/mm (in./in.).

$Z$ and $\epsilon_{to}$ are dependent upon the applied stress only (independent of temperature). Their meaning is explained in Fig. 13, which also shows the three periods of creep. From a practical point of view, the secondary creep is the most important (Eq 2 for $\epsilon_t$ does not cover the tertiary creep).

Values of $\Delta H/R$ for three important steels were given by Harmathy and Stanzak [17]. Numerical techniques have been reported [15,24,25] that apply creep information to the calculation of deflection history of joists and beams during fire exposure.

A significantly different behavior was observed when the same load was applied before the temperature rise. When the temperature rise took place under the sustained load, thermal expansion was prevented to a degree that only partly can be attributed to the change in stress-strain relationship and the development of creep. The complete course of events for these two types of tests is shown in Fig. 11.

Figure 12 shows creep information for two stress levels and several different temperature levels for a 3-h period. From these data it appears that creep plays a very limited role in the overall behavior of concrete except when the temperature is above 400°C (752°F). The authors worked out an equation for creep after 3 h as affected by stress and temperature when these two parameters are held constant. The expression also takes into account the influence of time.

*Steel*—In high temperature processes, the time-dependent nonrecoverable (plastic) unit deformation of steel is referred to as creep strain. When dealing with fire problems, it is convenient to express creep strain according to Dorn's concept [22] in terms of a "temperature-compensated time" defined as

$$\theta = \int_0^t (e^{-\Delta H/RT}) dt \qquad (1)$$

where

$\theta$ = temperature-compensated time, h,
$t$ = time, h,
$\Delta H$ = activation energy of creep, cal/g mole (Btu/lb mole),
$R$ = gas constant, cal/g mole K (Btu/lb mole °$\overline{R}$), and
$T$ = temperature, K (°$\overline{R}$).

18



FIG. 11—*Measured total strain as a function of time* [5] (*load applied during heating in curve 2*).

FIG. 13—*Interpretation of creep parameters and three periods of creep* [21].

Further simplifications to Harmathy's creep model were made by Plem [26] and Anderberg [8,14].



FIG. 14—*Compressive strength of carbonate aggregate concrete at high temperature and after cooling* [27].



FIG. 15—*Compressive strength of siliceous aggregate concrete at high temperatures and after cooling.* [27].

## Strength

Information on the effect of elevated temperature on strength properties of inorganic materials has been available in the literature for a number of years. Some information for several materials is summarized in the following paragraphs.

*Concrete*—Figures 14, 15, and 16 [27] show the compressive strength of concretes made with different types of aggregates. Specimens heated to test temperature with no superimposed load and tested hot are designated as "unstressed." Strengths of specimens heated while stressed to $0.4f_c'$ and then tested hot are designated as "stressed to $0.4f_c'$," where $f_c' = 28$-day moist cure compressive strength. The "unstressed residual" strengths were determined from specimens heated to test temperature, cooled to room temperature, stored at 75 percent relative humidity for 6 days, and then tested in compression.

Abrams [27] found that applied stress levels during heating of 0.25 to 0.55 $f_c'$ had little effect on the strength obtained. He also noted that original concrete strength between 27 600 and 44 800 kN/m² (4000 and 6500 psi) had little effect on the percentage of strength retained at test temperature. In Fig. 16, the "unstressed" sanded specimens were made with sand replacing 60 percent of the lightweight fines, by volume. The unsanded lightweight concrete was the kind used in the manufacture of masonry block.

19

maximum at about 300°C (572°F). Strength then decreased as the temperature continued to increase. Generally, the concrete stressed to $0.3f'_c$ during heating had higher strengths than unstressed concrete. With exception of the initial decrease in strength, results obtained by Kordina approximated those obtained by Abrams [27] for lightweight concrete.

Few results have been reported of tests to determine tensile strength under elevated temperature. Figure 17 shows the effect of temperature on split-cylinder tensile strength of a siliceous aggregate concrete. These tests were conducted in Sweden [5,8,35].

Steel—The influence of temperature on strength of certain steels are shown in Fig. 18. Included are data on yield-strength of structural steels [36] and ultimate strengths of cold-drawn steel [37,38] and high-strength alloy bars [39,40]. In these tests, specimens were heated unloaded and then stressed under elevated but constant temperature to failure. Generally, strengths of steel decreased with increasing temperature. Strength of hot-rolled steels are often slightly higher than at room temperature up to about 260°C (500°F). In Germany [34] considerable differences in ultimate tensile strength have been found between hot-rolled and cold-drawn reinforcing steel of the same original strength when subjected to the same test conditions [8].

Information on the decrease of yield strength caused by heating of four reinforcing steels and information on the decrease of tensile strength due to heating of four prestressing steels are given in Ref 8.

Thermal Conductivity, Thermal Diffusivity, and Specific Heat—The thermal properties of building materials are required to calculate heat flow through materials and determine temperature distribution. Not only is this information required to predict performance of the structure, but also to determine fire severity in the compartment. Harmathy [41] pointed up that structural performance of a building and fire severity depend on the thermal properties of the boundary or lining materials. To understand
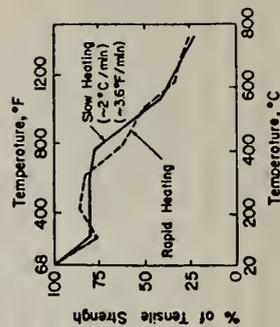


FIG. 17—*Effect of temperature on split-cylinder tensile strength of a siliceous aggregate concrete* [8].



FIG. 16—*Compressive strength of lightweight concrete at high temperature and after cooling* [27].

Several investigators [5,8,28,29] reported results of tests made on samples of siliceous aggregate concretes heated without mechanical stress and loaded when the maximum temperature had been reached. Test results obtained showed similar trends. However, lower values of the compressive strength were obtained by some investigators.

In the results reported by Abrams [27] the "stressed" strengths are higher than the "unstressed" strengths. Anderberg and Thelandersson [5] obtained similar results for a siliceous aggregate concrete. Abrams [27] also found that the "unstressed residual" strengths were lower in all cases than strengths determined by the other two procedures.

Harmathy and Berndt [11] reported data on compressive strength of cement paste and a lightweight concrete. Tests were conducted on specimens held at target temperature with no load for periods of 1 to 24 h. Further data on the strength of concrete at high temperatures have been recorded by Saeman and Washa [12], Malhotra [28], Zoldners [30], Binner et al [31], and Weigler and Fischer [32,33].

Recently, Kordina et al [34] reported the compressive strength at elevated temperature of a lightweight concrete made with expanded clay aggregate. Some tests were conducted in the "unstressed" condition with no load applied during heating. Other tests had a load equal to $0.3f'_c$ applied during the heating period.

For both conditions of loading, strength decreased as the temperature increased to about 165°C (329°F). Strengths then increased and reached a

20

FIG. 19—*Thermal conductivity for granite aggregate concrete under heating and subsequent cooling* [8,9].

conductivity results are shown for a granite aggregate concrete heated to different maximum temperature levels [8,9].

A method for the calculation of the thermal conductivity of all concretes up to 982°C (1800°F) has been presented by Harmathy [45]. He defined four concretes: Nos. 1 and 2 represent limiting cases, from the point of view of thermal properties, among normal-weight concretes, and Nos. 3 and 4 among lightweight concretes. Thermal conductivities of concretes, together with some experimental data, are shown in Fig. 20.

Carman and Nelson [46] determined thermal conductivity and diffusivity of a carbonate aggregate concrete between 49 and 199°C (120 and 390°F). Anderberg [43] gives thermal conductivity information of a quartzite aggregate concrete. The thermal conductivity was determined by the Stalhane Pyk's Method [47]. Schneider and Haksever [8,48] developed data on the diffusivity of a siliceous aggregate concrete at high temperature. This information is shown in Fig. 21.

The specific heat of various concretes was studied by Harmathy [6,45]. Typical ranges for the "volumetric specific heat" (product of specific heat and density) for normal weight and lightweight concrete are shown in Fig. 22. Odeen [9] also studied the volumetric specific heat of concrete over a temperature range of up to 982°C (1800°F). Collet and Tavernier [49] studied the variation of the specific thermal capacity as a function of temperature for three different types of concrete made with gravel, limestone, and lightweight aggregates, as shown in Fig. 23. It can be observed that the specific thermal capacity increases slowly with increasing temperature. Also, the type of aggregate has only a small influence on this factor.

*Concrete Masonry*—Information on the thermal conductivity, thermal diffusivity, and specific heat of 16 masonry unit concretes for a temperature
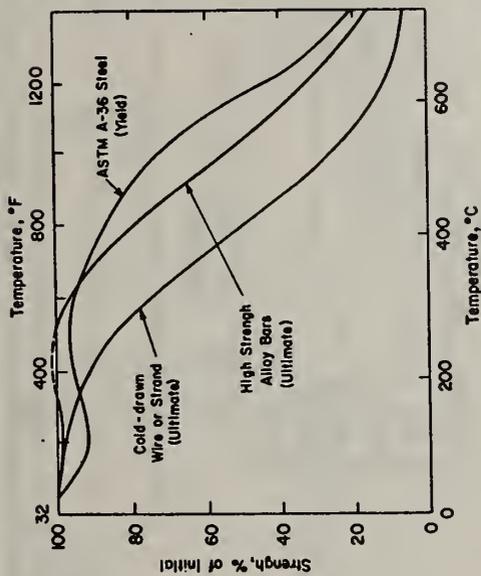
FIG. 18—*Strength of certain steels at high temperature* [36,37,39].

this, imagine that experimental fires are set in two rooms. Each room contains the same amount of combustibles and are identical in every respect, except that one room is lined with poor, the other with good noncombustible insulating materials. Obviously, the temperature in the room lined with good insulation will climb higher, and the fire will appear to be more severe than in the other room. Yet, because of the lesser penetration of heat into the boundary elements, structural damage is less likely to occur in this room.

Over the past 15 or 20 years, thermal property information has been developed for a number of important inorganic building materials. Harmathy [42] developed a variable state method by which all three thermal properties can be determined from a single measurement. Some thermal property information for concrete, concrete masonry, and other inorganic materials are presented.

*Concrete*—Anderberg [43] pointed up that test results on thermal properties may differ considerably from one laboratory to another, even at room temperature. This is shown in a paper by Collet [44]. Test results from four different laboratories on three different types of concrete were studied. In some instances, the results on identical specimens varied by more than 70 percent. Anderberg [43] also pointed up that thermal conductivity is usually taken as invariant with respect to direction of heat flow. He and other investigators found that thermal conductivity decreases with increasing temperature. However, during subsequent cooling, the change is not reversible. This is illustrated in Fig. 19, where thermal

21

FIG. 22—*Volumetric specific heats of normal weight and lightweight concretes* [6,45].



FIG. 23—*Specific thermal capacity for different types of concrete* [49].

FIG. 20—*Thermal conductivity of four "limiting" concretes and some experimental thermal conductivity data* [45].



FIG. 21—*Thermal diffusivity of siliceous aggregate concrete* [8,48].

range of 20 to 675°C (68 to 1247°F) was reported by Harmathy and Allen [5].

*Steel*—Some thermal properties of steel are shown in Fig. 24 [50].

*Other Materials*—Information on the effects of temperature on the volumetric specific heat and thermal conductivity of brick and gypsum have been reported by Harmathy [51]. Thermal property information has been developed for other inorganic materials [52]. For mineral fiber ceiling tile over a temperature range of from 20 to 700°C (68 to 1292°F), the thermal conductivity varied from (3.8 to 13.9) × 10⁻³ W/mK [(2.2 to 8.0) × 10⁻³ Btu/ft h°F]. Over the same temperature range, the thermal

diffusivity varied from (1.21 to 2.76) × 10⁻⁷ m²/s [(4.69 to 10.70) × 10⁻³ ft²/h]. The specific heat varied from 760 to 1149 J/kgK [(1.82 to 2.75) × 10⁻¹ Btu/lb°F].

Asbestos-board products had the following thermal properties over a temperature range of 22 to 300°C (72 to 572°F): thermal conductivity, 0.148 to 0.814 W/mK [(8.55 to 47.05) × 10⁻² Btu/ft h°F]; thermal diffusivity, (2.202 to 0.407) × 10⁻⁶ m²/s [(7.83 to 15.77) × 10⁻³ ft²/h]; and specific heat, 869 to 1205 J/kgK [(2.08 to 2.88) × 10⁻¹ Btu/lb°F]. The density of the asbestos material varied from 700 to 1790 kg/m³ (43.7 to 111.7 lb/ft³). "Gyproc" gypsum wallboard had the following thermal

be used for 1, 2, or 3 dimensional heat flows. In addition, the program can handle composite materials, such as reinforced concrete.

Temperature distribution information has been developed for concrete members made with different types of concrete. Some typical distributions are given for concrete slabs, beams, and tapered sections.

*Slabs*—Temperature distributions in flat slabs at selected distances from the exposed surface during fire exposure are shown for structural concretes made with siliceous, carbonate, and lightweight aggregates in Figs. 25, 26, and 27, respectively [8,55-57]. Similar information is available for other types of concrete and for combinations of materials. Slab thickness does not significantly affect temperatures in the materials except for very thin slabs or when the temperatures are less than 200°C (392°F).

Temperatures within flat slabs made of lightweight insulating concretes in three density ranges are shown in Figs. 28, 29, and 30 [58].

*Beams*—Temperature distributions within rectangular beams and tapered sections are considerably different than those obtained for flat slabs. Temperatures within beams are affected not only by width of the beam, but also by distance from the fire surface. Temperature distributions are strongly influenced by the fact that three faces of the beam are usually exposed to the fire.

FIG. 25—*Temperatures within slabs during fire tests—siliceous aggregate concrete* [8,55-57].

FIG. 24—*Thermal properties of steel.* [50].

properties over a temperature range of 33 to 337°C (91 to 639°F): thermal conductivity, (1.6 to 2.1) × 10⁻⁵ W/mK [(9.25 to 12.14) × 10⁻⁶ Btu/ft h °F]; thermal diffusivity, (1.9 to 2.4) × 10⁻⁷ m²/s [(7.36 to 9.30) × 10⁻³ ft²/h]; and specific heat at 33°C (91°F) 1.43 × 10³ J/kgK (0.34 Btu/lb°F). The density of this wallboard was 722 kg/m³ (4.5 × 10³ lb/ft³).

Estimates of the thermal properties of neat gypsum plaster, gypsum-perlite plaster, and gypsum-vermiculite plaster were reported by Ryan [53].

Data developed in Europe for several materials are given in Ref 15.

## Temperature Distributions

To use high temperature property information for various building materials in predicting performance, it is necessary to know the temperature distribution in the members of a structure exposed to fire. Due to the transient nature of fire, various parts of the structure usually will be at different temperatures. Temperature distribution information has been obtained for various steel and concrete members of various sizes and thicknesses. Different concretes were used in many tests.

In addition to the experimental work, calculation methods have been developed for determining temperature distributions in building members.

## Concrete

Iding et al [54] developed a computer program for calculating temperature distribution in various types of concrete members. The program can

FIG. 26—*Temperatures within slabs during fire tests—carbonate aggregate concrete* [8.55-57].

Gustaferro and Martin [56] show temperatures along the vertical center-lines of beams 76.2 to 254.0 mm (3 to 10 in.) wide for exposure periods ranging for ½ to 4 h. Data were developed from results of fire tests of prestressed stemmed units at Underwriters Laboratories and of beam and joist sections tested at the Portland Cement Association [59]. Using the temperatures along the vertical centerline, the authors developed a method to estimate temperatures throughout the cross section by constructing isothermal diagrams. This method is outlined in Ref 56.

Temperature distributions in normal-weight concrete ribs and beams are shown in Figs. 31 to 36 [57]. These graphs were developed from information given in Ref 56. From these graphs, temperatures within the concrete member ranging in thickness from 100 mm (3.94 in.) to over 300 mm (11.81 in.) can be determined for fire exposure times from 1 to 4 h. For lightweight aggregate concrete, it is suggested that the distance from an exposed surface of the temperature, °C, corresponding to the distance from an exposed surface obtained from Figs. 31 to 36, be reduced by 20 percent.

Much of the temperature distribution information for beams resulted from a test program in which 32 rectangular "T" beam specimens were tested [59]. Beams were 406.4 mm (16 in.) deep and had widths from

24
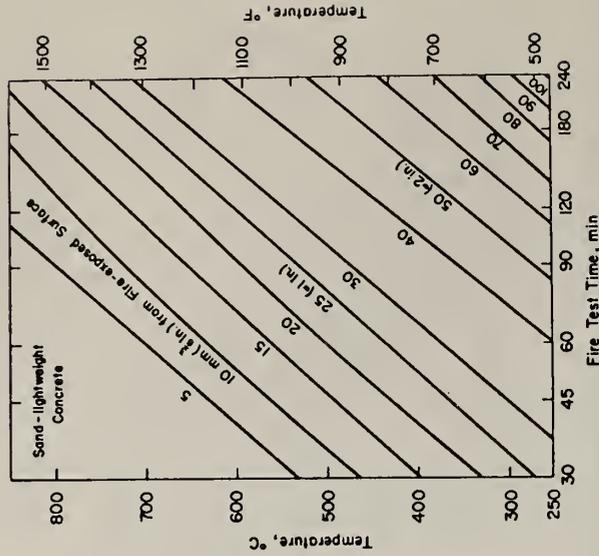
FIG. 27—*Temperatures within slabs during fire tests—sand lightweight concrete* [8.57]. *(A concrete using lightweight coarse aggregate and natural sand fine aggregate.)*

50.8 to 609.6 mm (2 to 24 in.). Several types of aggregates were included in the test program. All specimens were exposed to ASTM Fire Tests of Building Construction and Materials (E 119). Representative temperature distributions for a 304.8-mm (12-in.)-wide normal-weight concrete rectangular unit at fire exposure times of 1 and 3 h are shown in Figs. 37 and 38, respectively. Similar distributions for selected exposure periods have been prepared for all 32 beams of the test program.

In addition to this test program, a computer program has been prepared using a finite difference solution of the transient heat-flow problem [59]. Calculated isothermal distributions using the computer program closely approximate those obtained experimentally. The program accommodates nonrectangular geometries, such as tapered sections, and exposures different from the standard fire.

*Double Tee Units*—Odeen [9] investigated the temperature distribution in double "Ts" during fire tests. Temperatures within 8 sizes of double "Ts" have been calculated at ½, 1, 1½, and 2 h of fire exposure.

*Columns*—A numerical technique was developed by Lie and Harmathy [60] by which the temperature distribution in concrete-protected steel columns was analyzed. Lie and Allen [61] studied the temperature distribu-
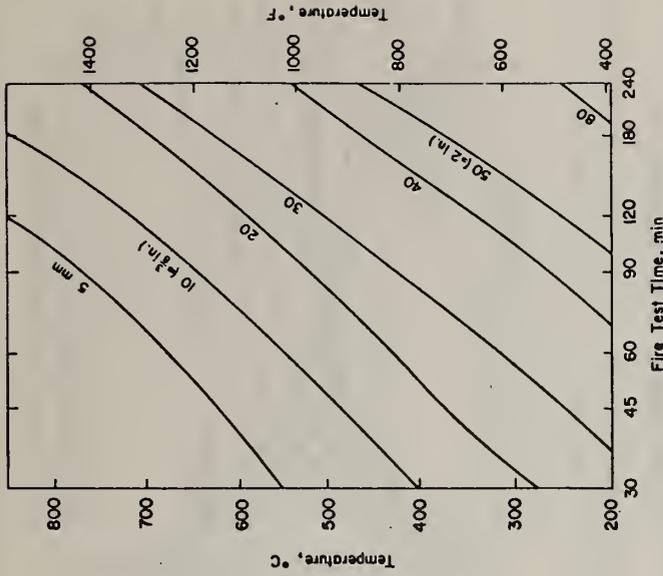
FIG. 29—*Temperature within lightweight insulating concrete slabs during fire tests.* 800 to 960 kg/m³ (50 to 60 lb/ft³) [58].

### Concrete Masonry

Harmathy [64] performed an extensive series of computer calculations to study heat flow during fire tests of masonry walls. Calculations take into account geometry of the unit, concrete type, temperature dependent thermal properties, and heat flow mechanisms. Figure 42 shows the calculated temperature distribution in a masonry unit at time of its thermal failure (2.11 h). The masonry unit is of a lightweight expanded shale concrete, having an overall thickness of 203.3 mm (0.667 ft), a face-shell thickness to overall thickness ratio of 0.167, and a web thickness to face-shell ratio thickness of 0.5.

### Steel

Graphical displays of temperature distributions in structural steel members are not readily available. Temperatures within steel members are influenced by a number of factors, including geometry, size of the member, and type of protection.
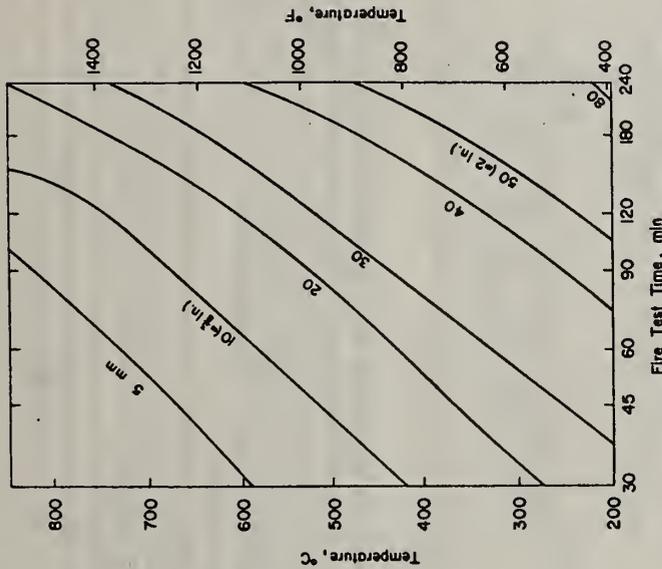
FIG. 28—*Temperature within lightweight insulating concrete slabs during fire tests, 320 to 480 kg/m³ (20 to 30 lb/ft³)* [58].

tion in solid concrete columns during fire. Similar studies were also conducted by Iding et al [54].

*Spray-Applied Coatings*—If the fire-exposed surface of a concrete member is coated with an insulating material, lower temperatures result within the concrete member. Abrams and Gustaferro [62] developed data on the effect of three types of insulating materials: sprayed mineral fiber (SMF), vermiculite-type cementitious material (VCM), and intumescent mastic (IM), on the temperature within the concrete member. Data are given in Fig. 39 in terms of equivalent concrete thickness. These data can be converted to temperatures by use of some of the other figures in this report.

Figures 40 and 41 show temperature distributions along the centerlines in carbonate aggregate concrete joists, 101.6 mm (4 in.) wide by 406.4 mm (16 in.) high, coated with 12.7 or 6.4-mm (½ or ¼-in.) spray-applied material. The materials used were vermiculite type MK (VMK), and sprayed mineral fiber (SMF). These tests were made at the Portland Cement Association [59]. The coating materials are described in Ref 63.

25

FIG. 31—*Temperature distribution in a normal weight concrete rib or beam—100 mm wide beam* [57].
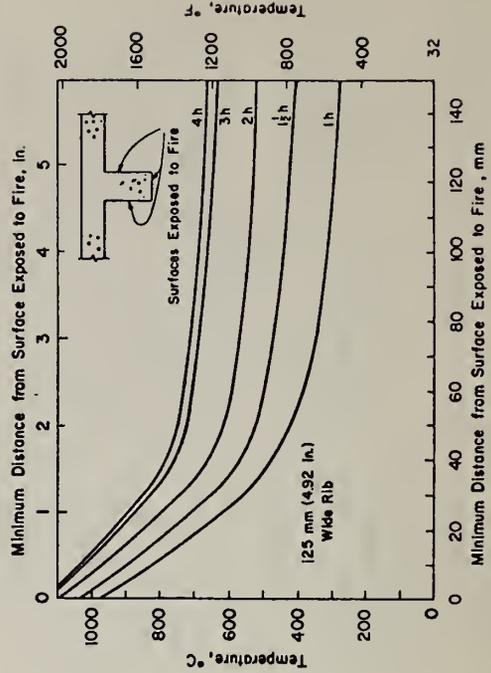


FIG. 32—*Temperature distribution in a normal weight concrete rib or beam —125 mm wide beam* [57].



FIG. 30—*Temperature within lightweight insulating concrete slabs during fire tests, 1120 to 1280 kg/m³ (70 to 80 lb/ft³)* [58].

Bletzacker [65] determined the temperature distribution for a 12WF27 wide-flange protected steel beam. This information is given in Fig. 43. The beam was protected with 22.2-mm (7/8-in.) Type MK fire insulation and a spray-applied vermiculite cementitious mixture, and supported a 101.6-mm (4-in.)-thick by 914.4-mm (36-in.)-wide concrete slab cast on a 22-gage steel deck.

Calculation methods have been developed for determining the temperature distributions in protected and unprotected steel members. Lie and Harmathy [60] developed a numerical procedure to calculate the temperature of protected steel columns exposed to fire. Lie [66] described a procedure based on a finite-difference method for calculating the temperature history of fire-exposed protected steel columns with rectangular cross-sections. The method also is suitable for calculation of temperatures in monolithic building components such as solid concrete columns, beams, and walls. It can also be used for the calculations of temperatures of any system in which a perfect conductor or well-stirred fluid is enclosed in an encasement, such as water-filled hollow steel columns or beams, and exposed to a

26

FIG. 33—Temperature distribution in a normal weight concrete rib or beam—150 mm wide beam [57].



FIG. 34—Temperature distribution in a normal weight concrete rib or beam—200 mm wide beam [57].



FIG. 35—Temperature distribution in a normal weight concrete rib or beam—250 mm wide beam [57].
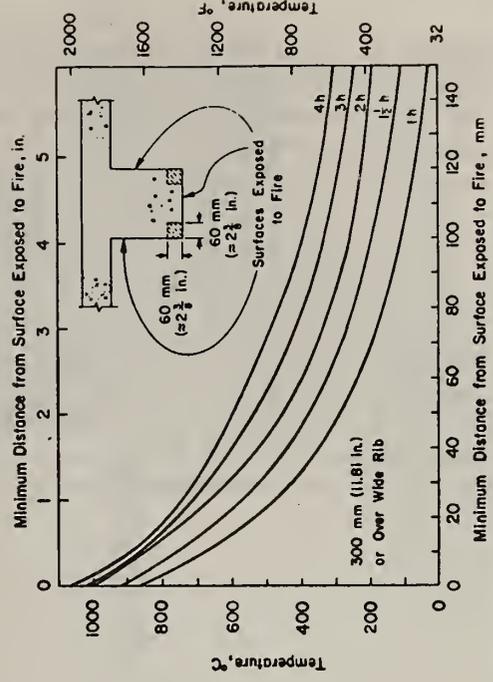


FIG. 36—Temperature distribution on a normal weight concrete rib or beam—300 mm wide beam [57].

FIG. 38—*Temperature distribution in normal weight rectangular unit at 3 h of fire exposure* [59].
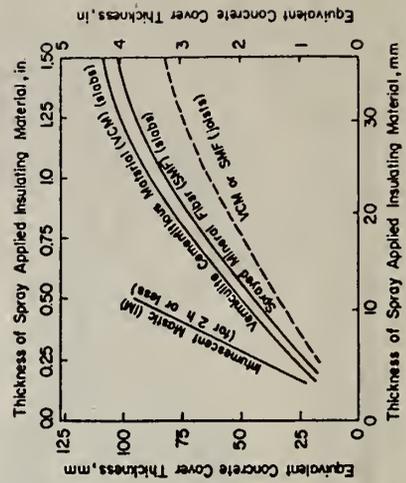


FIG. 39.—*Equivalent concrete cover thickness for spray-applied coatings* [62].

FIG. 37—*Temperature distribution in normal weight rectangular unit at 1 h of fire exposure* [59].

radiative heat source of varying temperature. Stanzak and Lie [67] presented temperature distribution information on unprotected square solid steel columns.

## Estimating and Predicting Fire Performance

In Ref 57, it is pointed up that a number of different approaches can be used to estimate or predict the fire resistance of a structure. Among these are: application of fire resistance test data, use of tabulated data on important parameters derived from tests, use of rules and design aids based on test data, and analytical techniques based on test data and other research studies. By the use of analytical techniques, it is possible to estimate the fire severity, heat transfer, and change of material properties. Also, analytical techniques are available to perform a structural analysis of a component or the structure in its altered condition. Use of these different approaches to estimate or predict the fire resistance of structural members made with inorganic materials is discussed.

FIG. 41—Temperature along vertical centerlines at various fire exposures for 101-mm-wide rectangular units coated with SMF [59].
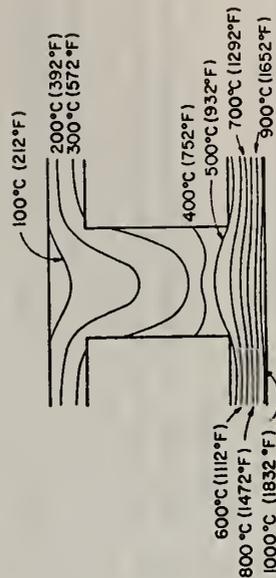


FIG. 42—Temperature distribution in a masonry unit at the time of its thermal failure [64].

FIG. 40—Temperature along vertical centerlines at various fire exposures for 101-mm-wide rectangular units coated with VMK [59].

## General

Over the past 50 years, thousands of fire tests have been conducted on all types of inorganic materials and combinations of those materials. Most of the tests were conducted to satisfy some particular regulatory requirement. The most comprehensive document containing fire test results of many inorganic materials and combinations of materials for various structural members such as beams, columns, floors, roofs, walls, and partitions is the *Fire Resistive Directory* [68]. The *Directory* is updated every year. Another comprehensive document containing fire test results is published by the American Insurance Association [69]. This document contains fire resistance classifications for various materials of beams, girder and truss protections, ceiling constructions, column protections, floor and ceiling constructions, roof constructions, and walls and partitions. This document also is updated annually.

Other documents containing fire tests results are more restrictive in that one inorganic material is used to provide fire resistance for the elements of the building. One such document is the *Fire Resistance Design Manual* [70]. Designs in this manual utilize gypsum products to provide fire resistance

29

usual methods of structural mechanics often can be applied to predict structural performance. Some examples of the use of this rational design approach for concrete, concrete masonry, and steel are given.

### Concrete Construction

Design information for estimating or predicting fire performance of concrete members or structures can be broadly divided into two classes. Part of the information is oriented to determine the requirements for performance in fire, based on the heat-transmission characteristics of the materials. Usually this relates to the unexposed surface temperature criteria given in ASTM Test E 119. The other part of the information relates to prediction of structural performance of concrete members or buildings.

*Heat Transmission Approach*—In designing a concrete member for a specific fire-resistance period, all applicable end-point criteria must be satisfied. One of these criteria relates to an average temperature rise of 139°C (250°F) on the unexposed surface of the member. The rate at which the temperature will rise on the unexposed surface is directly a function of the heat-transmission characteristics of the material.

Information has been published on single-course slabs and multicourse assemblies. Shown in Fig. 44 are data reported by Abrams and Gustaferro [55] and Gustaferro and Martin [56]. Curves in the figure can be used

FIG. 44—*Fire endurance (heat transmission) of concrete slabs as a function of thickness— interpolation for varying concrete unit weights is reasonably accurate [55,56].*
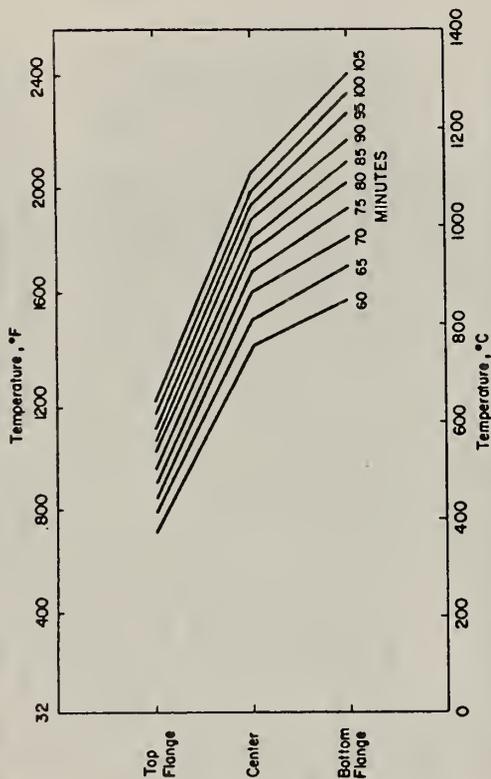
FIG. 43—*Idealized temperature distribution in cross section of protected steel beams [5].*

for walls, partitions, floor-ceilings, columns, beams, and roof decks. Another document of the latter type is Technical Note 16 on Brick Construction [71] that gives several designs using brick in combination with other materials.

Often, fire tests results are tabulated in such a manner to give data to satisfy minimum requirements for particular fire resistance classifications. Such an approach lacks flexibility because it does not take into account variations from one situation to another. However, it is widely used. A more useful application of fire test results, and results from special research projects, is to establish relationships between important variables required for determining various fire resistance characteristics. Such relationships for major building materials are presented in many publications. Applications are presented where information contained in some of these graphical design aids is used.

The most comprehensive method for determining fire resistance is the analytical approach. Availability of high temperature property information and temperature distribution information permits a mathematical approach to predicting performance of various members in a building exposed to fire. When the building element is subjected to a time versus temperature exposure during fire, this exposure will cause a predictable temperature distribution in the member. Increased temperatures cause deflections and property changes in the member and in the materials of which it is composed. With a knowledge of deformation and property changes, the
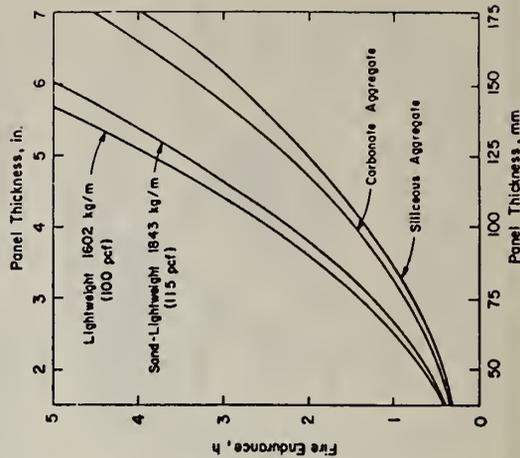
DESIGN OF BUILDINGS FOR FIRE SAFETY

to determine thickness required for a specific fire endurance of four different concretes. Gustaferro and Martin also reported the effect on the fire endurance of 15.9-mm (5/8-in.) gypsum wallboard attached to three different types of concrete with no air space, and a 152.4-mm (6-in.) air space between the gypsum board and concrete. Figure 45 [58] shows the relationship between slab thickness, oven-dry unit weight, and fire endurance for low-density concretes.

Concrete floors and roofs often consist of base slabs, with undercoatings or overlays of other types of concrete or insulting materials. Reference 63 gives results of many fire tests of assemblies consisting of various thicknesses of two materials. Results of some of these tests are shown graphically in Figs. 46 to 49.

*Structural Approach*—Methods for predicting structural performance have been applied to simple and complex situations. Computational methods have been used to analyze floor sections exposed to fire but actually restrained from thermal expansion [72–74]. The behavior of reinforced concrete columns has been analyzed using calculation methods by Lie and Allen [61] and Bizri [75]. In the past few years, the more complex problem of evaluating behavior of reinforced concrete frames in fire environments has been studied by several investigators [76–78].

Anderberg [43] recently completed an experimental and theoretical study of behavior of hyperstatic concrete structures exposed to fire. Although his method is capable of evaluating the detailed structural behavior of reinforced concrete frames exposed to fire, the study is limited to a type of structural member used in his experimental investigation. He studied four separate boundary conditions including simple support, simple support but restrained against axial movement, complete rotational restraint at

both ends and a free axial movement, and complete restraint against rotation as well as axial movement at both ends. The study also took into consideration cooling after the fire. His study illustrated the capability of an analytical procedure or model to predict a quite realistic fire response for hyperstatic concrete structures.

A rational approach for the design for fire resistance of precast, pre-stressed concrete was recently presented by Gustaferro and Martin [56]. Application of a rational design approach is given for simply supported, continuous, and restrained concrete members.

*Simply supported members*—Consider a simply supported concrete slab either conventionally reinforced or prestressed. If a fire is applied to the underside of the slab, the bottom will become hotter and the slab will

31



FIG. 46—*Combinations of base slabs and overlays of normal weight and lightweight concretes* [56,63].



FIG. 45—*Effect of dry unit weight and thickness on fire endurance of low-density concretes* [58].
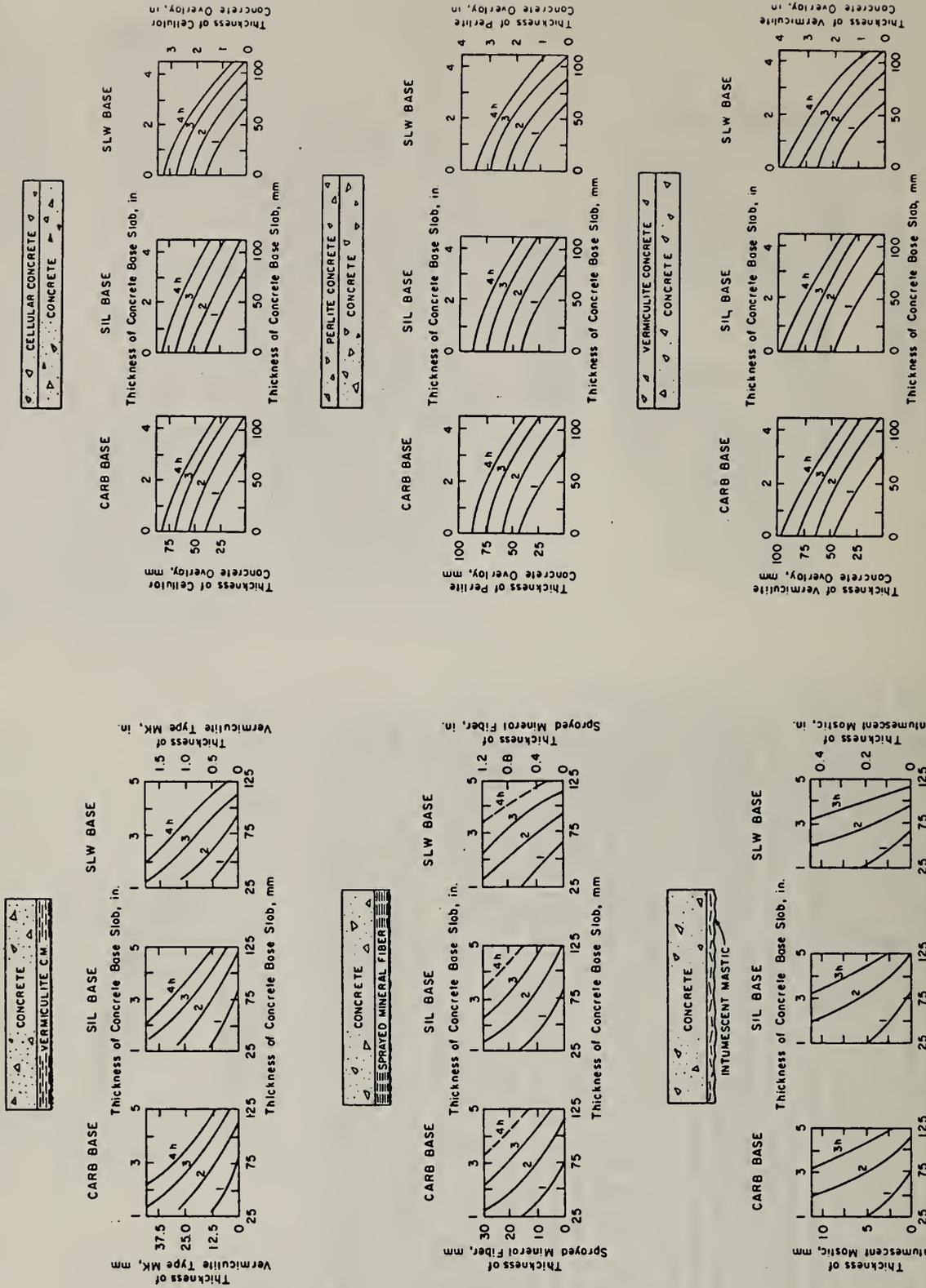
FIG. 48—*Concrete base slabs with overlays of cellular, perlite, and vermiculite concretes* [56,63].
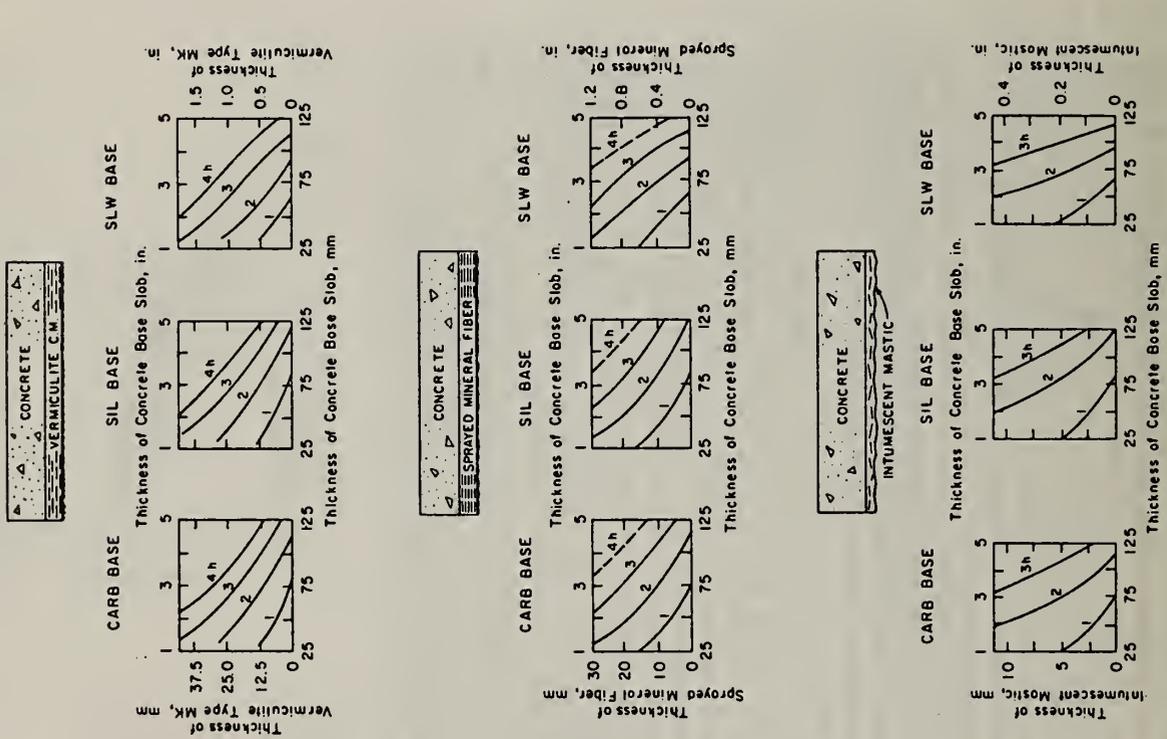
FIG. 47—*Concrete slabs undercoated with vermiculite cementitious material, sprayed mineral fiber, and intumescent mastic* [56,63].

32

$A_{ps}$ = area of the steel,
$f_{ps}$ = stress in the steel at ultimate,
$d$ = distance between the steel centroid and the extreme fiber, and
$a$ = the depth of the equivalent stress block at ultimate.

This formula is from the American Concrete Institute (ACI) Code with the capacity reduction factor equal to 1 [79].

For conventionally reinforced members, $f_{ps}$ is replaced by $f_y$, the stress in the steel at yield.

When the temperature of the reinforcement is increased to a temperature $\theta$, values of $f_{ps}$ and $a$ must be reduced to reflect the new temperature. Then, $M_{t\theta}$ is the residual moment capacity with the steel at temperature $\theta$. During a fire test, a structural end-point will occur when the residual moment capacity is reduced to that of the applied moment.

To verify this behavior, several prestressed concrete slabs were fire tested while simply supported on spans of either 3.66 m (12 ft) or 6.1 m (20 ft) [80]. Load intensity in the test program ranged between 40 and 60 percent of the calculated capacities. Normal weight and lightweight concretes were included in the program. Steel temperatures were monitored during each test. The temperature of the reinforcement when collapse was imminent was used in calculating the residual moment capacity.

A comparison of the residual moment capacity and the applied moments due to the loads is shown in Fig. 50. Values are almost equal indicating that the effect of fire on moment capacity can be predicted.

*Continuous members*—At midspan of a continuous beam, the reinforce-

FIG. 50—Comparison of residual moment capacity and applied moment [80].

FIG. 49—Concrete roof assemblies with mineral board or glass fiber board insulations [56,63].

deflect toward the fire. Temperature of the reinforcement will increase and strength of the steel will decrease. When steel strength approaches steel stress caused by dead and live loads, the steel will yield. As this occurs, deflection of the member will increase rapidly until a flexural failure occurs, usually at midspan.

During a fire, failure of simply supported and axially restrained members is generally by bending. Consequently, the calculation of the moment-capacity is usually sufficient to predict performance. The moment-capacity, $M_t$, of a prestressed concrete beam or slab at normal temperature can be computed from the following equation

$$M_t = A_{ps}f_{ps}\left(d - \frac{a}{2}\right)$$ (3)

where

33

## DESIGN OF BUILDINGS FOR FIRE SAFETY

ment is located near the bottom, while over the support, the reinforcement is located near the top. Assume that this type of construction is repeated for several spans and that a fire occurs beneath one span. As the underside of the beam heats up, the heated span tends to deflect downward. Due to this deflection, the beam tends to rotate over the supports, but since the adjacent spans are continuous, upward deflection is resisted.

During a fire, important changes in moments and moment capacities of a continuous beam occur. The redistribution increases moments over the supports and decreases moments at midspan. The effect of the fire decreases the positive moment capacity much more rapidly than the negative moment capacity. This occurs because top reinforcement on which the negative moment capacity depends is well protected from the fire. For failure to occur, three plastic hinges must form. One will be located at midspan and the other two at adjacent supports. A hinge forms at any section whenever the applied moment equals the moment capacity at that section.

The temperature of the positive reinforcement is the primary index in the behavior of simply supported members exposed to fire, because one hinge is required for failure to occur and no moment redistribution can take place. In the case of continuous members, the temperature at failure is dependent on the moment redistribution capacity and the mechanism for development for the three hinges. Consequently, the fire endurance of a continuous beam is generally much longer than that of a simply supported member, with the same cover thickness.

Effects of continuity were demonstrated in a series of tests simulating simple support, and one and two-end continuity [81]. The simply supported member failed at 80 min, after the fire test started. A similar beam was tested with one end simply supported and the other end continuous. This simulated an exterior span of a structure. The fire resistance was 2 h. A third identical beam tested with both ends continuous had a fire endurance of 210 min.

These test results demonstrate that a broad range of fire resistance can be designed into continuous members through the application of established engineering principles.

*Restrained members*—When a fire occurs beneath an interior portion of a floor or roof slab, the heated portion tends to expand and exert forces on the surrounding cooler slab. The surrounding slab pushes against the heated portion and externally prestresses the slab. The line of action of the thermal thrust or restraint force acts near the bottom of the slab early in the test. Its effect on the capacity of the slab is similar to that of "fictitious reinforcement" located at the line of action of the thrust.

Issen et al [82] showed that the magnitude of thermal thrust, $P$, for a given expansion, varied directly with the heated perimeter and the concrete modulus of elasticity according to the formula

$$\frac{P_1}{P_0} = \frac{s_1 E_1}{s_0 E_0} \tag{4}$$

or

$$\frac{P_1}{A_1 E_1} = \frac{P_0}{A_0 E_0} \frac{z_0}{z_1} \tag{5}$$

where

$z = A/s$ in mm (in.),
$P =$ thrust in kN (lb),
$s =$ heated perimeter in mm (in.)
$E =$ concrete modulus of elasticity in kN/m² (lb/in.²), and
$A =$ cross section area normal to the thrust in mm² (in.²).

Subscripts 0 and 1 refer to the reference specimens described in Ref 82 and the member in question. The magnitude of $P$ for a given member is a function of the expansion.

A set of nomograms that relate thermal thrust, expansion, and heated perimeter for normal weight and lightweight concrete members that are prestressed or reinforced are shown in Fig. 51 [8,56,82]. The thrust and expansion are expressed in the dimensionless parameters $T/AE$ and $\Delta l/l$.

Generally, it is necessary to estimate deflection in the member in design problems involving restraint forces. This can be done by using data developed during fire tests of the reference specimens. Figure 52 [56] represents closely the deflection of the reference specimens in which minimal restraint occurred.

Deflection of the specimen can be calculated by the following formula

$$\Delta_1 = \frac{l_1^2 \Delta_0}{89\,000 y_{bl}} \qquad \Delta_1 = \frac{l_1^2 \Delta_0}{3500 y_{bl}} \tag{6}$$

(SI units)      (English units)

where

$\Delta_1 =$ deflection of specimen in mm (in.),
$\Delta_0 =$ deflection of reference specimen in mm (in.),
$l =$ heated length of member in mm (in.), and
$Y_b =$ distance between the centroidal axis of the member and the extreme bottom fiber in mm (in.)

A procedure for estimating the thrust requirements for a given fire endurance for simply supported slabs or beams is given in Refs 8 and 56.

34

Research is continuing to produce additional information and provide experimental verification for the analytical approach for predicting fire performance of structures. Krampf [83] recently reported on three types of investigations concerning behavior of structural elements and the entire buildings under fire attack. One investigation deals with theoretical and experimental investigations on one-legged reinforced concrete frames. This type of construction is regarded as the most characteristic part of multibay and multistory frames. The second investigation attacks the problem of how to relate effects of actual fires to those of standard fire conditions. The third investigation reports on a full-scale fire test carried out in a four-story dwelling house of modern, but conventional construction (reinforced concrete slabs on brickwork walls). Interesting and new information should become available from these investigations.

*Concrete Masonry Construction*

Until recently, concrete masonry construction was designed on the basis of individual fire tests or design aids in which relationships between fire resistance and other important parameters were given. In recent years, analytical methods for designing concrete masonry construction were developed. Information concerning two approaches follows.

*Heat Transmission Approach*—The fire endurance of most concrete masonry walls, as established by ASTM Test E 119, has been determined by heat transmission based upon the criteria of temperature rise on the unexposed side. Consequently, it has become general practice in building codes to state fire resistances required of concrete masonry walls in terms of "equivalent solid thickness." The fire resistance of concrete masonry walls as a function of aggregate type and equivalent solid thickness is shown in Fig. S3 [84].

The effect on fire endurance of filling the cores of concrete masonry units with various materials, as well as the effect of sand substitutions for lightweight fines in the concrete masonry unit are discussed in Ref 85.

The equivalent solid thickness concept for estimating required fire resistance in concrete masonry construction has also been adopted in Supplement No. 2 of the *National Building Code of Canada* [86]. Classifications used in Canada are slightly lower than those accepted in the United States. The *National Building Code of Canada* also contains detailed provisions for contributions of wall finishes to fire resistance of concrete masonry walls.

*Analytical Approach*—In 1970, Harmathy [64] introduced an empirical method for calculating the fire endurance of masonry units in a dry condition. The method was based on 1180 computer calculations performed to study heat flow during fire through concrete masonry unit walls. His calculations covered large ranges of four geometric variables, and four concretes that
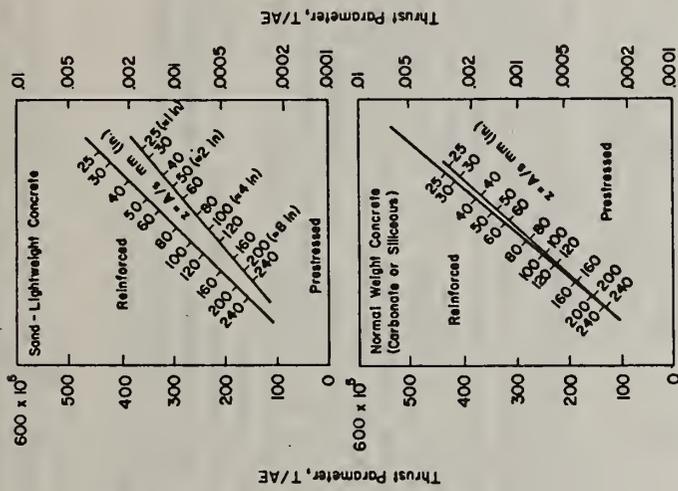
FIG. S1—*Nomograms relating thrust parameter, strain parameter, and ratio of cross-sectional area to heated perimeter* [8,56,82].
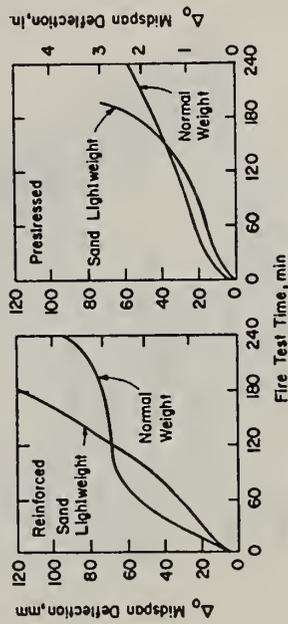
FIG. S2—*Midspan deflection of reference specimens* [8,56,82].

FIG. 53—*Fire resistance of concrete masonry* [84].

could be regarded as "limiting materials" in the normal and lightweight groups. Subsequent to the introduction of Harmathy's empirical method, 71 fire tests were conducted on 44 different types of concrete masonry units [87–89]. Based on results of the computer simulations and fire tests, three empirical equations were developed for estimating fire endurance from the geometric variables and material properties only in the case of concretes made with chemically stable aggregates. The real usefulness of these equations lies in showing the most economical design, and as extrapolation formulas in extending test information to geometries and materials not covered by fire tests.

Many of the results of fire tests were used by Williams-Leir and Allen [90] to predict fire endurance of concrete masonry walls. The authors presented results of a statistical procedure used to establish fire performance of most types of concrete masonry walls.

*Steel Construction*

In the past 20 years, hundreds of tests on steel floor and roof assemblies, beams, and columns have been conducted. Generally, results of these tests have been used to establish the fire endurance of the members or assemblies. As in the case of other materials, efforts have been made to extend the use of the individual test by developing design aids that relate fire resistance to some important parameters.

In the past 3 years, calculation methods have been presented for determining fire-resistive characteristics of steel construction.

*Fire-Resistance Classifications*—It was pointed out earlier in this report that fire resistance classifications for many materials are published in several referenced documents. Due to the large amount of material in these documents, it often is difficult for the designer to locate the specific test establishing the fire resistance for a particular set of design conditions.

A recent document published by the American Iron and Steel Institute [91] provides a guide to the proper source for detailed information for steel construction. In this document, summaries of fire-resistance classifications are presented. The summaries give sufficient information to locate the source of additional information relating to construction details and fire-endurance classifications. The summaries describe the systems that have been tested and the range of fire endurance classifications thus established.

Although some work concerned with the fire resistance of unprotected steel members [67] has been done, most of the published fire-endurance classifications for steel construction pertain to fire-protected elements. Fire protection used for modern steel framed buildings include gypsum, perlite and vermiculite, mineral fiber, ceiling panels and tile, portland cement concrete, portland cement plaster, masonry materials, and intumescent coatings. Two fire-protection methods result from the use of these fire-protection materials. The first method is classified as membrane fire protection. In this method a fire-resistant barrier is placed between the potential fire source and the member to be protected. The second method is by direct application of the fire-protection material. In this method, the fire-protection material generally comes into actual contact with the surfaces of the structural components to be protected. The direct-applied fire-protection method is widely used to safeguard structural steel columns that are enclosed with other building finishing materials.

*Use of Design Aids*—As mentioned previously, fire test results may often be used to develop design aids for determining the fire resistance of steel members. In some cases, the fire tests constitute a research program with a particular objective to be achieved. Such a research program is reported in another American Iron and Steel Institute publication [92]. In this program, 14 columns with different sizes and shapes were tested in accordance with ASTM Test E 119. The various columns were boxed in with one or more layers of gypsum wallboard in order to achieve fire endurance protection of from 1 to 4 h.

For steel columns of any size and shape, the gypsum wallboard thickness needed for a specific fire resistance rating can be obtained from Figs. 54 and 55. The graphs in these figures are diagrammatic representations of a formula for fire resistance developed in the study. Reference 92 also gives information on designing fire protection for steel columns using spray-

applied cementitious mixture and mineral fiber, and concrete to encase the steel column.

Information given in Fig. 55 also can be used in designing fire protection for steel trusses [93]. Other methods of achieving truss fire protection, such as ceiling membrane insulation systems and enclosing every member of the truss, are discussed in this publication.

Recently, some information on the use of precast concrete column covers was presented [94]. Figure 56 gives the thickness of concrete cover required for either normal weight or structural lightweight concretes, for various sizes of steel columns, for different fire endurance periods. Graphs are based on a study by Lie and Harmathy [95].

*Calculation Methods*—Calculation methods for steel construction vary from single formulas for determining the fire resistance of a particular structural member protected by a specific protection material to comprehensive rational design procedures. Studies made at Underwriters Laboratories, Inc. [96] and by Lie and Stanzak [97] resulted in a formula for calculating the fire resistance of protected steel columns. This general formula is

$$R = \left(\frac{215.2 W}{D\rho} + \frac{C}{25.4}\right)h \qquad R = \left(\frac{20W}{D\rho} + C\right)h \qquad (7)$$

$$\text{(SI Units)} \qquad\qquad \text{(English Units)}$$

where

$R$ = fire resistance in h (hours),
$W$ = weight of steel in kg/m (lb/ft),
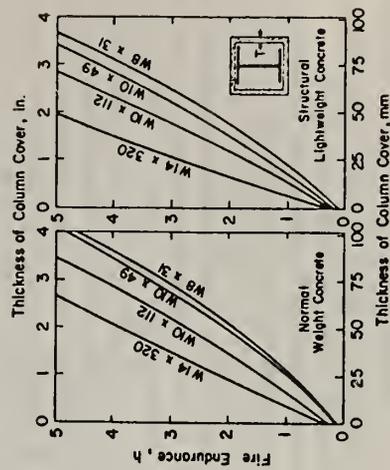


FIG. 56—*Fire endurance of steel columns afforded protection by precast concrete column covers [94].*

D = Heated Perimeter of Steel (backside of protection), mm (in.)
W = Weight of Steel Section with Protection, kg/m (lb./ft.)
h = Thickness of Protection, mm (in.)

FIG. 54—*Fire resistance of steel columns protected with gypsum wallboard [92].*

37



W = Weight of Steel Section with Protection kg/m
D = Heated Perimeter, mm
W/D for Steel Column (W=lb/ft, D=in.)

FIG. 55—*Thickness of gypsum wallboard needed to obtain fire resistance for various sizes and shapes of steel columns [92].*

## DESIGN OF BUILDINGS FOR FIRE SAFETY

$D$ = perimeter of protection, at the interface between protection and steel through which heat is transferred to steel, in mm (in.),

$\rho$ = density of insulation in kg/m³ (lb/ft³),

$h$ = thickness of insulation in mm (in.), and

$C$ = constant for sprayed mineral fiber and cementitious mixtures. The recommended value for C is: 0.5 where $\rho$ = 240 to 320 kg/m³ (15 to 20 lb/ft³).

The constant, C, for mineral fiber and cementitious mixtures is based on fire test data developed at Underwriters Laboratories, and the American Iron and Steel Institute research project at Smithers Scientific Services, Inc. [92].

Figure 57 [91] shows a comparison between experimental and calculated fire resistances determined by using the formula for cementitious-protected steel members. Good correlation was obtained between test results and calculated fire endurance classifications.

A more comprehensive treatment for determining the fire resistance of steel members exposed to fire was presented by Brozzetti [98]. Some of the information contained in this publication was presented by Barthelemy [99]. The author presents a method for calculating the heating-up behavior of steel members protected by dry or wet products. He also presents information on the heating-up behavior of unprotected members.

The most comprehensive method available for designing steel structures for fire is given in Ref 15. Babrauskas [100] pointed up that the objective of this manual is to enable a building designer to calculate simultaneously both the expected fire and response of the structure to it without the use of a computer. He noted that from a design approach the real interest is in the last part of the manual where the recommended approximate procedures for rational fire endurance design are given. The procedures are

different for walls than those for floors and columns. Walls are treated as nonload-bearing slabs failing by thermal transmission. The critical temperature concept is used for floors and columns.

The basic methodology for floors and columns is as follows. Tables are given for suggested fuel load. The designer identifies ventilation openings and wall materials for which a list of thermophysical properties is also given. These variables would suffice to determine the room fire gas time-temperature curve. Instead of producing the time-temperature curve, the next step is immediately incorporated. The designer identifies thickness and insulating properties of the steel protection and uses knowledge of the critical steel temperature to determine the fire endurance time.

Use of the design manual and information on its contents were summarized by Thor et al [101]. This publication points out that the rational fire engineering method presented in the manual is based on four main steps: (1) determination of fire load, (2) determination of the gas temperature in the fire compartment, (3) determination of the maximum steel temperature, and (4) determination of critical load.

The manual is divided into four major sections. The main section gives the background and principles of the differentiated design method. Theories and equations used are thoroughly discussed. In the design section, all diagrams and tables necessary for practical design work are presented. The example section contains ten different examples with solutions describing the design procedure and manner in which to use the design tables and diagrams. The last section contains an alternate design method based upon the equivalent time of fire duration concept. Rules and diagrams for translating results from standard fire tests of steel structures to real fire conditions are given.

Additional work on the design of steel structures for fire has been done by Lie [102] and Ove Arup and Partners [103].

### Other Materials

Ryan [53] reported experimental results from a study in which small gypsum plaster specimens were exposed to controlled fires similar to those to which large building elements have been subjected in tests by a recognized standard method.

The small specimens were tested without either structural load or restraint. From the test results, fire resistance based on time of the unexposed surface temperature to rise 139°C (250°F) is expressed as a function of the plaster thickness. The results of the study are plotted in Fig. 58.

*Additional Design Information*—A well-developed systematic approach to building fire safety was published in 1972 [104]. This method considers all aspects of the fire safety problem, including fire severity, spatial requirements, economic considerations, and movement of people.
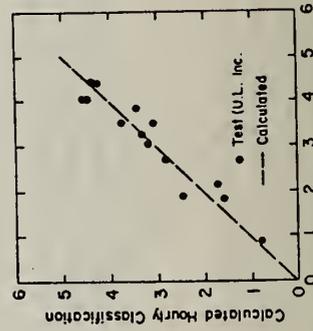


FIG. 57—*Comparison between experimental and calculated fire resistance for cementitious protected steel members* [91].

Here, $x$ is taken as a space variable that increases in a pseudo-exponential fashion.

Figure 59 expresses the results of this method graphically. Two main curves are drawn; one represents the probability of success demanded by the owner, and the second curve shows the expected performance for a given design. The design is acceptable if the expected fire curve is always below the critical curve.

### Actual Fires

Fire-resistive structures made of inorganic materials historically have performed well when exposed to fire. In most cases, structural collapse of members or of the entire building occurred after longer periods than required by the design. Often, collapse during fire can be associated with poor judgment in design of the structure, a more severe fire than anticipated due to higher fire loads, overloading of members of the structure, and code requirements not adequate for the intended occupancy.

Recently, Malhotra [105] presented a paper in which seven fires in concrete buildings of various sizes, types, and occupancies were examined. The publication establishes the extent of damage and the role of the



FIG. 59—*General Services Administration's fire spread probability diagram* [104].



FIG. 58—*Time to 139°C (250°F) rise versus thickness of vermiculite, perlite, and sand aggregate plasters* [53].

Babrauskas [100] reviewed the method and gives a quotation from Ref 104 concerning the guiding principle of the method.

A basic premise through the entire system development is that there is no absolute state of fire safety. All activities and all structures involve a degree of risk to people, property, and operational continuity. The acceptable degree of risk is the controlling criterion. This criterion, which is to be established by management, becomes the controlling parameter for the designer.

The heart of the approach is a decision tree which in diagram form sets forth the fire safety goals, and then gives all the possible ways that protection can be accomplished. No consideration is excluded from the solution. To apply the method to a specific building, the designer observes that the paths through the tree branch in two ways: with "and" gates, and with "or" gates. At an "and" intersection, both pathways must be utilized while at an "or" gate only one of several alternatives, or more commonly a bit of each, can be used. Babrauskas points out that the system is quantified by use of a probabilistic variable. The variable can be expressed as

$P(x)$ = probability that, given ignition, the fire will be stopped at or before it reaches size $x$.

structural components in the behavior of the structure are discussed in the following paragraphs. Also, two fires in structural steel buildings are discussed.

The purpose of examining structures exposed to actual fires is to show that if such factors as fire severity, design details, material properties, and occupancy are given proper consideration in the design of the building, performance of the building when exposed to fire can be predicted. In fact, analytical methods are now available by which the performance of the structure during a fire can be compared with calculated results.

*Andraus Building*

The Andraus Building is a 31-story reinforced concrete department store and office building located in Sao Paulo, Brazil. Fire occurred on 24 Feb. 1972 [*106*]. Although the building was designed as a fire-resistive structure, many factors added to the high combustible content of the building. Wood floor forms were left in place, combustible ceiling tile was used, all floors were wood parquet, and there were many wood partitions. A solid flame front engulfed the entire building within 15 min after the fire started. It continued at high intensity for 3 to 4 h, and was not completely extinguished for several hours after that.

The fire gutted many areas of the building, consuming construction materials and practically all other combustible contents. There was no collapse of the building although some load-bearing members on the 25th floor were severely damaged. One floor slab deflected and the adjacent beam cracked. Some spalling of the concrete occurred. The building was inspected after the fire and declared structurally safe. It was eventually repaired and put back into use.

Three-hundred and fifty people were rescued from the roof during the 4-h period when the fire was most intense. Two hundred additional people were rescued from a stairwell in the upper floors of the building where they sought refuge from the fire. It is interesting to note that the fire damage was less severe on the four vacant top floors, apparently because of the suspended gypsum tile ceiling used here, and less fire load from the contents.

The building maintained its structural integrity during the fire. The damage that occurred to members of the structure can be related to the severity of the fire, the temperatures that developed in the structural members due to fire exposure, and the reduction in material properties associated with these temperature distributions.

*Military Personnel Record Center*

The Military Record Center is a building 86 m (282 ft) wide by 221 m

(725 ft) long. This 6-story structure was constructed of reinforced concrete. Floor and roof construction did not have expansion joints.

The fire began on 12 July 1973 [*107*]. It started on the 6th floor and burned out of control for about 20 h. It was extinguished finally after 4 days.

The sixth floor contained a fire load of about 975 kg/m³ (200 psf). The roof was reported to suffer displacement at about 2½ h, but did not begin to collapse until 12 h after the fire began. Eventually 30 percent of the roof slab concentrated in the vicinity of the estimated point of origin of the fire collapsed onto the sixth floor.

The building was inspected during and after the fire. Practically no structural damage occurred to the building below the sixth floor. The sixth story was removed and the structure is now used as a 5-story building.

A computational procedure developed at the University of California was used to analyze the performance, during fire, of the Military Personnel Record Center [*108*]. Uncertainties about the fire spread, duration and intensity of the fire, and the complexity of the structural system made detailed study of behavior difficult. However, correlation of observed behavior and analytical predictions demonstrated good agreement and helped to explain failures that could not otherwise be accounted for.

*McCormick Place Fire*

McCormick Place at the time of the fire in 1976 [*109,110*] was the nation's largest exhibition center. The building was 296.6 m (1130 ft) long by 106.7 m (350 ft) wide. It was divided into three levels. The lower and intermediate levels of McCormick Place were reinforced concrete. The upper level and roof construction were of structural steel.

Final arrangements were being completed to prepare the National Housewares Manufacturers Association's 46th Semi-Annual Exhibit for opening the following morning.

At approximately 2:00 a.m., a small fire was noted in one of the booths on the upper level. Ineffective fire fighting by untrained personnel, a 6-min delay in sounding the alarm, lack of sprinkler protection, malfunctioning of the private water supply, pumps, and controls, damaged water supply mains and hydrants, and a combustible content having large surface area contributed to the rapid spread of the fire. Roof collapse had already begun by the time water could be effectively applied to the level where the fire started. This was about 30 to 45 min after the fire was reported. The fire was finally struck out about 7 h after it began.

Damage to the building was extensive. Practically the entire roof of the building collapsed. The reinforced concrete construction below the exhibition or top level was not seriously damaged structurally. There were extended areas on the underside of the slab where spalling of the concrete

40

extended below the reinforcing steel. Spalling was also noted on some of the columns on the bottom level.

Collapse of the roof occurred because the unprotected steel could not sustain the severe temperatures produced in this fire. These temperatures were obviously high enough to cause the steel to reach its critical temperature for the load it was carrying. There was no redistribution of moments since the roof structure was of a statically determinate design. Based on the fire severity from an estimated fire load of 73.1 to 97.6 kg/m² (15 to 20 psf) of floor area, distributed to have a large surface area conducive to rapid involvement of all combustibles, the temperature development in the steel members and property changes of the steel materials could be determined. Hence, the response of the structure to the fire was predictable.

McCormick Place was rebuilt into a much larger exhibition center. Many changes were made in the fire-protective system and design of the structure. Steel members were coated with fire protection material. Certain redundancies were built into the steel frame of the structure, and sprinkler systems were installed in the new building.

*One New York Plaza Fire*

This building is a 50-story skyscraper having a reinforced concrete center core containing elevator shafts, stair towers, utilities, and air-conditioning supply and return air shafts. The structural frame was steel. Columns, girders, beams, and the underside of the floors were protected by sprayed-asbestos fiber to provide a 4-h fire resistance for columns, and a 3-h rating for filler beams and floors. A fire believed to have started on the 33rd floor of the building occurred on 5 Aug. 1970 [111]. This fire was brought under control after 5 h.

Most of the damage to the steel frame occurred at the interior portions in parts of the 33rd and 34th floors. Steel filler or intermediate beams on these floors were twisted or deflected several inches and the connecting bolts sheared off, allowing the filler beams in some sections to rest on the flange of the girder.

Damage to the structure resulted from several factors. The most important one was the loss of the sprayed-asbestos fiber fire protection on various steel members. In many places, the insulation fell off shortly after its application along with an oxidized scale that formed on the steel beams while in transit from England. Also, the fire protection insulation was removed in many areas to accommodate certain construction details.

In spite of a very severe fire, there was no structural collapse of the steel frame or floor system. Damage that did occur can be explained in terms of the fire severity, and expansion and strength properties of the members as affected by the temperature distribution caused by the fire.

**Summary**

When fire-resistive structures are exposed to fire, temperature changes usually occur in many members of the building. These temperature changes cause properties of the materials in the structure to change. Information has been presented on effects of temperature on some of the more important strength, elastic, and thermal properties of several inorganic materials. Representative temperature distributions in slabs, beams, and other members are given.

Fire test results and design aids relating fire resistance with various parameters are often used to determine the fire endurance of structural members. With property and temperature distribution information, it is possible to use a rational approach for predicting performance of structures. Several of these approaches were discussed and illustrated for members made of different inorganic materials. Predicted performance using these methods have been verified by results of fire test programs.

Finally, four actual fires involving concrete and steel structures were discussed. Three of the structures were "protected" and performed well structurally for periods equal or longer than contemplated by the design, even though the fire conditions were very severe. The structure that collapsed during the fire was permitted by the Chicago Building Code to be "unprotected." A computational method was used to analyze the effects of the fire on one of the structures. Calculated results verified observed performance.

**References**

[1] ASTM Fire Tests of Building Construction and Materials (E 119), American Society for Testing and Materials, Philadelphia, Pa.
[2] Abrams, M. S., "Performance of Concrete Structures Exposed to Fire." 9th National SAMPE Technical Conference, Vol. 9, "Materials and Processes-In Service Performance," Society for the Advancement of Material and Process Engineering. Azusa, Calif., 1977.
[3] Philleo, R., *Proceedings*. American Concrete Institute, Vol. 54. April 1958: *PCA Research Bulletin 97.*
[4] Dettling, H. in *Behavior of Concrete at High Temperatures*, Deutscher Ausschus fur Stahlbeton, Vol. 164, Part 2, 1964, pp. 1-64; PCA Foreign Literature Study 458.
[5] Anderberg, Y. and Thelandersson, S., *Division of Structural Mechanics and Concrete Construction, Bulletin 54*, Lund Institute of Technology, Lund, Sweden, 1976.
[6] Harmathy, T. Z. and Allen, L. W., *Journal of the American Concrete Institute*. Vol. 70, Feb. 1973.
[7] "Steel for Elevated Temperature Service," U.S. Steel Corporation, Pittsburgh, Pa.
[8] "FIP/CEB Report on Methods of Assessment of Fire Resistance of Concrete Structural Members," Great Britain, 1978.
[9] Odeen, K., "Fire Resistance of Prestressed Concrete Double T-Units," National Swedish Institute for Materials Testing, Stockholm, 1968.
[10] Cruz, C. R., "Elastic Properties of Concrete at High Temperatures," *PCA Research Bulletin 191.*
[11] Harmathy, T. Z. and Berndt, J. E., *Proceedings*. American Concrete Institute, Vol. 63, Jan. 1966.

[41] Harmathy, T. Z., *Fire Technology*, Vol. 12, Nos. 2 and 3, National Fire Protection Association, Boston, Mass., 1976.

[42] Harmathy, T. Z., *Journal of Applied Physics*. Vol. 35, No. 4, 1964.

[43] Anderberg, Y., "Fire-Exposed Hyperstatic Concrete Structures—An Experimental and Theoretical Study," Bulletin 55, Division of Structural Mechanics and Concrete Construction, Lund Institute of Technology, Lund, Sweden, 1976.

[44] Collet, Y., "Conductivite Thermique du Materiau Beton, (Thermal Conductivity of Concrete)," Groupe de Travail "Beton Leger de Structure" et "Comportement du Materiau Beton en Fonction de la Temperature," 1970.

[45] Harmathy, T. Z., *ASTM Journal of Materials*, Vol. 5, No. 1, 1970, p. 47.

[46] Carman, A. D., and Nelson, R. A., "The Thermal Conductivity and Diffusivity of Concrete," *Bulletin No. 122*, University of Illinois Engineering Experimental Station, 1921.

[47] Stalhane-Pyk., Electrovarmeinstitutet, 1923–1933.

[48] Schneider, W., and Haksever, A., "Bestimmung der Aquivalenten Branddauer von Statisch Bestimmt Getlagerten Stahlbetonbalken bei Naturlichen Branden." Report of Institut fur Baustoffkunde und Stahlbetonbau der TU Braunschweig. 1976.

[49] Collet, Y. and Tavernier, E., "Etude des Proprietes du Beton Soumis a des Temperatures Elevees," "Comportement du Materiau Beton en Fonction de la Temperature," Bruxelles, 1976.

[50] "Physical Constants of Some Commercial Steels at Elevated Temperatures," British Iron and Steel Research Association, Butterworks Scientific Publications, London, England, 1953.

[51] Harmathy, T. Z. in *Symposium on Fire Test Methods. ASTM STP 301*, American Society for Testing and Materials, 1961.

[52] Unpublished, private communication from National Research Council of Canada.

[53] Ryan, J. V., *Journal of Research*, Vol. 66C, No. 4, 1962.

[54] Iding, R., Bresler, B., and Nizamuddin, Z., "Fires-T3, A Computer Program for the Fire Response of Structures–Thermal," UCB FRG 77-15, Fire Research Group. University of California, Berkeley, 1977.

[55] Abrams, M. S. and Gustaferro, A. H., "Fire Endurance of Concrete Slabs as Influenced by Thickness, Aggregate Type and Moisture," *PCA Research Department Bulletin 223*.

[56] Gustaferro, A. H. and Martin, L. D., "PCI Design for Fire Resistance for Precast Prestressed Concrete," Prestressed Concrete Institute, Chicago, 1977.

[57] "Design and Detailing of Concrete Structures for Fire Resistance." Interim Guide by a Joint Committee of the Institution of Structural Engineers—The Concrete Society. The Institution of Structural Engineers, London, 1978.

[58] Gustaferro, A. H., Abrams, M. S., and Litvin, A., "Fire Resistance of Lightweight Insulating Concrete," *Lightweight Concrete. ACI Special Publication 29.* American Concrete Institute, Detroit, Mich.; *PCA Research and Development Bulletin RD104.* 1970.

[59] Lin, T. D. and Abrams, M. S., "Temperature Distribution in Rectangular Beams Subjected to Fire," Portland Cement Association, in preparation.

[60] Lie, T. T. and Harmathy, T. Z., "A Numerical Procedure to Calculate the Temperature of Protected Steel Columns Exposed to Fire," Fire Study No. 28, NRCC 12535. Div. of Building Research, National Research Council of Canada. 1972.

[61] Lie, T. T. and Allen, D. E., "Further Studies of the Fire Resistance of Reinforced Concrete Columns," Technical Paper No. 378 of the Division of Building Research, National Research Council of Canada, Ottawa, Canada.

[62] Abrams, M. S. and Gustaferro, A. H., *Journal of the Prestressed Concrete Institute.* Jan.-Feb., 1972, *PCA Research and Development Bulletin RD017.* 1973.

[63] Abrams, M. S. and Gustaferro, A. H., *Journal of the American Concrete Institute.* Vol. 66, No. 2, Feb. 1969, *PCA Research and Development Bulletin RD048,* 1976.

[64] Harmathy, T. Z. in *Fire Test Performance. ASTM STP 464.* American Society for Testing and Materials, 1970.

[65] Bletzacker, R. W., "Effect of Restraint on the Fire Resistance of Protected Steel Beam Floor and Roof Assemblies," Building Research Laboratory Final Report EES 246-266,

[12] Saeman, J. C. and Washa, G. W., *Journal of the American Concrete Institute*, Vol. 29, No. 5, Nov. 1957; *Proceedings.* Vol. 54.

[13] Garofalo, E., Malenock, P. R., and Smith, G. V. in *Symposium on Determination of Elastic Constants, ASTM STP 129*, American Society for Testing and Materials, 1952, p. 10.

[14] Anderberg, Y., "Mechanical Properties of Reinforcing Steel at Elevated Temperatures," Lund Institute of Technology, in preparation.

[15] Pettersson, O. et al, "Fire Engineering Design of Steel Structures," Division of Structural Mechanics and Concrete Construction, Lund Institute of Technology, Bulletin 52, Lund, Sweden, 1976.

[16] Kordina, K. and Schneider, U., *Beton Herstellung Verwendung*, Vol. 25, No. 1, 1975.

[17] Harmathy, T. Z. and Stanzak, W. W. in *Fire Test Performance, ASTM STP 464*, American Society for Testing and Materials, 1970.

[18] Cruz, C. R., "Apparatus for Measuring Creep of Concrete at High Temperatures," *PCA Research Department Bulletin 225*.

[19] Mukaddam, M. A. and Bresler, B., *Concrete for Nuclear Reactors*, SP-34, American Concrete Institute, Detroit, Mich., 1972.

[20] Mukaddam, M. A., *Journal of the American Concrete Institute*, Vol. 71, 1974.

[21] Nasser, K. W. and Neville, A. H., *Journal of the American Concrete Institute*, Vol. 64, 1967.

[22] Dorn, J. E., *Journal of the Mechanics and Physics of Solids*, Vol. 3, 1954.

[23] Harmathy, T. Z., *Journal of Basic Engineering*, Vol. 89, Series D, 1967.

[24] Harmathy, T. Z. in *Symposium on Fire Test Methods, ASTM STP 422*, American Society for Testing and Materials, 1967.

[25] Harmathy, T. Z., "Creep Deflection of Metal Beams in Transient Heating Processes with Particular Reference to Fire," *Canadian Journal of Civil Engineering*, 1976.

[26] Plem, E., "Theoretical and Experimental Investigations of Point Set Structures," Swedish Council for Building Research, Document D9, Stockholm, 1975.

[27] Abrams, M. S., *Temperature and Concrete*, SP-25, American Concrete Institute Detroit, Mich., 1971.

[28] Malhotra, H. L., *Magazine of Concrete Research*, Vol. 8, No. 22, London, 1956.

[29] Schneider, U., "Zur Kinetik Festigkeitsmindernder Reaktionen in Normalbetonen bei Höhen Temperaturen," Thesis, TU Braunschweig, 1973.

[30] Zoldners, N. G., "Effect of High Temperatures in Concretes Incorporating Different Aggregates," *Mines Branch Research Report 64*, Department of Mines and Technical Survey, Ottawa, 1960.

[31] Binner, C. R., Wilkie, C. B., and Miller, P., "Heat Testing of High-Density Concrete," Supplement to HKF-1 (Declassified Atomic Energy Commission Report), 1949.

[32] Weigler, H. and Fischer, R., *Behavior of Concrete at High Temperatures*, Deutscher Ausschus fur Stahlbeton, Vol. 164, 1964.

[33] Weigler, H. and Fischer, R., *Beton*, Vol. 2, 1968.

[34] Kordina, K. et al, *Sonderforschungsbereich 148*, TU Braunschweig, 1977.

[35] Thelandersson, S., "Effect of High Temperature on Tensile Strength of Concrete," Nordisk Betong, 1972.

[36] Brockenbrough, R. L. and Johnston, B. G., "Steel Design Manual," U.S. Steel Corporation, Pittsburgh, Pa., 1968.

[37] Abrams, M. S. and Cruz, C. R., "The Behavior at High Temperature of Steel Strand for Prestressed Concrete," *PCA Research Department Bulletin 134*.

[38] Day, M. F., Jenkinson, E. A., and Smith, A. I., *Proceedings of the Institution of Civil Engineers*, Vol. 16, 1960.

[39] Gustaferro, A. H., Abrams, M. S., and Salse, E. A. B., "Fire Resistance of Prestressed Concrete Beams. Study C: Structural Behavior During Fire Tests," *PCA Research and Development Bulletin (RD009.01B)*, Portland Cement Association, 1971.

[40] Carlson, C. C., et al, "A Review of Studies of the Effects of Restraint on the Fire Resistance of Prestressed Concrete," *Proceedings. Symposium on Fire Resistance of Prestressed Concrete*, Braunschweig, Germany 1965. International Federation for Prestressing (FIP), Bauverlag GmbH, Wiesbaden, Germany; *PCA Research Department Bulletin 206*.

Engineering Experiment Station, The Ohio State University, Columbus, Ohio, Sept. 1966.

[66] Lie, T. T., *Journal of Heat Transfer*, Vol. 99, Series C, No. 1, Feb. 1977.

[67] Stanzak, W. W., and Lie, T. T., *Journal of the Structural Division*, American Society of Civil Engineers, Vol. 99, No. ST5. Proc. Paper 9719, May 1973.

[68] *Fire Resistance Directory*, Underwriters Laboratories Inc., Northbrook, Ill., 1978.

[69] "Fire Resistance Ratings of Beams, Girder and Truss Protection, Ceiling Constructions, Column Protections, Floor and Ceiling Constructions, Roof Constructions, Walls and Partitions," American Insurance Association, New York, N.Y.

[70] *Fire Resistance Design Manual*, Gypsum Association, Evanston, Ill., 1978.

[71] "Technical Notes on Brick Construction," No. 16, Brick Institute of America, McLean, Va. 1974.

[72] Nizamuddin, Z. and Bresler, B., "Fire Response of Reinforced Concrete Slabs," Report No. UCB FRG WP 77-1, Department of Civil Engineering, University of California, Berkeley, 1977.

[73] Abrams, M. S. et al, "Fire Tests of Concrete Joist Floors and Roofs," *PCA Research and Development Bulletin RD006.*

[74] Abrams, M. S. and Lin, T. D., "Simulation of Realistic Thermal Restraint During Fire Tests of Floor and Roof Assemblies," *Report to the National Bureau of Standards*, submitted by Portland Cement Association, Skokie, Ill., Jan 1974.

[75] Bizri, H., "Structural Capacity of Reinforced Concrete Columns Subjected to Fire Induced Thermal Gradient," Report No. UC SESM 73-1, Department of Civil Engineering, University of California, Berkeley, 1973.

[76] Becker, J. and Bresler, B., "Fire-RC—A Computer Program for the Fire Response of Structures-Reinforced Concrete Frames," Report No. UCB FRG 74-3, Department of Civil Engineering, University of California, Berkeley, 1974.

[77] Bresler, B., "Response of Reinforced Concrete Frames to Fire," Report No. UCB FRG 76-12. Department of Civil Engineering, University of California, Berkeley, 1976.

[78] Bresler, B., Thielen, G., Nizamuddin, Z., and Iding, R., "Limit State Behavior of Reinforced Concrete Frames in Fire Environments," Report No. UCB FRG 76-12, Department of Civil Engineering, University of California, Berkeley, 1976.

[79] ACI Committee 318, "Building Code Requirements for Reinforced Concrete (ACI 318-71)," American Concrete Institute, Detroit, Mich., 1971.

[80] Gustaferro, A. H. and Selvaggio, S. L., *Journal of the Prestressed Concrete Institute*, Vol. 12, No. 1, Feb. 1967; *PCA Research Bulletin 212.*

[81] Abrams, M. S., Gustaferro, A. H., and Lin, T. D. "Fire Endurance of Continuous Reinforced Concrete Beams," *Preliminary Report, Tenth Congress*, International Association for Bridge and Structural Engineering, Tokyo, 1976.

[82] Issen, L. A. et al in *Fire Test Performance, ASTM STP 464*, American Society for Testing and Materials, 1970.

[83] Krampf, L., "Recent Progress in Fire Research," *Proceedings of the Eighth Congress of the Federation International de la Precontrainte*, London, 1978.

[84] "Estimating the Fire Resistance of Concrete Masonry," NCMA TEK 6, National Concrete Masonry Association, McLean, Va., 1966.

[85] Randall, F. A., Jr. and Panarese, W. C., "Concrete Masonry Handbook for Architects, Engineers, Builders," Portland Cement Association, Skokie, Ill. 1976.

[86] "Fire Performance Ratings 1975," Supplement No. 2 of the National Building Code of Canada, NRCC No. 13978, National Research Council, Ottawa, Ont., Canada, 1975.

[87] Allen, L. W. and Harmathy, T. Z., *Journal of the American Concrete Institute*, Vol. 69, Detroit, Mich., 1972.

[88] Allen, L. W., "Fire Endurance of Selected Non-Load Bearing Concrete Masonry Walls," National Research Council of Canada, Division of Building Research, NRCC 11275, 1970.

[89] Allen. L. W., "Effect of Sand Replacement in the Fire Endurance of Lightweight Aggregate Masonry Units," National Research Council of Canada, Division of Building Research, NRCC 12112, 1971.

[90] Williams-Leir, G. and Allen, L. W., "Prediction of Fire Endurance of Concrete Masonry Walls," National Research Council of Canada, Division of Building Research, NRCC 13560, Ottawa, Canada, 1973.

[91] "Fire Resistant Steel Frame Construction," 2nd ed., American Iron and Steel Institute, Washington, D. C. 1974.

[92] "Designing Fire Protection for Steel Columns," American Iron and Steel Institute, Washington, D.C., 1978.

[93] "Designing Fire Protection for Steel Trusses," American Iron and Steel Institute, Washington, D.C., 1976.

[94] Gustaferro, A. H., *Journal of the Prestressed Concrete Institute*, Vol. 19, No. 5, Chicago, Ill., 1974.

[95] Lie, T. T. and Harmathy, T. Z., *ACI Journal, Proceedings*, Vol. 71, No. 1, Detroit, Mich., 1974.

[96] "Methods of Predicting the Fire Resistance of Column Assemblies," Underwriters Laboratories, Inc., Northbrook, Ill., 1973.

[97] Lie, T. T. and Stanzak, W. W., *Engineering Journal*, Third Quarter, 1973.

[98] Brozzetti, J., "Project de Recommendations Concernant la Prevision par la Calcul du Comportement au Feu de Structures en Acier," Technical Center for Steel Structures, Puteaux, France, 1975.

[99] Barthelemy, B., "Heating Calculation of Structural Steel Members," *Journal of the Structural Division*, American Society of Structural Engineers, 1976.

[100] Babrauskas, V., "Fire Endurance in Buildings," Report No. UCB FRG 76-16, Fire Research Group, University of California, Berkeley, 1976.

[101] Thor, J., Petterson, O., and Magnusson, E., *Engineering Journal*, Third Quarter, 1977.

[102] Lie, T. T., *Engineering Journal, Third Quarter*, 1978.

[103] Arup, Ove. and Partners, "Design Guide for Fire Safety of Bare Exterior Structural Steel—Designers Manual and Technical Reports," American Iron and Steel Institute, Washington, D.C., 1977.

[104] "Building Fire Safety Criteria," Draft of GSA Handbook PBS P 5920-9A, Public Building Service, General Services Administration, Washington, D.C., 1975.

[105] Malhotra, H. L., "Some Noteworthy Fires in Concrete Structures," *Proceedings of the Eighth Congress of the Federation International de al Precontrainte*, London, 1978.

[106] Willey, E. A., "High Rise Building Fire," *Fire Journal*. National Fire Protection Association, Boston, Mass., 1972.

[107] "Military Personnel Records Center Fire," *Fire Journal*, National Fire Protection Association, Boston, Mass., 1974.

[108] Bresler, B., "Fire Protection of Modern Buildings; Engineering Response to New Problems," Eleventh Annual Henry M. Shaw Lecture in Civil Engineering, North Carolina State University, 1976.

[109] "The McCormick Place Fire," Illinois Inspection and Rating Bureau, Chicago, Ill., 1967.

[110] "McCormick Place Fire," An Engineering Report, American Iron and Steel Institute, Washington, D.C., 1968.

[111] "One New York Plaza Fire," Report by The New York Board of Fire Underwriters Bureau of Fire Prevention and Public Relations, New York, N.Y. 1970.

# CALCULATION OF FIRE RESISTANCE LIMITS FOR
# FLEXURAL REINFORCED CONCRETE STRUCTURES

Dr. V. V. Zhukov, PhD. and Dr. V. N. Samoylenko, PhD.
NIIZhB, Gosstroy USSR

At present the fire resistance of reinforced concrete structures, especially of those newly being designed is mainly determined experimentally. The Experimental method for determining the fire resistance limits of structures is rather labor-consuming and expensive. Therefore both in our country and abroad one should search for ways of determining the fire resistance limits of structures without performing fire tests.

On the basis of numerous test analyses on fire resistance of reinforced concrete members tables and diagrams were made to give the fire resistance limits of structures by their sizes, thickness of concrete cover; reinforcing steel, types of concrete, etc. These methods of determining the fire resistance limits are given in SNiP 11-A.5-70(1) and in Recommendations (2). It should be noted that according to this method heating of elements will be regulated to follow the curve given in ISO DIS 834.

For structures of new materials, different cross-sections as well as other fire exposures, this method of determining the fire resistance limits for reinforced concrete structures is unusable. For this reason a calculation method for the fire resistance limits of reinforced concrete structures has been developed.

The calculation approach consists of two stages: the first is the determination of transient heat flow in cross-sections of structures, and the second one is an analysis of structure under static load, considering the change of concrete and steel properties with respect to temperature during their heating period.

The transient heat flow computation method in our country is based on A. V. Lykov's theory of total heat mass exchange (3). In general it is necessary to solve a system of partial differential equations in order to find the interrelationship between temperature, moisture content and steam pressure in concrete.

For determining the fire resistance limits of reinforced concrete structures, this system is considerably simplified to solving two (4, 5) or one (6, 7) differential equation.

Calculation of temperatures in reinforced concrete structures is a non-linear differential equation, which is written as

$$C \cdot \rho \cdot \frac{\partial T}{\partial \alpha} = \text{div} (\lambda \cdot \text{grad } T) + L \qquad (1)$$

where T - temperature;
    $\lambda$ - thermal conductivity;
    L - heat of liberation and absorption due to phase transition
       of water in concrete;
    C - specific heat;
    $\rho$ - density of concrete.

This is the Fourier's equation in its general form. A digital computer was used to solve this equation considering the transformation of mechanically combined water in concrete structure into steam only through an adjustment in the value of "C" (6). Another way for thermal calculations (4, 7) is based on the method of smoothed heat transfer coefficients that takes into account different phase transitions of cement paste in concrete. This was done by introducing the latent heat, H(T) as a temperature function to justify the effect of phase transitions. In reference (5), equation (1) is solved directly with data measured during a test of a column that was exposed to a non-isothermic fire.

It is natural that all heat-flow calculations are performed on the basis of correct initial and boundary conditions. However, one may encounter difficulties of physical sense and mathematical order in specific solution steps.

The above basic calculation methods of transient heat flow for fire resistance limits give a reasonable agreement between calculated and measured temperatures in concrete members exposed to fire. This agreement is attributed to the right formulation of the problem, and accurate experimental data on the thermodynamic parameters of material. Recently there has emerged a better method that accounts for phase transition of water in the concrete capillary system at any calculated temperature level.

The calculation of flexural reinforced concrete structures subjected to static load and high temperature mainly involves the computation of moment capacity and the associated deflections.

The moment capacity of the structure is computed at the stage under · which the strength of the most stressed cross-section decreases so much that it is unable to bear the load and dead weight any longer.

Calculation methods for the strength of heated flexural members have been elaborated rather well in our country and abroad (6, 8). For calculations one may use formulas under ambient temperature. Nevertheless the coefficients that account for a decrease of yield stress of reinforcement due to heating must be introduced.

The influence of temperature on reinforcement yield stress has been investigated by many experimenters. The published data provide accurate values of the above-mentioned coefficients.

Decrease of concrete strength in the compressed zone is not usually taken into account due to its low temperature. It should be noted that investigations, carried out by A. I. Yakovlev (6), have shown that consideration must be given to the decrease of cross-sectional area in the compression zone caused by stress relaxation of reinforcement due to the high thermal strains of reinforcing steel.

The time shortly after a considerable increase of deflection in the test members is often assumed to be the end point of flexural reinforced concrete structures exposed to fire. Therefore, for the sake of accuracy, one should calculate the fire resistance of flexural reinforced concrete structures throughout the fire test. Calculations for thermal strains in a reinforced concrete member are considerably more complicated than the determination of bearing capacities of that member and have not been elaborated in depth. For example, in Recommendations (2) there are no proposals for strains calculation for flexural members.

Experimental and theoretical investigations on the development of calculational methods for strains in reinforced concrete flexural members, subjected to fire have been conducted for some years in NIIZhB, Gosstroy USSR. These calculation methods given in Manual (9), are assumed as a basis for computing thermal strains according to the following formula:

$$1/\rho = 1/\rho_H + 1/\rho_t \tag{2}$$

where $1/\rho_H$ and $1/\rho_t$ - axis curvatures of member due to load and temperature respectively.

The curvature of heated reinforced concrete flexural members due to external load and dead weight is determined from the formula

$$1/\rho_H = \frac{M}{h_o \cdot Z_1} \left[ \frac{\psi_a}{E_a \cdot \beta_a \cdot \nu_a \cdot F_a} + \frac{\psi_\delta}{\xi \cdot b \cdot E_\delta \cdot \beta_\delta \cdot \nu} \right] \tag{3}$$

where M - bending moment due to dead weight and external load;

   b - width of the flexural member

   $h_o$ - distance from extreme compression fiber to centroid of tensile reinforcement;

   $Z_1$ - distance from centre of gravity of reinforcing steel to the reference axis;

$E_a$, $E_\delta$ - elastic moduli of reinforcement and concrete respectively;

$\beta_a, \beta_\delta$ - coefficients, accounting for decrease in elastic moduli of reinforcement and concrete under heating, respectively;

$\nu_a, \nu$ - coefficients, accounting for development of plastic deformations in reinforcement and in compressed concrete of member;

$\psi_a, \psi_\delta, \xi$ - coefficients, determined in accordance with Manual (10);

   $F_a$ - area of tensile reinforcement.

The Axis of curvature of a reinforced concrete member due to heating, is determined from:

$$1/\rho_t = \frac{\alpha_{at} \cdot t_a - \alpha_{\delta t} \cdot t_\delta}{h_o} \qquad (4)$$

where   $\alpha_{at}, \alpha_{\delta t}$ – coefficients of linear thermal expansion of reinforcement and concrete, correspondingly;

$t_a, t_\delta$ – temperatures of tensile reinforcement and extreme compression fiber of concrete, correspondingly.

In order to solve equations (1) through (3) for the deflections of flexural reinforced concrete members under fire according to proposed methods, one should know the temperature distribution on the member cross-section and the temperature related coefficients $\beta_a, \beta_\delta, \nu_a, \nu, \alpha_{at}, \alpha_{\delta t}$. The effect of temperature on physical and mechanical properties of reinforcement and concrete has been determined in numerous experiments (6,8,10). On the basis of test results analyzed for the coefficients $\beta_a, \beta_\delta, \nu_a, \nu, \alpha_{at}, \alpha_{\delta t}$ for various types of steel and concrete, it is possible to form mathematical relationships between the temperature and the above coefficients.

Formulas (3) and (4) were used in the computer program for calculating the strains in flexural reinforced concrete members under temperature and load action. The program is also used to determine the strength of members due to heating.

Figure 1 shows deflections obtained by the methods developed by A. F. Milovanov and experimental results, obtained by Kh. U. Kambarov on ceramsite concrete slabs with steel percentage of $\mu = 0.44\%$ (10). Comparing calculated and experimental values one find that calculated values are in a good agreement with the measured ones throughout the fire test. As the member reaches its fire resistance limit ($\tau = 95$ min), the calculated deflection sharply increases.

The above-mentioned methods may also be used for determining the rigidity and temperature effect on statically indeterminate reinforced concrete structures.

<div align="center">References</div>

1.  SNiP II A.5-70 "Fire-prevention design codes for buildings".

2.  FIP/CEB Recommendations for the Design of Reinforced and Prestressed Concrete Structural Members for Fire Resistance", FIP/CEB 1975.

3.  Lykov, A. V., "Heat Exchange", Publishing House "Energiya" ("Energy"), M., 1972.

4.  Robsman, V. A., Investigation of heat and mass transfer in refractory capillary porous bodies.   Candidate thesis, M., 1975.

5.  Roitman, V. M., Lyrina, G. N., Solution of heat and technical problem of structure fire resistance considering the processes of moisture transfer on digital computers according to implicit finit- separation diagram.   Collection N 2, "Fire resistance of building structures", VNIIPO MVD USSR, M., 1974.

6.  Byshev, V. P., Pchelintsev, V. A., Fedorenko, V. S., Yakovlev, A. I., "Fire resistance of buildings", Stroyizdat, M., 1970.

7.  Zhukov, V. V., Robsman, V. A., Shevchenko, V. I., Tsygankova, L. R., Heat and physical calculations of structures from refractory concrete on digital computers, Volgograd, 1971.

8.  Report on methods of assessment of the fire resistance of concrete structural members, FIP/CEB, 1978.

9.  Design Manual for Concrete and Reinforced Concrete Structures for Fires, Stroyizdat, 1977.

10. Milovanov, A. F., Kambarov, Kh. V., Malkina, T. N., Fire resistance of ceramsite concrete structures, FIP Notes 76, 1978.
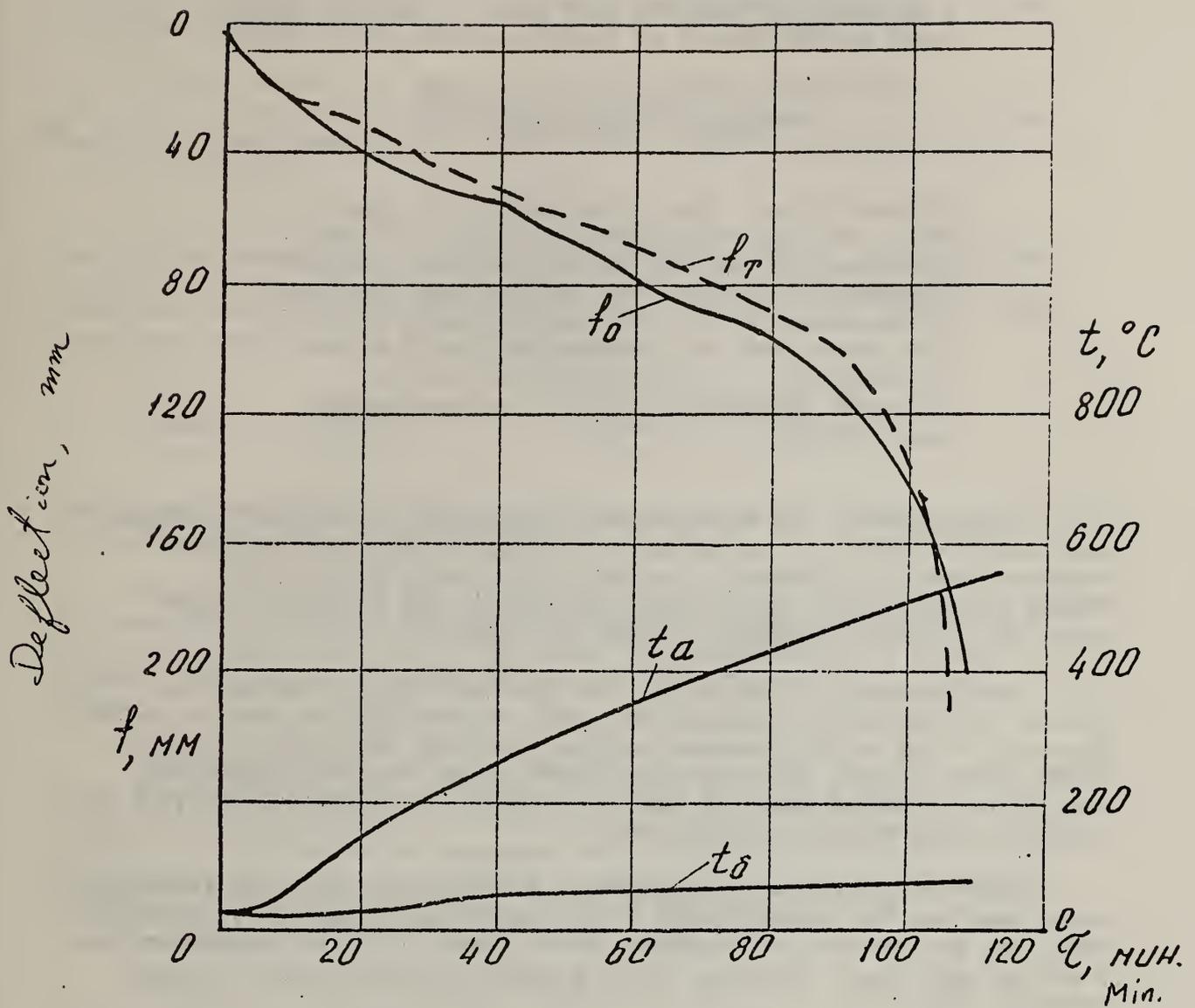
Прогиб в середине пролета плиты

— опытный,
--- теоретический,
$t_a$ температура арматуры,
$t_б$ температура крайнего сжатого волокна бетона

49

A MATHEMATICAL MODEL OF HEAT FLOW IN CONCRETE BEAMS
BASED ON THE RESULTS OF THIRTY-TWO FULL SCALE TESTS

T. D. Lin and M. S. Abrams
Portland Cement Association

Editors' Note:  This presentation was given by
Dr. T. D. Lin from slides and notes.  A final
text has not yet been released by the Portland
Cement Association.  The text has been prepared
from several of Dr. Lin's slides and his notes,
and constitutes an "extended abstract" of the
presentation.  A full publication will be
released subsequently by the Portland Cement
Association.


In the 1960's, the Fire Research Laboratory of the Portland Cement
Association carried out an extensive program to determine isotherms in
concrete beams in a furnace 13 m long, 3.5 m deep, and 2 m wide.
Figure 1 shows six of the 32 specimens used in the program.  A beam
being placed in the furnace is shown on figure 2.

The temperature information from the test program was used to
develop and validate a mathematical model of heat flow in concrete beams.
The major steps in the computer program, outlined in figure 3, include
input, nodal points, the time-temperature curve, boundary conditions,
assignment of volume specific heat and thermal conductivity, and then the
iterative heat transfer calculation.

Input data include the dimensions of the beam.  The time-temperature
curve used was the standard ASTM E 119, which was presented by parabolic
equations as indicated in figures 4 and 5, where y is the temperature and
x is the test time.  There are (n-1) parabolic equations for n control
points.

      Figure 1 = slide 4
      Figure 2 = slide 36
      Figure 3 = slide 6
      Figure 4 = slide 10
      Figure 5 = slide 11

The general solution for the unknown constants of the nth parabolic
equation can be expressed as shown in figure 6, and the temperature com-
puted as shown in figure 7.

The temperatures on the exposed surfaces were prescribed according
to the measured data.  They varied with position on the beam surface
because some of the heat transfer from the furnace to the beam was by

radiation, and the radiative view factor varied with position as shown in figure 8.

Figure 9 indicates the increases in surface temperature, $\Delta U_1$, $\Delta U_2$, etc., at a point on the beam surface for time intervals, $\Delta T_1$, $\Delta T_2$, etc. Combining these measurements, one obtains temperature boundary conditions shown in figure 10.

The initial volume specific heat data (specific heat x density) used in the program were taken from a paper by Harmathy, and are shown in figure 11. The high values at temperatures near 500°C are associated with heat absorption due to chemical decomposition. The symbol $\varepsilon$ represents the extent of the chemical reaction.

Figure 6 = slide 13          Figure 9  = slide 18
Figure 7 = slide 14          Figure 10 = slide 19
Figure 8 = slide 17          Figure 11 = slide 21

The thermal conductivity as a function of temperature, shown in figure 12, was also taken from Harmathy's data.

The equation used for temperature calculation in the computer program is shown in figure 13. Using $\Delta t$ steps of 1/2 minute, convergence was obtained without difficulty. The value of temperature at a central nodal point is taken as the arithmetic mean of the values at four neighboring points.

The specimen used in the computation to be shown is a T beam. Only half of the cross section is shown in figure 14. For simplicity, only temperatures in the circle are shown at t = 1/2 hour in figure 15. The numbers in parentheses are measured data. Those not in parentheses are computed using a program developed at the University of California; the computed results under-estimated the true temperature as much as 220°C. Similar errors were calculated at other times.

Figure 16 shows a measured temperature-position curve along the centerline of a rectangular beam after 1 hr exposure. The dashed line would be expected if the heat flow reached a steady state. Because of the steep slopes of both lines, the temperature difference between the two can be substantial; on the order of 100°C.

Figure 12 = slide 23          Figure 15 = slide 34
Figure 13 = slide 24          Figure 16 = slide 37
Figure 14 = slide 33

To obtain better agreement between calculated temperatures and the data, the literature values of the volume specific heat were adjusted, as a function of temperature, by the empirical correction factors shown in figure 17.

Typical results at 1/2 hr, 1 hr, 2 hr, and 4 hrs of test are shown in figures 18, 19, 20, and 21, showing reasonable agreement. Calculated temperatures at 1 hr in a T beam (that was not tested) are shown in figure 22.

Figure 17 = slide 42          Figure 20 = slide 46
Figure 18 = slide 44          Figure 21 = slide 47
Figure 19 = slide 45          Figure 22 = slide 50

SLIDE – 4

53

SLIDE - 36

SLIDE - 6

TIME, min.

SLIDE-10

56
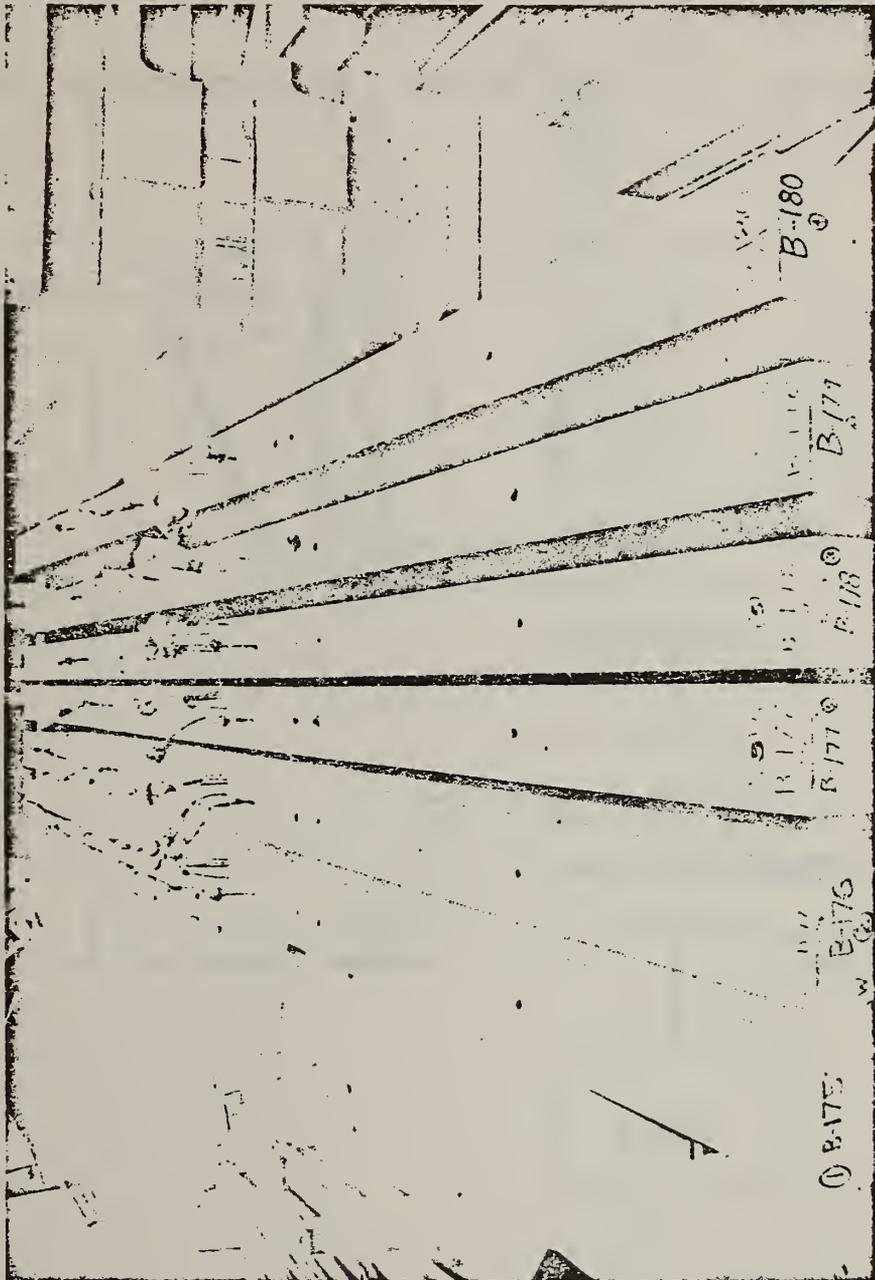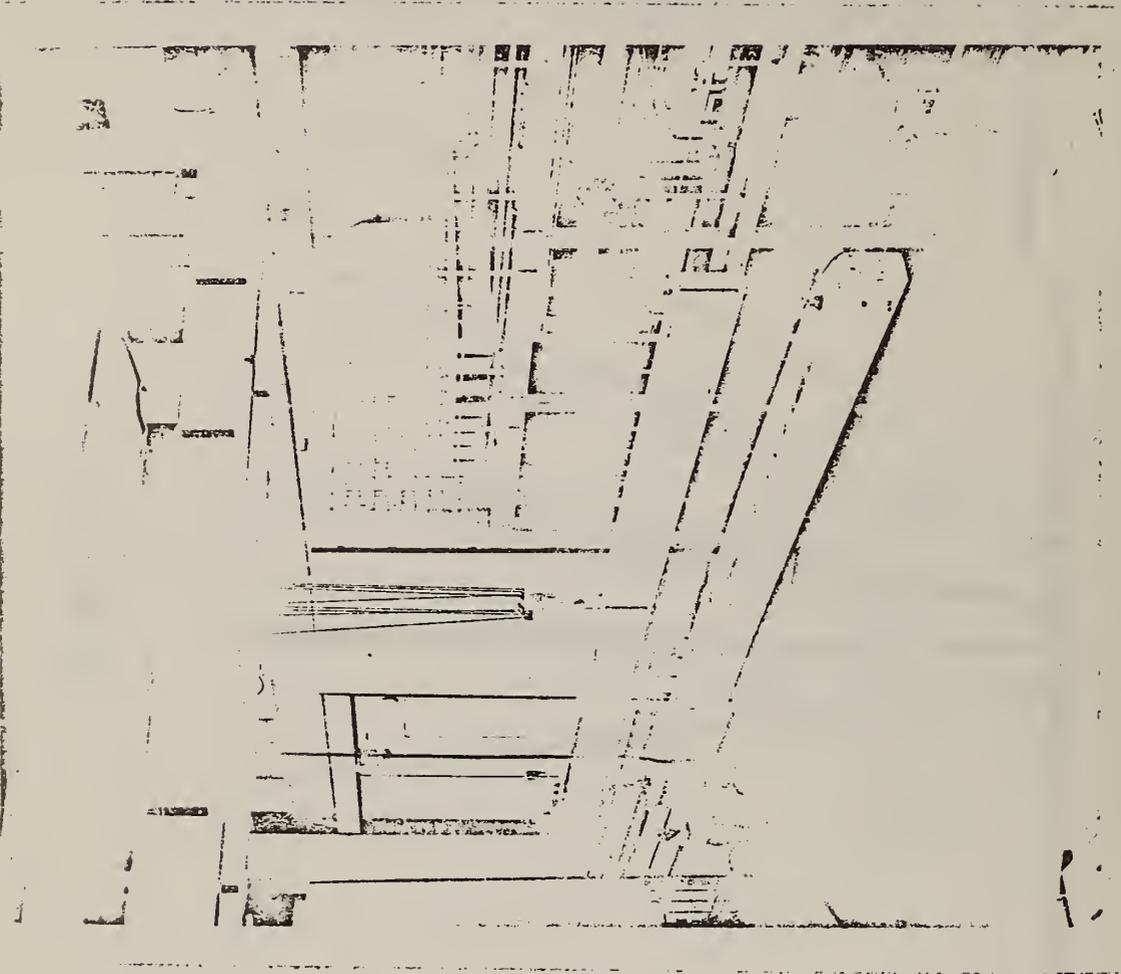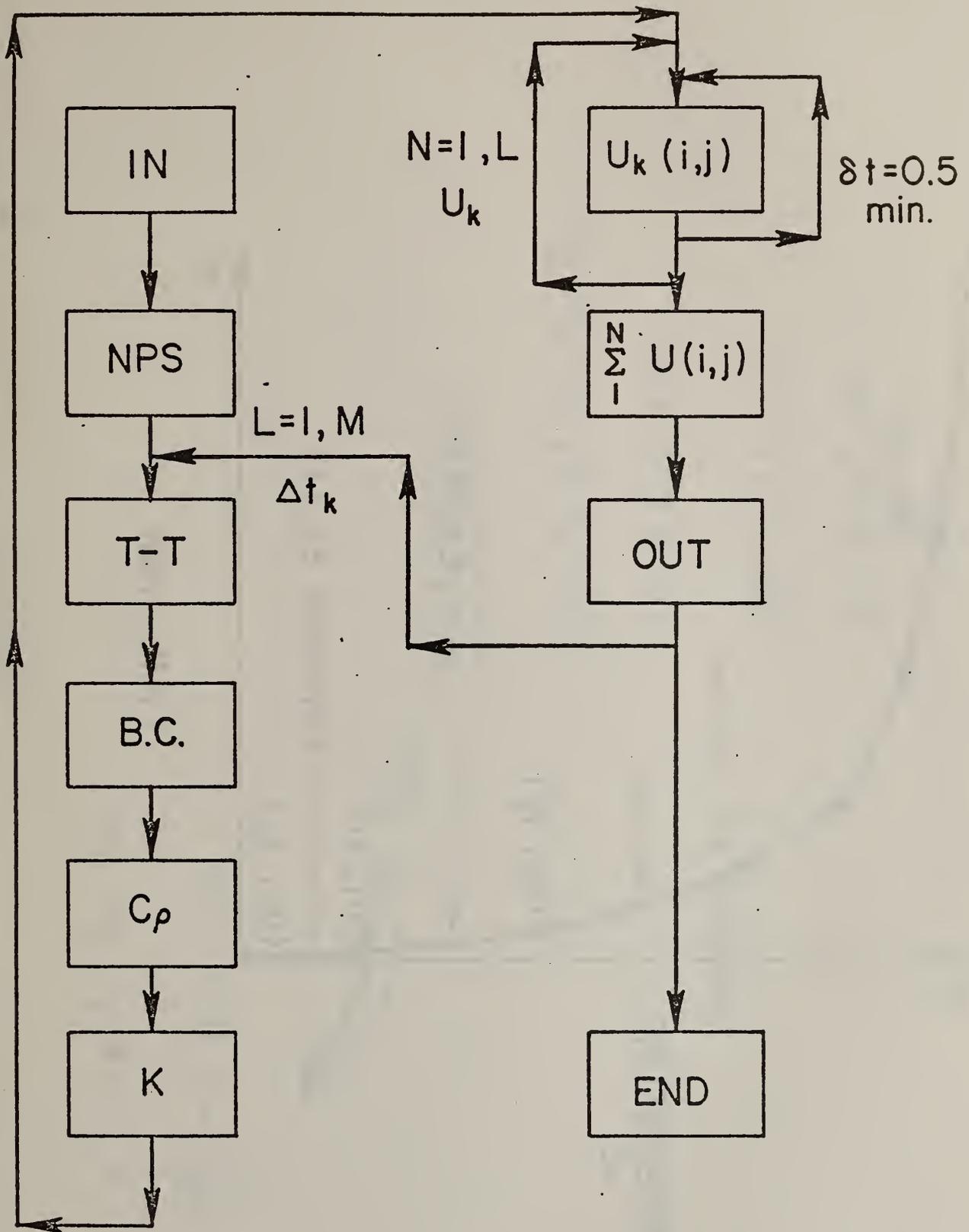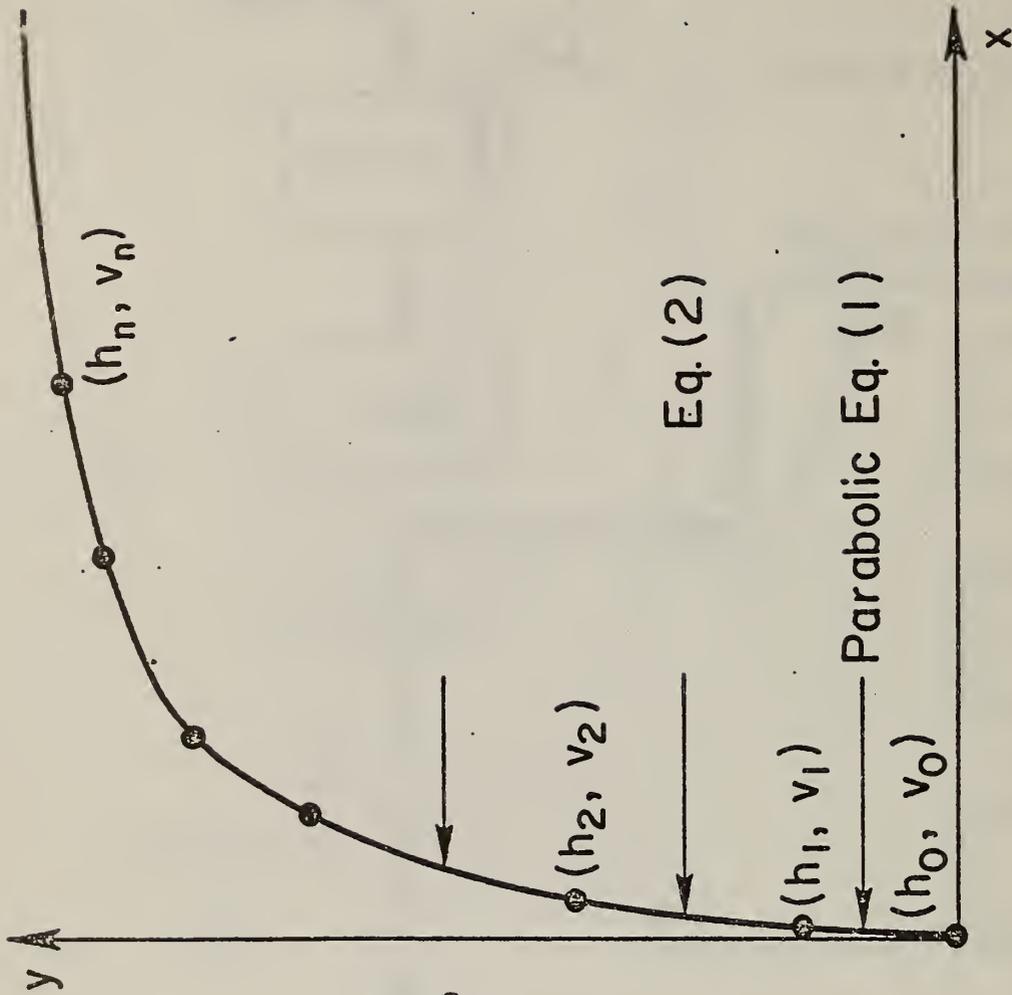
$$x = A_n y^2 + B_n y + C_n$$

$$\frac{dx}{dy} = 2 A_n y + B_n$$

B.C. :

@ pt. $(h_o, v_o)$

$$h_o = A_1 V_o^2 + B_1 V_o + C_1$$

$$0 = 2 A_1 V_o + B_1$$

Parabolic Eq. (1) →   @ = Pt. $(h_1, v_1)$

$$h_1 = A_1 V_1^2 + B_1$$

SLIDE-11

57

General Solution –

$A_n$, $B_n$, $C_n$:

$f(h_{n-1}, v_{n-1}, h_n, v_n, A_{n-1}, B_{n-1}, C_{n-1})$

SLIDE – 13

58

$$\text{Temp} = \frac{-B_n + \left[B_n^2 - 4 A_n (C_n - \text{time})\right]^{1/2}}{2 A_n}$$

SLIDE – 14

59

VIEW FACTOR

SLIDE-17

60
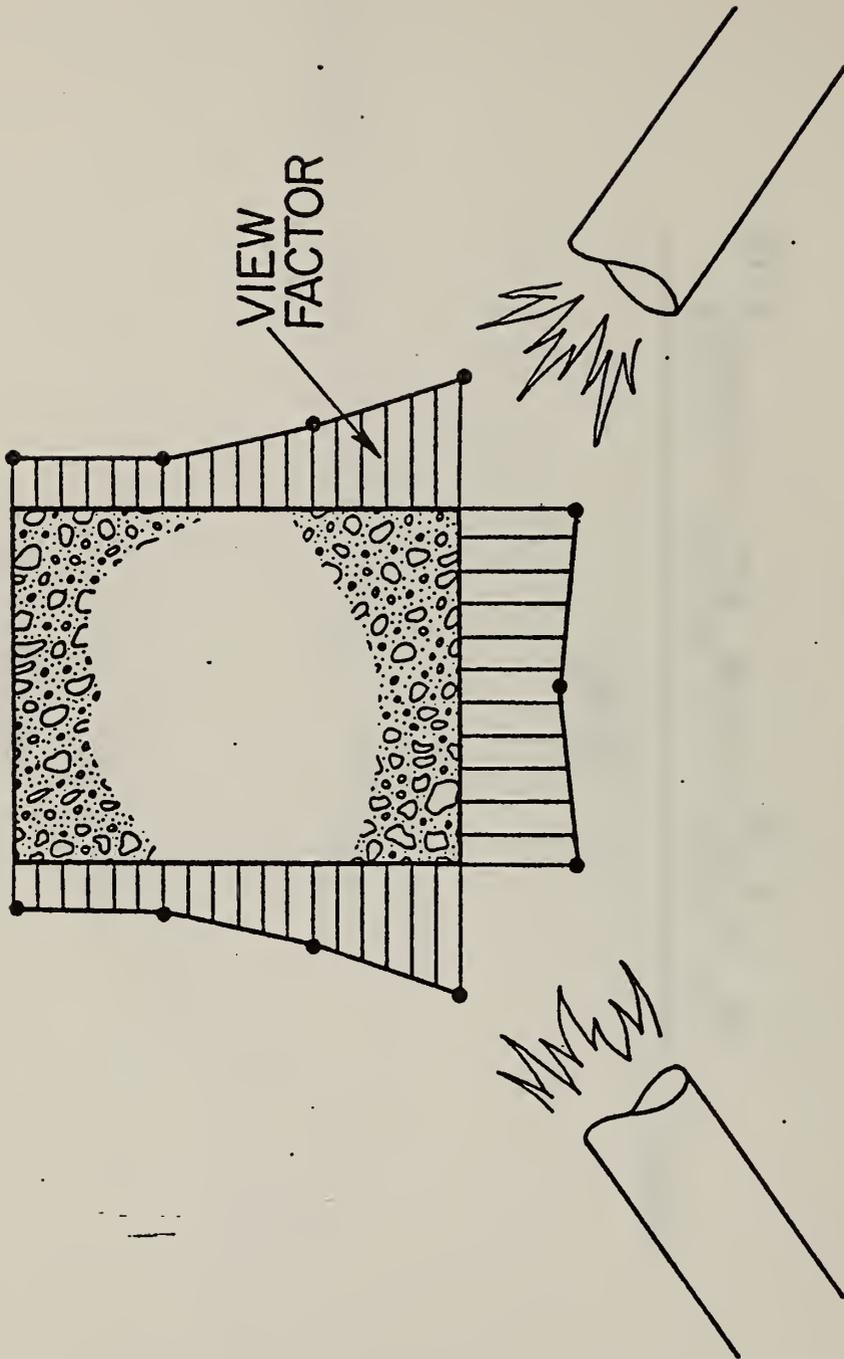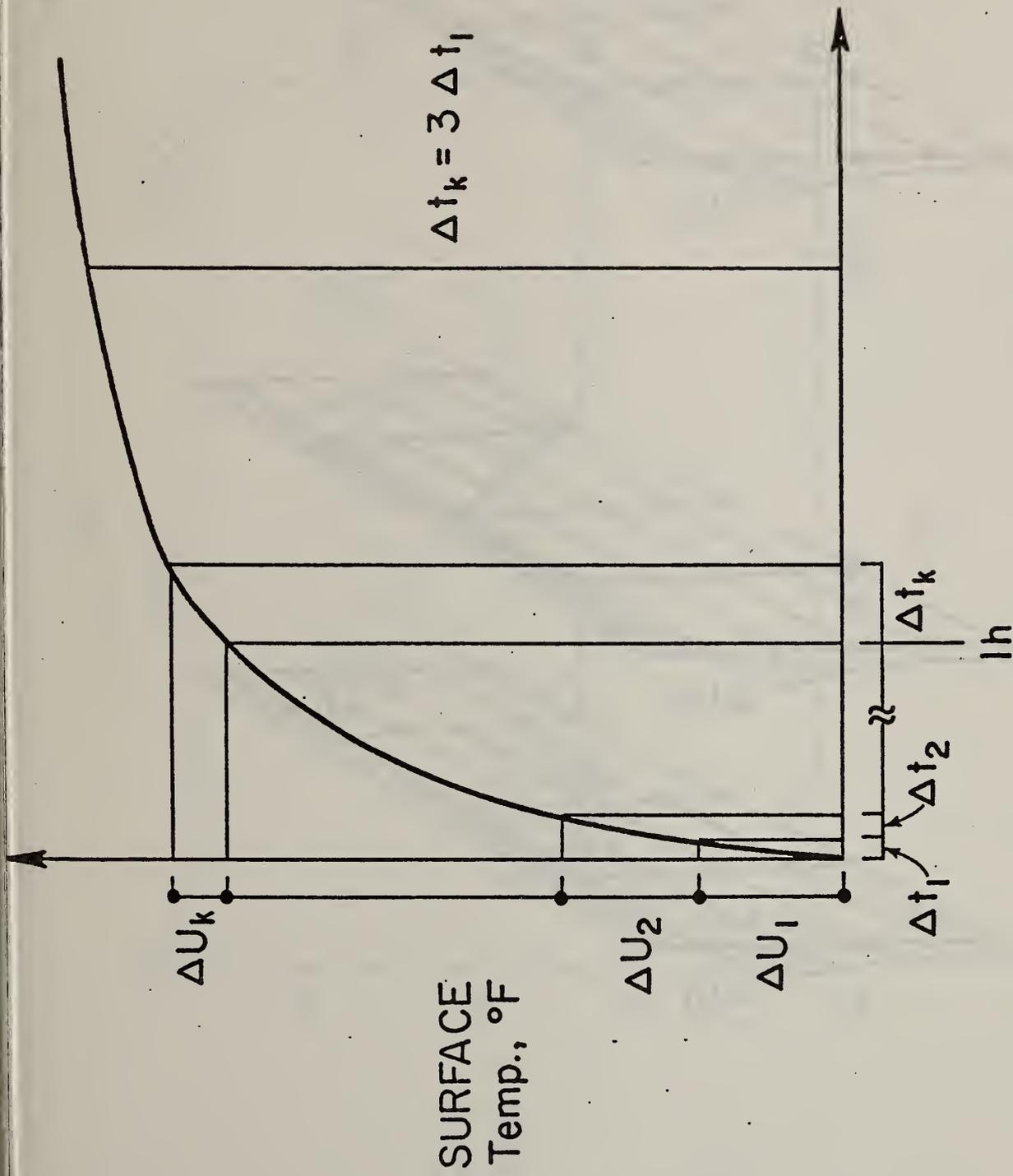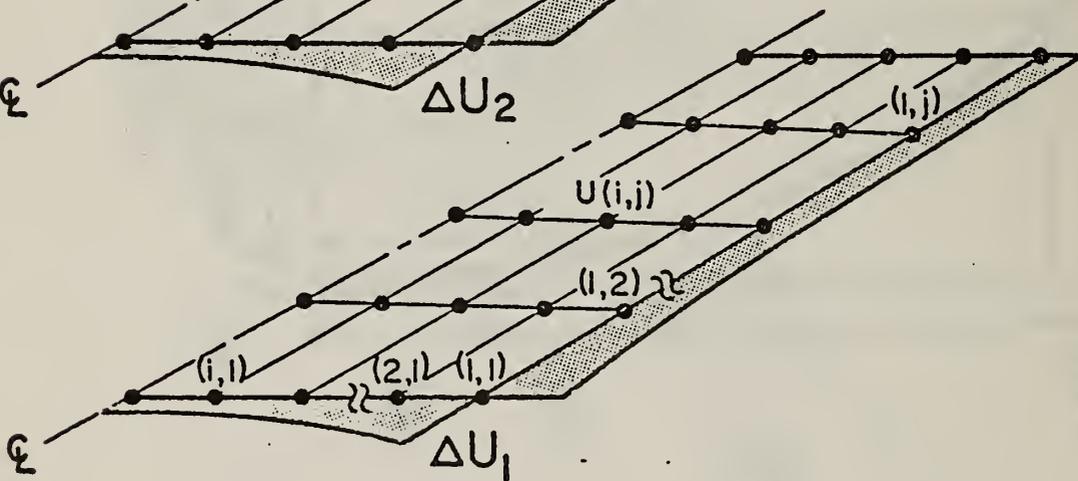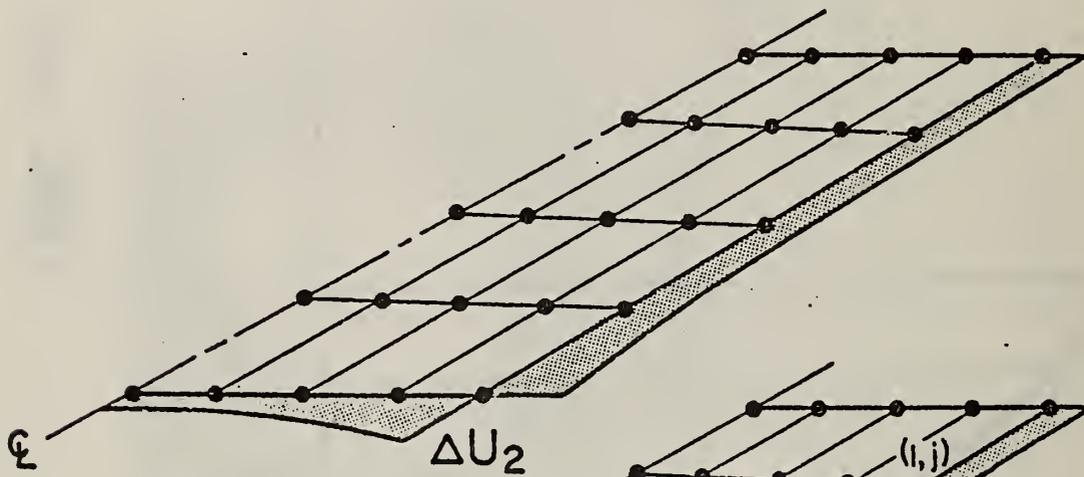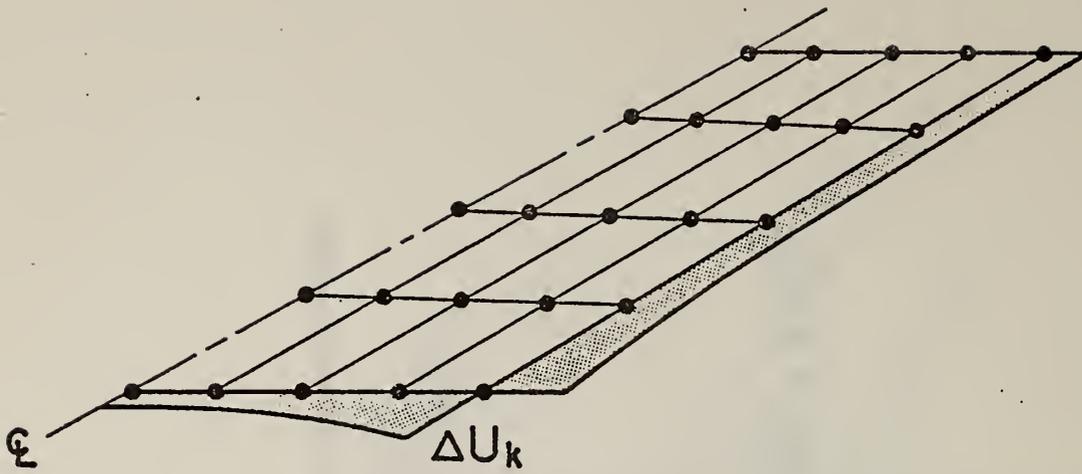
SLIDE-18

SLIDE-19

SLIDE - 21

SLIDE-23

64

65

SLIDE-33

66

SLIDE-34

SLIDE - 37

68

SLIDE-42

69
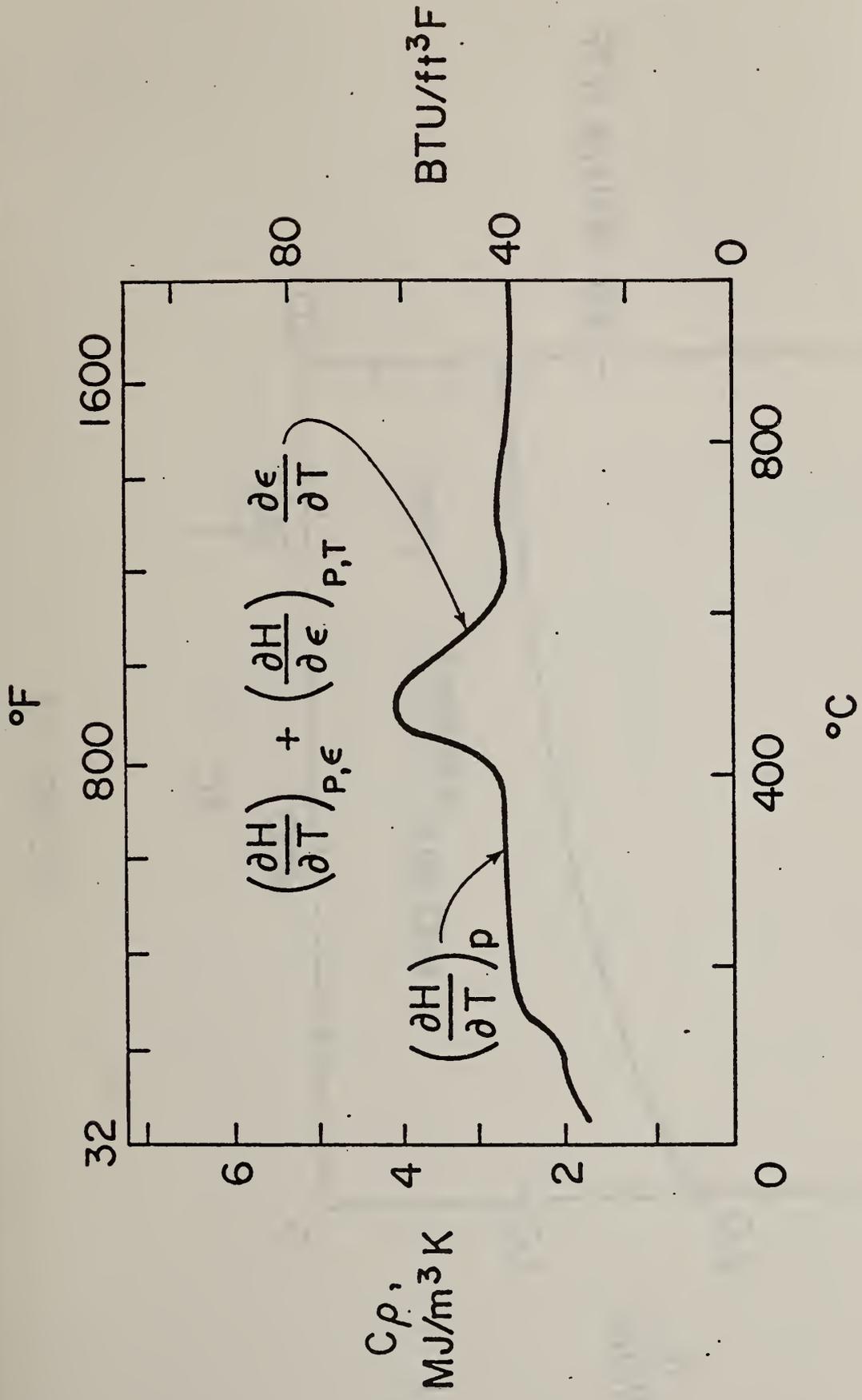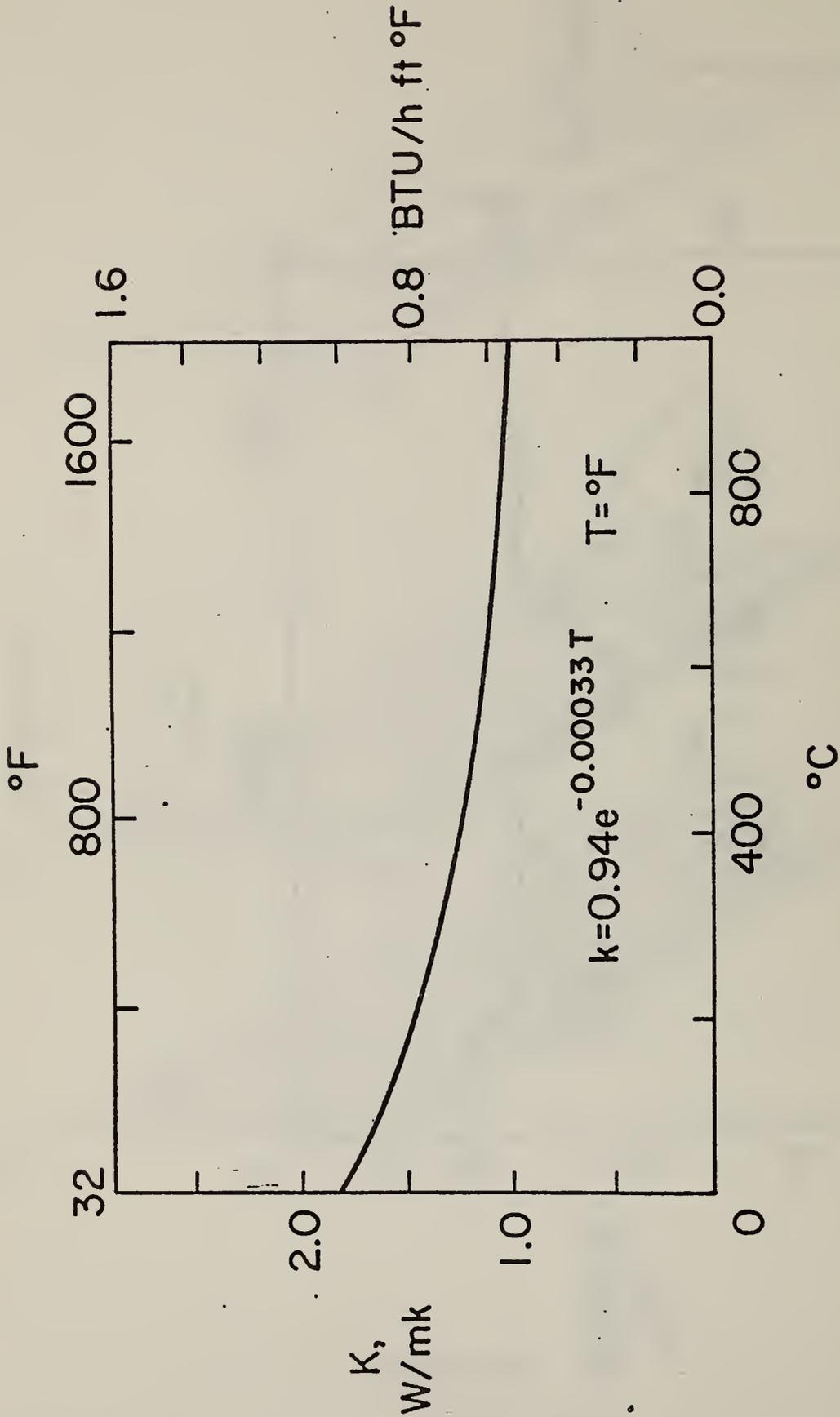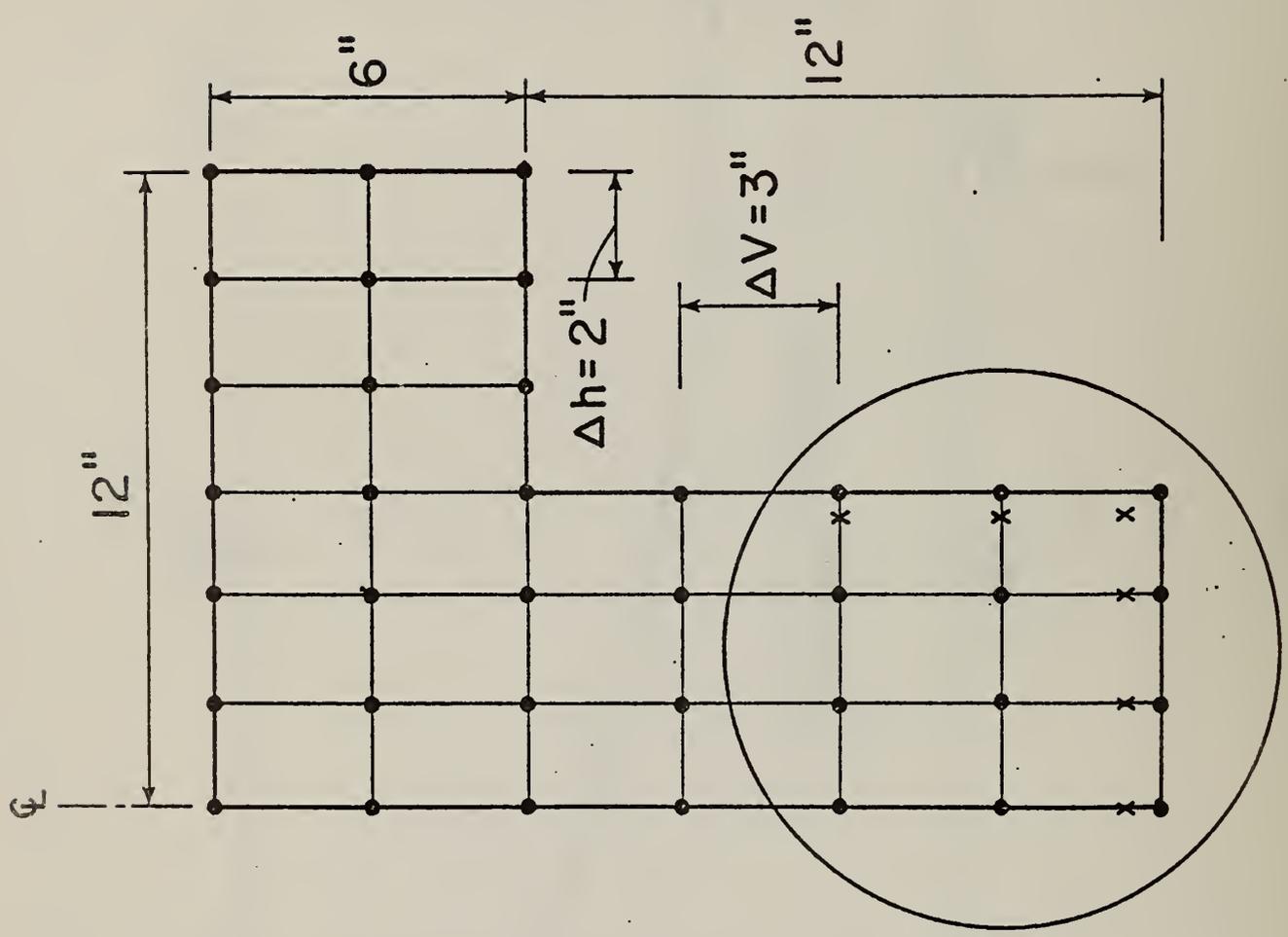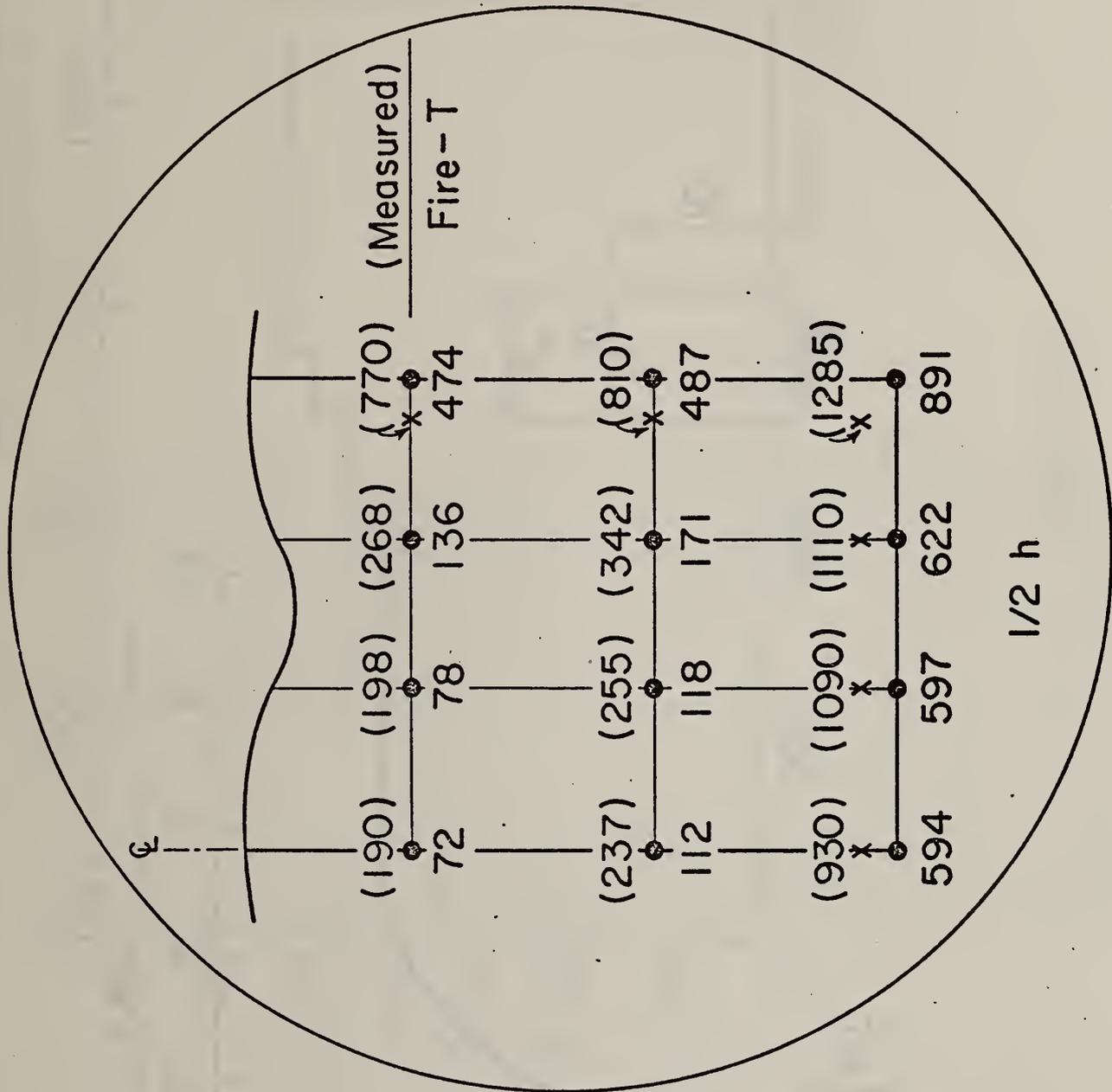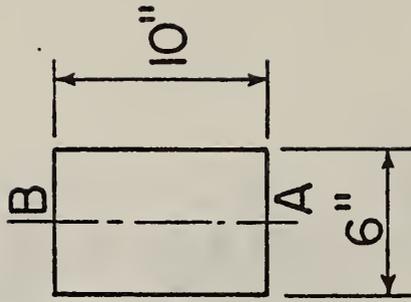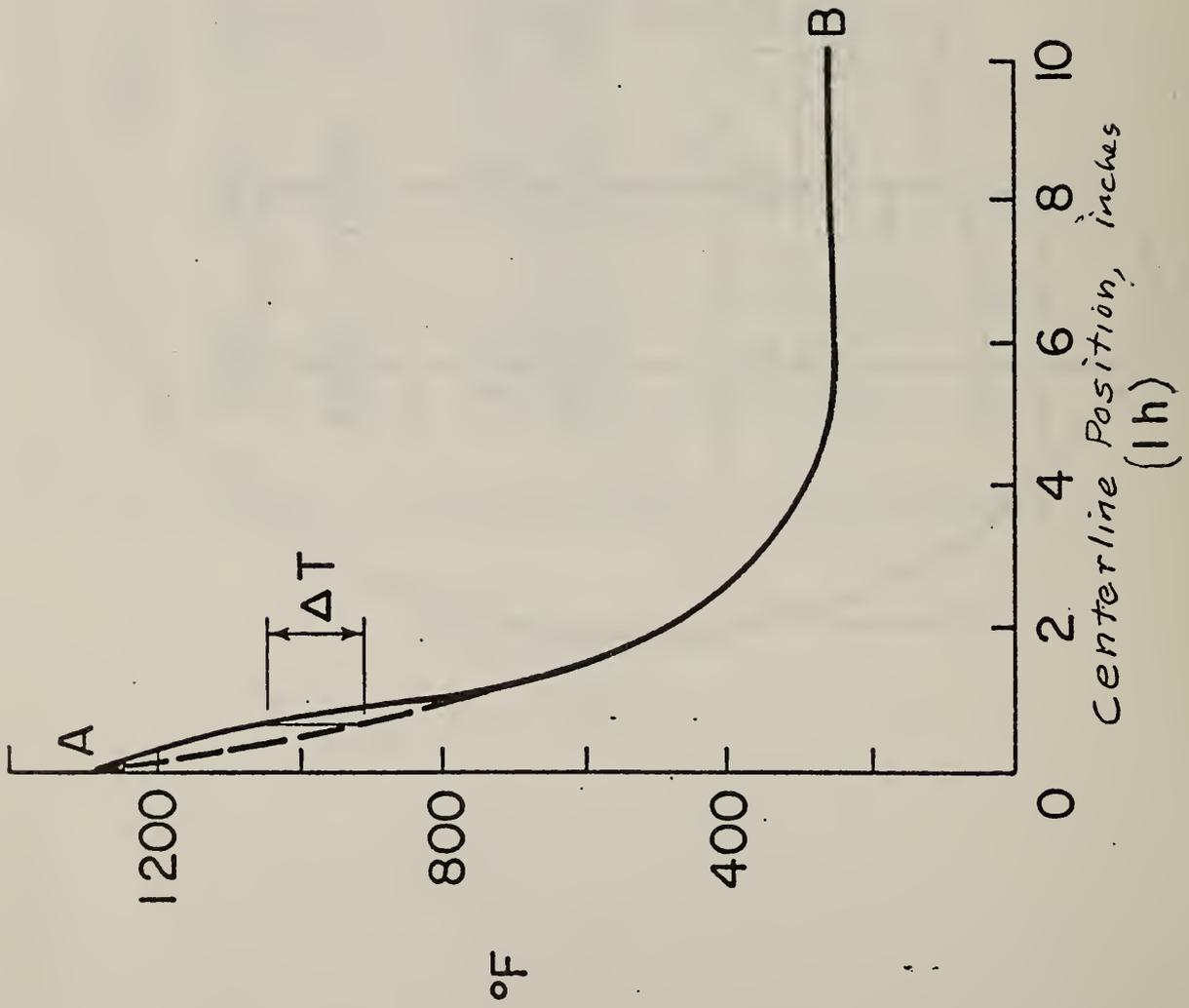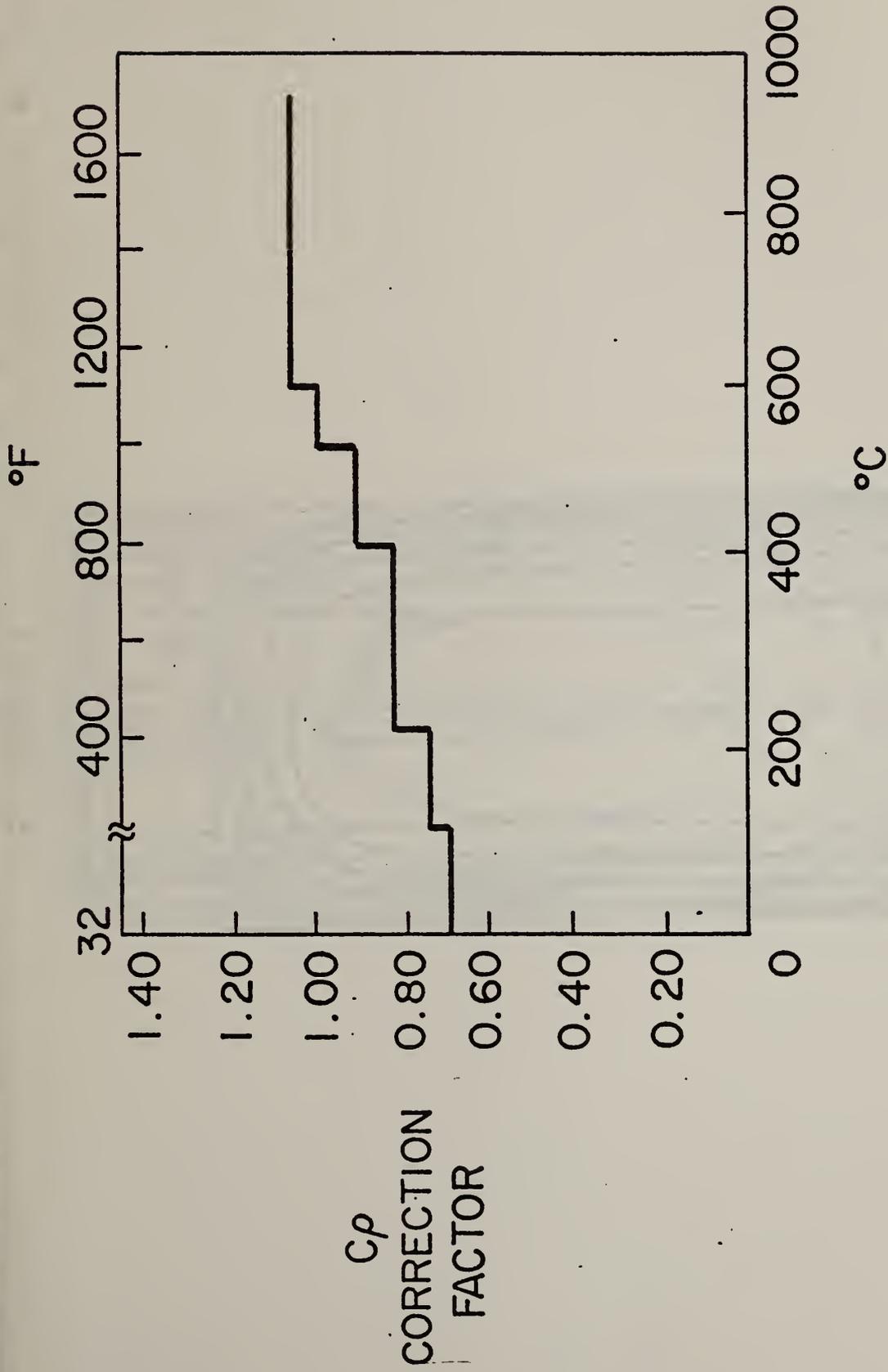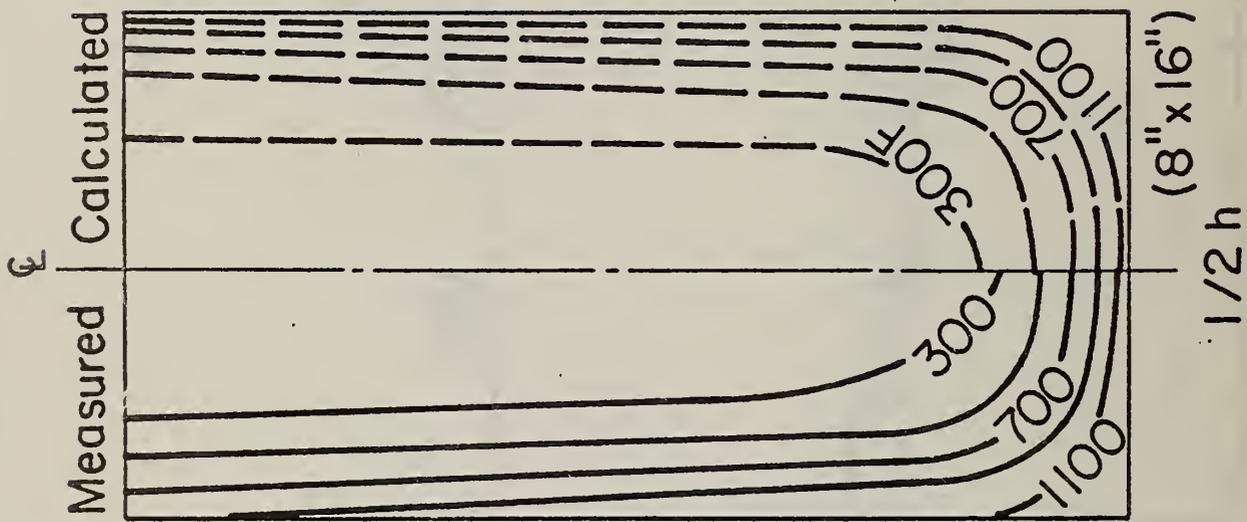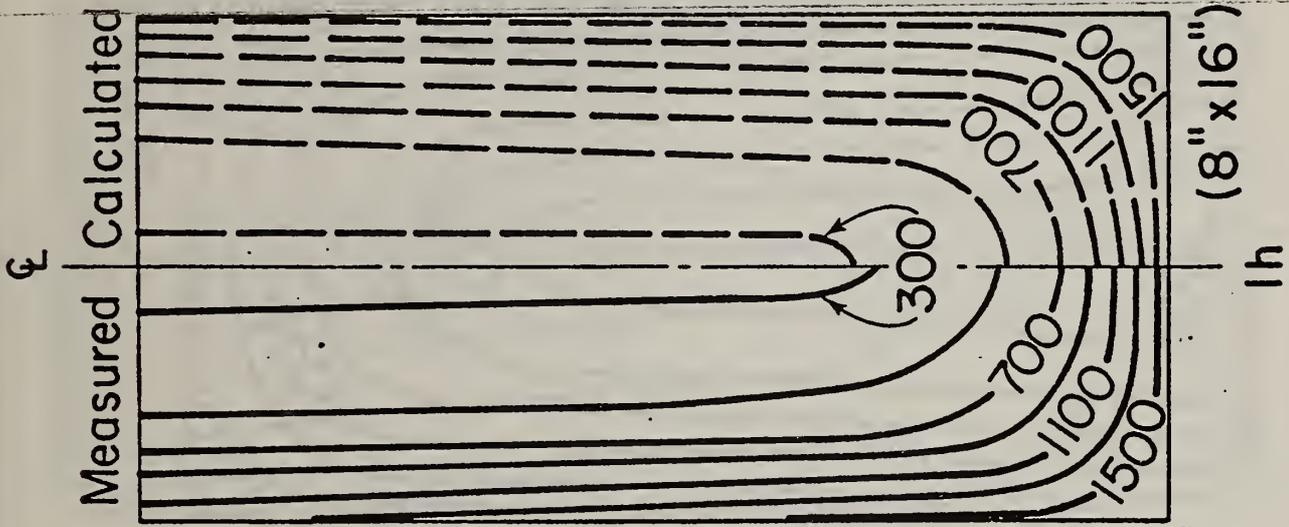
SLIDE – 44

SLIDE-45

SLIDE – 47

Calculated

300
400
600
800
1000
1200
1400

1200
1400

₵

Ih

SLIDE − 50

74
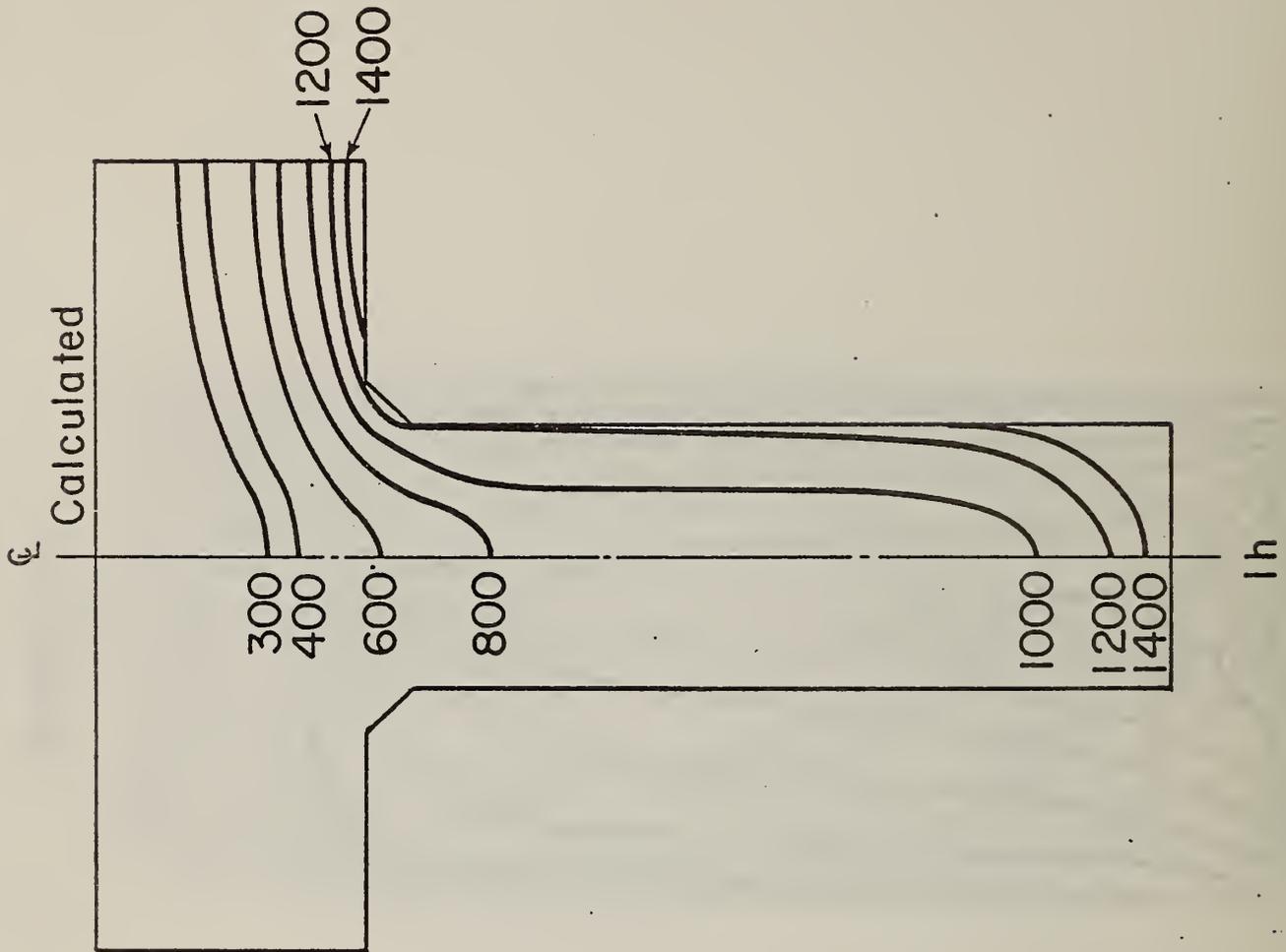
# CALCULATION METHOD FOR DETERMINING THE
# POSSIBILITY OF CONCRETE SPALLING DUE TO FIRES

Dr. V. V. Zhukov, PhD
NIIZhB, Gosstroy USSR

Spalling may take place in reinforced concrete structures exposed to
fire. It occurs suddenly with a great speed and therefore is a most
dangerous phenomenon. As a rule, spalling begins 5-20 min. after the
start of fire and manifests itself as splitting of concrete pieces in
the form of slab rocks about 1 cm$^2$ to 0.5 -1 m$^2$ in area and from 1 mm to
5 cm in thickness from the heated surface. Spalling may continue during
the entire period of fire test until complete destruction of the struc-
ture, accompanied by a sound like a light "slap", cracks of different
intensities or "explosions". Scattering of pieces up to some kilograms
as far as 10-20 m may take place.

Concrete spalling due to fire may quickly lead to failure of reinforced
concrete structures. In this case the limit of structural fire resis-
tance may be considerably less than the required one due to decrease in
size of the concrete cross-section of the structure; decrease in thickness
or complete elimination of concrete cover as well as the formation of a
penetration.

Decrease in cross-section and increase of bending moment due to unsymmetric
heating of columns or panels subjected to vertical loads, results in
stress concentration in the remaining part of cross-section (figure 1).

Thickness decrease or splitting of concrete cover in reinforced concrete
beams results in a quick rise of steel temperature up to a critical·
level (500-700°C) that causes structural failure (figure 2).

Decrease in slab thickness leads to a sharp temperature rise on its
unheated surface to a critical temperature (180-220°C). As a result the
structural fire resistance limit is met.

Spalling may cause a through-hole (penetration) in a slab system at once
or after a certain period of fire exposure. Therefore, the slab will no
longer be a barrier preventing fire passing from one room to another
(figure 3). The fire resistance limit in any structure is reached as
soon as a penetration forms.

Under fire conditions, the onset of spalling often does not take place
simultaneously with collapse of the entire structure, which occurs
considerably later. Sometimes, despite the occurrence of spalling, the
structure can resist fire for a long time. In this case its fire resistance
may be quite sufficient to meet the standard requirements.

When evaluating the effect of spalling on the fire-resistance limits of concrete and reinforced concrete structures one should consider every possibility that may cause a structural failure.

Spalling on load-bearing structures under fire conditions is most dangerous, especially for those with a small cross-section, carrying heavy loads. Their unpredictable failure may result in a collapse of other parts of the structure, or the entire building. For example concrete spalling in columns and panels on ground floors and basements of multi-story buildings is impermissible.

The cause of concrete spalling under fire conditions is the transformation of cracks formed before heating or during heating, from equilibrium state into a non-equilibrium one, and the spontaneous development (figure 4) of high stresses in a local area.

When working out new mix designs or those already available, one should evaluate the possibility of concrete spalling due to fire by a special computational method. This computational method determines the value of a spalling criterion, F, as shown in the following equation:

$$F = a \frac{\alpha \cdot E \cdot \rho}{K \cdot \lambda \cdot \Pi} \cdot W_o^\varepsilon \tag{1}$$

where a – proportionality factor;

$\alpha$ – coefficient of linear thermal expansion of concrete;
E – elastic modulus of heated concrete;
$\rho$ – density of dry concrete;
K – tensile strength of concrete;
$\lambda$ – thermal conductivity of concrete;
$\Pi$ – porosity of concrete;
$W_o^\varepsilon$ – moisture content of concrete by volume before fire.

Table 1

| "F" Value | Comments on spalling and necessary measures |
|---|---|
| $\leq 4$ | Concrete will not spall. No additional check or structural protection are required. |
| $> 4; < 6$ | Concrete may spall in the compression block due to long-term standard load or in members which have thickness less than 4 cm. Here one needs to further control concrete from spalling. |
| $\geq 6$ | Concrete will fail. Special measures should be applied for its protection. |

The possibility of concrete spalling due to fire in a non-load bearing structural element may also be estimated on the basis of mean critical moisture of concretes by weight ($W_b^{Kp}$); 3% - for heavy concrete with coarse aggregate of granite; 4% - for heavy concrete with coarse aggregate of limestone rocks; 5-10% - for lightweight structural concrete with coarse porous aggregate; 2-3% - for heavy silicate concretes.

If the moisture content of concrete by volume ($W_o^\varepsilon$) is less than the mean critical moisture by weight, multiplied by the concrete density and $10^{-3}$ i.e. $W_o^\varepsilon < W_o^{Kp} \cdot \rho \ 10^{-3}$, then the concrete will not spall.

Concrete, having "F" values more than 4 or less than 6, should be checked on the possibility of spalling due to fire in the compression block near the edge fibre on the exposed surface of the concrete member that carries the long term design load. In this case the compressive stresses ($\sigma$) in an independent member due to fire are determined by the long-term design load. The critical volumetric moisture content of concrete $W_o^{Kp}$ is calculated from the formula

$$W_o^{Kp} = \frac{C \cdot R_p^H \cdot \Pi}{\lambda \ (1 + 0, \ 1 + 0.15 \ \sigma_{sh}/R_p)} \qquad (2)$$

where C - proportionality factor;

$R_p^H$ - allowable tensile strength of concrete.

For steam cured concretes, the value of $W_o^{Kp}$ derived from formula (2) should be reduced by a factor of 1.4.

Value $W_o^{Kp}$ is compared with the moisture content $W_o^\varepsilon$.

If $W_o^\varepsilon > W_o^{Kp}$ then the concrete will be subject to spalling due to fire. One should take special measures to protect the concrete against spalling or should decrease the design compressive stresses in the concrete.

To assess concrete spalling in load bearing members under fire conditions one may use the mean critical concrete moisture in connection with a reduced factor "n" that depends on relative compressive stresses in the compression block of the load bearing members. Fire resistant limits of reinforced concrete structures based on spalling may be also determined by a conventional method that gives due regard to the rate of decrease in cross section with a maximum speed of 2.6 mm/min.

Application of these design methods to assess the possibility of concrete spalling due to fire can provide the following solutions: first - to eliminate spalling completely; second - to decrease the probability of manifesting spalling; or third, which serve as a preventative indicator of the spalling.

Among the first measures are the following: use of a water screen, sprinkler and other devices to protect the concrete and reinforced concrete structures from fire; by lowering the room humidity to dry the concrete to a moisture value which will decrease the possibility of spalling; the use of wire mesh with openings measuring from 3 to 15 mm and with the wire diameter from 0.7 to 1 mm at a distance of 0.5 cm from the heated surface to control the spalling; applying insulating plaster 1-2 cm thick on the concrete to retard spalling on the structure surface; application of refractory concretes made with chamotte aggregate to minimize the possibility of spalling; spreading reinforcing fibers such as admixtures (5% of the mass for binding) of materials like asbestos, glass fibre or metal fibre in refractory concrete layers about 1-2 cm thick on the concrete to prevent the concrete from spalling.

These measures may be used for concretes with $F \geq 4$.

Among the second group of measures are the following: placing wire mesh made with 3 mm diameter wires having 10 x 10 cm openings around the main reinforcement at a distance of not more than 0.5-1 cm from the heated surface in the concrete cover of beams and slabs; application of polymer admixture in amounts of 5-10% by weight in the heated surface layer of concrete; application of coarse aggregates that have low coefficients of linear thermal expansion, for example, limestone, basalt, diabases, blast furnace slag instead of granite or natural quartz sand; substitution of a part (not less than 1/3) or the whole natural sand by the sand from limestone, basalt, diabases, siennit or diorite; use of concrete composition with a limited amount of cement paste (portland cement of not more than 400 kg per 1 $m^3$ of concrete mix) and with high values of W/C ratio (not less than 0.5); use of concretes with lightweight aggregates; application of cement concretes with lightweight aggregates; application of cement with air entraining agent; application of cements with lower specific surface and slag portland cement; use of fine-ground admixtures from blast-furnace and cast slags.

All these measures are applied to the case when "F" is less than 6 or more than 4, but their full efficiency still requires spot checks by fire tests.

Among the measures of the third group are the following: application (in reinforced concrete structures) of reinforcement of the same area but of smaller diameter; use of structures with cross-sections without irregular angles, for instance, round columns without cut-off angles instead of columns of rectangular or square cross section.

## Conclusion

This calculation method allows us to evaluate the possibility of concrete spalling due to fires and to plan measures to prevent structural failures without conducting fire tests on reinforced concrete structures.

## Captions

For Recommendations on the Protection of Concrete and Reinforced Concrete Structures Against Spalling Due to Fires

Figure 1. Effect of spalling on the fire resistance limit of supporting reinforced concrete panels exposed to one-sided fire

$\quad$ a – panel scheme with load (P);
$\quad$ b – time ($\tau$) – temperature ($T_n$) curve under fire conditions;
$\quad\quad$ 1 – panel; 2 – spalled piece of concrete;
$\quad$ $\tau_1$ – fire-resistance limit of panel under spalling; $\tau_2$ – fire-resistance limit of panel without spalling; $t_n 1$ – fire temperature at time $\tau_1$; $T_{n,2}$ – fire temperature at time $\tau_2$.

Figure 2. Effect of spalling on fire resistance limit of reinforced concrete beam

$\quad$ a – scheme of beam; b – time-temperature curves for room atmosphere and reinforcement; 1 – beam; 2 – reinforcement; 3 – spalled piece of concrete; 4 – room time-temperature curve; 5 – time-temperature curve for reinforcement under spalling; 6 – time-temperature curve for reinforcement without spalling

Figure 3. Effect of concrete spalling on fire resistance limit of reinforced concrete enclosure structure

$\quad$ a – scheme of enclosure structure; b – time-temperature curve, 5 – fire exposure; 1 – ceiling (floor); 2 – floor; 3 – enclosure structure; 4 – spalled piece of concrete; 5 and 6 – rooms which are divided by the structure; 7 – time-temperature curve in room 5; 8 – the same on surface of enclosure structure from the side of room 6, where concrete spalling does not occur; 9 – the same under concrete spalling.

Figure 4. Trajectory of crack, resulting in concrete splitting under spalling

$\quad$ 1. Cross-section of concrete member;
$\quad$ 2. crack;
$\quad$ 3. trajectory;
$\quad$ 4. temperature diagram.

Рис. 1    Figure 1



Figure 2

80
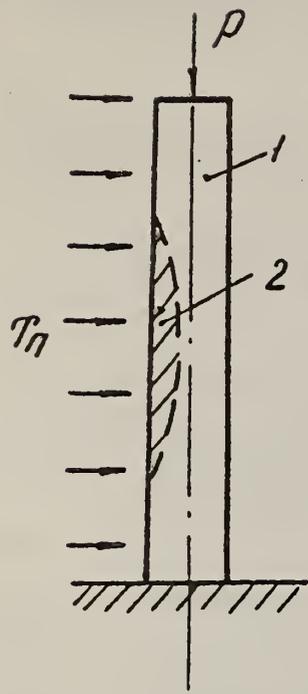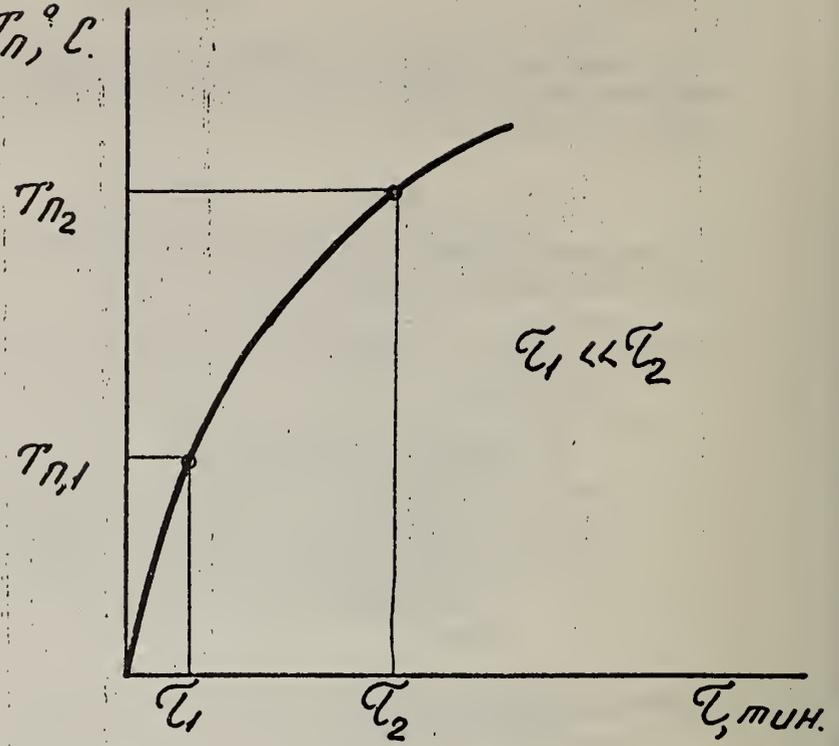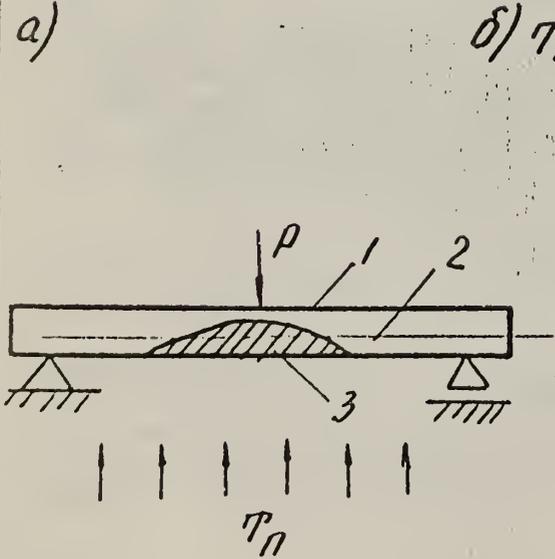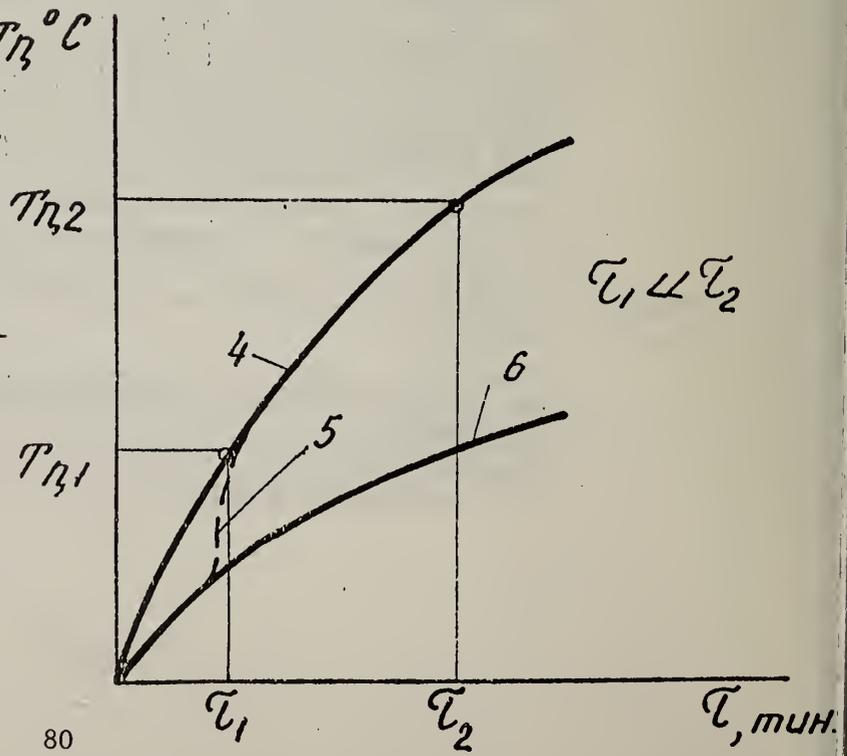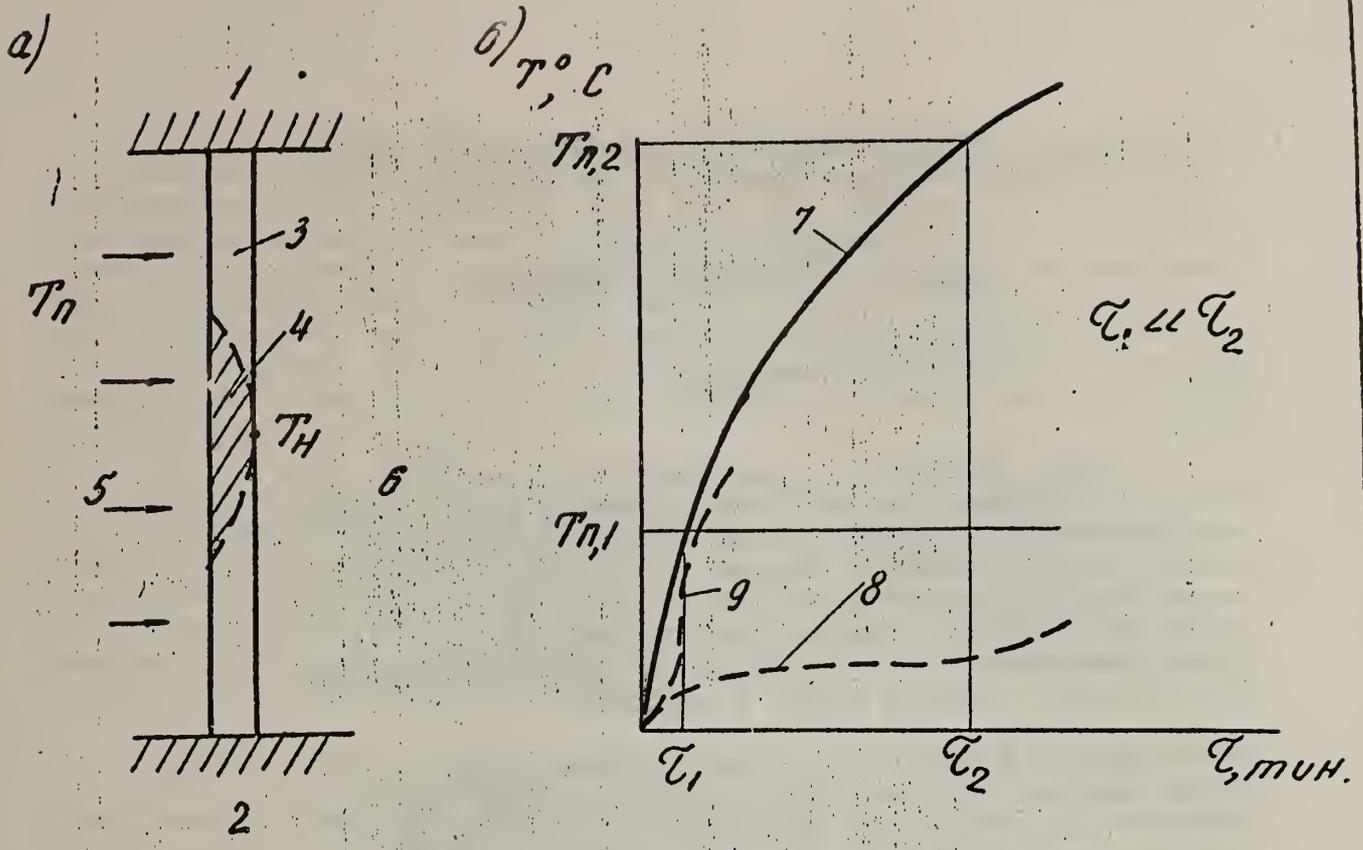
Рис. 3   Figure 3



Figure 4

81
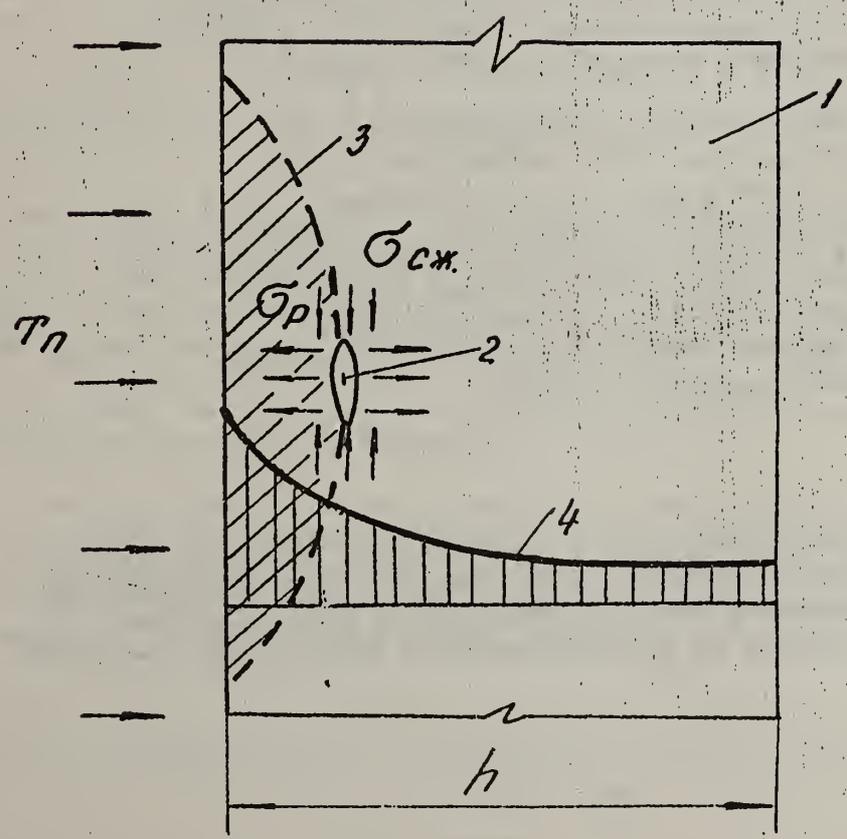
CALCULATING FIRE RESISTANCE FOR STEEL STRUCTURAL MEMBERS
LOCATED ON THE OUTER WALLS OF BUILDINGS

Richard G. Gewain
American Iron and Steel Institute

Abstract

In 1964, American Iron and Steel Institute (AISI) fire
research programs were initiated to develop data on factors
influencing fire intensity, flame projection and other
aspects of fire behavior relevant to a fire-safe design
method for structural members located outside the exterior
walls of buildings. The methods also were developed in
such a manner so as to be appropriate, with modifications,
for structural members inside a building.

Margaret Law of Ove Arup and Partners, under
joint contract with AISI and the Constructional Steel
Research and Development Organization (Constrado) of
England, prepared a detailed technical report setting
out the most plausible models of flame projection from
openings in building walls. The University of Maryland
Department of Fire Protection Engineering used the
technical report to prepare the AISI Design Guide
arranged for ready reference by fire protection officials
and designers. It presents a step by step analysis and
procedures for designing fire safe exterior members.

This paper deals with the establishment of the
conditions of fire exposure (fire temperature in the
fire compartment, flame geometry and temperature). This
paper is an explanation of Miss Law's work, for which
she was nominated for Engineering News-Record's Engineer
of the Year Award in 1979. The conditions of heat
transfer from the fire exposure to the structural
members are not covered in this paper but are contained
in the Design Guide available from AISI.

Introduction

"Fire exposure arises from interior and exterior origins. The
evaluation of the exterior exposure can be done only with difficulty in
quantitative terms, and the gradual accumulation of data from actual
fires will probably continue as the main guidance in providing the proper
protection."

This quote by Mr. S. H. Ingberg, then Senior Engineer, U.S. Bureau of Standards, introduced his paper, "The Severity of Fire in Buildings," published in the NFPA Quarterly, July 1928 (Vol. 22, No. 1, pp. 43-61). This indicated that the development of the ASTM E 119 fire test and fire protection requirements in building codes focused attention on structural elements located inside a building exposed to a fire inside a building. This is still true today; however, engineering methods continue to be developed to place structural fire resistance on the same basis as seismic design, and the design for structural performance when exposed to external loads such as wind and snow.

Building codes require fire resistance ratings for specific portions of a building. These ratings are based on a specific exposure period based on the Standard Fire Test, ASTM E 119. As a result of studies in the United States and abroad, it has been shown that the fire exposure in building fires (fig. 1) may not be the same as the standard fire exposure; little has been done except to modify the code-required fire endurance time for structural members.

Building members located in the interior of a building are surrounded by flames and by heated surfaces (walls, ceiling, and floor) of the fire compartment. These heating conditions are similar to those in the Standard Fire Test where the member is located within the test furnace.

Exterior structural members are exposed to two conditions; radiation through a window from the fire in the compartment, and radiation and convection from flames and hot gases issuing from windows. The value of the intensity of the radiation received by the exterior member varies with the relative position of the window and flame (radiator) and the surface of the structural member (receiver). Also the structural member loses heat to the air surrounding it at normal ambient temperature. Depending on the size and location of the structural member and the behavior of the fully developed fire, structural members may not need any fire protection.

Early attempts to assess the external fire exposure involved experiments with ASTM E 119 furnace tests which had a window in the furnace wall [1][1]. This effort showed that no matter how long the E 119 fire test is conducted, the flame exposure is generally less severe than from a more realistic building fire. As a result, there have been full-scale experimental fire tests with exterior structural elements exposed to flames and radiation from "real" fires. As a result of these tests, approvals have been obtained for specific buildings [2] (fig. 2).

A design approach has been developed to assess the fire exposure from a building fire including fires of a size beyond the size limits of practical fire tests. This approach will permit analysis of the external heat transfer to structural members and enables engineers to calculate the amount of fire protection if any is needed.

---

[1]Figures in brackets refer to references at the end of this paper.

For structural steel elements, critical conditions can be defined in terms of a critical steel temperature and given the heat transfer conditions, calculation of the steel temperatures is relatively simple.

The main problem is to define the external heat transfer. A large body of data on building fire and flame behavior exists. It has been collected and analyzed by Margaret Law at Ove Arup and Partners, London, England, to estimate external heat transfer for practical designs in buildings [3]. Correlations have been derived, not only from model-scale experiments but also from measurements for a wide range of experimental fires in large-scale building compartments.

The Designers Manual prepared by Ove Arup and Partners was used by the University of Maryland, Fire Protection Engineering Department to develop a Design Guide [4] for Exposed Exterior Steel.

The principal elements needed to make this design approach useful are:

(1)  Flame shapes must be based on parameters which can be readily identified by the designer.

(2)  Temperatures of the room fire and the external flame plume must be determined by relatively simple equations.

(3)  Heat transfer must be simplified to facilitate calculation.

Research

Most flame and structural damage occurs in the post flashcver period. This phase of the fire has been studied by many researchers and Dr. Philip Thomas [5] has summarized this work. Analysis of a fully developed fire is complex and the model developed used a number of simplifying conclusions--principally, a uniform temperature throughout the compartment and that fuel burns in a uniform way. Important parameters involving the way a fully developed fire burns have been defined by Margaret Law and the large amount of test data has been used to show how these parameters interact.

Ingberg was the first to study the relationships between fire load density and fire severity and these studies have formed the basis for building code requirements for the fire resistance of structures. Later, Fujita [6] quantified the effect of ventilation in terms of the area and height of ventilation openings, usually the window. Later work on models was carried out cooperatively by the Counseil International de Batiment (CIB) [7] which modified the Fujita relationship on ventilation by introducing the size and shape of the fire compartment (fig. 3). In addition to using scale models in the CIB program, the various factors were studied in full scale studies at Borehamwood [8], Maisieres-les-Metz [9] and Carteret, New Jersey [10].

## INTERIOR FIRE BEHAVIOR

A number of full scale experiments have been carried out using wood cribs as fuel; in still or lightly moving air, although some tests were conducted with additional air supply.

Two of the most important factors affecting exterior fire exposure from a fully developed interior fire are rate of burning, which affects flame size and fire duration; and fire temperatures, which affects the radiation from the window.

### Rate of Burning

In the case of natural draft conditions where the fire behavior and compartment dimensions control the air flow, continuous weighing of the fire load during tests have shown that the rate of weight loss is fairly steady over the fully developed fire period when the weight of the fire load falls from 80 percent to 30 percent of its initial value. This rate of burning R is defined as:

$$R = \frac{L}{T} \tag{1}$$

Where T is the effective fire duration and L is the total fire load in the fire compartment.

For a free burning condition the value of $T$ is $T_F$ and is determined by the characteristics of the fire load--thin fuels with large surface areas give a smaller value for $T_F$.

Where ventilation is restricted, as is generally the case, there is an upper limit for R regardless of how large the fire load. It has been shown that the important parameters are the window area $A_w$, and its height h, and the area of the heat absorbing surfaces of the fire compartment $A_T$, and the ratio of the depth D to width W of the fire compartment (fig. 4).

Thomas has drawn a line through the points in figure 3 which include measurements for R which have been reported for large-scale, ventilation restricted fires. The values for R are in reasonable agreement with the CIB data.

The following equation for R results from the Thomas Line:

$$R = \frac{1.22}{E} \cdot 1-e^{-065\eta} \tag{2}$$

where the ventilation factor is:

$$\eta = \frac{A_T}{A_w \sqrt{h}} \tag{3}$$

EXTERIOR FLAME BEHAVIOR

Yokoi [11] made the first comprehensive study of flame projection from windows to evaluate the risk of vertical fire spread. He demonstrated several influences on the trajectory of the flame plume and temperature of the flame plume. The wall above the window absorbs heat but restricts air from entering at the flame edges which will force the flame plume away from the wall; the wider the window, the closer the flame plume remains to the wall. Yokoi defined the shape of the window as the ratio of the width to the height of the upper half of the window and derived a series of plume shapes for different window shapes. In checking the results of his experiments against large scale tests using wood cribs he obtained good agreement. He also observed that where ventilation is restricted the emerging gases will continue to burn after leaving the window and will affect correlation.

Thomas [12] correlated results of model tests by Webster [13-15] using dimensional analysis similar to that used by Yokoi. By assigning a flame tip temperature of 1000°F or 1460°R reasonable agreement is obtained between these data and those of Yokoi.

Additional work by Seigel [16] on tests conducted at Underwriters Laboratories in which he treated the flames as forced horizontal jets, defined their projection by a temperature of 1000°F at the flame tip and recorded flame temperature in the exterior flame plume.

Other work was conducted at Borehamwood and full scale tests in the United States. All of this work was used to establish the relationships defining the flame plume dimensions outside of windows.

Flame Plume Dimensions

No Draft Condition--The flame dimensions are an important factor in calculating radiation from the flame to the receiver or exposed structural member. Thomas and Law [17] analyzing the data of Yokoi, Webster et al. showed a correlation that takes into account the dominant role of buoyancy and the turbulent mixing of hot gases in a flame emerging from a window. The recommended correlation shown in figure 8 is expressed as follows:

$$\frac{Z+h}{h} = 16 \left[ \frac{R}{A_w P_z (gh)^{1/2}} \right]^{2/3} \qquad (11)$$

This may be written for the flame height (Z) as follows:

$$Z = 3.55 \left[ \frac{R}{w} \right]^{2/3} -h \qquad (12)$$

This distance of the center of the flame tip away from the exterior face of the building (x) depends on the shape of the window and if there is a wall above the window. A wall is defined as a vertical surface which

the fire compartment geometry is:

$$E = (A_w)^{-1} \sqrt{\frac{D}{hW}} \qquad (4)$$

For a particular fire load and compartment, R should be calculated for both equations (1) and (2) and the lower value used.

Fire Temperature

There is a maximum temperature developed within the fire compartment, depending on the fire load and compartment dimensions. Thomas gives the correlation of the CIB measurements of average fire temperature rise $\theta_f$ over the fully developed fire period as a function of $\eta$ as shown in figure 5. The significance of this data is that the fire temperature rises to a maximum for $\eta = 5$ to 10 then declines. The average fire temperature also depends on the fire load as shown in figure 6 for plots of large scale tests with low fire load densities which fall well below the Thomas curve. There is justification to assume that the following equation for a no draft or natural draft condition gives a maximum or upper limit fire temperature ($\theta_f$ or $T_f$) for a given value of $\eta$:

$$T_f = 8025 \text{ (Function of } \psi)(\text{Function of } \eta) + 520 \qquad (5)$$

where the fire load and fire compartment is

$$\psi = \frac{L}{\sqrt{A_w A_t}} \quad \text{and} \qquad (6)$$

the function of $\psi$ and $\eta$:

$$f_x \psi = 1 - e^{-0.25\psi} \quad \text{and} \qquad (7)$$

$$f_x \eta = \frac{1 - e^{-0.18\eta}}{\sqrt{\eta}} \qquad (8)$$

There is limited information in the rate of burning under forced draft conditions. The results of fire tests using excess air at Underwriters Laboratories show no significant variation of temperature with $\eta$ or air supply but fire temperature ($\theta_f$ or $T_f$) can be related to $\psi$ as shown in figure 7 with the curve shown having the following equation:

$$T_f = 2160 \text{ (Function of } \psi) + 520 \qquad (9)$$

where the function of $\psi$ is:

$$f_x \psi = 1 - e^{-0.20\psi} \qquad (10)$$

87

retains its integrity exceeding two-thirds the flame height. A flame will be projected away from the wall surface if air can get behind it. In situations where there is either a narrow window or a wide window with no wall above, air can move more easily between the flame and the wall thereby deflecting the flame or flames outward. The work of Yokoi was studied and a regression analysis for flame tip projection gives:

$$\frac{x}{h} = \frac{0.454}{n^{0.53}} \tag{13}$$

where n is the ratio of width to height of the upper half of the windows.

Data plotted in figure 9 indicates the flame tip projection decreases with n and is less than half the window height for values of n exceeding unity, which includes most situations. Therefore the value of x is independent of n and may be represented by the following equation if there is no wall above:

$$x = 0.6h \left[\frac{Z}{h}\right]^{1/3} \tag{14}$$

If there is a wall above the window and where h (window height) is less than 1.25 times the window width

$$x = \frac{h}{3} \tag{15}$$

Where there is a wall above the window and where h is greater than 1.25 times the window width and the distance to any other window on the same floor exceeds four widths of an individual window, use the following equation:

$$x = 0.3h \left(\frac{h}{w_1}\right)^{0.54} \tag{16}$$

Forced Draft

The effect of a forced draft on a fire is to increase the rate of burning of a ventilation controlled fire. Also for a given rate of burning, wind or a draft blowing flames out a window may also affect the flame size and direction. Experimental data from tests at Underwriters Laboratories is plotted in figure 10 and indicates that the correlation proposed by Seigel with $R/A_w^{1/2}$ raised to the power of unity, is reasonable provided the wind effect (u) is included. The following solves for the height of the flame above the bottom of the window:

$$Z+h = 17.7 \left(\frac{1}{u}\right)^{0.43} Q \tag{17}$$

where

$$Q = \frac{R}{\sqrt{A_w}} \tag{18}$$

88

Analysis of experimental data shown in figure 11 shows a correlation between horizontal projection, flame height, window height and wind speed. Comparison with this correlation shows that as wind speed increases, flame height decreases, but that the horizontal projection increases. The horizontal projection (x) of the flame tip away from the building is given thus:

$$x = 0.077 \ J^{0.22}(Z+h) \tag{19}$$

where

$$J = \frac{u^2}{h} \tag{20}$$

The maximum width $w_z$ of a flame emerging from a window usually exceeds the window width. The angle made by the emerging flame as shown in figure 12 averages 11 degrees giving:

$$\frac{W_z-w}{2x} = 0.194 \tag{21}$$

therefore

$$w_z \cong w+0.4x \tag{22}$$

## EFFECTIVE FLAME BOUNDARY

In order to estimate heat transfer from a flame plume, boundaries must be defined. The temperature distribution across a flame section as shown in figure 13 shows one approach is to define the flame boundary by the 1000°F contour. Margaret Law proposed that since radiative transfer will be an integrated effect, which can be made equivalent to a uniform effective temperature, an equivalent step function distribution be used. Since radiant transfer is so sensitive to the value of temperature, she suggested adoption of the axial temperature (maximum) for the step function with a defined effective thickness. The problem is to define this effective thickness bearing in mind an assumption of maximum temperature across the flame thickness.

Natural draft: In figure 14 the flame emerges above the neutral plane from the upper two-thirds of the window. The flame width varies little with the distance from the window plane. Therefore it is reasonable to assume the step function remains the same size throughout the trajectory $(wx2h/_3)$. This assumption is consistent with estimated values of emissivity. Wind may deflect the flame sideways and it is assumed that the deflection will not exceed 45 degrees.

Forced draft: The flame shown in figure 14 can emerge from the entire window opening. The width of the flame does increase with distance out from the window. It is also reasonable to assume the vertical dimension increases, however, the upper vertical increase is already contained in the value for Z, it is proposed that the size of the flame

89

at the window opening be h x w, increasing to h x (w + 0.4x) at the flame tip as shown in figure 14.

TEMPERATURE AT FLAME AXIS

Correlation of test data to analyze the temperature distribution in flames for natural draft or no draft condition is illustrated in figure 15. The line in figure 15 has the equation:

$$\frac{\theta_Z}{\theta_0} = 1 - 0.33 \frac{\ell w}{R} \tag{23}$$

A similar correlation for the forced draft data is shown in figure 16 and the line has the following equation:

$$\frac{\theta_Z}{\theta_0} = 1 - 0.33 \frac{\ell A_w^{1/2}}{R} \tag{24}$$

Note in equations (23) and (24) that the decrease in flame temperature is directly proportional to the distance along the center line of the flame. By substituting $\theta_Z$ or $T_Z$ = 940°F (1000°F-60°F) and $\ell$ = X in equations (23) and (24) the value of $\theta_0$ or $T_0$ may be derived. For fires with natural draft, this may give values of $\theta_0$ or $T_0$ (at the window) greater than the fire temperature $\theta_f$ or $T_f$ in the fire compartment. This results from ignition of unburned gases outside the fire compartment. Where forced draft exists the opposite can be expected.

Conclusion

In order to be able to calculate heat transfer to a structural member from flames, it is necessary to establish the shape and size of flame emerging from the window, and the temperature distribution within the flame. The flame height and its horizontal projection from the building can be calculated, as can the temperature at any point on the flame axis. From this information an "idealized" flame is determined so that heat transfer calculations can be made.

The temperature of the fire within the building is determined. Although the fire temperature in a building fire will vary with time, the maximum temperature reached by the fire is used since this will result in the highest temperature in the material exposed.

The assessment of fire exposure using the procedures given in this paper will provide a conservative basis for calculating temperatures of exterior structural members. In some building fires the duration of the fire may be sufficiently long that bare or unprotected structural members will be heated to "steady-state-conditions." In other words the material may reach an equilibrium temperature such that the heat falling on the material will be balanced by the heat losses to the surroundings. The steady state condition assumes the most conservative approach to heat transfer.

90

# REFERENCES

[1] Pryor, A.J. Fire Exposure of Exterior Structural Members Final Report, July 1965, Southwest Research Institute, San Antonio, Texas, 1965.

[2] Seigel, L.G. Fire Test of an Exposed Steel Spandrel Girder Materials Research and Standards, MTRSA 10(2), 1970, pp. 10-13.

[3] Ove Arup and Partners. Design Guide for Fire Safety of Bare Exterior Structural Steel -- Technical Reports and Designers Manual, Report for American Iron and Steel Institute, Ove Arup and Partners, London, England. January 1977.

[4] American Iron and Steel Institute. Design Guide for Fire Safe Structural Steel. March 1979

[5] Thomas, P.H. Fires in Model Rooms: CIB Research Programmes Building Research Establishment Current Paper CP 32/74 BRE, Borehamwood, 1974.

[6] Fujita, K. Characteristics of Fire Inside a Non-combustible Room and Prevention of Fire Damage Report2(2). Japanese Ministry of Construction, Building Research Institute, Tokyo.

[7] Heselden, A.J.M. and P.J. Thomas. Fully Developed Fires in Single Compartments, CIB Report No. 20 Fire Research Note 923/1972, Joinst Fire Research Organization, Borehamwood, 1972.

[8] Heselden, A.J.M., P.G. Smith, and C.R. Theobald. Fires in a Large Compartment Containing Structural Steelwork -- Detailed Measurements of Fire Behavior. Fire Research Note 646/1966, Joint Fire Research Organization, Borehamwood, 1966.

[9] Arnault, P., H. Ehm and J. Kruppa. Rapport Experimental sur les Essais avec de Feux Naturels Executes dans la Petite Installation, CECM 3/73-11-FCTICM, Puteaux, France, June 1973

[10] Gross, D. Field Burnout Tests of Apartment Dwelling Units Building Science Series 10, National Bureau of Standards, September 29, 1967.

[11] Yokoi, S. Study on the Prevention of Fire-spread Caused by Hot Upward Current. Report No. 34, Japanese Building Research Institute Tokyo, 1960.

[12] Thomas, P.H. On the Heights of Buoyant Flames Fire Research Note 489/1961, Joint Fire Research Orangization, Borehamwood, 1961.

91

[13] Webster, C.T., Monica M. Raftery, and P.G. Smith
The Burning of Fires in Rooms Part II.  Fire Research Note 401/1959
Joint Fire Research Organization.  Borehamwood, 1959.

[14] Webster, C.T., Monica M. Raftery, and P.G. Smith
The Burning of Fires in Rooms, Part III.  Fire Research Note
474/1961, Joint Fire Research Organization, Borehamwood, 1961.

[15] Webster, C.T. and P.G. Smith.  The Burning of Fires in Rooms,
Part IV. Fire Research Note 574/1964, Joint Fire Research Organization,
Borehamwood, 1964.

[16] Seigel, L.G.  The Projection of Flames from Burning Buildings
Fire Technology, 5(1), pp. 43-51, 1969.

[17] Thomas, P.H. and Margaret Law.  The Projection of Flames
from Buildings on Fire  Fire Prevention Science and Technology,
No. 10, pp. 19-26, December 1974.

Explanation of Symbols

| SYMBOL | MEANING | AMERICAN | METRIC |
|--------|---------|----------|--------|
| $A_T$ | Total room surface area $= 2A_F + 2H(DxW)$ | $ft^2$ | $m^2$ |
| $A_W$ | Window area | $ft^2$ | $m^2$ |
| $D$ | Depth of compartment | $ft$ | $m$ |
| $E$ | $\left(A_W\right)^{-1}\sqrt{\dfrac{D}{Wh}}$ | $lb/min\ ft^{5/2}$ | $kg/sec\ m^{5/2}$ |
| $e$ | Base of Natural logs | | |
| $H$ | Height of compartment | $ft$ | $m$ |
| $h$ | Height of window | $ft$ | $m$ |
| $L$ | Fire load | $lb$ | $kg$ |
| $\ell$ | Distance along flame centerline from window | $ft$ | $m$ |
| $Q$ | $\dfrac{R}{\sqrt{A_W}}$ | $lb/min/ft$ | $kg/sec/m$ |
| $R$ | Rate of burning | $lb/min$ | $kg/sec$ |
| $T$ | Absolute temperature | $R$ | $K$ |
| $u$ | Velocity | $ft/min$ | $m/sec$ |
| $W$ | Width of compartment | $ft$ | $m$ |
| $w$ | Width of window | $ft$ | $m$ |
| $X$ | Centerline distance of flame tip from window | $ft$ | $m$ |
| $x$ | Horizontal distance of center of flame tip from window | $ft$ | $m$ |
| $z$ | Vertical distance of flame above top of window | $ft$ | $m$ |
| $\rho$ | Density | $lb/ft^3$ | $kg/m^3$ |
| $\tau$ | Fire duration | $min$ | $sec$ |
| $\tau_F$ | Free burning fire duration | $min$ | $sec$ |
| $f,o,z$ | These subscripts denote fire, window plane, and flame respectively. | | |

(UNITS)

93

Summarized Relationships

|  | U.S. Units <br> lb, ft, min, Btu, °R | S.I. Units <br> kg, m, s, kJ, °K |
|---|---|---|

**Natural Draft**

Flame  $z + h$
$$3.55\left(\frac{R}{w}\right)^{2/3} \qquad 12.8\left(\frac{R}{w}\right)^{2/3}$$

x "no-wall"
$$0.60h\left(\frac{z}{h}\right)^{1/3} \qquad 0.60h\left(\frac{z}{h}\right)^{1/3}$$

$\dfrac{\theta_z}{\theta_o}$
$$1 - 0.33\frac{lw}{R} \qquad 1 - 0.027\frac{lw}{R}$$

Fire  $R$  or  $\dfrac{L}{\tau_F}$
$$\frac{1.22(1 - e^{-0.065\eta})A_w h^{1/2}}{(D/W)^{1/2}} \qquad \frac{0.18(1 - e^{-0.036\eta})A_w h^{1/2}}{(D/W)^{1/2}}$$

$\theta_f$
$$\frac{8025(1 - e^{-0.18\eta})(1 - e^{-0.25\psi})}{\eta^{1/2}} \qquad \frac{6000(1 - e^{-0.10\eta})(1 - e^{-0.05\psi})}{\eta^{1/2}}$$

**Forced Draft**

Flame  $z + h$
$$17.7\left(\frac{1}{u}\right)^{0.43}\left(\frac{R}{A_w^{1/2}}\right) \qquad 23.9\left(\frac{1}{u}\right)^{0.43}\left(\frac{R}{A_w^{1/2}}\right)$$

x
$$0.077\left(\frac{u^2}{h}\right)^{0.22}(z + h) \qquad 0.61\left(\frac{u^2}{h}\right)^{0.22}(z + h)$$

| | Flame | Fire |
|---|---|---|
| $w_z$ | $w + 0.4x$ | $w + 0.4x$ |
| $\dfrac{\theta_z}{\theta_o}$ | $1 - 0.33 \dfrac{\ell A_w^{1/2}}{R}$ | $1 - 0.027 \dfrac{\tau A_w^{1/2}}{R}$ |
| $R$ | $\dfrac{L}{\tau_F}$ | $\dfrac{L}{\tau_F}$ |
| $\theta_f$ | $2160(1 - e^{-0.20\psi})$ | $1200(1 - e^{-0.40\psi})$ |

| Test Number | Fire Load (PSF) | Forced Air (CFM) | Windows ||| 
| | | | Number | Size, Ft X Ft | Area, Sq Ft |
| --- | --- | --- | --- | --- | --- |
| 1 | 10 | 0 | 1 | 2X6 | 12 |
| 2 | 10 | 0 | 1 | 2X8 | 16 |
| 3 | 10 | 0 | 2 | 2X6 | 24 |
| 4 | 10 | 0 | 2 | 2X8 | 32 |
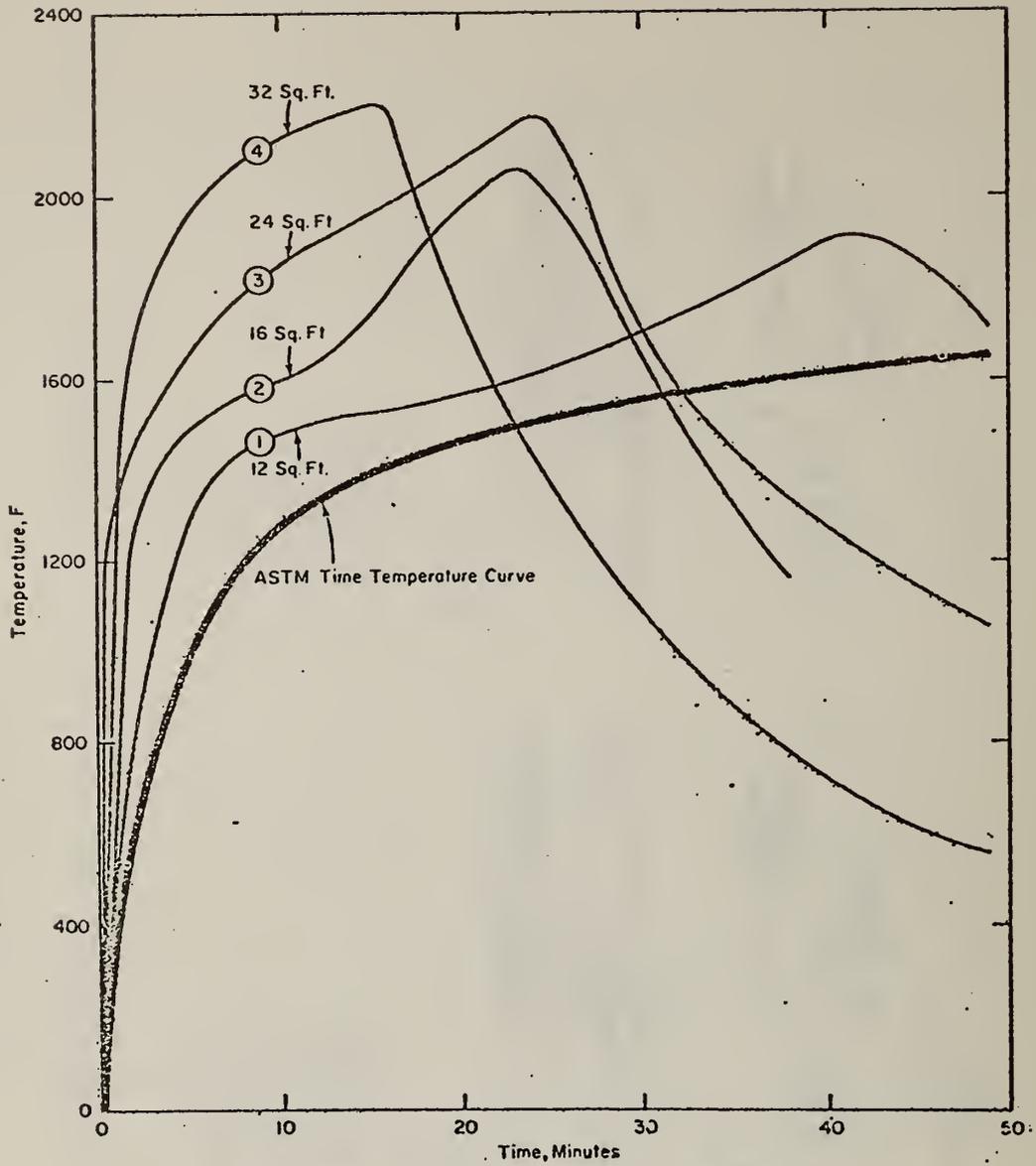
Figure 1 -- Effect of window area on fire temperatures during burnout tests (natural air flow).

Figure 2 -- One Liberty Plaza, N.Y.C.,
exterior surfaces of steel spandrel beams
have the web bare and the flanges flame-
shielded.
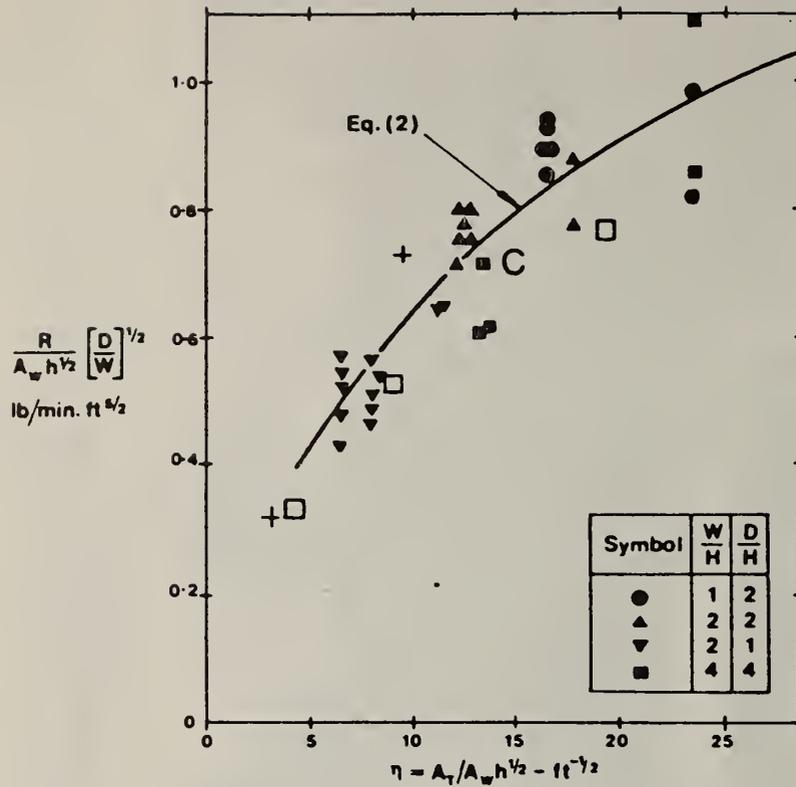
*Fig.* 3. *Variation of* $R/A_w h^{1/2}$ *with compartment size and ventilation, as given by Thomas for CIB data*

$A_F = D.W$

$A_w = w.h$

$A_T = 2A_F + 2H(D+W) - A_w$
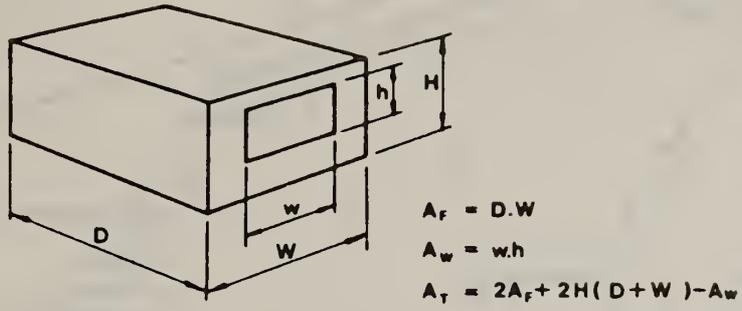
*Fig.* 4. *Simple fire compartment*
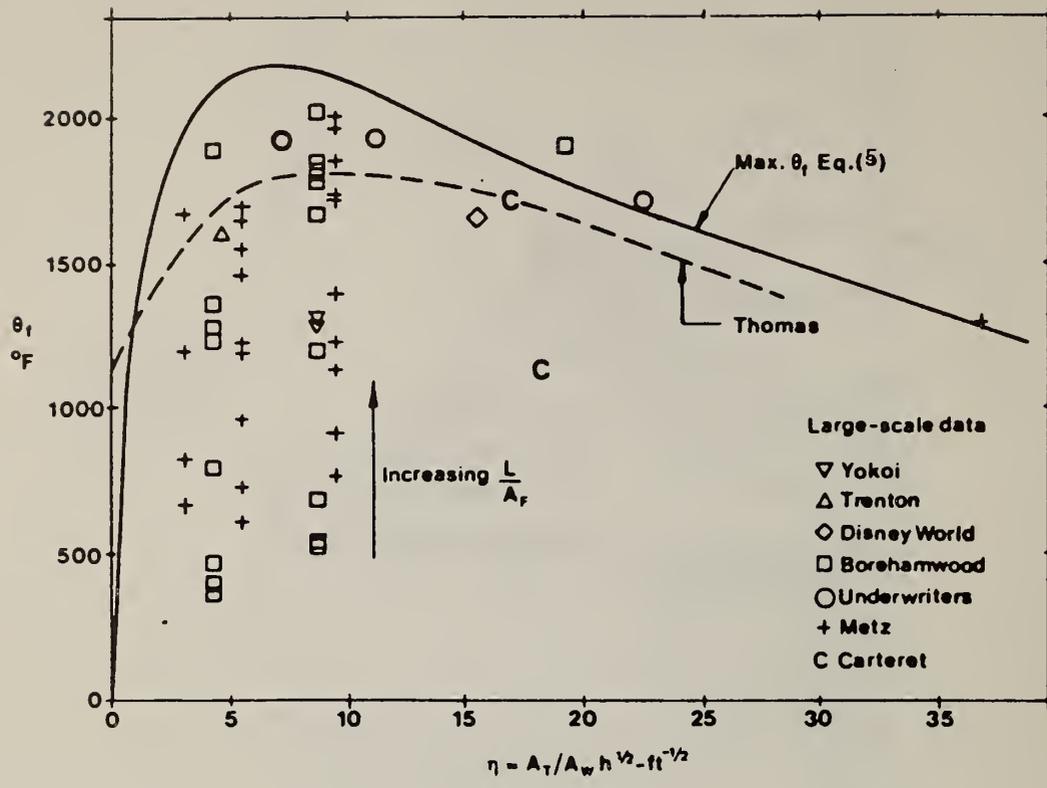
*Fig.* 5. *Variation of average fire temperature rise with compartment size and window area, natural draft*
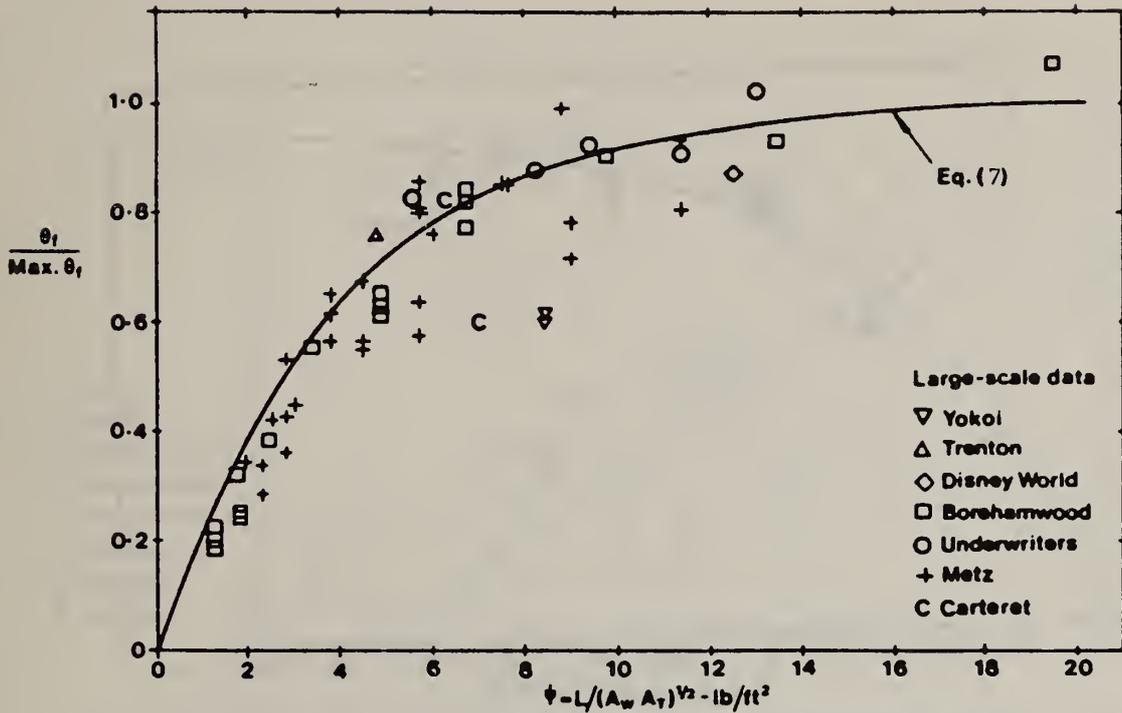
Fig. 6. *Variation of average fire temperature rise with fire load, compartment size, and window area, natural draft*
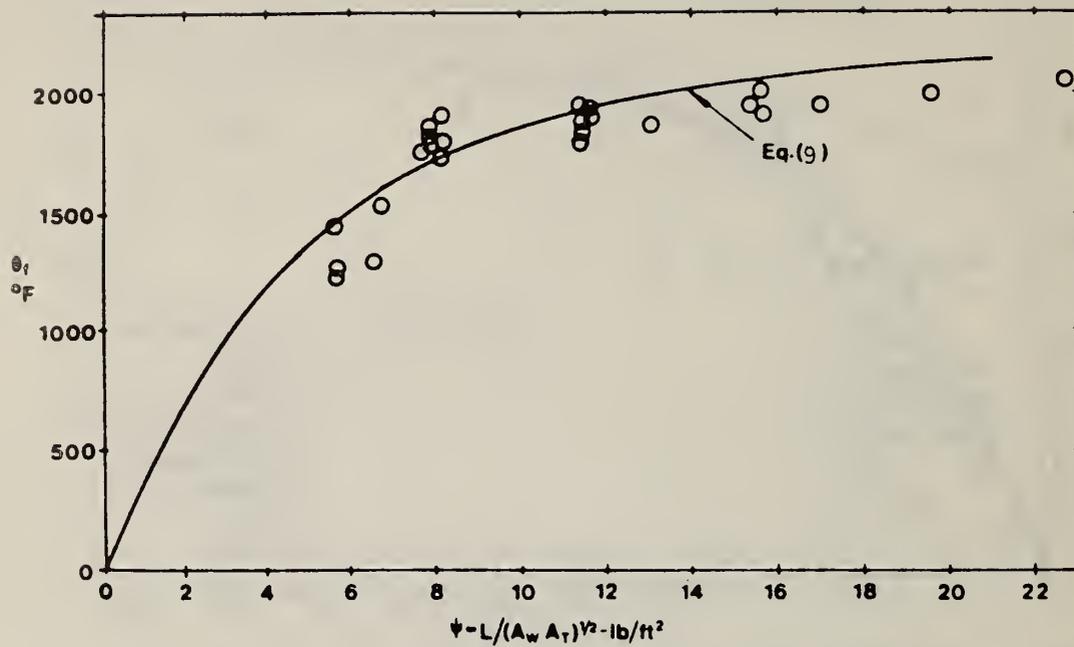
Fig. 7. *Variation of average fire temperature rise with fire load, compartment size, and window area, forced draft, Underwriters' Laboratories data*

10 ― $(z + h)/h$

Eq.(8) Thomas and Law ―

Eq.(11)

5

∇ Yokoi
△ Trenton
◇ Disney World
□ Borehamwood
○ Underwriters
✕ Tranas
C Carteret
K Kordina

K

C

1
0·01   0·02   0·05   0·1   0·5
$R/A_w P_z(gh)^{1/2}$
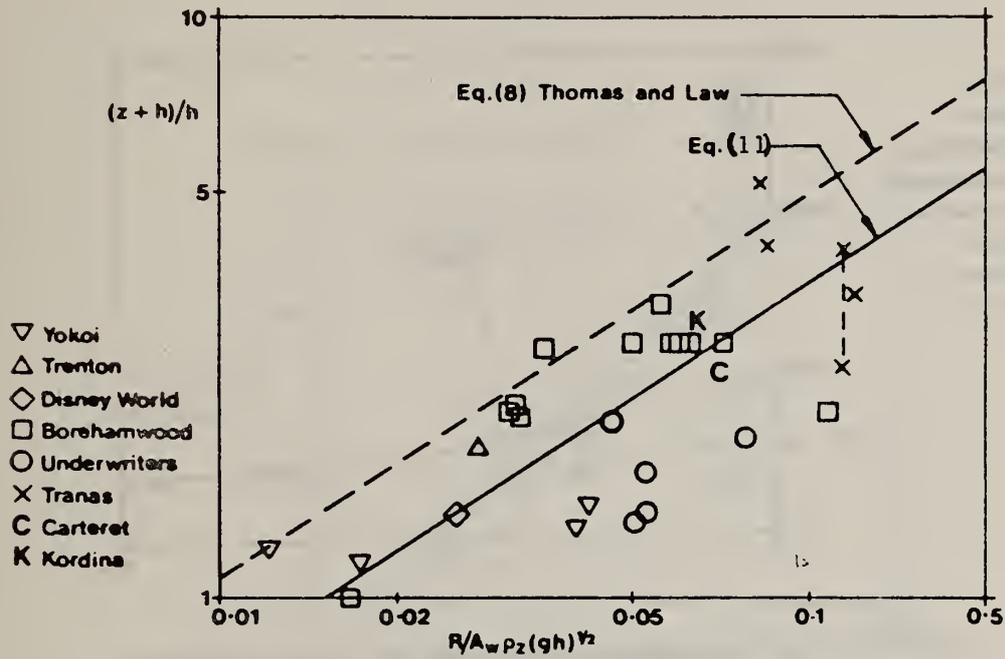
Fig. 8. *Flame heights for large-scale tests with natural draft (Note: Range of n: 0.5-18.7)*
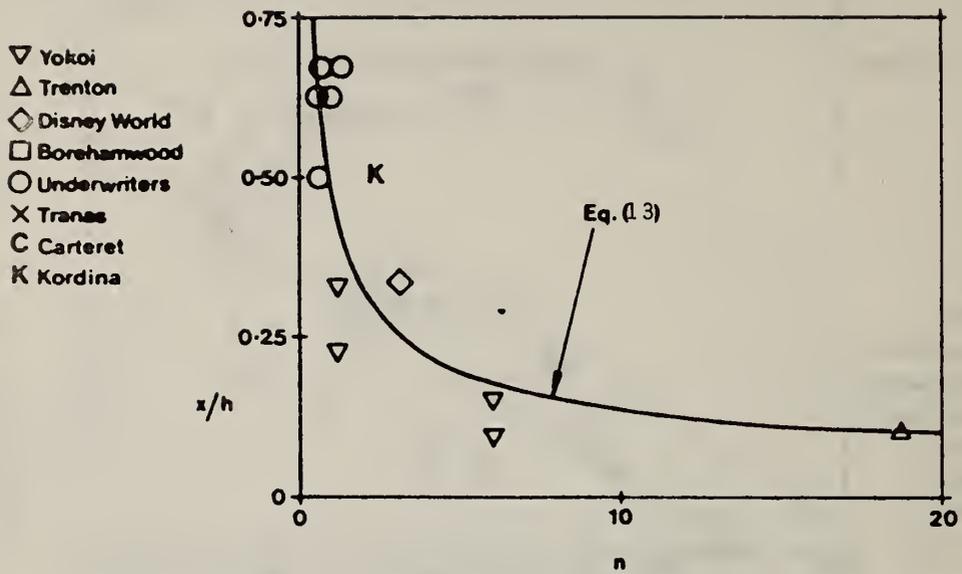
Fig. 9. *Horizontal projection of flame tip for large-scale tests with natural draft, wall above*
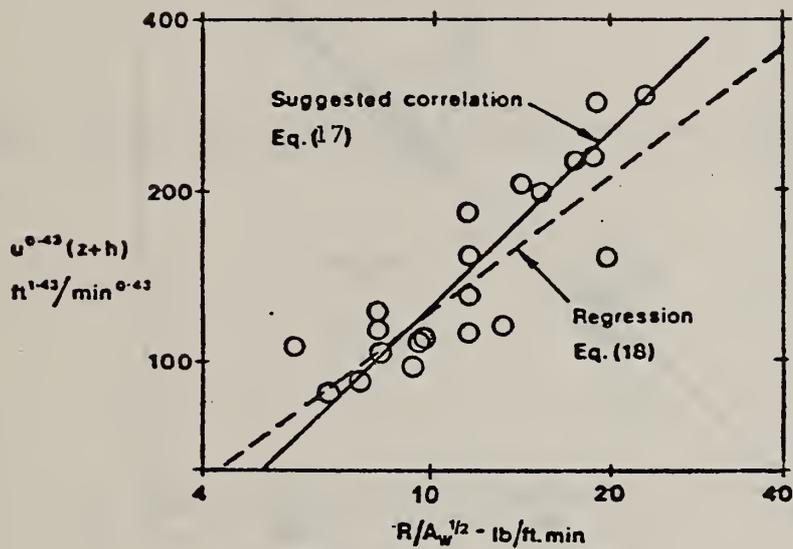
Fig. 10. *Flame heights for large-scale tests with forced draft,*
*Underwriters' Laboratories data*
*(Note: Range of u: 100-367 ft/min)*
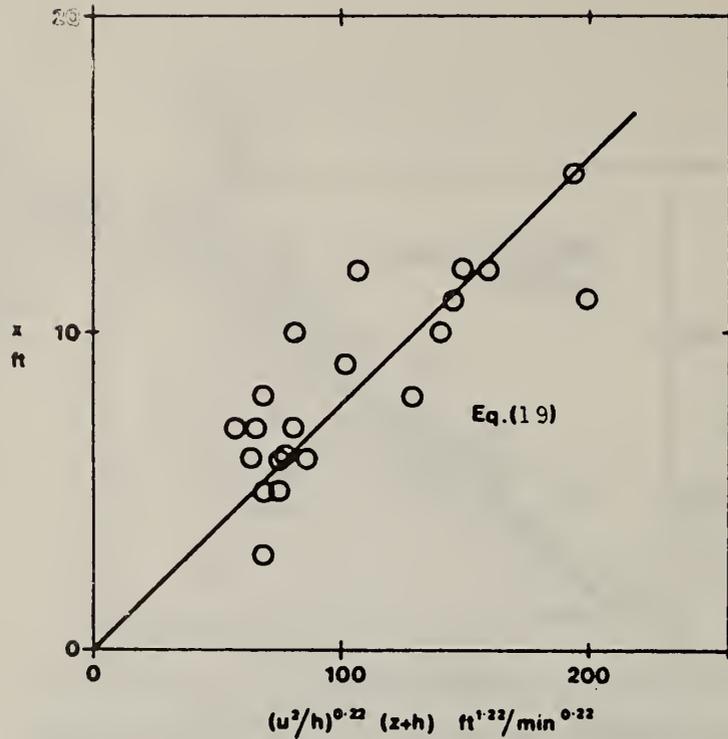
*Fig.* 11. *Horizontal projection of flame tip for large-scale tests with forced draft, Underwriters' Laboratories data (Note: Range of $u^2/h$: 1000-22,500 ft/min$^2$)*
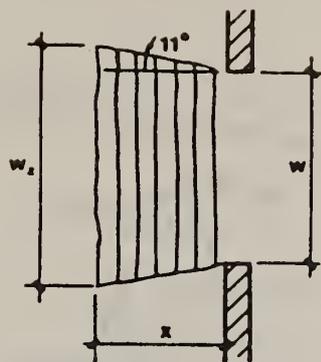
*Fig.* 12. *Plan view of emerging flames with forced draft*
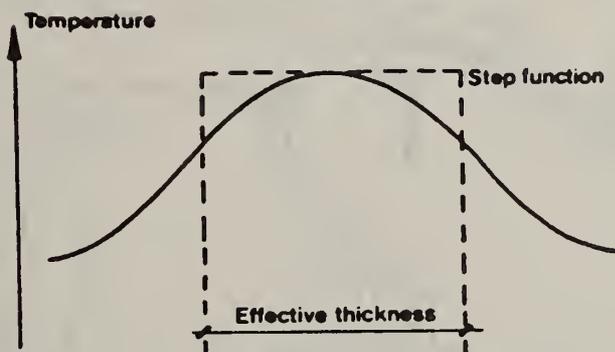


*Fig.* 13. *Temperature distribution across flame section*
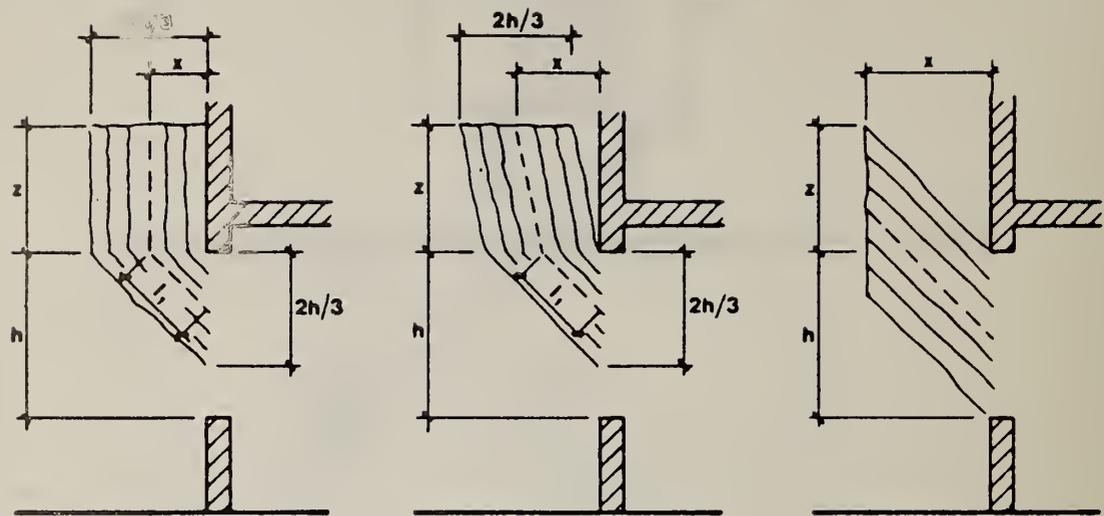
$$l_1 = \sqrt{x^2 + (\tfrac{h}{3})^2} \approx \tfrac{h}{2}$$

$$X = z + l_1$$

Natural draught
w > 0·8h wall above

$$l_1 = \sqrt{x^2 + (\tfrac{h}{3})^2}$$

$$X = \sqrt{z^2 + (x - \tfrac{h}{3})^2} + l_1$$

Natural draught
w < 0·8h wall above
or no wall above

$$X = \sqrt{z^2 + x^2}$$

Forced draught
wall or no wall above

Natural draught
Plan

wind

45°
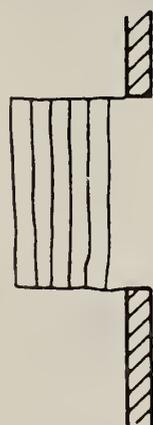
Natural draught
Plan
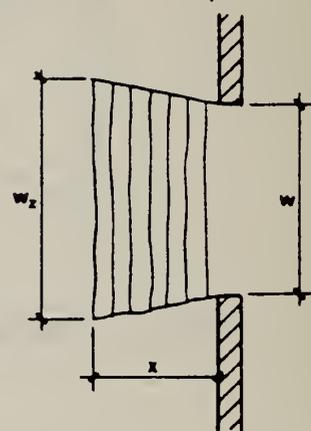
$$w_1 = w + 0·4x$$

Forced draught
Plan

*Fig.* 14 *Assumed trajectories of emerging flames*
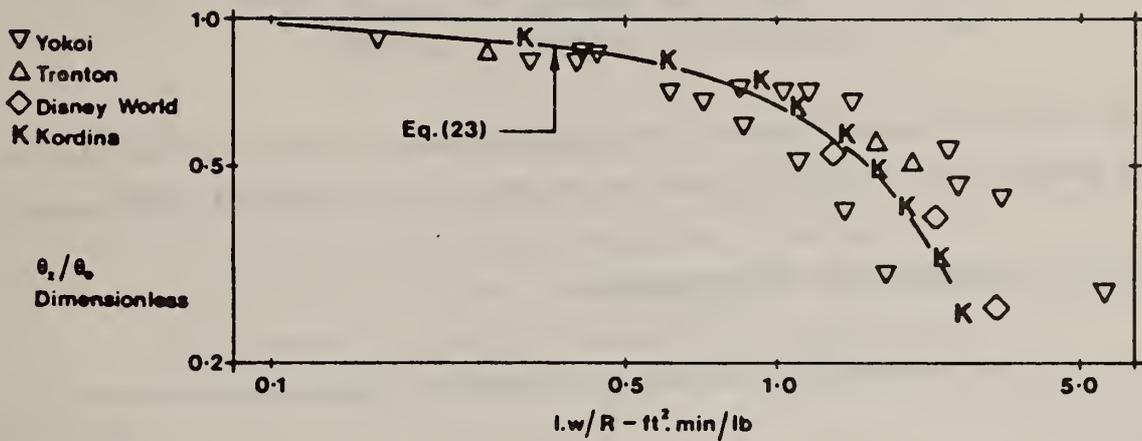
*Fig. 15. Flame temperature distribution for large-scale tests
with natural draft*
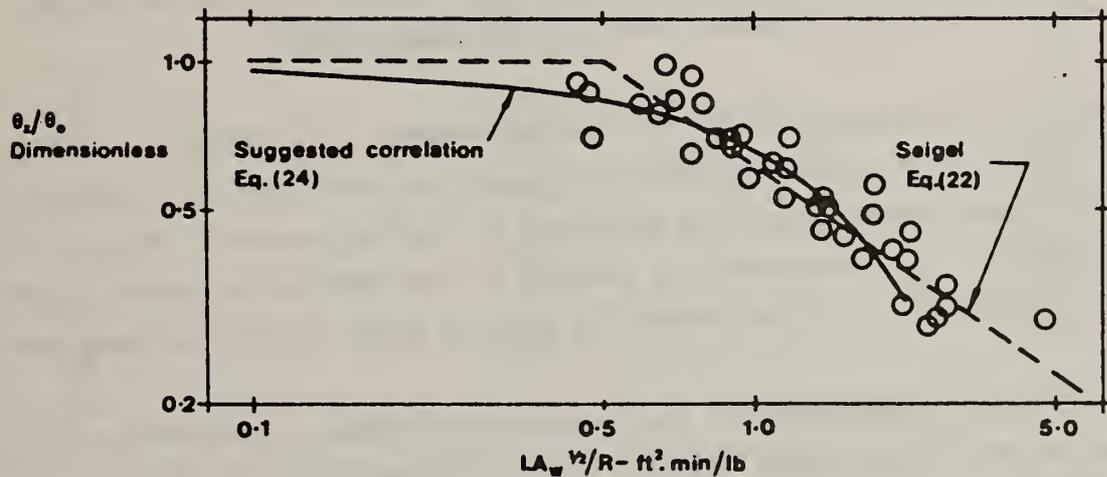


*Fig.* 16. *Flame temperature distribution for large-scale tests
with forced draft, Underwriters' Laboratories data*

$$\gamma_E = \frac{N_H \cdot \ell_o^2}{Si^2 \cdot E_H \cdot T_{min}}$$

# FIRE RESISTANCE CALCULATION METHODS
## FOR STEEL STRUCTURES

### Dr. A. I. Yakovlev
### (VNIIPO, Ministry of Interior of the USSR)

The fire resistance limit of steel structures is defined as the time for the bearing member or its separate parts to be heated to a critical temperature.

## I.  Critical Temperatures' Determination

The critical temperature for structure members subjected to a standard load is:

> 500°C - for steel members,
> 250°C - for aluminum alloy members.

In case the structure is subjected to considerably less load the critical temperature calculations take into consideration the type of structure, the support conditions, load level, and material characteristics in order to more precisely estimate the fire resistance limit.

The critical temperature of the bearing member is determined according to the table (for steel structures) with regard to coefficients $\gamma_T$ and $\gamma_E$. The coefficients characterize the reduction in bearing capacity for the heated element: $\gamma_E$ - the stability failure of the compression member under elastic deformation; $\gamma_T$ - the durability failure under plastic deformation.

The critical temperature of the compression element is defined as the least of the two values taken from the table with regard to $\gamma_E$ and $\gamma_T$ coefficients.

$\gamma_E$ and $\gamma_T$ coefficients are derived from the formulas (1)-(4).

For compressed elements:

$$\gamma_E = \frac{N_H \cdot \ell_o^2}{Si^2 \cdot E_H \cdot T_{min}} \tag{1}$$

110

where      $N_H$   - is the working load, kg;

             $E_H$   - is the metal elasticity initial modulus, $kg \cdot cm^{-2}$;

            $T_{min}$   - is the least moment of inertia, $cm^4$;

             $\ell_o$   - is the design bar length, cm.


Table


$\gamma_T$ and $\gamma_E$ Coefficients Relative to Nominal
Strength ($R^H$) and Elastic Modulus ($E_H$) for Hot-Rolled
Steel Grades $C_T.3$ and $C_T.5$ Depending on Temperature

| Temperature – °C | $\gamma_T$ | $\gamma_E$ |
|---|---|---|
| 20 | 1.0 | 1.0 |
| 100 | 0.99 | 0.96 |
| 150 | 0.93 | 0.95 |
| 200 | 0.85 | 0.94 |
| 250 | 0.81 | 0.92 |
| 300 | 0.77 | 0.90 |
| 350 | 0.74 | 0.88 |
| 400 | 0.70 | 0.86 |
| 450 | 0.65 | 0.84 |
| 500 | 0.58 | 0.80 |
| 550 | 1.45 | 0.77 |
| 600 | 0.34 | 0.72 |
| 650 | 0.22 | 0.68 |
| 700 | 0.11 | 0.59 |


$\ell_o$ value is equal to:

- $\ell$ ($\ell$ - is the bar's length) for hinged end conditions;
- $0.5\ell$ for fixed end conditions;
- $2\ell$ for one end fixed and another end loose (cantilevered);
- $0.7\ell$ for one end fixed and the other end hinged.

111

For members with axial compression and tensile loads

$$\gamma_T = \frac{N_H}{\phi_t \cdot F \cdot R^H} \tag{2}$$

where $F$ - is the cross-section, $cm^2$;

$R^H$ - is the standard initial metal strain, $kg \cdot cm^{-2}$;

$\phi_t$ - is the longitudinal bending ratio in heating conditions;

- for compressed members with slenderness ratio $\lambda < 40$ and for tensile bars, $\phi_t = 1.0$;

- for compressed members with slenderness ratio $\lambda \geq 40$, $\phi_t = 0,95$.

For members with eccentric compression or tensile loads

$$\gamma_T = \frac{N_H}{R^H} \left( \frac{e \cdot y}{T} + \frac{1}{F} \right) \tag{3}$$

where $e$ - is the eccentricity of the applied load, cm;

$T$ - is the moment of inertia for bending in one plane, $cm^4$;

$y$ - is the distance between the central axis and the section extreme fiber, cm.

For bending elements

$$\gamma_T = \frac{M_H}{W_{\pi\ell} \cdot R^H} \tag{4}$$

where $M_H$ - is the maximum bending moment under working load, $kg \cdot cm$;

$W_{\pi\ell}$ - is the section modulus, $cm^3$.

The given static calculation formulas are simple enough to use.

Having determined the critical temperature the thermotechnical calculation is carried out aimed at estimating the heating time until critical temperatures are reached, e.g. structure's fire resistance limit.

## 2. Thermotechnical Calculation

The boundary conditions for the thermotechnical calculation are given in the report "The General Fire Resistance Calculation Principles of Building Structures" and are not referred to in this paper.

The thermotechnical calculation for steel structures is carried out by the elementary heat balance method using computers.

### a) Exposed Steel Structures

Steel is known to have great thermal conductivity resulting in a rather quick temperature distribution over the structural section. That makes it possible to assume a uniform temperature distribution over the sections of steel structures exposed to heating.

Thus the heat balance equation for the unit length of the infinitely long member exposed to heating over the whole of its surface is as follows:

$$\alpha(t_B - t_{\overline{cm}}) \cdot \pi \cdot 1 \cdot \Delta\tau = \gamma_{\overline{cm}} \cdot F \cdot 1(C_{\overline{cm}} + D_{\overline{cm}} \cdot t_{\overline{cm}}) \cdot$$

$$(t_{\overline{cm},\Delta\tau} - t_{\overline{cm}}) \tag{5}$$

Making the necessary transformations we obtain a computer formula for the exposed member temperature determination:

$$t_{\overline{cm},\Delta\tau} = t_{\overline{cm}} + \frac{\Delta\tau \cdot \alpha \cdot (t_B - t_{\overline{cm}})}{60 \cdot \gamma_{\overline{cm}} \cdot \delta_{\pi p} \cdot (C_{\overline{cm}} + D_{\overline{cm}} \cdot t_{\overline{cm}})} \tag{6}$$

where    $t_{\overline{cm}}$ – is the temperature of the member at a given moment, °C;

   $t_{\overline{cm},\Delta\tau}$ – the temperature of member in a definite interval – $\Delta\tau$, °C;

   $t_B$ – the "standard fire" temperature at a given moment, °C;

   $\alpha$ – thermal conductivity ratio from the "standard fire" region to the surface of the member, $kcal \cdot m^{-2} \cdot hr^{-1} \cdot °C^{-1}$;

   $\gamma_{\overline{cm}}$ – the specific weight of metal, $kg \cdot m^{-3}$;

   $C_{\overline{cm}}$ – initial heat capacity of the metal, $kcal \cdot kg^{-1} \cdot °C^{-1}$;

113

$D_{\overline{cm}}$ – change in heat capacity of steel with regard to temperature increase, $kcal \cdot kg^{-1} \cdot {}^{\circ}C^{-2}$;

$\delta_{\pi p} = \dfrac{F}{100 \cdot \pi}$ – the given steel thickness, m;

$\qquad$ F – is the member cross-sectional area, $cm^2$;

$\qquad$ $\pi$ – is the heated perimeter of the section, cm.

It follows from (6) that in order to determine the temperature of the unprotected member its geometry is characterized by the parameter $\delta_{\pi p}$ – the equivalent metal thickness equal to the ratio of the cross-sectional area to its perimeter.

The stability of the algorithm for a calculation according to (6) is dependent on the choice of a $\Delta\tau$ value that must not exceed $\Delta\tau_{max}$ derived from the following formula:

$$\Delta\tau_{max} = \frac{60 \cdot \gamma_{\overline{cm}} \ \delta_{\pi p} \cdot (C_{\overline{cm}} + D_{\overline{cm}} \cdot t_{\overline{cm}, max})}{\alpha_{max}} \quad \text{minutes} \qquad (7)$$

where $\alpha_{max}$ and $t_{\overline{cm}, max}$ – are the maximum allowable values in the calculation process.

The heating curves for steel members with various $\delta_{\pi p}$ values are given in Fig. 1. The curves are drawn with regard to temperatures calculated according to (6). Computer program "Nairy-2" is used for the calculation process making use of the following data:

$\Delta\tau = 0.1$ min; $\qquad \gamma_{\overline{cm}} = 7800 \ kg \cdot m^{-3}$; $\qquad C_{t\overline{m}} = 0,105 \ kcal \cdot kg^{-1} \cdot {}^{\circ}C^{-1}$

$D_{\overline{cm}} = 0.000114 \ kcal \cdot kg^{-1} \cdot {}^{\circ}C^{-2}$;

$S_{\ell} = 0.85$ – is the emissivity of the surrounding fire box;

$S_{o} = 0.69$ – is the emissivity of the surface of the steel member

114

b) Structures with a Fire Protection Coating

Coated structures exposed to fire are subjected to considerable
temperature variation over the thickness of the protection. Besides this,
some fire protected elements (e.g. of I-shaped section) also suffer tem-
perature variation over the depth of the web and width of the flanges. In
this case the thermotechnical calculation is carried out with regard to
two-dimensional heat flow by the elementary heat balance method.

For this purpose a net (mesh) is attached to the section. The
temperatures in the net (nodes) are determined in successive time
intervals - $\Delta\tau$ with the help of a computer.

An example of the computer mesh for a fire protected concrete column
or a wide-flanged double-T beam is given in Fig. 2. Due to symmetry of the
section about the "y" axis the temperatures are only estimated in one half
of the section.

The temperatures at the nodes are estimated according to formulas
derived from the heat balance equations of finite element analysis. The
latter are formed by dotted lines drawn through the centers of the net cells.
To compose the heat balance equations it is necessary to consider tempera-
ture variation over the flange width and the web depth only; temperature
variation depending on the flange and web thicknesses is assumed to be zero.
In addition, the heat balance equations of elements include the heat of
free water evaporation in pores of the coating.

Considering these peculiarities, the design formulas for temperature
estimation in the most typical net nodes take the form (see Fig. 2):

Node 9, Fig. 2

$$t_{9,\Delta\tau} = t_9 + \frac{\Delta\tau\left\{[A(t_3 - t_9) + 0.5B\,(t_3^2 - t_9^2)] \cdot \dfrac{\left(\Delta X_1 + \Delta X_2\right)}{2\cdot\Delta Y_1}\right.}{30(\Delta X_1 + \Delta X_2)\cdot\Delta Y_1\cdot\gamma(C + Dt_9)} +$$

$$\frac{[A(t_8 - t_9) + 0.5B\,(t_8^2 - t_9^2)]\,\dfrac{\Delta Y_1}{\Delta X_1} + [A(t_{10} - t_9) + 0.5B\,(t_{10}^2 - t_9^2)]\,\dfrac{\Delta Y_1}{\Delta X_2}}{1} +$$

115

$$\frac{[A(t_{15} - t_9) + 0.5B (t_{15}^2 - t_9^2)] \cdot \left(\dfrac{\Delta X_1}{2\Delta Y_1} + \dfrac{\Delta X_2}{2\Delta Y_1 - d_{\pi 1}}\right)}{1} - t_9^\infty \tag{8}$$

where $t_9^\infty = \dfrac{p \cdot \tau}{100(C + 100D)}$

Node 15.  Fig. 2

$$t_{15,\Delta\tau} = t_{15} + \frac{\Delta\tau}{30}\left\{ \frac{[A(t_9 - t_{15}) + 0.5B (t_9^2 - t_{15}^2)] \cdot \left(\dfrac{\Delta X_1}{2\Delta Y_1} + \dfrac{\Delta X_2}{2\Delta Y_1 - d_{\pi 1}}\right)}{[0.5(\Delta X_1 + \Delta X_2)(\Delta Y_1 + \Delta Y_2) - d_{\pi 1} \cdot \Delta X_2] \cdot \gamma \cdot (C + Dt_{15})} + \right.$$

$$\frac{[A(t_{21} - t_{15}) + 0.5B (t_{21}^2 - t_{15}^2)] \cdot \left(\dfrac{\Delta X_1}{2\Delta Y_2} + \dfrac{\Delta X_2}{2\Delta Y_2 - d_{\pi 1}}\right)}{d_{\pi 1} \cdot \Delta X_2\, \gamma_{st}\, (C_{st} + D_{st} \cdot t_{15})} +$$

$$\frac{[A(t_{14} - t_{15}) + 0.5B (t_{14}^2 - t_{15}^2)]\, \dfrac{\Delta Y_1 + \Delta Y_2}{2\Delta X_1} + [A(t_{16} - t_{15}) + 0.5B (t_{16}^2 - t_{15}^2)]\, \dfrac{[0.5(\Delta Y_1 + \Delta Y_2) - d_{\pi 1}]}{X_2}}{1} +$$

$$\left. \frac{[A_{st}(t_{16} - t_{15}) + 0.5B_{st} (t_{16}^2 - t_{15}^2)]\, \dfrac{d_{\pi 1}}{\Delta X_2}}{1} \right\} - t_{15}^\infty \tag{9}$$

116

$$t_{15}^{\infty} = \frac{p \cdot \tau}{100} \left\{ (C + 100D) + \frac{d_{\pi 1} \cdot \Delta X_2 \ \gamma_{cm}(C_{st} + 100D_{st})}{[0.5(\Delta X_1 + \Delta X_2)(\Delta Y_1 + \Delta Y_2) - d_{\pi 1} \cdot \Delta X_2] \cdot \gamma} \right\}$$

## Node 18, Fig. 2

$$t_{18,\Delta\tau} = t_{18} + \frac{\Delta\tau}{30} \left\{ [A(t_{12} - t_{18}) + 0.5B \ (t_{12}^2 - t_{18}^2)] \frac{\Delta X_2}{2\Delta Y_1 - d_{\pi 1}} \cdot (C + Dt_{18}) + \right.$$

$$\frac{[A(t_{17} - t_{18}) + 0.5B \ (t_{17}^2 - t_{18}^2)] \left[ \frac{0.5(\Delta Y_1 + \Delta Y_2) - d_{\pi 1}}{2} \cdot \left( \frac{1}{\Delta X_2} + \frac{1}{\Delta X_2 - dc} \right) \right]}{[\Delta X_2 \cdot d_{\pi 1} + (\Delta Y_2 - d_{\pi 1})dc \ldots] \gamma_{st}(C_{st} + D_{st} \ t_{18})} +$$

$$\frac{[A_{st}(t_{17} - t_{18}) + 0.5B_{st} \ (t_{17}^2 - t_{18}^2)] \frac{d_{\pi 1}}{\Delta X_2} + [A(t_{24} - t_{18}) + 0.5B \cdot (t_{24}^2 - t_{18}^2)] \cdot \frac{0.5\Delta X_2 - dc}{\Delta Y_2 - 0.5d_{\pi 1}}}{1} +$$

$$\left. \frac{[A_{st}(t_{24} - t_{18}) + 0.5B_{st} \cdot (t_{24}^2 - t_{18}^2)] \frac{dc}{\Delta Y_2}}{1} \right\} - t_{18}^{\infty} \tag{10}$$

where

$$t_{18}^{\infty} = \frac{p \cdot \tau}{100} \left\{ (C + 100D) + \frac{[\Delta X_2 d_{\pi 1} + (\Delta Y_2 - d_{\pi 1})dc] \cdot \gamma_{st} \cdot (C_{st} + 100D_{st})}{[0.5\Delta X_2(\Delta Y_1 + \Delta Y_2) - \Delta X_2 \cdot d_{\pi 1} - (\Delta Y_2 - d_{\pi 1})dc] \cdot \gamma} \right\}$$

117

where: $\tau$ – is the latent heat of water, $kcal \cdot kg^{-1}$;

A, B, $\gamma$, C, D – are the thermophysical characteristics of the coating;

$A_{st}$, $B_{st}$, $\gamma_{st}$, $C_{st}$, $D_{st}$ – are the thermophysical characteristics of the steel;

$d_{\pi}$ – is the flange thickness of profile, m;

2dc – is the web thickness of profile, m;

p – is the moisture content of coating, wt. %.

The maximum design time interval – $\Delta\tau_{max}$ – is calculated according to the following formula:

$$\Delta\tau_{max} = \frac{30 \cdot \gamma_{st} \cdot \Delta X^2 \cdot C_{st}}{A_{st}} \quad minutes \qquad (11)$$

where $\Delta X$ – is the net cells' minimum dimension within the steel profile limits, m.

It is possible to simplify the thermotechnical calculation of some coated steel elements with rectangular or round sections and also double-T sections with contour protection by reducing these sections to a non-dimensional plate coated on one side and having perfect heat isolation on the other side (Fig. 3).

The temperature nomogram for the steel plate with various thickness – $\delta_{cm}$ – and coated with cement-sand plaster 30 mm in thickness is given in Fig. 4. The nomogram was prepared based on computations using the following baseline data:

118

$\Delta\tau = 0.1$ min, $\quad\quad\quad \Delta X = 0.005$ m, $\quad\quad\quad \gamma = 1930$ kg·m$^{-3}$

$A = 0.72$ $\quad\quad\quad\quad\quad B = -0.00038,$ $\quad\quad C = 0.184,$ $\quad\quad\quad D = 0.00015$

$Z = 539,$ $\quad\quad\quad\quad\quad p = 2\%,$ $\quad\quad\quad\quad S_o = 0.625,$ $\quad\quad\quad S_B = 0.85$

$\gamma_{st} = 7800$ kg·m$^{-3}$ $\quad\quad C_{st} = 0.105$ $\quad\quad\quad D_{st} = 0.000114$

The computation was carried out with an algorithm developed according to Fig. 3 and including the following formulas:

- the temperature – $t_{o,\Delta\tau}$ of the exposed coating surface:

$$t_{o,\Delta\tau} = t_o + \frac{\Delta\tau\left\{\alpha(t_B - t_o) + \frac{1}{\Delta X}[A(t_1 - t_o) + 0.5B(t_1^2 - t_o^2)]\right\}}{30 \cdot \gamma \cdot \Delta X(C + Dt_o)} - t_o^\infty \tag{12}$$

- the temperatures – $t_{n,\Delta\tau}$ of "n"-coating middle layer:

$$t_{n,\Delta\tau} = t_n + \frac{\Delta\tau}{60 \cdot \gamma \cdot \Delta X^2(C + D \cdot t_n)}[A(t_{n-1} + t_{n+1} - 2t_n) +$$

$$0.5B(t_{n-1}^2 + t_{n+1}^2 - 2t_n^2] - t_n^\infty \tag{13}$$

where

$$t_{o(n)}^\infty = \frac{p \cdot \tau}{100(C + 100D)}$$

- the temperature $t_{st,\Delta\tau}$ of steel plate;

$$t_{st,\Delta\tau} = t_{st} + \frac{\Delta\tau[A(t_{i-1} - t_{st}) + 0.5B(t_{i-1}^2 - t_{st}^2)]}{60 \cdot \Delta X[0.5 \cdot \gamma \cdot \Delta X(C + D \cdot t_{st}) + \delta_{st} \cdot \gamma_{st}(C_{st} + Dt_{st})]} - t_{st}^\infty \tag{14}$$

where

$$t_{st}^\infty = \frac{p \cdot \tau}{100\left[(C + 100D) + \frac{2 \cdot \delta_{st} \cdot \gamma_{st}(C_{st} + 100D_{st})}{\Delta X \cdot \gamma}\right]}$$

The data formulas were derived from the heat balance equations for the elementary layers shown in Fig. 3 by dotted lines.

The reduction of the actual cross-section of the member to a non-dimensional plate is carried out according to formulas based on the following conditions.

The box-shaped section of a coated member is presented in Fig. 5.

Let us compose the heat balance equation for $mmm^1n^1$-element restricted by the axes of x and y and $mm^1$-line, crossing the middle of coating thickness.

Heat transfer is not observed through the lines $mn^1$, $nn^1$ and $m^1n^1$ as: mn lies on the axis of section's symmetry, $nn^1$ adjoins the closed air space with the symmetry axis – "y" and $m^1n^1$ – is the symmetry axis for isotherms in the section corners of a structure.

Consequently, only heat passing through the $mm^1$-line to the restricted element results in the element's heating.

Therefore, the heat balance equation for $mnm^1n^1$-element takes the form:

$$\left( A + B \, \frac{t_o + t_{st}}{2} \right) \, \frac{(t_o - t_{st})(0.5B + 0.5\delta_o)\Delta\tau \, . \, 1}{\delta_o} =$$

$$(C + D \, . \, t_{st}) \, . \, \gamma \, . \, \frac{\delta_o}{2} \, (0.5B + 0.25\delta_o) + \tag{15}$$

$$(C_{st} + D_{st} \, . \, t_{st}) \, . \, \gamma_{st} \, . \, \delta_x \, (0.5B - 0.5\delta y) \, . \, (t_{st,\Delta\tau} - t_{st})$$

Having derived the left and the right parts of the equation by 0.5 $(b + \delta_o)$ and setting the derived expression in square brackets equal to the heat capacity value of an element of non-dimensional coated plane with the given thickness of $\delta_{np,x}$ we may derive the following design formula:

120

$$\delta_{np,x} = \delta_x \frac{b - \delta_y}{b + \delta_o} - 0.25 \frac{(C + D \cdot t_{st}) \cdot \gamma}{(C_{st} + D_{st} \cdot t_{st}) \cdot \gamma_{st}} \cdot \frac{\delta_o^2}{b + \delta_o} \qquad (16)$$

In this expression the heat capacity of the coating and of the steel at high temperature may be substituted for the initial heat capacities of these materials.

Therefore:

$$\delta_{npx} = \delta_x \frac{b - \delta_y}{b + \delta_o} - 0.25 \frac{C \cdot \gamma}{C_{st} \gamma_{st}} \frac{\delta_o^2}{b + \delta_o} \qquad (17)$$

Analogously for $\delta_{np,y}$ we have:

$$\delta_{np,y} = \delta_y \cdot \frac{a - \delta_x}{a + \delta_o} - 0.25 \frac{C \cdot \gamma}{C_{st} \cdot \gamma_{st}} \cdot \frac{\delta_o^2}{a + \delta_o} \qquad (18)$$

In the given formulas the second member of the right part having the coating thickness of $\delta_o \leq 20$ mm has insignificant value and may be neglected in the process of practical calculations. Thus, the design formulas for the given thickness will take the forms:

$$\delta_{np,x} = \delta_x \cdot \frac{b - \delta_y}{b + \delta_o} \qquad (19)$$

$$\delta_{np,y} = \delta_y \cdot \frac{a - \delta_x}{a + \delta_o} \qquad (20)$$

The general plate's thickness $- \delta_{np}$ is:

$$\delta_{np} = \frac{\delta_{np,x} \cdot b + \delta_{np,y} \cdot a}{a + b} \qquad (21)$$

Of concern is that the value of $\delta_{np}$ (at $\delta_o = 0$ and lack of coating) is equal to:

$$\delta_{np} = \frac{\delta_x \cdot \dfrac{b - \delta_y}{b} \cdot b + \delta_y \cdot \dfrac{a - \delta_x}{a} \cdot a}{a + b} =$$

$$\frac{2b\delta_x + 2a \cdot \delta_y - 4\delta_x \cdot \delta_y}{2(a + b)} = \frac{F}{n}$$

i.e. equal to the given thickness value for the exposed bars.

According to the curves given in Fig. 4 the heating time of the plate to the critical temperature is determined for $\delta_{np} = \delta_{st}$. The time determined will be the fire resistance limit of the member with a box-shaped section.

For a circular section;

$$\delta_{np} = \delta_{st} \frac{d_H - \delta_{st}}{d_H - \delta_o} - 0.25 \frac{C \cdot \gamma}{C_{st} \cdot \gamma_{st}} \cdot \frac{\delta_o^2}{d_H \cdot \delta_o} \tag{22}$$

where $\delta_{st}$ – is the thickness of section wall;

$d_H$ – is the external diameter of the section.

In case of a solid circular section:

$$\delta_{np} = \frac{0.25}{d_H + \delta_o} \quad d_H^2 - \frac{C \cdot \gamma}{C_{st} \cdot \gamma_{st}} \cdot \delta_o^2 \tag{23}$$
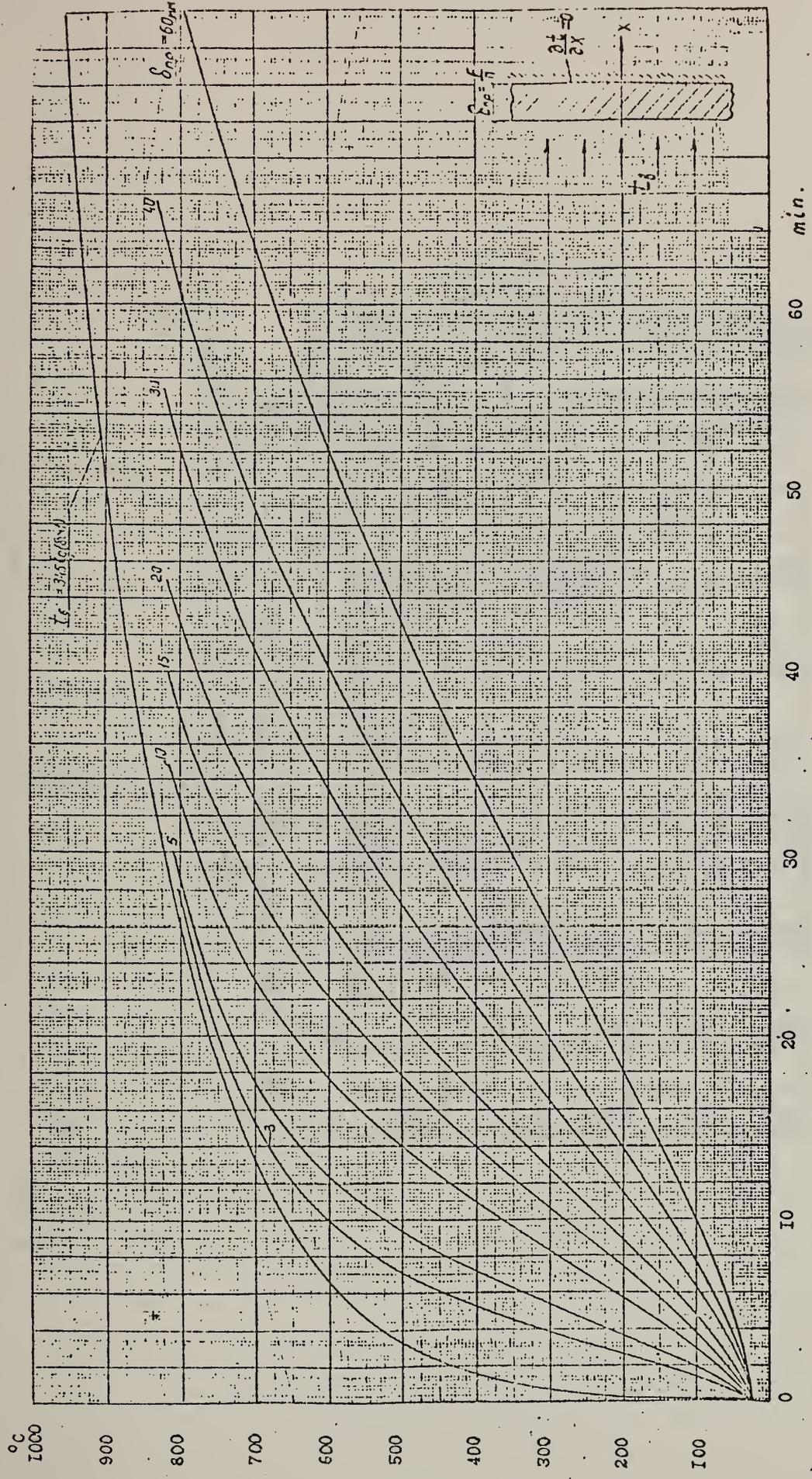
Figure 1
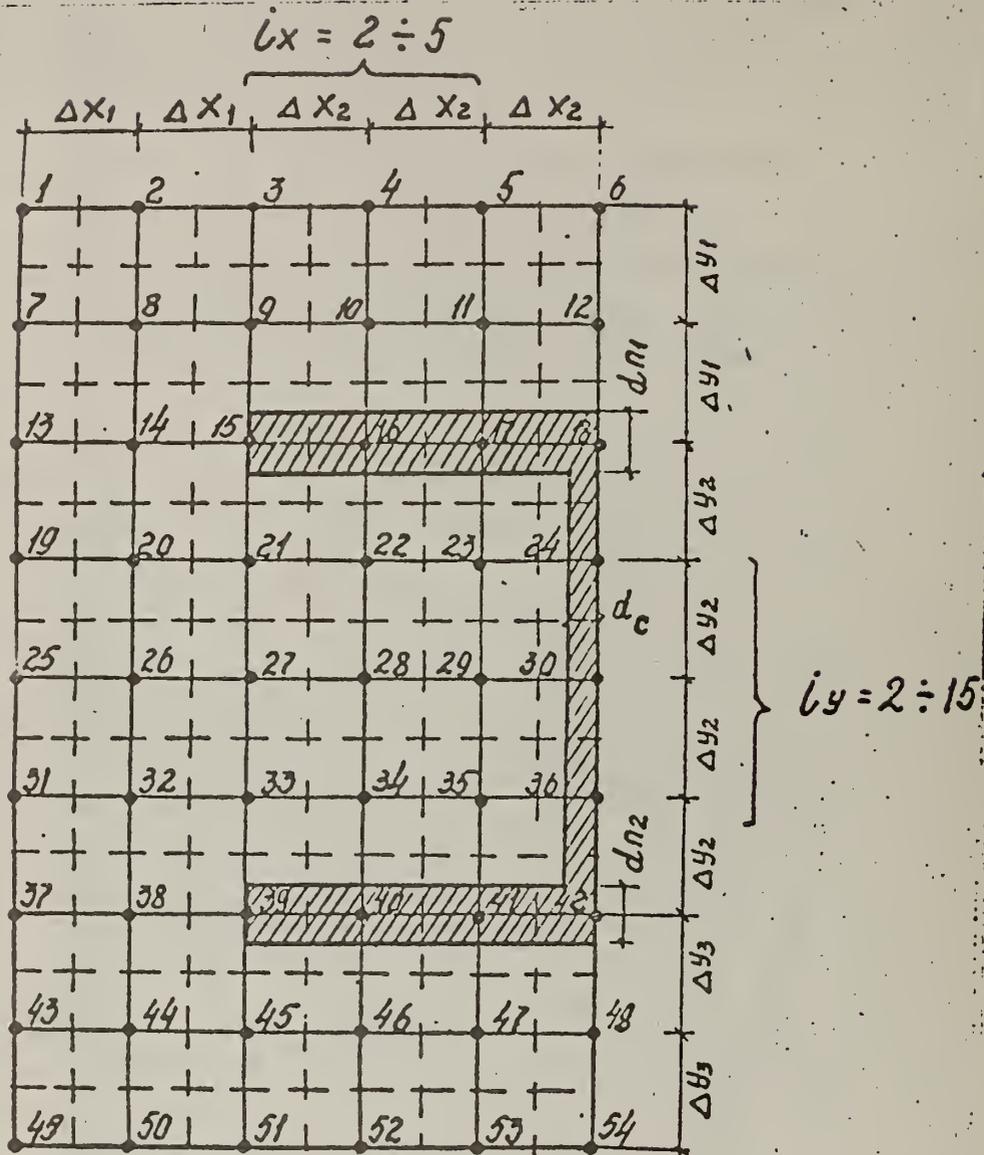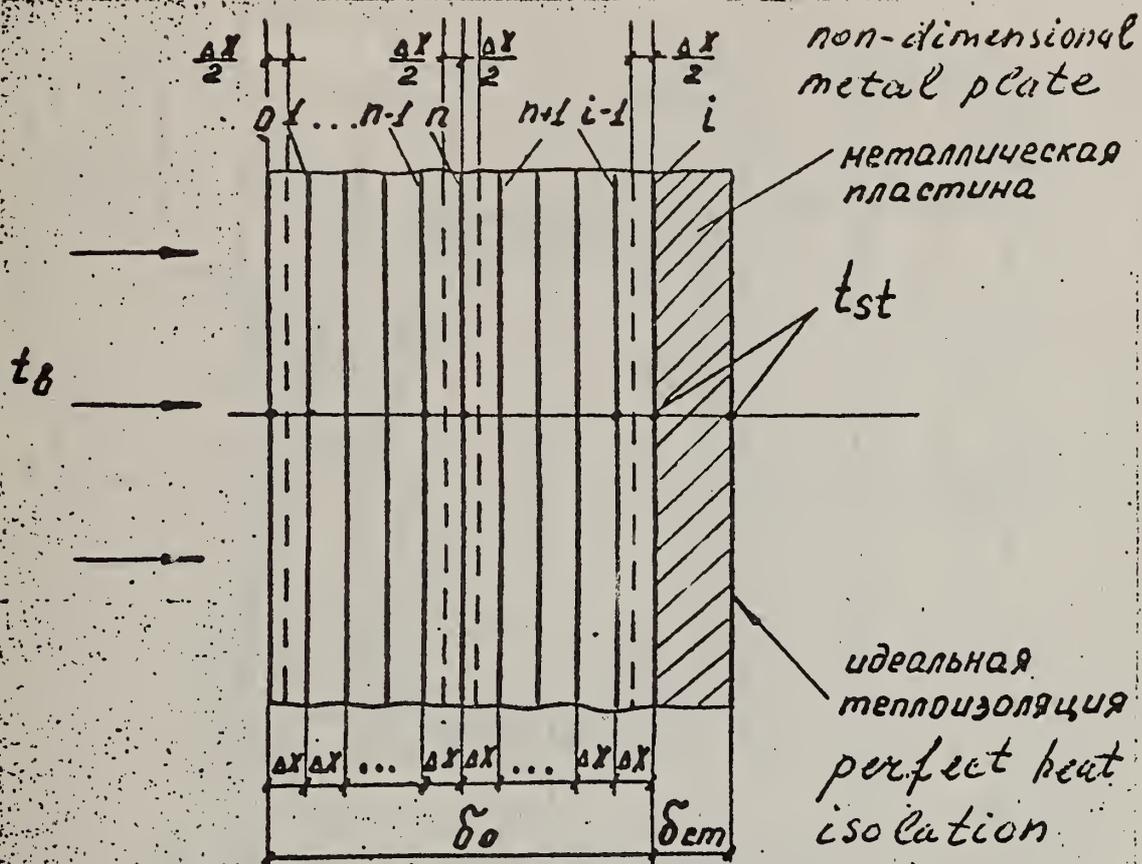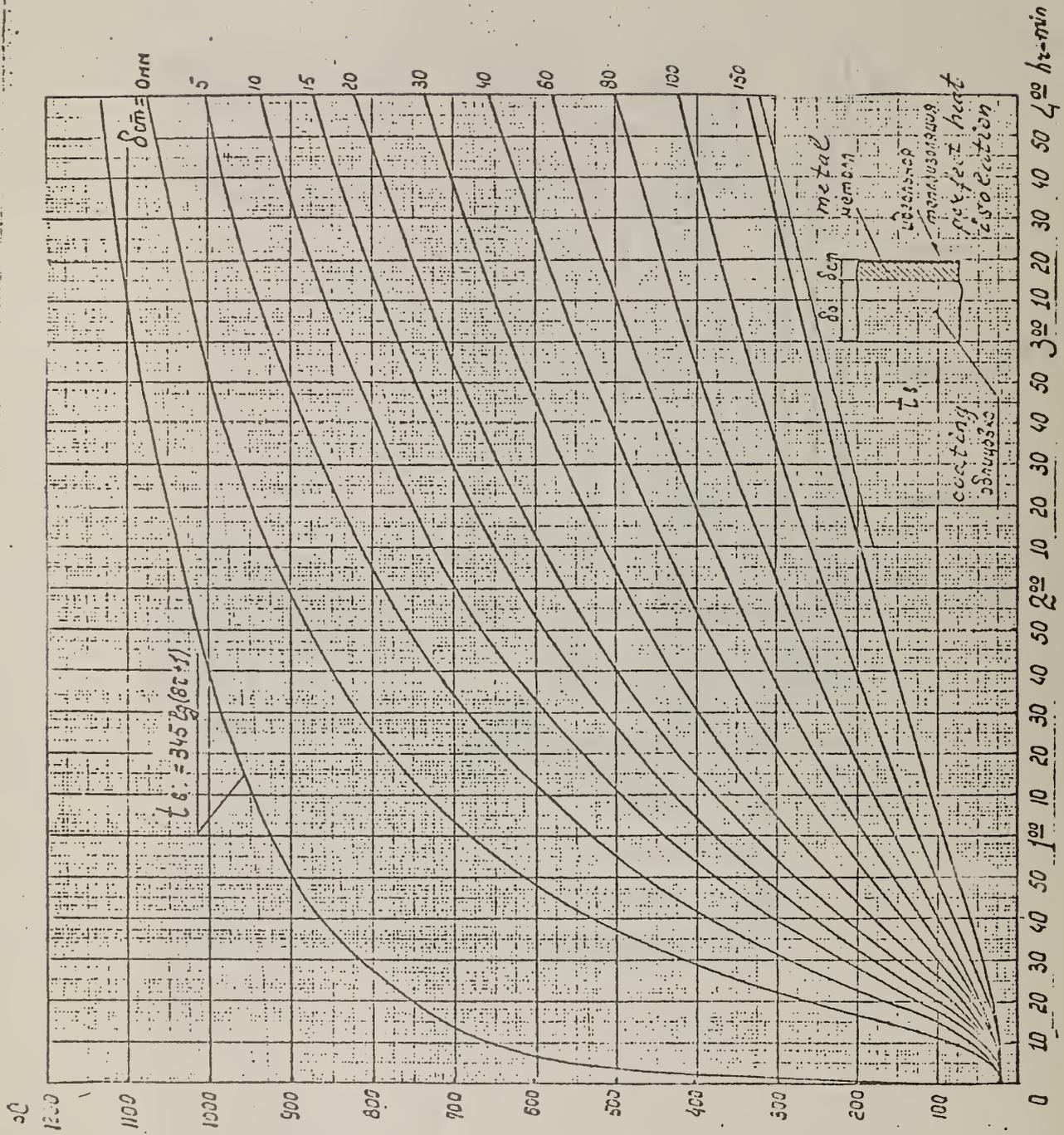
123

Figure 2

Figure 3

125

Figure 4

Figure 5

изотермы
isotherms

облицовка
coating

стальной
стержень
steel bar

127
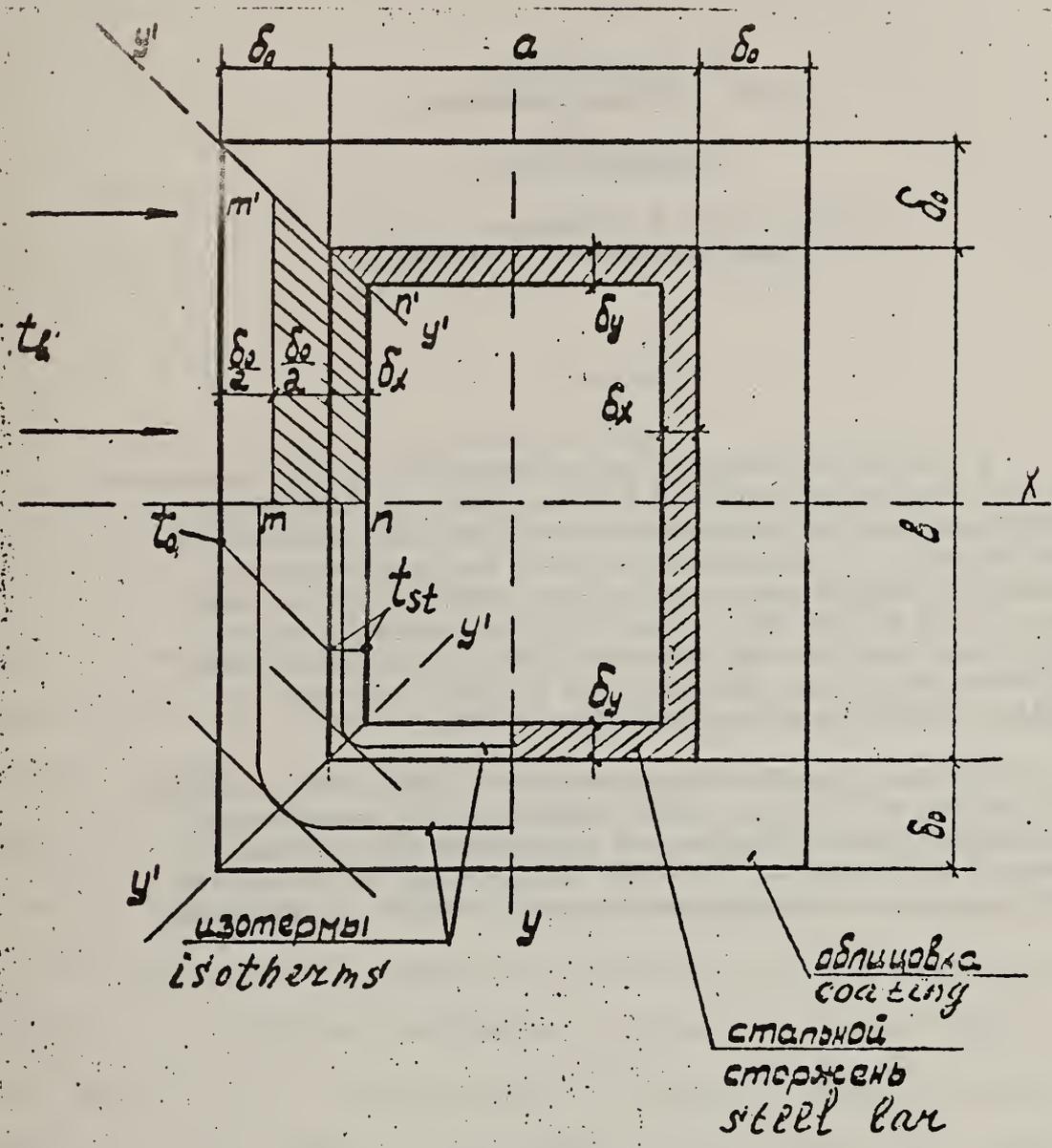
# RELIABILITY ANALYSIS OF FIRE-EXPOSED LIGHT-FRAME
## WOOD FLOOR ASSEMBLIES

by

E. L. Schaffer
Forest Products Laboratory

presented by

F. E. Woeste
Virginia Institute of Technology

## Abstract

A reliability analysis using second-moment approximations
is conducted on two types of fire-exposed, unprotected wood
floors--conventional wood joist and floor truss assemblies.
A methodology is illustrated by which the probability of
structural failure of a wooden floor assembly can be evalu-
ated.  This probability, along with the probabilities of
failure of other system components, can be used in a syste-
matic analysis which appears to be a viable approach to
realistic analysis of building fire safety.

The use of reliability analysis to compare the relative
fire safety of different floor components is demonstrated.
A procedure for introducing new components into the market,
based on the concept of an equal safety index as calculated
for a component with a proven inservice record, is discussed.

# Reliability Analysis of Fire-Exposed

## Light-Frame Wood Floor Assemblies

By

F. E. Woeste[1]
and
E. L. Schaffer, Engineer

Forest Products Laboratory,[2] Forest Service
U.S. Department of Agriculture

----

## Introduction

The effectiveness of structural assemblies--walls, floors, ceiling roofs--
to act as barriers to fire growth is currently measured by using the American
Society for Testing and Materials (ASTM) E-119 (3)[3] fire endurance test.  This
method requires that a typical loaded assembly be exposed to fire and the time
to failure recorded.  This time is then employed to "rate" the assembly.  An
assembly that maintains its integrity for 30 minutes (or more) is said to have
a 30-minute fire endurance rating.  The rating procedure is then used by codes
to regulate which assembly designs are satisfactory for buildings of various
occupancies.  The Department of Housing and Urban Development (HUD), for
example, specifies that exterior walls shall have a 20-minute and floors a
10-minute endurance rating in one- and two-family residences (42).  This is

---

1/ Agricultural Engineering Department, Virginia Polytechnic Institute
and State University, Blacksburg, Va. 24061.

2/ Maintained at Madison, Wis., in cooperation with the University of
Wisconsin.

3/ Underlined numbers in parentheses refer to literature cited at end of
report.

believed to protect occupants and enable firefighters to safely combat dwelling fires

One of several shortcomings of the present fire endurance evaluation and rating system is that it does not realistically measure the fire safety afforded by assemblies. It simply compares the fire performance of one assembly with another through the use of a single performance measure--that of a single test of each to measure an assembly's fire endurance under a standard fire condition. When one discusses safety, one is soon led to the need for a measure of risk associated with an event occurring. Hence, the present fire endurance rating system provides little information on the safety provided by structural assemblies. This is somewhat unfortunate because of the potential benefits accruing to resident owners, developers of new assemblies, and the firefighting and code enforcement community.

### Approach

This paper illustrates a risk-based methodology and its application to assessing the fire endurance safety of two unprotected light-frame assemblies-- the conventional joist assembly and a floor-truss assembly.

In the case of a floor, there are three primary modes of failure: structural collapse, flame penetration, and excessive temperature rise on the unexposed surface (3). In a system analysis the probability of occurrence of each of these events would be required. In one- and two-family dwellings, only structural assembly failure criteria are evaluated (42).

One objective of this research was to propose and illustrate a methodology by which the probability of structural failure of wooden floor assemblies can be evaluated.

A second objective, perhaps more important for the immediate future, is a method by which new components can be introduced into the market. The underlying premise is that a new component can be substituted for a conventional and code acceptable component if it provides the same "degree of safety" when exposed to the natural elements such as live and dead load, loads due to earthquakes, fire, and so on. The investigations of this research will address the fire performance aspects of floor assemblies only.

## Background

One rational approach to the accomplishment of both objectives is an analysis using probabilistic engineering methods. Probabilistic engineering is by no means a new discipline. Ang, as of 1972 in a review of literature, reports on some 355 research papers on structural reliability (4). Textbooks have been published on the subject, and the number of research publications dealing with steel, concrete, applications in wood engineering number as few as 20. The use of this same theory in fire situations has been suggested and illustrated by researchers (5,9,18,22).

### Fire Endurance of Floor Assemblies
   (Deterministic)

In the areas of reinforced concrete and steel design, the concept of fire design engineering as opposed to strictly fire tests is gaining acceptance (1, 2,13,35,41). Wooden floor assemblies are qualified or fire rated based on test only, and these data have been published for assemblies with at least a 1-hour fire rating (14). Various researchers have been promoting a combination of design and testing much in the way the field of structural engineering emerged throughout the years. Sunley reports that the variability of strength of

timber assemblies, when exposed to ASTM E-119 conditions, is less than the variability of assembly strength at normal temperature (39). Additional support for this is evident in the results of work of Schaffer, and Knudsen and Schniewind on the strength of small, clear specimens of wood at elevated temperature (19,34). Sunley argues further that fire design engineering should be no more difficult than designing for other load types.

Equations have been developed to predict the fire endurance of fire-exposed joist floor (20,21). The method of analysis was empirical, having as a starting point the flexure formula for pure bending. In each case, the solutions to these equations are obtained by graphical methods (fig. 1). These equations cannot be used conveniently in a probabilistic analysis, thus additional modeling is needed. A purely analytical approach to the prediction of strength at elevated temperatures would be most desirable, and a considerable amount of basic input data exists (35). However, such modeling has not been accomplished, thus simplified strength models will be used in the analysis to follow.

## Analysis

The first step of a probabilistic solution to an engineering problem is to identify two (preferably independent) random variables, one of which represents a load effect and the other a resistance effect. These variables are normally denoted by load $S$ and resistance $R$. When $R$ and $S$ have the same units and the probability of $R$ being less than $S$ can be interpreted physically as failure, the stage is set for a meaningful solution. In a fire situation, when fire endurance is associated with load $S$ and time to failure of the component is associated with resistance $R$, the above requirements are met.

132

Modeling the time to failure of various floor assemblies and the fire severity
to which they may be exposed is the first required step to further estimate
safety of the assemblies.

Fire Duration

The prediction of fire duration, and more generally fire severity, is a
research topic in itself (6,12,23,28,30,40). For this analysis, it will suf-
fice here to use the approach reviewed by Lie (21). For ventilation controlled
fires, in which case the duration would be the longest, the relation which
relates fire duration to available ventilation (e.g., window area and window
height) is given by

$$t_d = \frac{WA_F}{5.5 \, A_W H^{1/2}} \ (min)$$

(1)

where $\underline{W}$, $\underline{A}_F$, $A_W$, and $\underline{H}$ will be treated as random and defined as

W = fuel load density $(kg/m^2)$

$A_F$ = floor area $(m^2)$

$A_W$ = window are $(m^2)$

H = window height (m)

The constant 5.5 has units $kg \, min^{-1} \, m^{-5/2}$

Model Building for an Exposed
  Floor Joist

It is assumed that the failure during fire exposure is due to charring of
the three exposed sides of the joist, and this loss of section coupled with
the strength reducing influence of elevated temperature causes rupture of the
joist. While burn-through and elevated temperatures of the unexposed surface

133

can be additional failure criteria, they are not considered in this analysis.
(These failure criteria relate directly to the floor-subfloor design which can
be analyzed separately.)  Load sharing and composite action is not accounted
for directly in the analysis; however, it should eventually be included in an
experimental verification of the model.

A typical floor joist section is shown in figure 2.  The shaded region
shows an idealized charred area.  Schaffer (33) reports that the bottom corners
round when charring occurs, and furthermore, the radius of the corners can be
approximated by the depth of char.  To account for this rounding by means of
the moment of inertia, would extremely complicate the computations in the
analysis, and it is clear that the error involved by assuming straight bounda-
ries is of minor concern.

By use of the flexure formula, an equation can be written to quantify
failure in a fire situation as

$$\frac{M \, Y \, (t_f, C)}{I(t_f, C)} = \alpha B \qquad (2)$$

where

$M$          = the applied moment due to both dead and live loads (in.-lb)

$t_f$         = time to failure (min)

$Y(t_f, C)$ = the distance to the extreme fiber being a function of the time
             to failure and char rate (in.)

$I(t_f, C)$ = the moment of inertia about an axis located midheight the
             remaining uncharred section (in.$^4$)

$\alpha$         = an exposed joist performance factor which relates normal
             temperature strength to high temperature strength

134

B            = the joist modulus of rupture at room temperature $(lb/in.^2)$.
This model is similar to that used by others for large beams under fire expo-
sure (20,21). It also neglects any contribution to strength by the flooring
itself.

The selection of the above model needs some justification. At room
temperature $\alpha = 1$ and the model is exact with the thought in mind that the
modulus of rupture is an idealized linear state. The actual state of stress
is nonlinear, but the model is adequate for design especially when the "depth
effect" is taken into account. In a fire situation, the nonlinearities are
expected to worsen since the joist cross section will not maintain a uniform
temperature. The movement of the neutral axis, due to a nonuniform modulus of
elasticity (MOE) resulting from a nonuniform temperature profile, can be
expected. At the same time, the compressive and tensile strengths of the wood
fibers are reduced due to elevated temperatures (Schaffer (33)). It may be
possible to model the net effect of the above-mentioned behavior when coupled
with the normal temperature nonlinearities of bending, but it has not been
reported in the literature. By introducing the exposed joist performance
factor, $\alpha$, these unknowns will be accounted for in an empirical sense. In
addition, the factor $\alpha$ will account for the rounding of the corners and to
some degree, load sharing and composite action of the flooring-joist assembly.

Referring to figure 2, it can be seen that equation (2) can be rewritten
as

$$\frac{M \ (d \ - \ C \ t_f)/2}{(b \ - \ 2C \ t_f) \ (d \ - \ C \ t_f)^3/12} = \alpha B \tag{3}$$

135

where

b = the initial joist width (in.)

d = the initial joist depth (in.)

The remaining variables have been defined with equation (2). All of the above except $\underline{b}$ and $\underline{d}$ are treated as random variables. It is assumed that the failure is due to charring of the three exposed sides of the joist and this loss of section coupled with the influence of elevated temperature on strength properties causes rupture of the joist. By rearranging (3), there results a cubic equation in time, $\underline{t}_f$

$$\frac{6M}{\alpha B} = bd^2 - 2Cd(d + b)\ t_f + C^2(b + 4d)\ t_f^2 - 2C^3\ t_f^3 \tag{4}$$

While cubic equations can be readily solved by hand calculation and computer, the derivation of the statistics of the variable $\underline{t}_f$ would be cumbersome. This fact led the authors to investigate the error introduced in $\underline{t}_f$ by dropping the cubic term and simply solving the quadratic equation for $\underline{t}_f$. Fortunately, the errors introduced are negligible, ranging from 1.58 percent for a 2 by 6 (38 by 140 mm) to 0.35 percent for a 2 by 12 (38 by 286 mm). It must be emphasized that this approximation was shown to be adequate for only 2 by 6 (38 by 140 mm), 2 by 8 (38 by 184 mm), 2 by 10 (38 by 235 mm), and 2 by 12's (38 by 286 mm).

The data and results of full-scale floor section (two Douglas-fir joists per assembly) tests reported by Lawson were used to study the applicability of the model (20). A question immediately arises with regard to the appropriate value of the modulus of rupture, $\underline{B}$. Since the test for the measurement of $\underline{B}$ and the fire test are both destructive tests, it is impossible to have knowledge of both properties for a single piece. At this impasse the alternative

136

was to investigate the mean and variability of the product of the two variables $\alpha$ and $\underline{B}$. This was done in the following way:

The 42 Douglas-fir floor assemblies tested by Lawson were divided into four grade groups as shown in table 1. These data indicate that there is little difference in the apparent high temperature modulus of rupture for the four different grades. More surprising are the calculated coefficients of variation (COV). From data collected by Hoyle in a world search of lumber data, a value of 0.45 for the COV of $\underline{B}$ is typical for Construction grade joist (15). With all grades combined, the $\Omega$ was only 0.271 which shows that E-119 exposure appears to have a variance-reducing influence on $\underline{B}$ just as suggested by Sunley (39).

To scrutinize the model further, an attempt was made to predict the fire endurance of two Douglas-fir assemblies tested by Son (36). Structural failures occurred at 11.63 and 13.00 minutes for nominal 2 by 10 and 2 by 8 joist floors respectively. By assuming the 2 by 10 and 2 by 8 joist floors to be of similar quality as of the Lawson report, i.e., $\underline{\alpha B}$ = 1,165 pounds per square inch (lb/in.$^2$) (8,032 kPa), the predicted time to failure was 2.58 minutes. The large discrepancy between actual and predicted time is attributable to the difference between live load levels used by Lawson and Son. In the tests of Son, the joists were stressed to 100 percent of the allowable design stress, as is specified by ASTM E-119, whereas the load levels used in the Lawson tests ranged from only 200 to 917 lb/in.$^2$ (1,378 to 6,322 kPa), which is approximately 16 to 75 percent of the allowable design stress. This results in failure times calculated using figure 1 of 23 and 11.4 minutes respectively for a nominal 2 by 8 joist floor as Son (36) tested. Hence, as one expects, the lower the load level, the greater is the time to failure and thus more thermal

degradation is allowed to occur. Beams more heavily loaded will have shorter times to failure and less thermal degradation. The right-hand side of equation (3), representing the retained strength due to temperature rise, cannot account for the influence of heat accumulation degrading the cross-sectional strength unless some measure of time dependence is introduced. By making several data plots, the following model was developed to include such time dependence where the variables have been previously defined.

$$\frac{M(d - Ct_f)/2}{(b - 2Ct_f)(d - Ct_f)^3/12} = \frac{B}{1 + \frac{b + 2d}{bd}\gamma t_f} \tag{5}$$

The $[(b + 2d)\gamma t_f]/(bd)$ term may be viewed as a time-dependent geometic fictor to account for heat flowing into the cross section, bd, through the perimeter, b + 2d.

While visual inspection of the data plots suggest the use of the above model, some variation of the model may be more suitable. Again, as before, the cubic term $\underline{t}_f$ of equation (4) is negligible. A least-squares nonlinear regression analysis was conducted on five variations of equation (4) as shown in table 2. The models were fitted to the 42 full-scale floor section tests of Lawson.

It is seen that the second single-parameter model of the table is the preferred model, since the residual standard deviation is only slightly more than the residual standard deviation of the two-parameter model listed first in the table. The range of predicted times-to-failure for the 42 floor assemblies was 7 to 29 minutes. This shows that the selected model is a reliable predictor when recognition is made of the fact that the residual standard deviation of 2.57 minutes includes the variability of $\underline{\alpha B}$ as shown in table 1.

138

Solving equation (5) for $t_f$ by omitting the cubic, results in

$$t_f = \frac{2Cd(d + b) + 6MK\gamma/B}{}$$

$$- \sqrt{\frac{\{2Cd(d + b) + 6MK\gamma/B\}^2 - 4C^2(b + 4d)(bd^2 - 6M/B)}{2C^2(b + 4d)}} \qquad (6)$$

where $K = (b + 2d)/bd$, which is an explicit expression for the time to failure. Time to failure, $t_f$, is compatible to the previously defined fire duration $t_d$, which is the load variable.

Results predicted by equation (5) were compared to four floor fire endurance test results obtained by National Forest Products Association ([44],[45],[46], [47]). The actual times to failure to carry load versus those predicted are given in table 3. It is observed that the predicted times are consistently and significantly less than the times to failure of the whole floor assembly. This deviation can be explained by the model parameter derivation based upon Lawson's ([20]) results. Lawson conducted fire endurance test of paired Douglas-fir joists with essentially noncontinuous floor sheathing. The NFPA tests are of assemblies consisting of many joists and a more or less continuous floor sheathing. Such assemblies result in load-sharing between joists and increased load-carrying capacity of the sheathing which is not similarly reflected in the paired joist tests by Lawson. If one takes note of the time when the first joist ruptures in the NFPA tests, the difference between the model predicted results and actually observed are closer in two of the tests where it was observed. This, again, illustrates the need to have a degrade parameter, $\gamma$, or other parameters which include both the effect of load-sharing and floor sheathing. As a result, such replicate experiments are planned.

## Model for Exposed Floor Truss

The lower chord of a floor truss is subjected to both bending and tension, and the well-known interaction equation is used for design purposes.

$$I = \frac{f_b}{F_b} + \frac{f_t}{F_t} \leq 1 \tag{7}$$

Here $f_b$ and $f_t$ denote applied stresses, $F_b$ and $F_t$ denote allowable design stresses in bending and tension, respectively.

As in previous reliability work (38), this interaction equation can be modified to indicate failure (with some reservations as discussed in the Forest Products Laboratory report No. 302). However, in a fire exposure case, we need to estimate one parameter, thus some slight inaccuracy in the neighborhood of the combined stresses associated with a floor truss will be corrected. The failure equation for fire exposure would read

$$\alpha = \frac{f_b}{B} + \frac{f_t}{T} = \frac{1}{1 + g(b,d,t_f,\gamma)} \tag{8}$$

where the right-hand side of the equation has a form similar to that for the exposed floor joist. Function $g$ accounts for the thermal degrade of the section, and its arguments are later defined. $B$ is the modulus of rupture from which $F_b$ was derived and $T$ is the ultimate tensile strength property from which the design value $F_t$ was derived.

140

Because four-sided fire exposure of the lower chord in a floor truss is critical,[4/] expansion of the interaction formula for this case is as follows:

$$\frac{\dfrac{P}{(b - 2C\, t_f)(d - 2C\, t_f)}}{T} + \frac{\dfrac{M(d - 2C\, t_f)/2}{(b - 2C\, t_f)(d - 2C\, t_f)^3/12}}{B} = \frac{1}{1 + \gamma K\, t_f} \qquad (9)$$

where

$K$ = $2(b + d)/(bd)$

$\gamma$ = the thermal degrade factor

$P$ = the axial tensile force due to dead plus live load

$b$ = the width

$d$ = the depth

$C$ = the char rate

$t_f$ = the time to failure

$M$ = the maximum bending moment due to dead plus live load

$B$ = the modulus of rupture

$T$ = the ultimate tensile stress.

Analogous to the floor joist case, $K$ is the ratio of the lower chord perimeter (or surface area for heat transfer) to the cross-sectional area (or volume for heat storage). After some manipulation, there results the cubic equation

---

[4/] It is assumed that the mode of failure is rupture of the lower chord. The upper chord has only three-side exposure, and the webs are only stressed to approximately one-half the level of the lower chord.

$$\{-8C^3\} \, t_f^3 + \{4C^2(b + 2d) + \frac{2PC \, \gamma K}{T}\} \, t_f^2 + \{-2dC(d + 2b)$$

(10)

$$- \frac{Pd}{T} \, \gamma K + \frac{2PC}{T} - \frac{6M \, \gamma K}{B}\} \, t_f + \{bd^2 - \frac{Pd}{T} - \frac{6M}{B}\} = 0$$

This equation will later be solved for $\underline{t}_f$ and used to estimate assembly reliability.

Model Parameters for an
  Exposed Floor Truss

To properly estimate model parameters, test data on 2 by 4 assembly members under combined tension and bending are required. Unfortunately, none are available for this purpose. Schaffer (32), however, has conducted fire exposure tests of constantly tensile loaded Select Structural coast Douglas-fir and southern pine 2 by 4 members. The time to failure was recorded (table 4).

For pure tension, the failure model reduces to

$$P(1 + \gamma K t_f) = T(b - 2C t_f)(d - 2C t_f) \tag{11}$$

This expression is easy to deal with, since it is only a quadratic in $\underline{t}_f$. Solving it for $\underline{t}_f$, there results

$$t = \frac{2T \, C(b + d) + P\gamma K - \sqrt{\{2T \, C(b + d) + P\gamma K\}^2 - 16T \, C^2(Tbd - P)}}{8T \, C^2} \tag{12}$$

where the minus root is the meaningful root.

An estimate is needed for the mean tensile strength, $\bar{T}$, and char rate, $\underline{C}$, to determine $\underline{\gamma}$ for the available tensile fire test data.

142

An estimate of $\bar{T}$ is available for inland Douglas-fir Select Structural [Hoyle (16)]. Based on a sample size of 30, the average tensile strength value was 5,020 lb/in.$^2$ (34,600 kPa) with a COV of 0.388.

This average tensile strength value can be compared to what might be calculated using normal distribution theory and the allowable tensile stress. From NDS 77 (26) the allowable tensile value for Select Structural Douglas-fir/larch is 1,200 lb/in.$^2$. Using the calculated COV of 0.388, the mean value is determined to be 6,811 lb/in.$^2$ by the following formulae:

$$1,200 = (\bar{T} - 1.645 * COV * \bar{T})/2.1 \qquad (13)$$

This value is significantly larger than the actual mean of 5,020 which illustrates the non-normal nature of tensile data. This shows, therefore, that one should use the mean value obtained from lumber tests whenever possible for the grade and species in question.

The nine Douglas-fir fire and tension test results can then be used to estimate $\underline{y}$ for Douglas-fir. By using $\bar{T}$ = 5,020 and C = 0.0245 inch per minute, $\underline{y}$ was estimated to be 0.113 with a residual standard deviation of the time to failure of 1.829 minutes.

A similar estimate of the fire exposure reduction factor $\underline{y}$ can be done for the southern pine test results of table 4. The southern pine lumber tested was nearly clear of defects, and it was ungraded. The lumber appeared to have a quality at least as good as Select Structural. There are data [Hoyle (17)] that show that high quality southern pine (2400f machine stress rated (MSR)) is stronger in tension than high quality Douglas-fir (2400f MSR)--the ratio in strengths being 1.24. To arrive at a mean value for the tensile strength T of Select Structural southern pine, the 5,020 lb/in.$^2$ value for Douglas-fir

was multiplied by 1.24 to yield 6,233 lb/in.$^2$ for southern pine. Using a mean char rate for southern pine of 0.03 inch per minute (33) in a nonlinear regression analysis of the fire test results, the yield is an $\gamma$ of 0.0839 inch per minute with a residual standard deviation of the time to failure of 1.077 minutes.

Both species value of the reduction factor, $\gamma$, (0.113 for Douglas-fir and 0.0839 for southern pine) are substantially lower than that of 0.17 obtained for the floor joist assembly in the preceding section. The reasons for this are not clear at present. It is known, however, that smaller sections (2 by 4, as compared to 2 by 8, or 2 by 10's) are likely to suffer a more rapid reduction in cross section than larger ones. The difference for 2 by 4 sections of southern pine and Douglas-fir are shown in figures 3 and 4 as a function of fire exposure time.

The developed model and parameters may be used to estimate the structural failure of a given floor truss assembly. This was done for the truss shown in figure 5. The lumber of the floor truss is No. 1 Dense KD southern pine. $\bar{B}$ for No. 1 Dense southern pine was obtained from table 2 of Doyle and Markwardt (7). As tensile strength data for Dense No. 1 was not available, data for No. 1 KD southern pine was taken from Doyle and Markwardt (8). The published value of 5,706 was adjusted to reflect current standards by Forest Products Laboratory personnel to 5,646 lb/in.$^2$.

The truss was then analyzed with Purdue Plane Structures Analyzer (37), and as normally is the case, the center panel of the lower chord was most highly stressed with an axial force of 4,209 pounds and a bending moment of 140 inch-pounds. A summary of the input parameters can now be given for the fire tested floor truss.

144

$\gamma$ = 0.0839 inch per minute

P = 4,209 pounds

b = 3.5 inches

d = 1.5 inches

C = 0.03 inch per minute

M = 140 inches-pounds

B = 9,410 lb/in.$^2$

T = 5,646 lb/in.$^2$

Substitution into and solution of the failure model equation (10) results in a time to failure estimate of 11.2 minutes. The actual failure time was estimated to be at 10.2 minutes (10). This test continued to be conducted under reduced load until 14.6 minutes, where fire exposure was terminated without occurrence of collapse. The predicted time to failure falls within this 10- to 15-minute range. This result is most promising for future use of the model.

It is interesting to examine how time to failure is altered for the same truss with a reduction in applied load. The failure model equation predicts times-to-failure as a function of applied load as shown in figure 6. For reduction in load to 50 percent of full design, it is seen that 5 minutes is added to the predicted time under full design load. If there were no load on the floor assembly except the dead weight (4.9 lb/ft$^2$) of the assembly itself, a failure time of 21.1 minutes results. Hence, failure times greater than this are theoretically impossible for this truss design.

## Estimating the Safety

In the preceding paragraphs we have developed models for predicting the time-to-failure of two floor assembly types and have given an accepted model to predict severity of fire exposure. Both are given in units of time.

Using the standard reliability notation, the assembly time to failure and the time duration of fire exposure, $t_f$ and $t_d$ are denoted as follows:

$$R = t_f \qquad (14)$$

and

$$S = t_d \qquad (15)$$

With $R$ and $S$ defined, the fire reliability (Rel) of an exposed joist or floor truss (as a part of a floor), given the occurrence of a fully developed fire, is given by

$$Rel = Pr(R > S) \qquad (16)$$

which reads the probability (Pr) that the fire resistance is greater than the fire load. It is convenient, from a calculations standpoint, that $R$ and $S$ be independent. In other words, the amount of fire load and associated parameters cannot be correlated to the members resistance, char rate, and so on. Conversely, the structural load, member resistance, and char rate cannot be influenced by the fire load. Unfortunately, it is known that the char rate is correlated with the variables of equation (1) which is discussed by Schaffer (35). However, in practice, the joist or component will be exposed to a standard fire condition such as ASTM E-119 where the char rate will not be influenced by the variables $W$, $F$, $A$, and $H$. The real problem lies in the

146

fact that the fire severity of E-119 may not be representative of the fire severities associated with actual fire situations. It is thus appropriate in this analysis to treat $\underline{R}$ and $\underline{S}$ as independent random variables.

Using the approach of Zahn (43),

$$Rel = Pr(R/S > 1) \tag{17}$$

and taking the logarithm of the arguments

$$Rel = Pr(\ln(R/S) > 0). \tag{18}$$

By making the following definition

$$J = \ln(R/S) \tag{19}$$

there results

$$Rel = Pr(J > 0) = 1 - F_J(0) \tag{20}$$

where $\underline{F}_J$ is the cumulative density function of the variable $\underline{J}$.

Using first order, second moment approximations, the mean and variance are given by

$$\mu_J \cong \ln \frac{\mu_R}{\mu_S} \tag{21}$$

$$\sigma_J^2 \cong \Omega_R^2 + \Omega_S^2 \tag{22}$$

Standardizing $\underline{J}$,

$$\lambda \equiv \frac{J - \mu_J}{\sigma_J} \tag{23}$$

and

$$Rel = Pr \left[ \lambda > -\left(\frac{\mu_J}{\sigma_J}\right) \right] \tag{24}$$

If the distribution of $\lambda$ is similar in all applications, then the variable

$$\beta \equiv = \frac{\mu_J}{\sigma_J} \quad \frac{\ln \frac{\mu_R}{\mu_S}}{\sqrt{\Omega_R^2 + \Omega_S^2}} \tag{25}$$

is a consistent measure of fire safety. $\beta$ is normally called the safety index.

The next step is to estimate the means and variances of the resistance and load, $\underline{\mu}_R$ and $\underline{\mu}_S$, $\underline{\sigma}_R^2$ and $\underline{\sigma}_S^2$. A first order approximation of the mean, E, of a function, Z, where

$$Z = h(X_1, X_2, \ldots, X_n) \tag{26}$$

is given by

$$E(Z) = h[E(X_1), E(X)_2), \ldots, E(Z_n)] \tag{27}$$

Performing this operation on equation (6) for the conventional joist floor assembly and replacing the expected values, E, of the component variables by their statistical estimates denoted by a superscript bar, the result is

148

$$\mu_R \cong \frac{2\bar{C}d(d + b) + 6\bar{M}K\bar{\gamma}/B}{}$$

$$- \frac{\sqrt{\{2\bar{C}d(d + b) + 6\bar{M}K\bar{\gamma}/B\}^2 - 4\bar{C}^2(b + 4d)(bd^2 - 6\bar{M}/B)}}{2C^2(b + 4d)} \tag{28}$$

where $\gamma$ is treated as a random variable and $\underline{B}$ will be treated as a constant equal to the average strength of the joist grade. In otherwords, $\underline{\gamma}$ will be used to account for the total variability associated with $\underline{\gamma}$ and $\underline{B}$.

For a floor truss assembly, the result for the mean time to failure is similarly obtained by dropping the cubic term in equation (10), solving the quadratic, and by placing the expected values of the component variables by their statistical estimates

$$\mu_R \cong \frac{-b_1 - \sqrt{b_1^2 - 4\,a_1 c_1}}{2a_1} \tag{29}$$

where

$$a_1 = 4\bar{C}^2(b + 2d) + 2\bar{P}\bar{C}\,\bar{\gamma}\,K/T \tag{29a}$$

$$b_1 = 2\bar{P}\bar{C}/T - 2d\bar{C}(d + 2b) - \bar{P}d\,\bar{\gamma}\,S/T - 6\bar{M}\,\bar{\gamma}\,K/B \tag{29b}$$

$$c_1 = bd^2 - \bar{P}d/T - 6\bar{M}/B \tag{29c}$$

149

Again, $\underline{y}$ is treated as a random variable, and $\underline{B}$ and $\underline{T}$ are treated as constants equal to the average bending and tensile strength of the lumber grade.

The same operation is performed on the fire severity equation, which results in

$$\mu_S \cong \frac{\bar{W} \bar{A}_F}{5.5 \bar{A}_W \bar{H}^{1/2}} \tag{30}$$

The first order, second moment approximation of the variance of $\underline{Z}$ defined by equation (26) is given by

$$\sigma_Z^2 \cong \sum_{i=1}^{n} \left( \frac{\partial h}{\partial X_i} \right)^2 \sigma_{X_i}^2 \tag{31}$$

provided the $X_i$'s are uncorrelated. The partial are evaluated at their respective mean values.

In the expression for the load variable $\underline{S}$, the floor area $\underline{A}_F$ and window area $\underline{A}_W$ could be correlated since one would expect $\underline{A}_W$ to be some way related to the perimeter which involves the same variables as the floor area. However, since data are not available to substantiate this correlation, a zero correlation will be assumed. In the case of light-frame construction, the other pairs of variables lack an obvious cause for correlation. Without showing the computations

$$\sigma_S^2 = \bar{S}^2 (\Omega_W^2 + \Omega_{A_F}^2 + \Omega_{A_W}^2 + \Omega_H^2/4) \tag{32}$$

150

$$\Omega_S^2 = \Omega_W^2 + \Omega_{A_F}^2 + \Omega_{A_W}^2 + \Omega_H^2/4 \tag{33}$$

where the $\underline{\Omega}$'s are the respective COV.

In the equation for resistance, or time to failure of the floor joist, there does not appear to be any obvious confounding correlations. Using equation (31) to estimate the variance of equation (6), three partial derivatives must be calculated. These derivatives are lengthy so they will only be substituted into equation (31) symbolically, which results in

$$\sigma_R^2 = \left(\frac{\partial R}{\partial C}\right)^2 \sigma_C^2 + \left(\frac{\partial R}{\partial \alpha}\right)^2 \sigma_\alpha^2 + \left(\frac{\partial R}{\partial M}\right)^2 \sigma_M^2 \tag{34}$$

Again, the partial derivatives are evaluated at the mean values of the component variables.

For the case of the floor truss, component variables $\underline{M}$ and $\underline{P}$ are perfectly correlated with a correlation of +1. Therefore, equation (31) must be altered to include correlations as

$$\sigma_Z^2 = \sum_{i=1}^{n}\left(\frac{\partial h}{\partial X_i}\right)^2 \sigma_{X_i}^2 + 2 \sum_{\substack{i \\ i<j}}^{n} \sum_{j}^{n} \left(\frac{\partial h}{\partial X_i}\right)\left(\frac{\partial h}{\partial X_j}\right) \rho_{ij}\, \sigma_{X_i} \sigma_{X_j} \tag{35}$$

where $\rho_{ij}$ is the correlation coefficient between variables $X_i$ and $X_j$. By assuming zero correlation for the other variables, as for the floor joist case, application of equation (35) to equation (29) yields

$$\sigma_R^2 = \left(\frac{\partial R}{\partial C}\right)^2 \sigma_C^2 + \left(\frac{\partial R}{\partial \gamma}\right)^2 \sigma_\gamma^2 + \left(\frac{\partial R}{\partial M}\right)^2 \sigma_M^2 + \left(\frac{\partial R}{\partial P}\right)^2 \sigma_P^2$$

$$+ 2\left(\frac{\partial R}{\partial M}\right)\left(\frac{\partial R}{\partial P}\right)\sigma_M \, \sigma_P \tag{36}$$

The variance of the char rate, $\sigma_C^2$, has been estimated by reanalyzing data previously developed (33). The mean charring rate, $\bar{C}$, and estimated variance, $\sigma_C^2$, under ASTM E-119 fire exposure for coast Douglas-fir and southern pine are

coast Douglas-fir    $\bar{C} = 0.0245$ in./min, $\sigma_C^2 = 5.56 \times 10^{-6}$

southern pine          $\bar{C} = 0.0299$ in./min, $\sigma_C^2 = 3.80 \times 10^{-6}$

The variance in the strength reduction factor, $\gamma$, is unavailable. Substantial information is available on the variation of the applied load which defines the variation of $M$ and $P$. Eventually, all the variances denoted by $\sigma^2$ will be replaced by statistical estimates from the data available or being researched now. Finally, the COV of $R$ can be obtained and is given by

$$\Omega_R = \frac{\sigma_R}{\mu_R} \tag{37}$$

As statistical data become available for the various parameters, the components of the safety index equation (25) may be defined and comparisons of assembly safety accomplished.

## Discussion

### Probability of Failure

Knowing the distribution of $\lambda$ of equation (23), the probability of structural failure of an exposed floor assembly, given the occurrence of a fully

developed fire, can be calculated. In general, the distribution of $\underline{\lambda}$ is not known, and some assumption about the distribution of $\underline{\lambda}$ must be made. It is common practice to assume that $\underline{\lambda}$ follows a normal distribution. In this analysis, the assumption of normality will be used realizing that the probability estimated will be in the neighborhood of 0.1; thus deviations from normality from one application to the next will not be amplified. Under these assumptions, the probability of failure, $P_f$, is given by

$$P_f = \phi(-\beta) = 1 - \phi(\beta) \tag{38}$$

where $\phi$ is the cumulative area under the standard normal curve.

Code Calibration

In recent years the use of engineering components has increased dramatically. Often these components are fabricated with manmade materials, and the variability of the mechanical properties of these materials is substantially less than the variability of a natural material such as wood. The shortcoming of the present "fire rating" system is that while it may account for the average response of a component to fire, it does not account for the variability of the component response. Quite simply, the present system of fire rating allows for the use of two different components with an equal "fire rating" of, say, 1 hour, but at the same time have unequal safety levels. This situation can best be illustrated by a hypothetical example using equation (25). The example involves the calculation of the safety index for two different components, the only difference being the variability of the time to failure or resistance of the component.

For the example, assume that the following data in table 4 applies to two component types A and B.

Each column is identical except for the column indicating the COV of fire resistance. Upon applying equation (25) to each case, the result is $\beta_A = 0.98$ and $\beta_B = 1.24$, which indicates an unequal level of safety. Converting these $\beta$'s by equation (38) to probabilities, the results are 0.163 for component A and 0.107 for component B. It may be hastily argued that there is no difference between a 16.3 percent and 10.7 percent failure rate, but upon closer examination, it can be calculated that component B could have a fire endurance time of 51.9 minutes and have the same relative safety as component A at 60 minutes.

The above hypothetical situation illustrates just one possibility of how the safety index could be used to obtain equal safety and give a "fair shake" to new materials and new components.

In the future it may be possible to identify where the fire load, and hence the fire duration, have different expected values and different levels of variability. In such a case, a lower or higher fire-rated component may be needed.

### Summary and Conclusions

1. Time to structural failure prediction models, based upon the residual load-carrying capacity of fire-exposed floor elements, are given for two unprotected light-frame floor assemblies. A reduction in strength factor, $\alpha$. was calculated from the limited fire exposure test data according to two equations:

Joist floor

$$\frac{MY(t_f, C)}{I(t_f, C)} = \alpha B$$

Floor truss

$$\frac{f_b}{B} + \frac{f_t}{T} = \alpha$$

The thermal reduction factor is further a function of fire exposure time and the geometry of small cross sections:

Joist floor

$$\alpha = 1/(1 + \gamma K t_f)$$

where

$$\gamma = 0.170 \text{ (in./min)}$$

Floor truss

$$\alpha = 1/(1 + \gamma K t_f)$$

where for

| | |
|---|---|
| Douglas-fir | $\gamma = 0.113$ in./min |
| Southern pine | $\gamma = 0.0839$ in./min |

2. A comparison of predicted times to failure versus those actually observed for four unprotected _joist_ floor assemblies results in predicted times consistently less than that observed. The difference is attributed to three factors:

--The model has parameters quantified on the basis of fire endurance tests of paired joists with negligible floor sheathing.

--The actual floors consist of many joists with load-sharing likely.

155

--The actual floors have floor sheathing that contributes to increased

load-carrying capacity.

Predicted times to failure for two of the floor assemblies were similar to
that of observed times of failure of the first joist (not total floor assembly
failure).

3. The time-to-failure model with input parameters for a southern pine
floor truss assembly that had been fire endurance tested, resulted in a pre-
dicted time to failure of 11.2 minutes. The fire test had been concluded at
10.2 minutes due to excessive deflection of the floor assembly, without col-
lapse evidenced.

4. The time-to-failure model for a loaded and fire-exposed floor truss
assembly was employed to examine the influence of various floor loads on the
time to failure. At full design load, failure was predicted to be 11.2 minutes,
but with dead load alone, the period was extended to 21.1 minutes. This indi-
cates the sensitivity of such a fire-exposed assembly to the load applied
during test. This analysis did critically assume that failure of the lower
chord, rather than connectors, would result in collapse of the assembly.

5. The procedure to be used to calculate the safety of unprotected
light-frame floor assemblies is given. An example is provided to show how
variability in assemblies can affect the comparative safety of assemblies.

6. The predictive capabilities for both proposed assembly models requires
further fire exposure experiments for independent validation and parameter
refinement.

156

## Nomenclature

| | |
|---|---|
| R | Member or structural resistance |
| S | Applied "load" |
| $t_D$ | Fire duration |
| W | Fuel load density |
| $A_F$ | Floor area |
| $A_W$ | Window or opening area |
| H | Window or opening height |
| M | Applied moment |
| Y | Distance from beam centroid to outer fiber |
| I | Moment of inertia |
| $\alpha$ | Ratio of high temperature to normal temperature strength |
| B | Modulus of rupture at room temperature |
| C | Char rate |
| MOE | Modulus of elasticity |
| b | Beam breadth |
| d | Beam depth |
| $\sigma$ | Standard deviation |
| $\Omega$ | Coefficient of variation |
| $\gamma$ | Thermal degrade factor |
| F | Allowable stress |
| P | Axial load |
| T | Ultimate tensile stress |
| $\mu$ | Statistical mean |
| $\beta$ | Safety index |

157

| | |
|---|---|
| $\rho$ | Correlation coefficient |
| $\phi$ | Accumulative density function for standard normal distribution |
| $K$ | Ratio of perimeter to area of cross section. |

## Subscripts

| | |
|---|---|
| b | Bending |
| t | Tension |
| f | Failure |
| d | Duration |
| R | Resistance |
| S | Load |

158

# Literature Cited

1. Abrams, M. S.
    1978. Behavior of inorganic materials in fire. ASTM E-5 Symp. on design of buildings for fire safety. Boston Park Plaza, Boston, Mass.

2. American Iron and Steel Institute.
    1978. Designing fire protection for steel columns. American Iron and Steel Inst., Washington, D.C.

3. American Society for Testing and Materials.
    1977. Standard methods of fire tests of building construction and materials (E-119). Annu. Book of ASTM Standards, Part 18, p. 739-757.

4. Ang, A., et al.
    1972. Structural safety--A literature review. J. Struc. Div. ASCE 98 (ST4), p. 845-884.

5. Burros, R. H.
    1975. Probability of failure of building from fire. J. Struc. Div. Proc. ASCE 101 (ST9), p. 1947-1960.

6. Coward, S.K.D.
    1975. A simulation method for estimating the distribution of fire severities in office rooms. Build. Res. Estab. Current Pap. No. 31/75. Fire Res. Stn., Borehamwood Hertfordshire. WD6 2BL.

7. Doyle, D. V., and L. J. Markwardt.
    1966. Properties of southern pine in relation to strength grading of dimension lumber. U.S. Dep. Agric., For. Serv. Res. Pap. FPL 64. For. Prod. Lab., Madison, Wis.

8. Doyle, D. V., and L. J. Markwardt.
    1967. Tension parallel-to-grain properties of southern pine dimension lumber. U.S. Dep. Agric., For. Serv. Res. Pap. FPL 84. For. Prod. Lab., Madison, Wis.

9. Ellingwood, B., and J. R. Shaver.
    1977. Reliability of RC beams subjected to fire. J. Struc. Div. Proc. ASCE 103 (ST5), p. 1047-1059.

10. Factory Mutual Research.
    1977. Fire endurance test of floor-ceiling assembly. Wood trusses with plywood floor design. ASTM E-119-76, FC-250. Factory Mutual Res.

11. General Services Administration.
    1972. Building fire safety criteria. PBS P 5920.9 CHGE 2. Gen. Serv. Admin., Washington, D.C.

12.   Gross, D.
          1977.   Measurements of fire loads and calculations of fire severity.
          Wood and Fiber 9(1):72-85.   Wood Sci. and Tech.

13.   Gustaferro, A. H., and D. P. Jenny.
          1978.   Design concrete structures for fire endurance.   South. Build.,
          p. 24-28.   June-July.

14.   Gypsum Association.
          1978.   Fire resistance design manual.   Gypsum Assoc., Evanston, Ill.

15.   Hoyle, R. J.
          1977.   Review of world literature on characteristic distribution of
          properties of 2-inch softwood dimension lumber.   Res. Rep.
          No. 77/57-11.   Washington State Univ., Col. of Eng. Res. Div.,
          Pullman, Wash.

16.   Hoyle, R. J.
          1976.   Digest of tension parallel-to-grain strength of Inland North
          Douglas-fir.   Res. Rep. No. 76/57-22.   Washington State Univ.,
          Pullman, Wash.

17.   Hoyle, R. J., and T. M. Maloney.
          1976.   Tension strength and bending elastic modulus of truss joist
          machine stress rated 2 by 4 lumber.   Res. Rep. No. 76/57-44.
          Washington State Univ., Pullman, Wash.

18.   Kameda, H., and T. Koike.
          1975.   Reliability theory of deteriorating structures.   J. Struc. Div.,
          Proc. ASCE 101 (ST1), p. 295-310.

19.   Knudsen, R. M., and A. P. Schniewind.
          1975.   Performance of structural wood members exposed to fire.   For.
          Prod. J. 25(2):23-32.

20.   Lawson, D. I., C. T. Webster, and L. A. Ashton.
          1952.   The fire endurance of timber beams and floors.   Struc. Eng.,
          p. 27-33.   Feb.

21.   Lie, T. T.
          1972.   Fire and buildings.   Appl. Sci. Pub., Ltd.   Ripple Road, Barking,
          Essex, England.

22.   Lie, T. T.
          Optimum fire resistance of structures.   J. Struc. Div. ASCE 98(ST1),
          p. 215-232.

23.   Lie, T. T.
          1974.   Characteristic temperature curves for various fire severities.
          Fire Tech. 10(4):315-326.   Res. Pap. No. 651.   Div. of Build. Res.,
          Nat. Res. Counc. of Canada.

160

24. Ligtenberg, F. K.
    1971. Structural safety and fire (1.3). Build. Int., p. 271-272.
    Sept.-Oct.

25. Malhotra, H. L.
    1977. The philosophy and principles of fire tests. Fire prevention
    Sci. and Tech. (17):24-31. Build. Res. Estab., Fire Res. Stn.

26. National Forest Products Association.
    1977. Design values for wood construction--a supplement to the 1977
    edition of national design specification for wood construction.
    Washington, D.C. 20036. 20 p.

27. Nelson, H. E.
    1977. Directions to improve application of systems approach to fire
    protection requirements for buildings. Wood and Fiber 9(2):107-126.
    Wood Sci. and Tech.

28. Raes, H.
    1977. The influence of a building's construction and fire load on the
    intensity and duration of a fire. Fire Prevention Sci. and Tech.
    No. 16:4-16. Build. Res. Estab., Fire Res. Stn.

29. Rashbash, D. J.
    1977. The definition and evaluation of fire safety. Fire Prevention
    Sci. and Tech. 16:17-22.

30. Robertson, A. F., and D. Gross.
    1970. Fire load, fire severity, and fire endurance. Special Tech.
    Pub. 464. Amer. Soc. for Test. and Mat., Philadelphia, Pa. p. 3-29.

31. Roux, H. J., and G. N. Berlin.
    1978. Toward a knowledge-based fire safety system. Amer. Soc. for
    Test. and Mat. Symp. on design of buildings for fire safety.
    Boston Park Plaza, Boston, Mass.

32. Schaffer, E. L.
    1961. The effects of fire on selected structural timber joints.
    Unpubl. M.S. thesis, Univ. of Wis., Madison, Wis.

33. Schaffer, E. L.
    1966. Charring rate of selected woods--transverse to grain. U.S. Dep.
    Agric., For. Serv. Res. Pap. FPL 69. For. Prod. Lab., Madison, Wis.
    Apr.

34. Schaffer, E. L.
    1973. Effect of pyrolytic temperatures on the longitudinal strength of
    dry Douglas-fir. ASTM J. Test Eval. 1(4):319-329.

35. Schaffer, E. L.
    1977. State of structural timber fire endurance. Wood and
    Fiber 9(2):145-170. Wood Sci. and Tech.

36. Son, B. C.
    1973. Fire endurance tests on unprotected wood-floor constructions for
    single-family residences. Cent. for Build. Tech. Inst. for Appl.
    Tech., Nat. Bur. of Stan., Washington, D.C.

37. Suddarth, S. K.
    1972. A computerized wood engineering system: Purdue plane structures
    analyzer. U.S. Dep. Agric., For. Serv. Res. Pap. FPL 168. For. Prod.
    Lab., Madison, Wis.

38. Suddarth, S. K., F. Woeste, and W. Galligan.
    Differential reliability: Probabilistic engineering applied to wood
    members in bending/tension. U.S. Dep. Agric., For. Serv. Res. Pap.
    FPL 302. For. Prod. Lab., Madison, Wis.

39. Sunley, J. G.
    Design concepts for fire-resisting constructions. Behavior of wood
    products in fire. Pergamon Press, Oxford. p. 95-101.

40. Thomas, P. H., and C. R. Theobald.
    1977. Part 2: The burning rates and durations of fires. Fire
    Prevention Sci. and Tech. 17:15-16. Build. Res. Estab., Fire Res. Stn.

41. U.S. Department of Commerce/National Bureau of Standards.
    1978. Building research translation--the behavior of concrete struc-
    tures in fire--a method for prediction by calculation. NBS Tech.
    Note 710-7110. U.S. Government Printing Office, Washington, D.C.

42. U.S. Department of Housing and Urban Development.
    1973. HUD minimum property standards--one- and two-family dwellings.
    U.S. HUD, Washington, D.C.

43. Zahn, J. J.
    1977. Reliability-based design procedures for wood structures.
    For. Prod. J. 27(3):21-28.

44. National Forest Products Association.
    1974. ASTM E-119 fire endurance test--2- by 10-inch wood joist floor
    assembly. Design FC 212. Nat. For. Prod. Assoc., Washington, D.C.

45. National Forest Products Association.
    1974. ASTM E-119 fire endurance test--2- by 10-inch wood joist floor
    assembly. Design FC 209. Nat. For. Prod. Assoc., Washington, D.C.

46. National Forest Products Association.
    1974. ASTM E-119 fire endurance test--2- by 8-inch wood joist floor
    assembly. Design FC 216. Nat. For. Prod. Assoc., Washington, D.C.

47.  National Forest Products Association.

1974.  ASTM E-119 fire endurance test--2- by 8-inch wood joist floor

assembly.  Design FC 213.  Nat. For. Prod. Assoc., Washington, D.C.


48.  Hoyle, R. J., and T. M. Maloney.

1976.  Bending strength tests of visually graded 2-inch dimension lumber

from western Canada.  Res. Rep. No. 76/57-36.  Wash. State Univ.,

Pullman, Wash.

Table 1.--<u>The apparent high temperature modulus of rupture, αB, for each grade group</u>

| Grade | Sample size | Apparent rupture strength | | Coefficient of variation (COV) |
|---|---|---|---|---|
| | N | $\alpha B^{1/}$ | | $\Omega_{\alpha B}$ |
| | | Lb/in.$^2$ | kPa | |
| 800 | 20 | 1,126 | 7,764 | 0.238 |
| 1,200-1,600 | 15 | 1,126 | 8,384 | .320 |
| 1,600 | 2 | 1,264 | 8,715 | .442 |
| Clear | 5 | 1,266 | 8,729 | .199 |
| Combined | 42 | 1,182 | 8,150 | .271 |

1/ A constant char rate, C, of 0.025 in./min (0.0635 mm/min) was used in the calculation; therefore, the $\Omega$ values reported are an upper bound since they include the variability of the char rate.

Table 2. A least-squares non-linear regression analysis was conducted on five different variations of a time-to-structural-failure model. In each case, 42 data points were used to estimate either one or two parameters, depending upon the form of the model. The parameters must carry the necessary units to make the equations dimensionally homogeneous

| Model | Parameter estimates | Residual standard deviation |
|---|---|---|
| | | Min |
| $$\dfrac{M(d - Ct_f)/2}{(b - 2Ct_f)(d - Ct_f)^3/12} = \dfrac{B}{\gamma_0 + \gamma_1\ Kt_f^{1/}}$$ | $\gamma_0 = 0.296$ <br> $\gamma_1 = 0.206$ | 2.54 |
| $$= \dfrac{B}{1 + K\ \gamma\ t_f}$$ | $\gamma = 0.170$ | 2.57 |
| $$= \dfrac{B}{1 + K^{\gamma_0}\gamma_1 t_f}$$ | $\gamma_0 = 1.20$ <br> $\gamma_1 = 0.160$ | 2.60 |
| $$= \dfrac{B}{1 + \gamma\ t_f}$$ | $\gamma = 0.216$ | 2.74 |
| $$= \dfrac{B}{1 + K(\gamma_1\ t_f + \gamma_2\ t_f^2)}$$ | $\gamma_1 = -0.324$ <br> $\gamma_2 = 0.0328$ | 3.26 |

1/ $K = (b + 2 * d)/(b * d)$.

165

Table 3.--Predicted and actual times to failure for NFPA unprotected floor fire endurance tests (44,45,46,47)

| Sample | Nominal size | Applied joist moment In. lb | $\bar{B}$[2] Lb/in.² | C In./min | Predicted $t_f$ Min | Assembly Observed $t_f$ Min | Joist[1] Observed $t_f$ Min |
|---|---|---|---|---|---|---|---|
| No. 2 Douglas-fir "S-dry" w/vinyl tile, 19/32 in. plywood | 2 x 8 | 19,054 | 4,308 | 0.0245 | 5.42 | 10.2 | 5.0 |
| No. 2 Douglas-fir "S-dry" w/nylon carpet, 19/32 in. plywood | 2 x 8 | 19,054 | 4,308 | 0.0245 | 5.42 | 12.86 | 11.5 |
| No. 2 MG southern pine "S-dry" w/vinyl tile, 23/32 in. plywood | 2 x 10 | 31,017 | 5,730 | 0.03 | 7.01 | 13.34 | 9.0 |
| No. 2 MG southern pine "S-dry" w/nylon carpet 23/32 in. plywood | 2 x 10 | 31,017 | 5,730 | 0.03 | 7.01 | 12.06 | 12.06 |

1/ Failure time for first joists to fail; not assembly failure time.
2/ Douglas-fir rupture strength derived from reference 48. Southern pine rupture strength derived from reference 7.

Table 4.--<u>Fire endurance of 2 by 4's under constant tensile</u>
<u>load.  Select Structural allowable stresses for</u>
<u>Douglas-fir and southern pine are taken from</u>
<u>1977 National Design Specifications (NDS)</u>

| Douglas-fir, coast | | Southern pine | |
|---|---|---|---|
| Test | Failure time | Test | Failure time |
| | <u>Min</u> | | <u>Min</u> |
| P = 6,100 lb, 90 pct $F_t$ | | P = 6,100 lb, 83 pct $F_t$ | |
| 1 | 11.20 | 1 | 10.00 |
| 2 | 7.67 | 2 | 11.61 |
| 3 | 9.35 | 3 | 12.85 |
| 4 | 11.25 | 4 | 12.34 |
| 5 | 8.74 | 5 | 11.80 |
| Mean | 9.64 | Mean | 11.72 |
| Standard deviation | 1.57 | Standard deviation | 1.08 |
| P = 4,960 lb, 73 pct $F_t$ | | | |
| 6 | 9.24 | | |
| 7 | 9.96 | | |
| 8 | 13.36 | | |
| 9 | 13.92 | | |
| Mean | 11.62 | | |
| Standard deviation | 2.36 | | |

Table 5.--Two components, A and B, have the same average fire endurance time (60 min) but different variabilities (COV of 0.25 versus 0.5). Each component is exposed to an identically distributed fire load, as illustrated by the last two columns of the table. The result is an unequal level of safety, as calculated by the safety index equation (25)

| Component | $\mu_R$ | $\Omega_R$ | $\mu_S$ | $\Omega_S$ |
|-----------|---------|-----------|---------|-----------|
|           | Min     |           | Min     |           |
| A         | 60      | 0.5       | 30      | 0.5       |
| B         | 60      | .25       | 30      | .5        |

168

Figure 1.--The family of curves for fire endurance of wood floors

$$\alpha^{1/2} = 1/2(1 - T\sqrt{s})[1 - (T/2\sqrt{s})]^2 \quad ((\underline{20})) \text{ where}$$

$$\alpha = \frac{\text{applied load}}{\text{breaking load}}\underline{1}/$$

$$= \frac{\text{design allowable stress}}{\text{ultimate stress}},$$

$s$ = D/B (depth/breadth),

$T = t/20\sqrt{\bar{A}}$,

$t$ = fire endurance (min), and

$A$ = cross-section area $(in.^2)$.

<u>1</u>/ Extreme fiber stress of 11,000 pounds per square inch at
    maximum load.
(M 145 178)

169
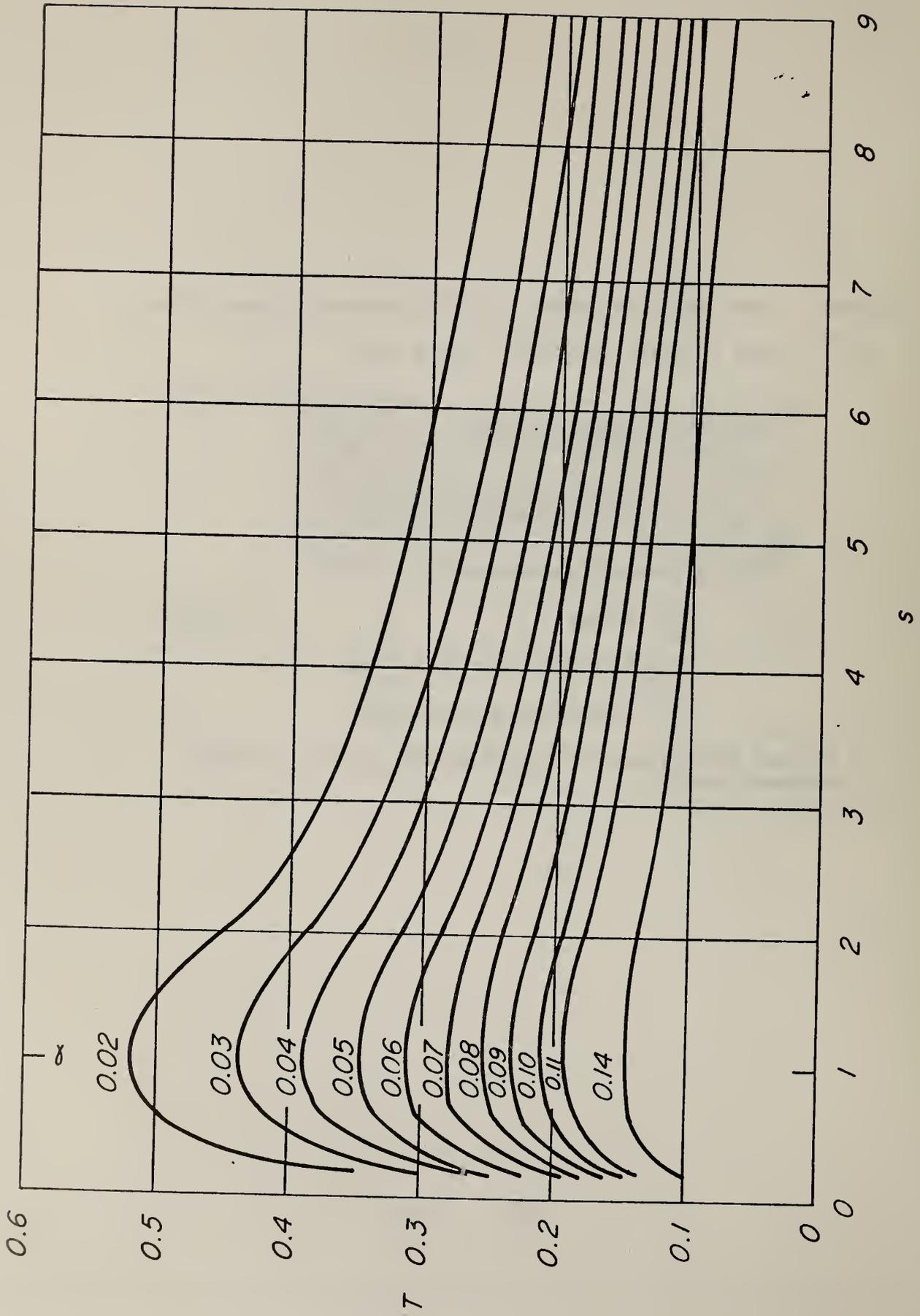
Figure 2.--An idealized exposed floor joist when subjected to fire chars on three sides.  The subfloor protects the top side of the joist.  While it is known that the bottom corners round, straight boundaries are used as an approximation.  After time, $t$, and char rate, $C$, the depth of char equals $C \cdot t$.

(M 148 531)

M 148 531

172
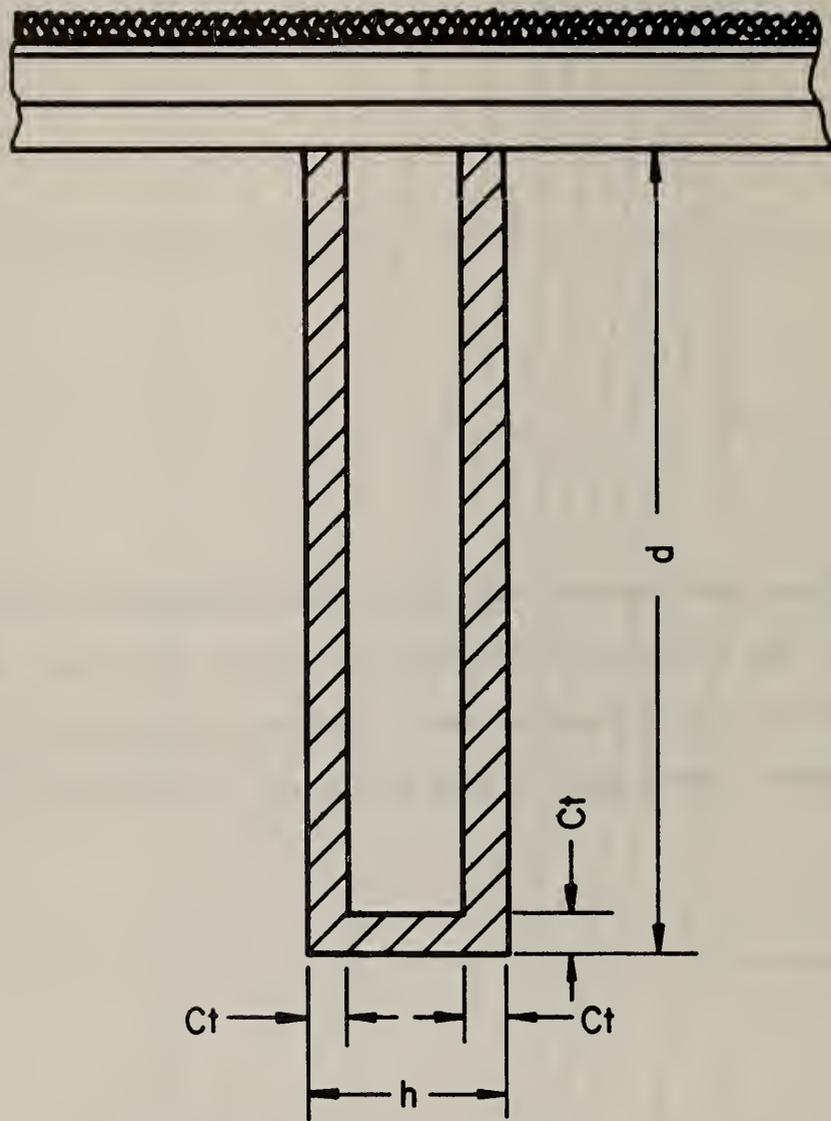
Figure 3.--Residual cross-sectional area divided by the initial area in percent
of coast Douglas-fir nominal 2 by 4 (1-5/8 by 3-5/8) members with duration of
exposure to ASTM E-119 fire conditions. The top curve is the result of using
the mean species charring rate, $\underline{C}_M$, of 0.025 in./min for large sections. The
bottom curve is the result of using an effective charring rate, $\underline{C}_f$, of
0.038 in./min. The straight line is the linear regression fit to the actual
data where the line was forced through 100 percent at time equal to zero.
(The model $Y = \beta X$ was fitted to one residual area/initial area.) The
equation of the curves is given by $100(b - 2Ct)(d - 2Ct)/(bd)$.

(M 148 528)

173

DOUGLAS-FIR 2 x 4

$A_f /A_i = (b-2C_m t)(d-2C_m t)/bd$

WITH $C_m = 0.025$ IN./MIN

$A_f /A_i =(b-2C_f t)(d-2C_f t)/bd$

WITH $C_f = 0.038$ IN./MIN

$A_f /A_i = 100-5.76t$

TIME, $t$ (MINS)

RESIDUAL AREA, $A_f /A_i$ (PCT)

174

M 148 528
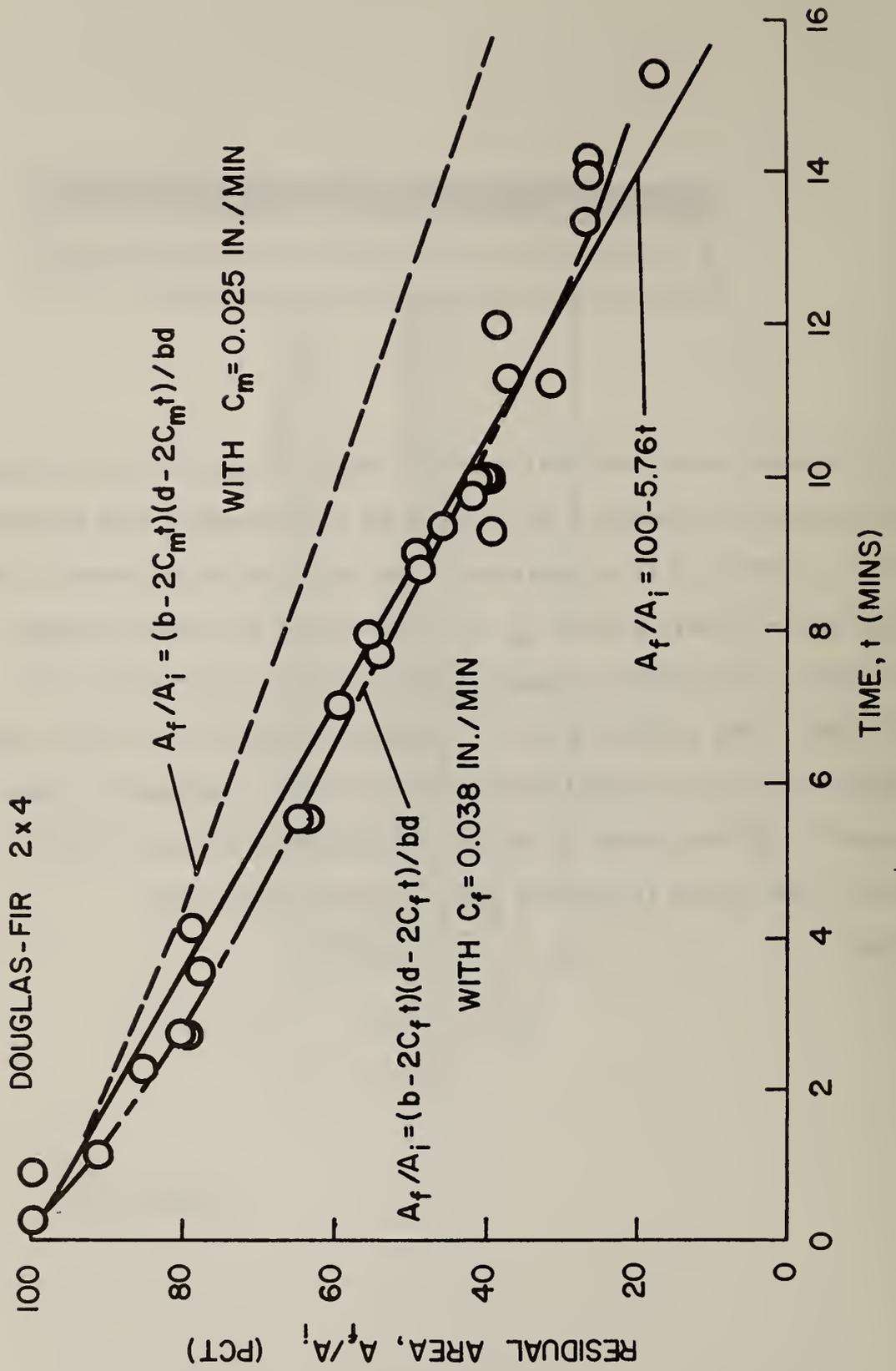
Figure 4.--Residual cross-sectional area divided by the initial area in percent

of southern pine nominal 2 by 4 (1-5/8 by 3-5/8) members with duration of

exposure to ASTM E-119 fire conditions.  The top curve is the result of using

the mean species charring rate, $\underline{C}_M$, of 0.030 in./min.  The bottom curve is

the result of using an effective charring rate, $\underline{C}_f$, of 0.45 in./min.  The

straight line is the linear regression fit to the actual data where the line

was forced through 100 percent at time equal to zero.  (The model $Y = \beta X$ was

fitted to the residual area/initial area).  The equation of the curves is

given by $100(b - 2Ct)(d - 2Ct)/(bd)$.

(M 148 529)

SOUTHERN PINE 2×4

$A_f/A_i = (b-2C_m t)(d-2C_m t)/bd$

WITH $C_m = 0.030$ IN./MIN

$A_f/A_i = (b-2C_f t)(d-2C_f t)/bd$

WITH $C_f = 0.045$ IN./MIN

$A_f/A_i = 100-6.98t$

RESIDUAL AREA, $A_f/A_i$ (PCT)

TIME, $t$ (MINS)

M 148 529

176
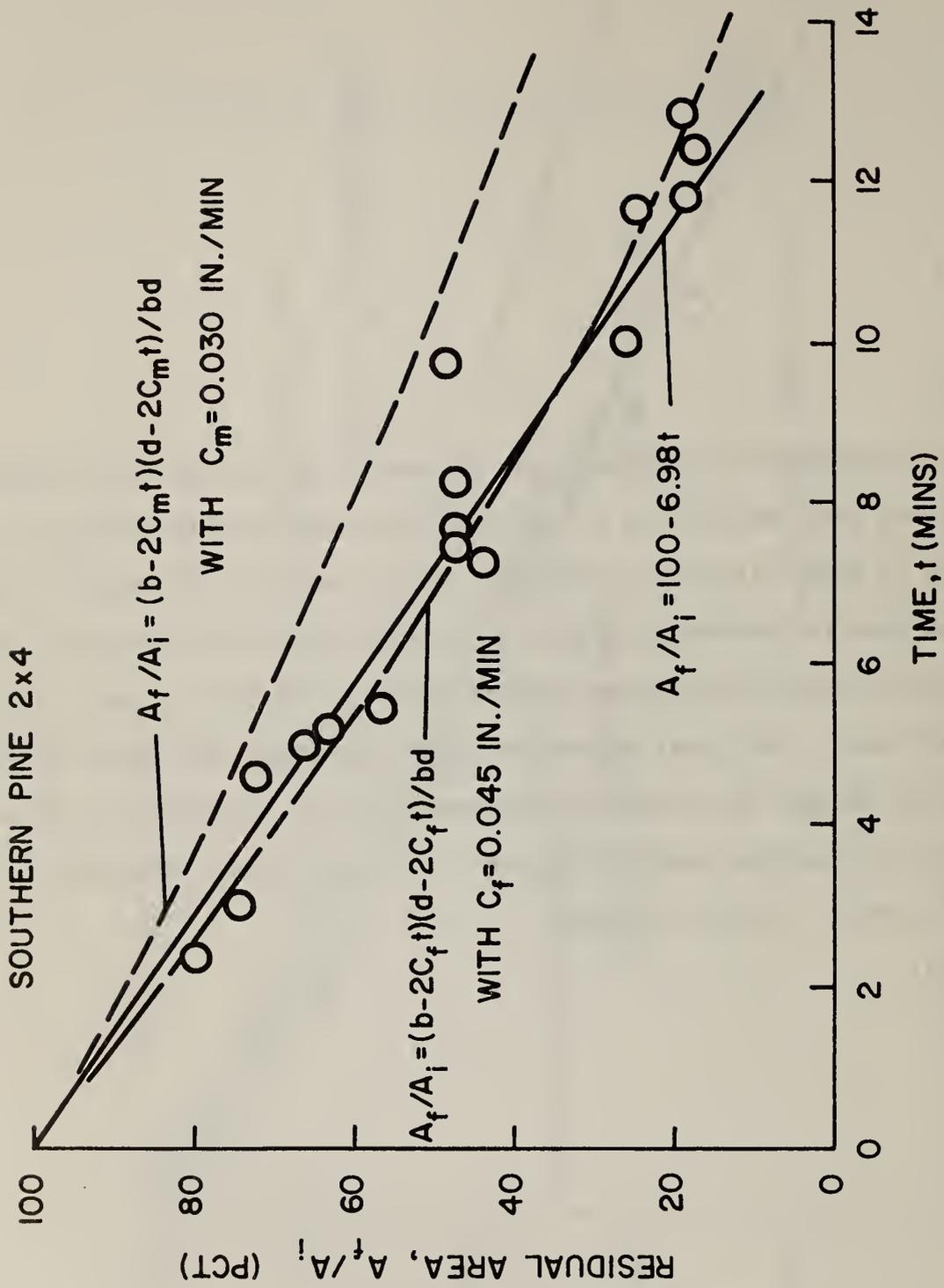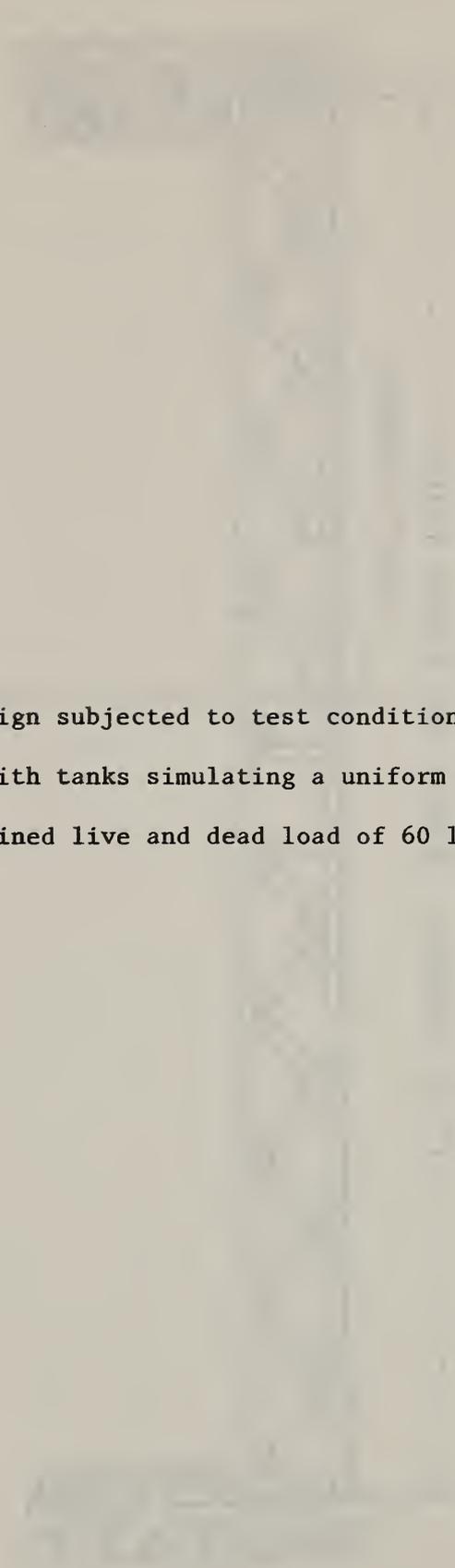
Figure 5.--Floor truss design subjected to test conditions of ASTM E-119.  The
upper chord was loaded with tanks simulating a uniform load of 55.1 lb/ft$^2$
which resulted in a combined live and dead load of 60 lb/ft$^2$.
(M 148 527)

17'-5" OVERALL LENGTH OF FLOOR TRUSS

3/4" PLYWOOD
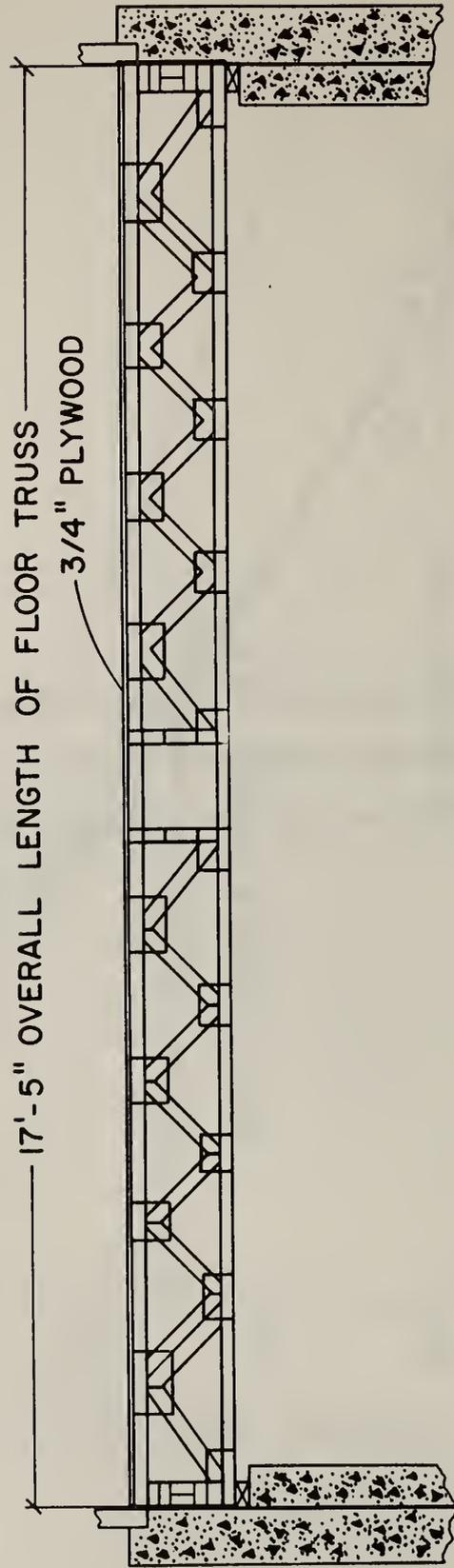
M 148 527

Figure 6.--Time to failure as a function of applied load for the floor truss
assembly of figure 5.

(M 148 530)

M 148 530

180
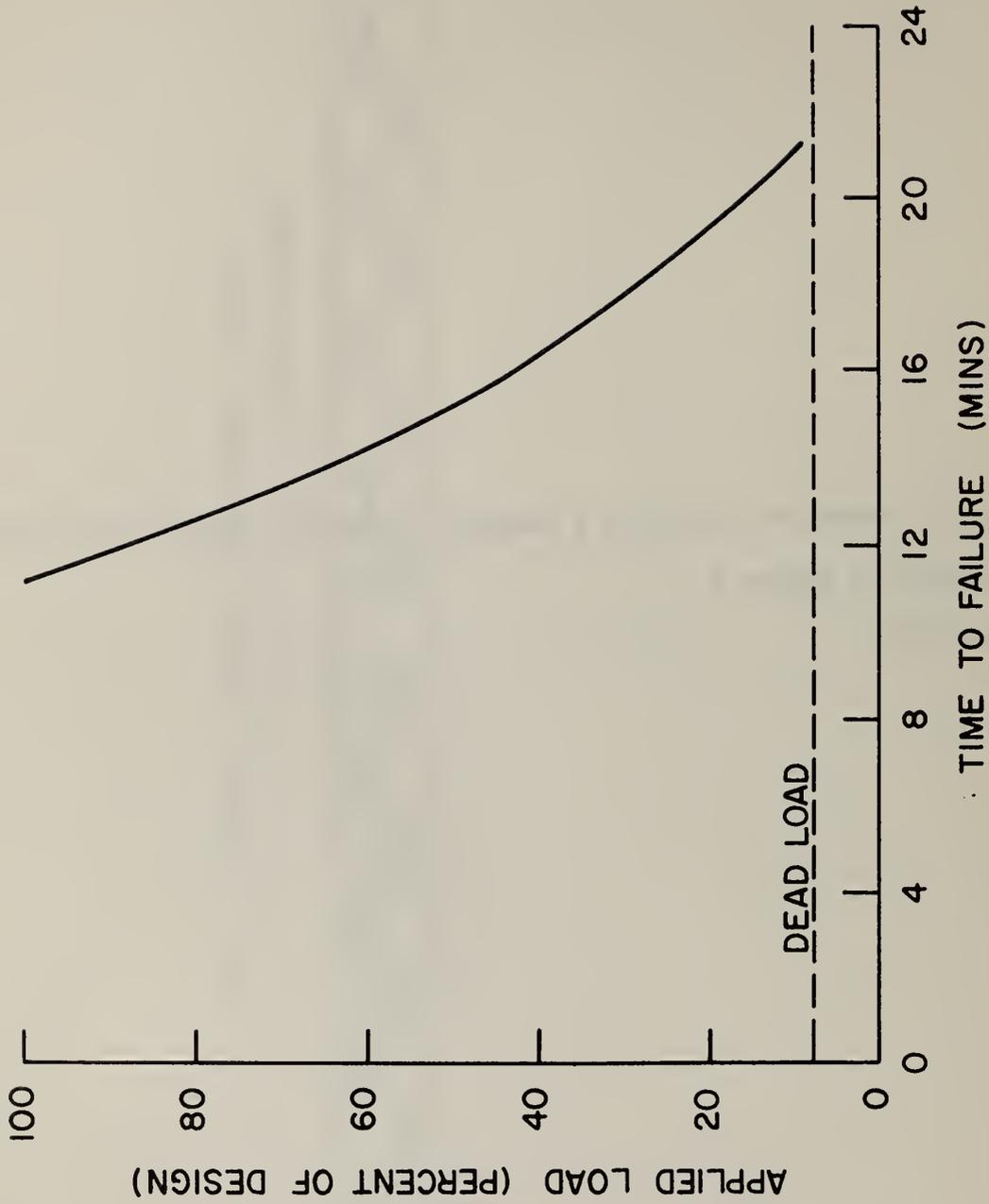
BASIC PRINCIPLES OF CALCULATING THE
FIRE RESISTANCE OF TIMBER STRUCTURES

Dr. G. M. Kirpichenkov
and
Dr. I. G. Romanenkov
(CNIISK, GOSSTROY USSR)

Timber structures are a tradition in the Soviet Union. The
nomenclature of timber structures includes beams of constant depth,
lean-to, gable, triangular and segmental trusses, triangular arches,
curved glue-laminated beams, three-hinged arches, etc. When exposed to
fire, timber structures burn and contribute to fire spread over the
surface of the structure. The latest fire tests show that timber
structures of massive cross-sections are highly resistant to fire
exposure. In 1976, building regulations were supplemented with an
additional requirement concerning the values of fire resistance limits
for timber structures. Depending on the structure type the required
fire resistance is 0.5-2.0 hours. The introduction of fire protection
requirements has stimulated the development of a fire resistance calcu-
lation method for timber structures.

The pecularity of timber structure performance in fires consists
in the loss by timber surface layers of their initial physical properties
and alterations in the mechanical properties of the unexposed timber
cross-sections. The stresses of the imposed load reach their extreme
values and there is a loss of strength of the structure due to the
reduction of timber cross-section and the temperature increases.

The main factors that influence the fire resistance limit are as
follows: timber carbonization rate and depth, changes in the timber
structures cross-sections, stress values in the structural members before
fire exposure and stress increase in the working sections at fire exposure,
changes in the elastic properties of timber in fire conditions, and
changes in load. Other factors are also known that are capable of
exerting influence on the fire resistance value, dependent on definite
types of stresses: change in elasticity and lateral stability; the
correlation of tangential and normal stresses in bending members, etc.
The principal aspects of timber structure fire resistance design based
on the solution of the equations for heat transfer and statics are con-
sidered in this report; the results of fire tests are also given. The
structures are subjected to "standard" fire exposure. The structure's
fire resistance is determined by the structural member with the least
resistance to fire exposure. The failure of a structural member results
in a functional loss of the structure.

The heat transfer solution consists of establishing the temperature distribution in the cross-section of a structural member and determining the change in the geometrical characteristics of a member's cross-section due to fire exposure.

Timber is considered to be a combustible material; it ignites and burns on exposure to high temperatures. The timber ignition temperature may be assumed to be 280°C. According to the standard fire, the time from the fire exposure until timber ignition ($\tau_b$) takes 3 min. In case of a fire retardant coating the time to timber ignition is determined by the coating's effectiveness and its thickness. The fire exposure results in the partial carbonization (combustion) of a member's cross-section which, however, remains partially undamaged. The carbonized area of a cross-section loses the physical properties of timber. The thickness of the carbonized layer depends on the fire exposure duration. The temperature of the carbonized region is assumed to correspond to the fire exposure temperature.

The temperature of internal (undamaged) timber layers changes with the fire exposure duration, so for this reason the cross section dimensions are of great importance. The isotherms are distributed over the cross-section in such a way that the timber temperature does not exceed 100°C after an hour-long fire or high temperature exposure.

Timber carbonization is one of the main factors to be considered in the process of stress and deformation analysis of timber structures with respect to time. Timber carbonization takes place successively from the surface layer at an equal rate for similar timber species of the same moisture content. The timber carbonization rate ($V_n$) is influenced by moisture content, timber density and air supply for combustion. Carbonization rate is determined experimentally by timber carbonization depth for rather large and straight members. The carbonization rate at 90 min. fire exposure is assumed to be constant. The carbonization rate for members with a minimum cross-section dimension of 120 mm made from air-dried solid timber is assumed to be 0.8 mm/min; for members with the cross-section dimension less than 120 mm-1.0 mm/min. Fire-retardant treatment is assumed not to have an influence on timber carbonization rate. Timber carbonization depth (Z) is a linear function of a fire exposure duration ($\tau_n$), i.e. $Z = V_n(\tau_n - \tau_b)$.

The change in the geometry of a cross-section takes place due to timber carbonization. The change in the geometric properties included in the design formulas is stated according to "time-carbonization depth" dependence by reducing the cross-section dimensions from each fire exposed side. Thus the fire resistance value of bending structures depends on the cross-section area, the resisting moment and the profile factor (the relation of the beams' side surfaces to the cross-section area).

More intensive timber carbonization at the corners of the section results in changes in the geometry of a cross-section and causes an additional alteration in the geometric parameters. A marked difference between the actual and an assumed rectangular cross-section after 10-15 min. of carbonization is noted. After a long-term fire exposure period the uncharred portion of a rectangular cross-section tends to acquire a round shape. Timber beams of rectangular shape with the initial cross-section dimensions 12 x 40 cm subjected to a 60 min. fire exposure on the lower exposed surface took an approximately round shape with the diameter of a circle equal to the width of the carbonized member.

Depending on the cross-section height to width ratio and on the fire exposure duration, its area may be reduced by 22% and the resisting moment of the cross section by 32% compared with the residual cross-section area estimated from the carbonization depth on each side. The additional reduction in the resisting moment and the cross-section area is taken into account by multiplying the coefficient η which depends on the relationship between the cross-section dimensions (height and width) and carbonization time.

The fire resistance limit determination for timber structures is calculated by one of three approximate methods: "time cross section area", "time resisting moment", "time profile factor". Each of these methods estimates the unknown value differently, and their correlation has no causal relation. To determine the fire resistance limit it is necessary to take the alterations in geometric properties into account as well as variation of stresses in a fire exposed structure.

The static problem consists of the calculation of the structures' bearing capacity under the conditions of fire exposure and working load. The load-bearing capacity of a structure is insured by the existing safety factor. The problem solution is based on calculation methods introduced in the building regulations for timber structure design. Variations in mechanical and strength characteristics of timber members at fire and load exposure are analyzed. Reduction of timber strength properties occurs upon heating. Timber strength reduction under high temperature conditions is considered to occur due to the changes in moisture and change in size due to shrinkage. The fire exposure is characterized by partial moisture transfer from the region of carbonization and an increase of moisture content in the residual cross-section. The phenomenon of increase in temperature and moisture content causes a simultaneous timber strength reduction. It is difficult to estimate each of these factors separately from the methodical point of view in the process of fire tests.

Temperature and strength are considered, as a rule, to be parameters to be estimated. The influence of heating on timber and glue-line strength under different moisture conditions is examined. In the structural design process (for normal conditions of load) the ultimate

strength estimation at the datum temperature is substituted for the timber strength at the standard temperature of 20°C.  In case of a temperature increase from 20°C to 100°C (at an initial moisture content of 12%) the magnitude of the timber strength reduction depends on the type of stress.  In compression conditions the strength is reduced by 20%; in conditions of tension, by 15%; in bending, by 20%; at fracture along the glue line, by 22%.  The stated reduction of timber mechanical properties when exposed to fire is for short-term load exposure and the possibility of a safety factor reduction of the material taken into consideration.  The design resistance value is stated for each stress type based on the nature of destruction due to both fire and load exposure.

The changes of stress in timber members at constant carbonization rate and external load are examined with regard to fire exposure conditions.

The given fire and static tests allowed us to specify the modes of failure and transfer regularities of glued timber structures to an ultimate state in fire and load exposure conditions.  The experimental stress values were determined from the residual cross section and the actual load at the time of failure.

Two failure schemes for bending members were described.  They depend on the relationship between the bending moment value and axial force and various combinations of beam length and depth.  The beams of rectangular section with dimensions 12 x 40 cm including the control ones, were tested without fire exposure up to failure.  The beams were subjected to shear failure in the maximum tangential stress area.  The average value of tangential stress was 11 kg/cm$^2$.  Normal stresses did not reach ultimate values at the failure point since the beams' failure took place at the shear plane.  The tests on a special series of beams with non-standard dimensions provided the researchers with useful information concerning the failure resulting from rupture on the tension side of the beam.  The average value of normal stresses at failure was 245 kgF/cm$^2$.  In case the load is distributed simultaneously, and assuming the given experimental values of normal and tangential stresses for the corresponding failure stages, their correlation makes 22.2.  Therefore, the destruction of beams with dimensions $\ell \leq 22.2h$ at fire and load exposure should occur due to shear at bending.  The given relation (or the relation of design resistance) may be used as a boundary condition for the design of a bending point at fire exposure.

The analysis of the experiments carried on for the compression members allows one to consider their load-bearing capacity and stress increase with regard to reduction of a cross-section, flexibility alterations, and lateral bending coefficient.  The average strength value at compression before failure was 250 kgF/cm$^2$, taking into account lateral stability and more intensive carbonization of members at their corners.

The fire resistance value (T) of timber structure is determined by the time from the fire exposure until timber ignition ($\tau_b$) and by the time from timber ignition until the bearing capacity loss by the design member ($\tau_n$), i.e. $T = \tau_b + \tau_n$. The value of $\tau_n$ is determined by the ultimate admissible reduction in the dimensions of the member's cross section ($\Delta_i$): $\tau_n = \Delta_i/V_n$. The timber carbonization depth should not exceed the admissible reduction in the dimensions of the cross section, i.e. $Z \leq \Delta_i$. The admissible $\Delta_i$ value is determined by the condition that the stress value ($\sigma_t$) in the non-carbonized cross-section part of the structural member at fire exposure does not exceed the design timber resistance ($R_o$) for fire resistance design, i.e. $\sigma_t \leq R_o$.

The determination of time until failure of the design member is carried on for the various types of stress conditions. In case of tension members the determination of value in question takes place with regard to the reduction of the cross-section area. The determination of time to failure of bending members in which the stability failure of a flat shape is not provided, is performed taking the reduction of resisting moment and the cross-sectional area into consideration. The $\tau_n$ estimation for the members designed for combined compression and bending stress is performed taking the area reduction of the cross-section, the resisting moment and $\eta$ ratio into account. The $\eta$ ratio accounts for the secondary moment's influence of the axial force due to member deformation. To determine the compressed members' strength, time to failure estimation is carried out by taking the cross-sectional area reduction into account. To calculate the members' stability, the cross-sectional area reduction is determined as well as a longitudinal bending ratio $\psi$.

In the process of the structural fire resistance determination the service load value is estimated on the basis of real load data. If this is not possible, the calculation is performed using standard, dead and live loads. The transient loads excluded are: people's weight, assembling loads, the loads transported by means of a hoisting crane. The snow load may be reduced in single-floor industrial, store, sport and other buildings without suspended ceilings and garrets. The snow load reduction is estimated depending on the quantity of snow melted in the process of fire exposure. The real stresses in timber members before fire exposure are estimated with regard to load according to the building regulations.

Taking the given preconditions into consideration, the nomograms and design formulas are worked out for the engineering fire resistance determination of timber structures (or their members) for the principle types of stress conditions: compression (central or eccentric), tension, bending, and compression with bending.

## CONTROL CALCULATIONS

### COMPRESSION

$$\frac{N}{\eta_F \cdot F'_o} \leq R^o_c \qquad\qquad \frac{N}{\eta_F \cdot \psi' F_o} \leq R^o_c \qquad\qquad \text{where:}$$

$N$ — longitudinal force at standard load;

$R^o_c$ — design resistance at compression in fire conditions;

$\zeta_F$ — cross-section reduction ratio due to carbonization of angles;

$F_o$ — cross-sectional area exposed to carbonization;

$\psi'_n$ — lateral bending ratio of a carbonized member.

$$\psi'_n = 1 - 0.8 \left(\frac{\lambda_o}{100}\right)^2 \; ; \; \text{at } \lambda_o \leq 75 \qquad \psi'_n = \frac{3100}{\lambda_o^2} \; ; \; \text{at } \lambda_o > 75$$

### TENSION

$$\frac{N}{\eta_F \cdot F'_o} \leq R^o_p \qquad \text{central tension;} \qquad \frac{N}{\eta_F \cdot F'_o} + \frac{N \cdot e' \cdot R^o_p}{\eta_w \cdot W'_n \cdot R^o_H} \leq R^\circ_p \quad \begin{array}{l}\text{eccentric} \\ \text{tension;}\end{array}$$

where:

$R^o_p$ — design resistance at tension in fire conditions;

$W'_o$ — resisting moment of a cross-section exposed to carbonization;

$\eta_w$ — resisting moment reduction ratio due to carbonization of angles;

$e'$ — eccentricity of normal force determined by alteration in gravity center of a cross-section at 3-sides carbonization.

AT 3-SIDES FIRE EXPOSURE:

$$F'_o = (b - 2\Delta)(h - \Delta)\eta_F$$

$$W = \frac{(b - 2\Delta)(h - \Delta)^2}{b} \cdot \eta_w$$

AT 4-SIDES FIRE EXPOSURE:

$$F'_o = (b - 2\Delta)(h - 2\Delta)\eta_F$$

$$W_o = \frac{(b - 2\Delta)(h - 2)^2}{b} \cdot \eta_w$$

186

## CHANGES IN THE GEOMETRICAL CHARACTERISTICS OF RECTANGULAR CROSS-SECTIONS IN FIRE CONDITIONS

$F = b \cdot h$ - rectangular cross-sectional area before fire exposure;

$F_O' = (b - 2\Delta)(h - 2\Delta)\eta_F$ - carbonized area of rectangular cross-section,

   where $\Delta$ - ultimately allowable reduction value of cross-sectional dimensions (b,h),

   $\eta_F$ - ratio of area reduction resulted from rounding of a rectangular section.

$$\eta_F = \psi(\tau_n \cdot \frac{h}{b})$$

at $\tau \geq 60$ min.

$$F_O' = (h - b)(b - 2\Delta) - \Pi/4\,(b - 2\Delta)^2$$

### CHANGES IN THE GEOMETRICAL CHARACTERISTICS OF A CROSS-SECTION AT CARBONIZATION
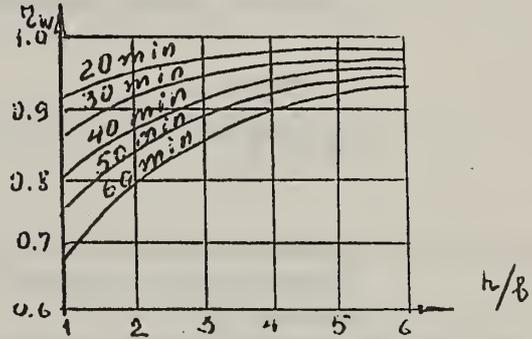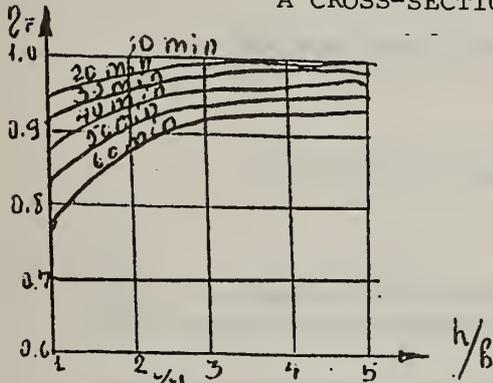




... area and ... ting mo- ... reduction ... rounded ... tion
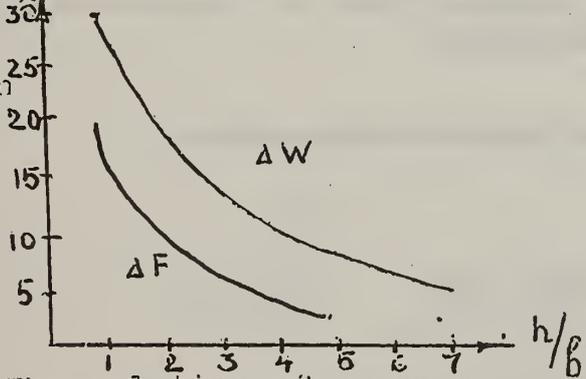


The relation of a cross-sectional hight to its width
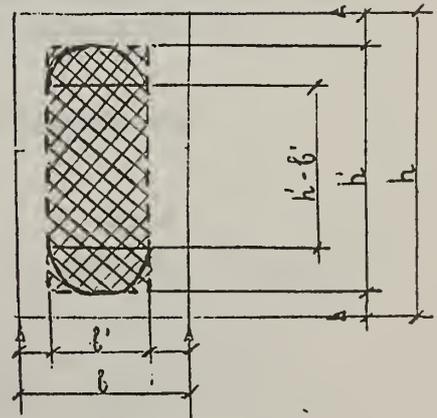
## BENDING.

$$\frac{3Q}{2Fn} \leq R^{\circ}_{ck} \text{ - shear at bending;} \qquad \frac{M}{\eta_w W'_n} \leq R^{\circ}_u \text{ - bending;}$$

where:  $M$  - lateral force at standard load;

$Q$  - design resistance to shear in fire conditions;

$R^{\circ}_{ck}$  - design resistance to bending in fire conditions;

$\eta_w$  - coefficient of changes in geometrical characteristics of sections due to more intensive carbonization of angles.

## COMPRESSION WITH BENDING.

$$\frac{N}{\eta_F \cdot F'_n} + \frac{N\xi \, R^{\circ}_c}{\xi \cdot \eta_w \cdot W'_n \cdot R^{\circ}_u} \leq R^{\circ}_c$$

where:  $\xi = 1 - \dfrac{\lambda^2_o \, N}{3100 R^{\circ}_c F'_n}$  $\qquad \lambda_o = \dfrac{\ell_o}{\eta_o}$

$\ell_o$  - member's design length;

$\eta_o$  - gyration radius of a carbonized cross-section.

$$\eta_o = \sqrt{\frac{\eta_y \cdot T_n}{\eta_F \cdot F'_n}}$$

where:  $T_n$  - gyration moment of a cross-section subjected to carbonization (angles' carbonization is not taken into account);

$\eta_y$  - gyration moment reduction ratio of a cross-section due to angles' carbonization.

## FOR MEMBERS OF RECTANGULAR CROSS-SECTIONS.

$$T_o = 0.29b$$

$$\Pi^{\circ} = T_{oi} + T_{ni} \qquad T_{ni} = \frac{Z_{ni}}{V_o} \qquad {}^{(}T_n \leq R^{\circ}$$

$R^{\circ}$  - timber resistance for fire resistance calculation.

# DURABILITY OF STRETCHED, COMPRESSED AND COMPRESSED-CURVED ELEMENTS

## 4-SIDES FIRE EXPOSURE

square section $\qquad Z_1 = \dfrac{b}{2}(1 - \sqrt{Ai})$

rectangular section $\qquad Z_1 = \dfrac{b+h}{4} - \sqrt{\dfrac{b+h}{4}^2 - \dfrac{bh}{4}(1 - Ai)}$

## 3-SIDES FIRE EXPOSURE

square section $\qquad Z = \dfrac{3}{4}b - \sqrt{\left(\dfrac{3}{4}\right)^2 - \dfrac{b}{2}^2(1 - Ai)}$

rectangular section $\qquad Z = \dfrac{b+2h}{4} - \sqrt{\left(\dfrac{b+2h}{4}\right) - \dfrac{bh}{2}(1 - Ai)}$

$Ai = \dfrac{\alpha_3^{c_1(p)}}{R_o^{c_1(p)}}$ $\qquad \alpha_3$ – stress in the element due to standard load before carbonization

## COMPRESSED ELEMENTS' STABILITY CALCULATION

$Ai = \dfrac{\psi \alpha_3^c}{\psi_n R_c^o}$ $\qquad \dfrac{\psi}{\psi_n} = \dfrac{1}{1 - \dfrac{2Z_1}{b}}$ $\qquad$ b – is the shortest side of a section

$\qquad\qquad\qquad\qquad\qquad\qquad\qquad \psi_1 \psi_n$ – is the longitudinal bending ratio before carbonization and destruction due to fire and load.

## COMPRESSED-CURVED ELEMENTS' CALCULATION

$Ai = \theta \dfrac{\alpha_3^c}{R_c^o}$ $\qquad \theta = \dfrac{1 + \dfrac{e}{\rho^n \cdot \xi^n}}{1 + \dfrac{e}{\rho \cdot \xi}}$ $\qquad$ e – eccentricity of normal force $\dfrac{M}{N}S$

$\qquad\qquad\qquad\qquad\qquad\qquad\qquad \rho_i \rho^n$ – cores radii of carbonized and and non-carbonized sections

$\qquad\qquad\qquad\qquad\qquad\qquad\qquad \xi_i \xi^n$ – the influence ratio of a longitudinal force's secondary moment.

189

APPROACH TO THE FIRE RESISTANCE DESIGN FOR LIGHT WALL PANELS
USING EFFECTIVE MATERIALS

V. N. Zigern-Korn
and
I. G. Romanenkov

Light enclosing prefabricated wall panels called "light structures" have been successfully used in the Soviet Union for the last ten years. The structures are characterized by the high degree of technological and installation effectiveness, transportability and good utilization qualities. The weight of these structures does not exceed 75 kg/m$^2$. Shaped and sheet, flat and corrugated steel, aluminum, asbestos-cement, plastics, timber, and other materials, as well as effective heat insulating materials of 200 kg/m$^3$ density, are used in the process of manufacturing. The words "light structures" include complex steel panels without framework intended for industrial buildings, asbestos-cement panels with or without framework for agricultural buildings, and partitioning panels using asbestos-cement, timber, plastics, etc.

In terms of fire security, the structures should meet the fire resistance and ignition requirements. Depending on the building's class of fire resistance the required fire resistance of wall panels, cap plates, and partitions is 0.25 hr to 0.5 hr (1)[1]. According to the combination of materials used, the structures are divided into non-combustible, combustible with difficulty, and combustible.

The actual fire resistances of light enclosing structures are estimated by means of fire tests carried on according to standard methods. The results of the tests cover a wide range of values.

According to their ignitability, the light enclosing structures are considered to be combustible or combustible with difficulty. Light enclosing structures possess specific properties that determine their behavior in fire conditions. But insufficient information concerning these properties together with the imperfection of fire protection requirements and estimation methods for the fire security level of buildings are likely to result in irrational usage of these structures. The structures' behavior in fire includes: 1) the resistance to fire exposure, expressed as the time that bearing and enclosing functions are maintained in a structure fire; 2) the degree of the structure's contribution to fire propagation and the accumulation of dangerous fire factors (heat, smoke, toxic products of combustion, etc., or fire hazard). Each of the two properties mentioned above is determined by a group of parameters. In the process of designing buildings for fire security, each group of parameters should be considered separately.

---

[1]Figures in parentheses refer to references at the end of this paper.

In terms of the terminology of 2) above, the structure reaches its limit with regard to fire resistance when the predicted failures take place, and its fire risk--if unanticipated events occur. Really, the load-bearing capacity loss of the structure or failure as an enclosing structure is seen as spasmodic fire development or by sudden accumulation of material losses due to fire propagation.

The increase of fire risk factors, i.e., fire propagation, results in the gradual accumulation of material loss. Besides this, losses of non-economic character, i.e., injuries and deaths of people, particularly during initial fire stages results from temperature increases or from the high concentration of toxic combustion products.

Of concern is that the methods of determining the fire resistance criteria for light enclosing structures are unsettled. The fire risk determination of these structures is limited, as a rule, to a fire propagation test.

The regulations (3) state three criteria of the structure's limiting condition regarding fire resistance: 1) the load-bearing capacity loss, failure or deflection; 2) heating to a definite temperature on the unexposed side; 3) the appearance of fire through cracks or openings.

Each of the criteria mentioned above 1), 2), and 3), has been of major importance for all types of buildings. Until 1978, the fire resistance of a structure was determined with regard to the minimum time necessary for the structure to reach one of the criteria.

Now that new types of structures with the use of effective materials have appeared, the determination of limiting conditions with regard to fire resistance have required a more concrete approach with regard to function. The structural design is likely to influence the method of determining the time until a limiting condition is reached. A more concrete approach to the limiting condition determination has already been partially given in the Standard (3). The limiting condition for external walls, beams, frames, columns, poles, and coatings is solely the load-bearing capacity loss by the structures and joints. It is suggested that the limiting condition of unloaded structures protected with fire resisting coverings be the critical temperature of the structural material. The criteria, 1), 2), and 3), are the limiting conditions for other types of structures.

While comparing the nomenclature of light structures used in national building practice and the types of structures with their function (bearing and non-bearing, external and internal, horizontal and vertical, etc.), it is easy to note the existence of fire resistance design method development for enclosing panels, cap plates, and external non-bearing walls.

As was stated, the fire resistance of light enclosing structures (non-bearing walls and cap plates) is specified according to factor 1).

191

The failure of panels used as separating walls occurs at fire tests after the insulation has burned out. However, it is impossible to determine the panel failure time analytically as the forces applied to it are close to zero.

The adopted list of possible structure limiting conditions with regard to fire resistance (1,2,3) does not correspond to the variety of the enclosing structure failures observed in practice. This circumstance makes difficult the development of fire resistance design methods for the enclosing structures useful for building fire security analysis. For example, during fire tests on the external walls (fragments) manufactured from light metal panels with the use of foam plastic insulation the steel covered panels' failure is not observed even after the insulation has burned out. But holes occur in aluminum covered panels. The hole dimensions increase with time--the panel failure occurs when it burns out along the whole of its width. The fire resistance remains undetermined in the first case and depends on the fragment's structural design in the second case. In both cases, the fire resistance determination is of some difficulty. The information on the fire resistance in the second case is of no use for the analysis of fire process development.

The fire resistance design consists of the following: determination of the unsteady state temperature field in the structure at a given temperature regime of fire exposure; bearing capacity estimation taking into account the structure's capacities during the fire and force exposure process; determination of the time from the fire exposure beginning until a limiting condition occurs (1,2,3). The structural load-bearing capacity is not controlled if the fire resistance is stated according to factor 2).

The change in the thermal properties and physical states of materials with temperature, the change in the geometrical dimensions of elements due to the material burning process, and the change in the heat transfer conditions on the surface of a structure due to temperature and properties alterations are taken into account in the unsteady state temperature field determination.

When determining the load-bearing capacity of a structure exposed to a fire it is necessary to take into consideration the change in the mechanical properties of materials with temperature, the extra stresses and the changes in the structures' design scheme that occur due to the thermal strains and the change in the structural members' properties.

There are no reasons for calculating the fire resistance of enclosing structures according to factor 3). It is possible to assume that concrete rupture research will develop ways for determining the possible failure of sheet material on the basis of mineral bending (4).

Also of importance is work on the burning out intensity of foam plastic insulation in three-layer panels with steel coverings. The results will help to estimate the possibility of open hole formation in panels with aluminum cover plates.

In terms of an impartial fire resistance evaluation of buildings it is of major importance to obtain information on the capacity of light wall enclosures to resist vertical and horizontal fire spread to the adjacent compartment, i.e. to high temperatures and fire spread along the internal surface through partitions and ceilings, adjacent to these walls. The formation of open orifices in the suspended external walls may influence the ventilation of the fire and, consequently, the fire temperature regime. This problem is likely to be of concern as well.

One-dimensional temperature fields for laminated enclosing structures using non-combustible materials are developed with regard to a non-stationary fire exposure regime (5). The structural fire resistance design criterion is the unexposed surface heating to 160°C (3). The calculation consists of solving the heat engineering problem of the heating time of the unexposed surface to this limiting temperature. The calculation is based on the elementary heat balance method permitting one to achieve calculation results without requiring the solution of differential equations (6). The non-stationary temperature field calculation of a multilayer enclosing structure of non-combustible materials is carried out using a numerical method. The structure cross-section is divided into a number of elementary layers. Their width remains constant within the limits of fixed material. The elementary layers and various materials limits as well as the points situated on the structure's surface and the air-exposed limits are considered to be points of calculation. The problem is reduced to the determination of temperature values at the structure's points of calculation at various time intervals until the limiting temperature is reached on the unexposed surface. The calculation is carried out by means of a step method. The heat balance equation is set up for each elementary layer. The sectional and surface temperatures of single-layer and multilayer structures are stated according to these equations. The calculation equations are algorithms for computers. The calculation permits determining the fire resistance of non-combustible structures according to factor 2). Of concern in this calculation process is the heat required to vaporize materials. The effect on the heating of air circulation in the hollow structure's layers after the structures have lost their tightness is also of concern. The problem grows more complex if combustible materials are used in a structure.

There is the necessity of solving the static problem for external horizontal bearing enclosures, e.g. membrane-type coverings, coverings with steel corrugated plates, coverings from frame-type panels with asbestos-cement, veneer, glass-fiber-reinforced plastics, and other types of sheetings. The load-bearing capacity of the first two coverings is determined solely by the bearing capacity of metal elements-membranes and

corrugated sheet. In this case, the method of calculating the enclosing structures' fire resistance is not difficult, as it does not differ from the calculation method for steel structures. The calculation of coverings on the basis of frame-type panels is more difficult. As the load imposed on these coverings during fire is significantly lower than the calculated one they may retain their shape even after openings occur in the coverings. Another phenomenon is observed in the process of calculating the fire resistance of any multilayer compressed or deflected structure if the layers and members are connected with each other mechanically and if these connections provide their mutual resistance to the imposed load. In these cases one, two, or three intermediate states with various sudden changes of calculation scheme will take place before the limiting condition with regard to structural bearing capacity is reached. The variety of the sudden changes in the calculation scheme is explained, for example, by rupture or melting of one of the facing layers, the beginning or completion of the burning process or the insulation melting.

The fire resistance of the structures mentioned is defined by the sum of time intervals corresponding to the definite states of the structure. The development of these calculation methods requires the accumulation and systematization of initial data both on the structure and material behavior in fire conditions.

The problem of the load level imposed on the structures in fire is one of the basic problems in the process of structural fire resistance evaluation. There is no unambiguous and well grounded opinion concerning this problem. For example, the existing Standard (3) suggests that a load should be determined on the basis of detailed analysis of conditions that may occur at fire. In case they cannot be defined, the load is considered to be the standard. The possibility of a load level reduction in fire in comparison with the calculated one is explained by the fact that a fire is a rare phenomenon. The possibility of its coincidence in time with the calculated load level is insignificant. The standard load level means the major technological loads (equipment, installation, materials, furniture, and people) and also on average annual unfavorable atmospheric loads. Therefore, the standard load level is also overestimated for the fire exposure conditions.

At present, the requirements for the choice of loads imposed on a structure during fire are unlikely to be formulated. It is necessary to study the statistical data concerning the fires that occur, comparing the fire beginning time and the stage of the daily or annual functional cycle of various types of buildings. The analysis of the data obtained will promote the evaluation of possible various technological and atmosphere load levels coincident with the time of the fire. In the process of developing recommendations, it is suggested that the existing design and calculation standards should be used for various types of structures (steel, timber, reinforced concrete). Of concern are the methods of investigation of possible various coincident loads (7).

The probabilistic-economic calculation methods of building structures and the concept of "failure" are widely used at present and aim at the optimization of failure possibility on the basis of the minimization of expenditures directed to engineering and possible losses resulted from failure.

To use the evaluation method of building structure fire resistance successfully, it is necessary to be aware of the possible moment of failure, which depends on the imposed load level, and take the physico-mechanical properties of materials and their variation into account. In this case only the development of analytical methods for the description of structure behavior during fire together with the statistical modeling methods will allow us to calculate the detailed characteristics of structural fire resistance, while a large scale test will be aimed at verifying the calculation methods.

Of major importance will be the accumulation of data concerning the physical and mechanical properties of materials under fire conditions when exposed to high temperatures and injury.

The fire security calculations of buildings will contain not a "standard" fire temperature regime but a real one. Therefore, it is desirable to prefer fire resistance calculation methods that will yield the working capacity at any temperature and fire exposure regime.

## REFERENCES

(1)   Fire safety norms of design of buildings and structures, SNiP II-A.5-70.

(2)   A. R. Rzhanitsyn, B. I. Snarskis, Yu. D. Sukhov, The main premises of the probability-economic technique for calculation of construction structures. Construction mechanics and calculation of structures, 1979, No. 3, pp. 67-71.

(3)   Fire safety norms of construction design. A method of testing of construction structures for fire resistance. ST COMECON 1000-78 standard.

(4)   Recommendations for protection of concrete and reinforced concrete structures from brittle failure during fires. NIIZHB of the State Construction Administration of the USSR, Moscow, 1979.

(5)   N. F. Gavrikov: Calculation of the fire resistance of incombustible protective structures. In the collection "Fire resistance of construction structures", Issue 3, 1975, pp. 100-108.

(6)   N. A. Strel'chuk et al. Engineering-Physical Journal, Vol. VII, No. 4, 1964, pp. 105-110.

(7)   A. R. Rzhanitsyn, The theory of calculation of construction structures for reliability.  Construction Publishing House, Moscow, 1978.

# SPRINKLER SYSTEMS: AN APPROACH TO ACTIVE FIRE RESISTANCE

Joseph Hankins
Factory Mutual Research Corporation

In discussions of fire resistance, what is normally considered is the resistance of structural components to the effects of heat produced by an assumed uncontrolled fire. A standard time-temperature curve was developed quite a number of years ago, and fire resistance is typically specified in terms of the period of time the component in question can withstand this standard fire exposure before exceeding some failure criteria. In more recent times, methods have been developed to approximate the exposure presented by various types of "real-world" fires, and relate those to the standard fire resistance measuring techniques to allow more realistic evaluations of fire resistance. A key point to note here is that the subject being dealt with is, in both cases, passive fire resistance.

I would like to suggest an additional step. That is to consider the active fire resistance offered by automatic sprinkler protection. In addition to the well known extinguishing effects of sprinklers, they also serve to reduce the temperature over a fire through the cooling effects of water. The combined effects of cooling and the reduction in the rate of burning can result in a marked reduction in temperatures above a fire. It is desirable to consider this factor when designing fire resistance into a structure.

Given the fact that automatic sprinkler protection is provided in many structures for the purpose of controlling and extinguishing fires, it is reasonable

to include the effects of sprinklers in an evaluation of a building's fire resistance. Also, trade-offs might be possible so that the fire extinguishing benefits of sprinklers can be obtained at a lower cost as a result of the reduced level of structural fire resistance needed.

It must be made clear at the outset that I am not proposing that automatic sprinkler protection is a replacement for fire resistance. It is equally important to note that fire resistance is not a final answer either. As in any design process, goals must be set before choices are made.

For example, in a hotel or apartment building, provision of reliably fire resistant walls, floors, and ceiling between each unit can assure that fire will be contained in the area that it originates, thereby limiting damage and risk to life. By the same token, provisions of a fire resistant structure used as a large, open manufacturing area will simply assure that there is a shell remaining after all contents have been consumed by fire.

Consideration must be given to reliability as well. Sprinkler systems are subject to mechanical failure; any fire resistance scheme that depends on doors, dampers, etc. is also subject to mechanical failure. There is no such thing as "close enough" in the design of sprinklers or structural fire resistance. If a sprinkler system is not designed to produce the discharge required to control a fire in the area it protects, it will be no more effective than rain

on a volcano. By the same token, structural fire protection must be complete in every detail. A fire resistant partition can be rendered useless by the collapse of a pipe passing through it.

I would like to begin by showing you an example of the effect sprinklers have on temperatures at the ceiling over a severe fire. This figure shows the results of one of a series of tests where pairs of tests, one sprinklered and one unsprinklered, were run for various plastic commodities. Also included in the figure is the standard time-temperature curve. It is interesting to note, by the way, that the unsprinklered test follows the standard time-temperature curve very closely. On the other hand, in the sprinklered test, the most important effect to note is the considerable reduction in maximum ceiling temperature resulting from the operation of sprinklers. Results of the other tests were similar: unsprinklered tests generally resulted in maximum temperatures well in excess of 1000°F for a considerable length of time, while temperatures stayed below 1000°F for most of the sprinklered tests. The 1000°F mark is widely used as the rule-of-thumb critical temperature for steel.
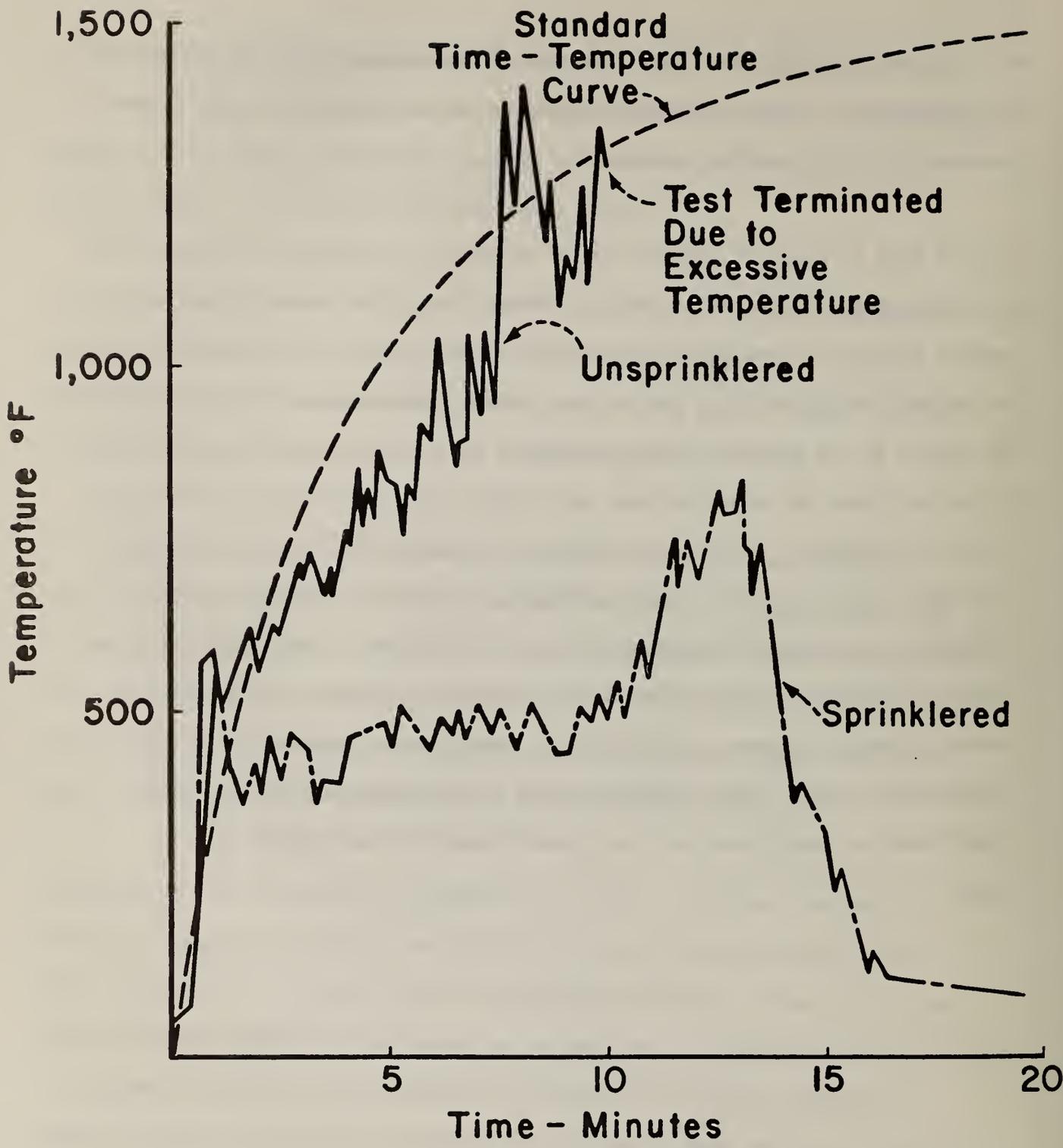
Sprinklered Vs. Non Sprinklered Test
of 2 Pallet x 2 Pallet x 11 ft. Array of
Polyethylene Bags in Cardboard Cartons

What I will attempt to do here today is present a simple method, developed by our Basic Research Group, for estimating the area of sprinkler operation and maximum anticipated ceiling temperature, given the type and configuration of combustibles present and the design parameters of the sprinkler system.

Equation 1 gives us the radius of sprinkler operation in terms of the location and freeburn heat release rate of the combustibles present; the distance between the top of the combustibles and the ceiling; and the sprinkler density and operating pressure. These relationships have proven to be accurate, within practical limits, when compared to results of actual tests.

Equations 2 and 3 allow the temperature near the ceiling, within and outside of the fire plume to be predicted, based on the above data. Again, these relationships compare well with temperatures measured in actual tests.

These relationships apply only to 1/2 in. orifice sprinklers. A relationship can also be developed for 17/32 in. orifice sprinklers.

The greatest problem in using these relationships comes in determining a realistic heat release rate of the combustible in question. As there is more easily accessible data on freeburn heat release rates, these are used in our calculations. Use of the freeburn rate also introduces a safety factor into the calculation. Freeburn heat release rates can range between 1,500 Btu/min/ft$^2$ and 96,000 Btu/min/ft$^2$. This chart shows some representative values.

$$r_0 = \frac{\left([B^3 + 193\, CpD\dot{Q}]^{1/2} - B^{3/2}\right)}{96pD} \qquad (1)$$

Where:

$$B = \frac{(T_L - T_{rm})\, H}{4.74}$$

C = Dimensionless location factor
    C = 1  far from walls
    C = 2 directly adjacent to walls
    C = 4 directly in corner
D = Sprinkler density (GPM/ft$^2$)
H = Ceiling height above top of combustibles (ft)
P = Pressure at operating sprinklers (psig)
$\dot{Q}$ = Free-burn heat release rate of combustibles (Btu/min.)
r = Radial distance from center of fire (ft.)
$r_0$ = Radius of arc of sprinkler operation (ft.)
T = Maximum gas temperature at ceiling at r (°F)
$T_L$ = Temperature rating of sprinklers
$T_{rm}$ = Room temperature (°F)

Outside of Fire Plume ( r ≥ .18H ):

$$T - T_{rm} = \left[\frac{C\dot{Q} - 48p\, Dr_0{}^2}{r}\right]^{2/3} \left[\frac{4.74}{H}\right] \qquad (2)$$

Inside of Fire Plume ( r < .18H ):

$$T - T_{rm} = \left[C\dot{Q} - 48p\, Dr_0{}^2\right]^{2/3} \left[\frac{14.87}{H^{5/3}}\right] \qquad (3)$$

202

TABLE

Heat-release rate per unit floor area of fully involved combustibles, bracketed between discrete values. (PE = polyethylene; PS = polystyrene; PVC = polyvinyl chloride; PP = polypropylene; PU = polyurethane)

|  | Btu/min per ft$^2$ of Floor Area | | | | | | |
|---|---|---|---|---|---|---|---|
|  | 1.5K | 3K | 6K | 12K | 24K | 48K | 96K |
| 1. Wood pallets, stack 1 1/2 ft high |  |  | x |  |  |  |  |
| 2. Wood pallets, stack 5 ft high |  |  |  | x |  |  |  |
| 3. Wood pallets, stack 10 ft high |  |  |  |  | x |  |  |
| 4. Wood pallets, stack 16 ft high |  |  |  |  |  | x |  |
| 5. Mail bags, filled, stored 5 ft high | x |  |  |  |  |  |  |
| 6. Cartons, compartmented, stacked 15 ft high |  |  | x |  |  |  |  |
| 7. PE letter trays, filled, stacked 5 ft high on cart |  |  |  |  | x |  |  |
| 8. PE trash barrels in cartons, stacked 15 ft high |  |  | x |  |  |  |  |
| 9. PE-fiberglass shower stalls in cartons, stacked 15 ft high |  |  | x |  |  |  |  |
| 10. PE bottles packed in item 6 |  |  |  |  | x |  |  |
| 11. PE bottles in cartons, stacked 15 ft high |  |  | x |  |  |  |  |
| 12. PU insulation board, rigid foam, stacked 15 ft high |  |  | x |  | .: |  |  |
| 13. PS jars packed in item 6 |  |  |  |  |  | x |  |
| 14. PS tubs nested in cartons, stacked 14 ft high |  |  |  |  | x |  |  |
| 15. PS toy parts in cartons, stacked 15 ft high |  |  | x |  |  |  |  |
| 16. PS insulation board, rigid foam, stacked 14 ft high |  |  |  |  | x |  |  |
| 17. PVC bottles packed in item 6 |  |  |  |  | x |  |  |
| 18. PP tubs packed in item 6 |  |  |  |  | x |  |  |
| 19. PP and PE film in rolls, stacked 14 ft high |  |  |  |  |  | x |  |
| 20. Methyl alcohol |  | x |  |  |  |  |  |
| 21. Gasoline |  |  |  |  | x |  |  |
| 22. Kerosine |  |  |  |  | x |  |  |
| 23. Diesel oil |  |  |  |  | x |  |  |

203

As an example, we will use the tests from which were derived the previously shown time-temperature curve.

For this test, the height of the test array was 12 ft and the ceiling height was 30 ft. The test array occupied 80 ft$^2$ of floor area. Sprinklers were of the 165°F rating and the sprinkler system maintained a density of .3 gpm/ft$^2$, requiring a pressure at the operating sprinklers of 28 psig. The ambient temperature at the test site was 55°F, and the test array was located well away from walls.

As the commodity tested was essentially a solid block of polyethylene in a cardboard box, it is reasonable to bracket the heat release rate somewhere between polyethylene bottles and 10 ft stacks of pallets. We chose 18 K Btu/min/ft$^2$.

Therefore:

$H = 18$ ft                                $D = 0.3$ gpm/ft$^2$

$P = 28$ psig                              $T_L = 165°F$

$\dot{Q} = 18$ K Btu/min/ft$^2$            $(80$ ft$^2) = 1.44 \times 10^6$ Btu/min

$C = 1$                                    $T_{rm} = 55°F$

$B = \dfrac{(165 - 55)\ (18)}{4.74} = 418$

The radius of sprinkler operation is:

$$r_o = \frac{[(418)^3 + 193 \ (1) \ (28) \ (.3) \ (1.44 \times 10^6)]^{1/2} - (418)^{3/2}}{96 \ (28) \ (.3)}$$

$$= 50 \ ft$$

In the actual test, the radius of sprinkler operation was 40 ft.

If we assume no sprinklers, the temperature directly of the fire would be predicted to be:

$$T - T_{rm} = [1.33 \times 10^6]^{2/3} \left[\frac{14.87}{(18)^{5/3}}\right]$$

$$= 1425°F$$

$$T = 1480°F$$

The actual measured value was 1305°F.

For the case where sprinklers were provided, the predicted temperature would be:

$$T - T_{rm} = [1.44 \times 10^6 - 48 \ (28) \ (.3) \ (50)^2]^{2/3} \left[\frac{14.87}{(18)^{5/3}}\right]$$

$$= 643°F$$

$$T = 698°F$$

The actual measured value was 700°F.

205

Obviously, this is not a procedure that is in a final, useable form. Work continues at Factory Mutual to develop a sophisticated and very accurate computer model of sprinklered fires. In the meantime, anyone doing research in numerical determinations of fire resistance should at least be aware that methods do exist to allow the inclusion of the effects of sprinklers in their calculations. Ultimately, it is hoped that a designer will have more flexibility in making choices among building materials or assemblies. One will be able to select a material alone with a higher fire resistance rating, or another material with a lower rating but with sprinkler protection provided to bring the overall fire resistance up to the desired level.

| U.S. DEPT. OF COMM.<br>BIBLIOGRAPHIC DATA<br>SHEET | 1. PUBLICATION OR REPORT NO.<br><br>NBSIR 80-2188 | 2. Gov't Accession No. | 3. Recipient's Accession No. |
|---|---|---|---|

| 4. TITLE AND SUBTITLE<br><br>Joint US-USSR Seminar on Mathematical Methods for Estimating the Fire Endurance of Structural Assemblies | 5. Publication Date<br><br>January 1981 |
|---|---|
| | 6. Performing Organization Code |

| 7. AUTHOR(S)<br><br>R. S. Levine, Editor | 8. Performing Organ. Report No. |
|---|---|

| 9. PERFORMING ORGANIZATION NAME AND ADDRESS<br><br><br>NATIONAL BUREAU OF STANDARDS<br>DEPARTMENT OF COMMERCE<br>WASHINGTON, DC 20234 | 10. Project/Task/Work Unit No. |
|---|---|
| | 11. Contract/Grant No. |

| 12. SPONSORING ORGANIZATION NAME AND COMPLETE ADDRESS *(Street, City, State, ZIP)* | 13. Type of Report & Period Covered |
|---|---|
| | 14. Sponsoring Agency Code |

15. SUPPLEMENTARY NOTES

| | Document describes a computer program; SF-185, FIPS Software Summary, is attached.

16. ABSTRACT *(A 200-word or less factual summary of most significant information. If document includes a significant bibliography or literature survey, mention it here.)*

This publication is a compilation of papers presented May 14, 1980, at a Joint US-USSR Seminar on "Mathematical Methods for Estimating the Fire Resistance of Structural Assemblies". The seminar was arranged by the US-USSR Panel on Fire Resistance of Buildings and Structures as a part of their continuing protocol (agreement) to cooperate in this field. In turn, this agreement is part of a wider US-USSR agreement to cooperate in the field of Housing and Other Construction. The responsible U.S. government agency for the parent agreement is the Department of Housing and Urban Development (HUD). Mr. Lawrence P. Simons, Assistant Secretary for Housing and Federal Housing Commissioner is U.S. Deputy Co-Chairman for the Parent Agreement. Dr. Robert S. Levine of the National Bureau of Standards, Center for Fire Research and Dr. Igor G. Romanenkov, Laboratory Chief, Central Research Institute of Building Construction, GOSSTROY, are the Co-Chairmen of the Fire Panel. This is the first of a series of planned yearly joint seminars on specific applied fire safety research topics. The Soviet papers were translated into English by the Soviets, but editorial changes have been made by U.S. personnel who are expert in the particular subject. It is intended that the original authors' meanings have not been changed. In some cases, the U.S. presentations are not yet available as published papers, or were summaries of work that has already been published elsewhere. Hence, one of the U.S. presentations is in the form of slides and commentary. These presentations, in the form given, are intended to represent up-to-date U.S. technology.

17. KEY WORDS *(six to twelve entries; alphabetical order; capitalize only the first letter of the first key word unless a proper name; separated by semicolons)*

Fires; fire endurance; mathematical models; reinforced concrete; steel structures; wood structures.

| 18. AVAILABILITY [X] Unlimited | 19. SECURITY CLASS<br>(THIS REPORT) | 21. NO. OF<br>PRINTED PAGES |
|---|---|---|
| | For Official Distribution. Do Not Release to NTIS | UNCLASSIFIED | 213 |
| | Order From Sup. of Doc., U.S. Government Printing Office, Washington, DC<br>20402, SD Stock No. SN003-003- | 20. SECURITY CLASS<br>(THIS PAGE) | 22. Price |
| [X] Order From National Technical Information Service (NTIS), Springfield,<br>VA. 22161 | UNCLASSIFIED | $17.00 |